Investigation ofblended fibroin/aloe gel extract film on the biomolecular mechanism(s) relating to fibroblast wound healing activity

Preeyawass Phimnuan

THESE DE DOCTORAT DE L'ETABLISSEMENT UNIVERSITE BOURGOGNE FRANCHE-COMTE
PREPAREE A ECOLE DOCTORALE « ENVIRONNEMENTS-SANTE »

Ecole doctorale n°9920A12627S

Docteur de l'Université de Franche-Comté

Doctorat de « Pharmacie »

Par

Preeyawass PHIMNUAN

Investigation of blended fibroin/aloe gel extract film on the biomolecular mechanism(s) relating to fibroblast wound healing activity

Thèse présentée et soutenue à « Thaïlande », le « 9 Décembre 2022 »

Composition du Jury :

Prof. Waraporn Putalun, Ph.D.	Khon kaen University	Président et Rapporteur
Prof. Patricia Rousselle, Ph.D.	Claude Bernard University Lyon 1	Rapporteur
Sophie Robin, Ph.D.	Cryonove Pharma SAS	Examinatrice
Assoc. Prof. Nanteetip Limpeanchob, Ph.D.	Naresuan University	Examinatrice
Assist. Prof. Saran Worasakwutiphong, M.D.	Naresuan University	Examinateur
Assoc. Prof. Anuphan Sittichokechaiwut, Ph.D.	Naresuan University	Examinateur
Prof. Jarupa Viyoch, Ph.D.	Naresuan University	Codirecteur de thèse
Céline Viennet-Steiner, Ph.D.	Bourgogne Franche-Comté University	Codirecteur de thèse

ÉCOLE DOCTORALE
PRES I Bourgogne I Franche-Comté
Environnement - Santé

Titre : titre (en français) Étude d'un film d'extrait de gel de fibroïne/aloès sur le(s) mécanisme(s) biomoléculaire(s) lié(s) à l'activité de cicatrisation des fibroblastes

Mots clés : fibroïne de soie, gel d'aloès, ulcère du pied diabétique, pansement, cicatrisation

Résumé : Chez les patients diabétiques, le processus de cicatrisation est généralement retardé ou altéré. Une complication chronique primaire est l'ulcère du pied diabétique. Un environnement diabétique pourrait être associé à un dysfonctionnement des fibroblastes dermiques, à une angiogenèse réduite, à la libération de cytokines pro-inflammatoires et à des caractéristiques de sénescence. Les traitements thérapeutiques alternatifs utilisant des produits naturels sont très demandés pour leur fort potentiel d'activité bioactive dans la réparation cutanée. Dans cette étude, les propriétés physicochimiques et biologiques d'un film d'extrait de gel de fibroïne/aloès irradié aux rayons gamma ont été étudiées pour soutenir l'efficacité de cicatrisation du film. Ce travail prolonge nos études précédentes in vitro et in vivo chez le rat diabétique induit par la streptozotocine et les essais cliniques chez les patients diabétiques souffrant d'ulcère du pied. Dans la présente étude, la fibroïne de soie et l'extrait de gel d'aloès ont été analysés séparément pour leur teneur en protéines, leur poids moléculaire et leurs caractéristiques chimiques. Les deux extraits ont ensuite été dissous dans une solution d'acide lactique et simplement coulés pour obtenir le film d'extrait de gel de fibroïne/aloès, et les propriétés physicochimiques et biologiques du film ont été déterminées. Nous avons constaté que l'irradiation gamma n'affecte aucune propriété physicochimique du film préparé, telles que l'apparence physique (translucidité de flexibilité et couleur jaunâtre), la morphologie de surface (morphologie non poreuse), les propriétés mécaniques et les caractéristiques chimiques (présentation d'amide I, II, III, unités glucanes, cycle pyranoside et mannose). Les cellules traitées avec le film ont stimulé la prolifération en initiant un passage de la phase G0/G1 à la phase S et à la phase G2/M. Les cellules traitées avec le film non traitée n'a pas été complètement cicatrisée, ce qui indique que l'activité biologique du film préparé améliore la prolifération et la migration des fibroblastes caractérisant ainsi une amélioration de la cicatrisation cutanée. Le film préparé a également été étudié pour ses effets bénéfiques sur les activités biologiques cellulaires et le(s) mécanisme(s) biomoléculaire(s) en utilisant des fibroblastes cutanés issus de patients sains et de patients diabétiques (avec et sans ulcère). Plusieurs paramètres ont été analysés dont la cytotoxicité, la prolifération cellulaire, le cycle cellulaire, la migration cellulaire, la sécrétion de la protéine VEGF et la régulation de la voie de signalisation ERK1/2. Le film préparé a démontré des activités préférentielles en favorisant la prolifération et la migration cellulaires, la sécrétion de VEGF et la prévention de la sénescence cellulaire. Son mécanisme d'action est principalement lié à l'activation de la voie MAPK/ERK, connue pour réguler diverses activités cellulaires, dont la prolifération. Par conséquent, le film d'extrait de gel de fibroïne/aloès peut être considéré comme une nouvelle approche thérapeutique dans le traitement des ulcères diabétiques non cicatrisants.

Title : Investigation of blended fibroin/aloe gel extract film on the biomolecular mechanism(s) relating to fibroblast wound healing activity

Keywords : silk fibroin, aloe gel, diabetic foot ulcer, wound dressing, wound healing

Abstract : In diabetic patients, the wound healing process is usually delayed or impaired. A primary chronic complication is diabetic foot ulcers. A diabetic environment could be associated with dermal fibroblast dysfunction, reduced angiogenesis, the release of pro-inflammatory cytokines, and senescence features. Alternative therapeutic treatments using natural products are highly demanded for their high potential of bioactive activity in skin repair. In this study, the physicochemical and biological properties of a gamma-irradiated blended fibroin/aloe gel extract film were investigated to support the wound healing efficacy of the prepared film. This work extends our previous studies in vitro and *in vivo* in the streptozotocin-induced diabetic rat and clinical trials in diabetic foot ulcer patients. In the current study, silk fibroin and aloe gel extract were separately analyzed for their protein content, molecular weight pattern, and chemical characteristics. Both extracts were then dissolved in lactic acid solution and simply cast to obtain the blended fibroin/aloe gel extract film, and the physicochemical and biological properties of the prepared film were determined. We found that gamma irradiation does not affect any physicochemical properties of the prepared film, such as physical appearance (flexibility translucence and yellowish color), surface morphology (non-porous morphology), mechanical properties, and chemical characteristics (presenting of amide I, II, III, glucan units, pyranoside ring, and mannose). The film-treated cells stimulated the proliferation by initiating a shift from G0/G1 phase to S phase and G2/M phase, which were higher than the untreated cells. The film-treated cells provided a completely healed scratch at 36 h after wound creation, while untreated wound was not fully healed, indicating that the biological activity of the prepared film enhances the proliferation and migration of the fibroblast cells and thereby stimulates wound healing improvement in diabetic foot ulcers. The prepared film was also investigated for its beneficial effects on cell biological activities and biomolecular mechanism(s) using normal dermal, diabetic dermal, and diabetic wound fibroblasts. This study aimed to elucidate the possible MAPK/ERK signaling pathway related to the biological effects of the film on fibroblast cells. The biological activities and biomolecular mechanism(s) were determined, including cytotoxicity, cell proliferation, cell cycle, cell migration, VEGF protein secretion, and ERK1/2 signaling pathway assays. The prepared film illustrated the preferential activities to promote cell proliferation and migration, VEGF secretion, and prevention of cell senescence. Furthermore, the prepared film displayed a biological behavior with interesting properties for delayed wound healing. Its mechanism of action is mainly linked to the activation of the MAPK/ERK pathway known to regulate various cellular activities, including proliferation. Therefore, the blended fibroin/aloe gel extract film can be considered as a novel therapeutic approach in treating diabetic non-healing ulcers.

ACKNOWLEDGMENTS

First of all, I would like to acknowledge Naresuan University and Bourgogne Franche-Comté University for providing the double doctoral degree program for thesis of doctorate agreement of co-supervisor. I acknowledge the Center of Excellent for Innovation in Chemistry (PERCH-CIC), Office of the higher Education Commissions and graduate school, Naresuan University for grant to graduate student and Faculty of Pharmaceutical Sciences, Naresuan University for facility support. Additionally, I also acknowledge UMR 1098 RIGHT INSERM EFS BFC, DImaCell Imaging Ressource Center, Bourgogne Franche-Comté University for useful facilities and equipment.

I would like to express my genuine and dutiful to my advisor, Professor Dr.Jarupa Viyoch for providing me the opportunity for the further education in Doctoral degree and for her continuous encouragement and support during my graduate study and also co-advisor, Dr Céline Viennet-Steiner for their invaluable advice and mercifulness as well as the whole unforgettable supporting for everything when I studied in France. Their patience, kindness and understanding are also deeply appreciated. In particular, Zélie Dirand, Marion Tissot, and Gwenael Rolin have been an incredible resource for novel ideas and innovative solutions involving the knowledges of biomolecular level and supported for the equipment.

I gratefully acknowledge to the members of my supervisory committee who associated for their suggestions and ideas that allowed me to accomplish my research proposal and project. And all of staff in Faculty of Pharmaceutical sciences, Naresuan University and unit laboratory of UMR 1098 RIGHT INSERM EFS BFC, DImaCell Imaging Ressource Center, Bourgogne Franche-Comté University for their advice.

Finally, I would like to express deeply my thanks to my parents and family for their endless love, supports, care and encouragement.

Preeyawass Phimnuan

ABSTRACT

In diabetic patients, the wound healing process is usually delayed or impaired. A primary chronic complication is diabetic foot ulcers. A diabetic environment could be associated with dermal fibroblast dysfunction, reduced angiogenesis, the release of pro-inflammatory cytokines, and senescence features. Alternative therapeutic treatments using natural products are highly demanded for their high potential of bioactive activity in skin repair. In this study, the physicochemical and biological properties of a gamma-irradiated blended fibroin/aloe gel extract film were investigated to support the wound healing efficacy of the prepared film. This work extends our previous studies *in vitro* and *in vivo* in the streptozotocin-induced diabetic rat and clinical trials in diabetic foot ulcer patients. In the current study, silk fibroin and aloe gel extract were separately analyzed for their protein content, molecular weight pattern, and chemical characteristics. Both extracts were then dissolved in lactic acid solution and simply cast to obtain the blended fibroin/aloe gel extract film, and the physicochemical and biological properties of the prepared film were determined. We found that gamma irradiation does not affect any physicochemical properties of the prepared film, such as physical appearance (flexibility translucence and yellowish color), surface morphology (non-porous morphology), mechanical properties, and chemical characteristics (presenting of amide I, II, III, glucan units, pyranoside ring, and mannose). The film-treated cells stimulated the proliferation by initiating a shift from G_0/G_1 phase to S phase and G_2/M phase, which were higher than the untreated cells. The film-treated cells provided a completely healed scratch at 36 h after wound creation, while untreated wound was not fully healed, indicating that the biological activity of the prepared film enhances the proliferation and migration of the fibroblast cells and thereby stimulates wound healing improvement in diabetic foot ulcers. The prepared film was also investigated for its beneficial effects on cell biological activities and biomolecular mechanism(s) using normal dermal, diabetic dermal, and diabetic wound fibroblasts. This study aimed to elucidate the possible MAPK/ERK signaling pathway related to the biological effects of the film on fibroblast cells. The biological activities and biomolecular mechanism(s) were determined, including cytotoxicity, cell proliferation, cell cycle, cell migration, VEGF protein secretion, and ERK1/2 signaling pathway assays. The prepared film illustrated the

preferential activities to promote cell proliferation and migration, VEGF secretion, and prevention of cell senescence. Furthermore, the prepared film displayed a biological behavior with interesting properties for delayed wound healing. Its mechanism of action is mainly linked to the activation of the MAPK/ERK pathway known to regulate various cellular activities, including proliferation. Therefore, the blended fibroin/aloe gel extract film can be considered as a novel therapeutic approach in treating diabetic non-healing ulcers.

GRAPHICAL ABSTRACT

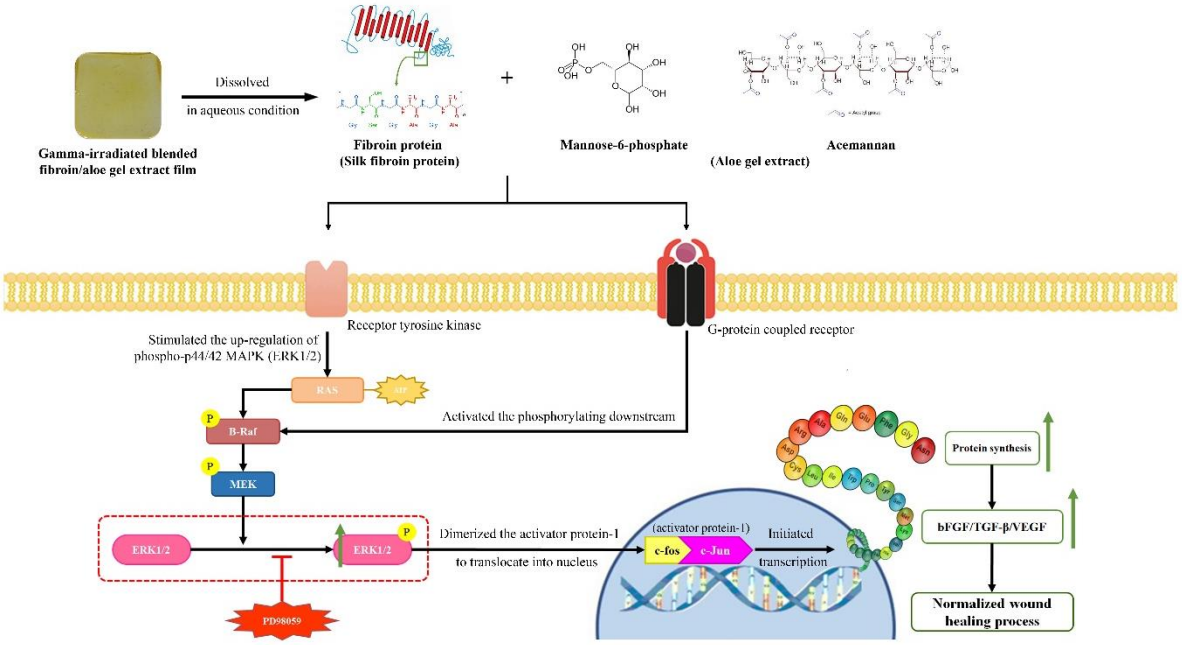

Schematic summary of the beneficial effects of blended fibroin/aloe gel extract film. The mechanism of action is mainly linked to the activation of MAPK/ERK phosphorylation pathway. Both of fibroin protein and aloe gel extract constituents (e.g., mannose-6-phosphate or acemannan) activate tyrosinase receptor and G-protein coupled receptor and stimulate the up-regulating downstream of MAPK/ERK pathway resulting in the normalized wound healing process. PD98059, a potent inhibitor of MEK/ERK1/2 cascade by binding to MEK/ERK1/2, induces an inactive MEK/ ERK1/2 form and prevents the activation of upstream activator.

TABLE OF CONTENTS

III RESEARCH METHODOLOGY

LIST OF TABLES

LIST OF FIGURES

ABBREVIATIONS

µg	=	microgram
µL	=	microliter
µm	=	micrometer
%	=	Percent
2-D	=	Two-dimensional
3-D	=	Three-dimension
AGEs	=	Advanced glycation end products
Ang-1	=	Angiopoietin-1
BSA	=	Bovine serum albumin
bFGF	=	basic Fibroblast growth factor
CDK	=	Cyclin-dependent kinase
CKIs	=	Cyclin-dependent kinase inhibitors
CLI	=	Critical limb ischemia
cm^{-1}	=	per centrimeter
COX	=	Cyclooxygenase
CRP	=	C-reactive protein
dL	=	Deciliter
DDF	=	Diabetic dermal fibroblast
DFU	=	Diabetic foot ulcer
DMEM	=	Dulbecco's modified eagle medium
DWF	=	Diabetic wound fibroblast
DI	=	Deionized
DM	=	Diabetic mellitus
ECM	=	Extracellular matrix

EGF	=	Epidermal growth factor
ERK	=	Extracellular signal-regulated kinase
FTIR	=	Fourier-transform infrared spectroscopy
FGF	=	Fibroblast growth factor
GAGs	=	Glycosaminoglycans
h	=	hour
HbA1c	=	Hemoglobin A1C
HIF-1	=	Hypoxia-inducible factor-1
IDF	=	International diabetes federation
IDDM	=	Insulin-dependent diabetes mellitus
IGF	=	Insulin-liked growth factor
IgG	=	Immunoglobulin G
IL-1α	=	Interleukin-1 alpha
IL 1β	=	Interleukin-1 beta
IL-1R	=	Interleukin-1 receptor
IL-6	=	Interleukin-6
iNOS	=	inducible Nitric oxide synthase
JNK	=	c-Jun N-terminal kinase
kg	=	kilogram
kDa	=	kilo Dalton
KGF	=	Keratinocyte growth factor
L	=	Liter
LPS	=	Lipopolysaccharide
MAPK	=	Mitogen-activated protein kinase
MEK-1	=	Mitogen-activated protein kinase-1
MEKK-1	=	Mitogen-activated protein kinase kinase-1

MI	=	Myocardial infarction
MIF	=	Macrophage Migration Inhibitors Factor
mg	=	Milligrams
mL	=	Milliliter
mins	=	Minutes
mm	=	Millimeter
mm^2	=	Millimeter square
mmol	=	Millimoles
MMPs	=	Matrix metalloproteases
N	=	Newton
NGF	=	Nerve growth factor
nm	=	nanometer
NDF	=	Normal Dermal Fibroblast
NHDF	=	Normal Human Dermal Fibroblast
NIDDM	=	non-insulin-dependent diabetes mellitus
NO	=	Nitric oxide
PAD	=	Peripheral artery disordered
PAI-1	=	Plasminogen activator inhibitor-1
PGE2	=	Prostaglandin E2
PKC	=	Protein kinase C
ROS	=	Reactive oxygen species
RT	=	Room temperature
SD	=	Standard deviation
SDS-PAGE	=	Sodium dodecyl sulfate-polyacrylamide gel electrophoresis
SEM	=	Scanning electron microscope

SF	=	Silk fibroin
TGF-α	=	Transforming growth factor-alpha
TGF-β	=	Transforming growth factor-beta
TLRs	=	Toll-like receptors
TNF-α	=	Tumor necrosis factor-alpha
TNFR	=	Tumor necrosis factor receptor
PDGF	=	Platelet-derived growth factor
VEGF	=	Vascular epidermal growth factor
v/v	=	Volume by volume
WHO	=	World Health Organization
w/o	=	without
w/w	=	Weight by weight

CHAPTER I

INTRODUCTION

Background and Significance of the Study

The International Diabetes Federation (IDF) estimated that approximately 463 million adults aged 20-79 had diabetes worldwide in 2019. In 2045, this number is estimated to rise to 700 million people living with the disease [1]. Additionally, IDF also reported that diabetes is prevalent in adults up to 4.3 million in Thailand. Diabetes Mellitus (DM) is a group of metabolic disorders characterized by hyperglycemia resulting from defects in absolute or relative insulin deficiency, or both. Chronic diabetes is associated with long-term damage, dysfunction, and failure of different organs, especially feet [2]. And 15-25% of DM patients can develop diabetic foot ulceration (DFU) [3]. Diabetic foot is one of the most considerable and disastrous complications of DM and is defined as a foot affected by ulceration related to neuropathy, vasculopathy, and immunopathy of the lower limb in a DM patient [4, 5]. These lesions are common, particularly on the lower extremities. Leg and foot ulcers have many causes that may further define their characters. For the peripheral neuropathy and ischemia, the problems affect the poor infiltrating of macrophage or antibiotic into the wound resulting in the longer wound healing and finally, amputation. At the molecular pathway, the metabolic abnormalities cause insufficient cellular growth factor responses, including Transforming growth factor (TGF-β1), Pellet-derived growth factor (PDGF), basic Fibroblast growth factor (bFGF), and especially Vascular epidermal growth factor (VEGF) [6-8]. During normal wound healing, these growth factors served as important roles in the inflammatory and proliferative process simultaneously with re-epithelialization [9]. In diabetes conditions, the healing process is dysfunctional by the changes in the levels and timing of their expression [10]. Therefore, the critical result affected the cellular level change, contributing to an increased risk of delayed wound healing. The stimulation of growth factor expression contributes to the cellular activity, including cell migration or proliferation into the provision of the wound, and promotes the protein synthesis or diminishes some conditions as normal healing progresses. The prevention of DFU is critical, considering the adverse impact on a patient's quality of life, experience chronic pain, loss of function and mobility, increased social stress and isolation, depression, anxiety, and

prolonged hospitalization [11]. We believe that both primary healthcare systems and medical innovations involved in the treatment and management of DFU are important.

The wound dressing is one of alternatively effective tools that is responsible for this problem. Wound dressing plays a pivotal role in managing of diabetic foot ulcers, which comprises cleaning the wound and the use of modern wound care techniques that promote a moist wound healing environment [12]. Wound dressing can be classified into 3 types including tissue-derived biomaterials, hydrogel-based biomaterials, and biomaterials with controlled-release of signaling molecules [13]. Recently, there are several developed artificial polymeric materials for application as a wound dressing. Additionally, biomaterials based on silk fibroin incorporating with aloe gel extract exerted potential properties in promoting wound healing evaluated *in vivo* and during clinical trials [14-16].

Silk fibroin (SF) from *Bombyx mori* has been highlighted for various biomedical field applications due to its superior mechanical properties, controllable biodegradability, hemostatic properties, non-cytotoxicity, and non-inflammatory characteristics [17-19]. SF also exhibits exceptional compatibility with a variety of cells and tissues [14, 20]. Furthermore, at the molecular level, SF accelerates signals, including AKT/mTOR and MAPK pathway, which provide prominent actions for the phosphorylation of ERK 1/2 and JNK 1/2 kinases and promote cellular migration through the expression of PAI-1, regards to the promotion migration, facilitating the re-epithelialization of the provisional wound bed and stimulates complete cellular adhesion [21, 22]. Because of its properties to promote the differentiation and proliferation of various cells, SF has been considered a potential biomaterial to use as wound dressings with various formulations.

Aloe vera (*Aloe barbadensis* Miller) has been traditionally used in diverse cultures for its therapeutic properties. The *Aloe vera* leaf contains chemical compounds (acetylated mannans, polymannans, anthraquinone C-glycosides, anthrones, anthraquinones, and lectins) [23]. Its leaf pulp containing mucilaginous gel has been applied to various alternative medicines for rejuvenation, dermatologic conditions, and wound healing properties [24, 25]. *Aloe vera* proteins (polypeptide) have low molecular weights (20-100 kDa) providing anti-inflammatory activity due to inhibition of bradykinin vasodilating action. Moreover, glucomannans are the main polysaccharides in *Aloe vera* that interfered with bradykinin activity [26]. For the cellular pathway, *Aloe vera* illustrates the acceleration of wound

repairing by promoting collagen type I synthesis, influencing the cyclin-dependent cell cycle progression, as well as stimulating cross-linking of collagen for wound contraction and promoting wound-breaking strength [27]. *Aloe vera* further induces stimulating effects of elevating the expression of VEGF and TGF-β1 genes in the wound of induced-diabetes rats [28, 29]. Hence, it clarifies the enhancing capabilities of growth factor expression associated with the wound healing process via penetration into cellular skin [30].

Although herbal products are widely used as a folk treatment, few approaches exist combining natural product extracts. We were interested in the association of SF and *Aloe vera* for wound healing properties through the development of a blended fibroin incorporating aloe gel extract. In accordance with Caesar L.K. & Cech N.B. reported that the constituents consisted of natural herbal composition as the therapeutic properties account more potential effects than the purified components owing to the efficacious synergistic effects [31].

According to our previous study, the developed film significantly accelerated the healing rate of the wound by 1 week in streptozotocin-induced diabetic rat and rapidly attenuated the healing time and the wound size to be completely healed within 4 weeks in 5 DFU patients [14, 16]. However, there are limitations of some points during the study. For these reasons we need to confirm and investigate more issues including 1) scaling up, we developed the film as a prototype based on lab scale model which applies preliminary *in vitro* and animal studies. In addition, we modified the production procedure to scale up in the larger amount for applying and transferring to the industrial field 2) sterilization procedure, we modified the sterilized technique from the previous study as ozonation technique to gamma irradiation. Gamma irradiation technique is undergone by exposing the continuous gamma rays to samples [32]. It is typically appropriate used for the up-scale level and avoids the heat-sensitive material in the medical device industry. This sterilization practically deactivated various contaminating microorganisms such as bacteria, fungi, viruses, and spores [33]. However, some studies are indicating the adverse effects of sterilization of products by gamma irradiation such as molecular mechanisms involved in gamma rays-induced cell damage, microorganisms-resistance, and structural changes in polymer medical devices using gamma rays. For these reasons, we need to investigate the physical, chemical characteristics, and sterility test of

the developed film using gamma-irradiated sterilization. 3) biological activity, we sought to emphasize the biological activities in the molecular level associating with healing property to support the efficacy described in the previous study of the developed film.

In this present study, we likewise anticipate that the developed gamma-irradiated film stimulates cellular activities in normal and diabetic fibroblast cells at the biomolecular level.

Purposes of the Study

To investigate the physicochemical properties and biomolecular activities of the blended fibroin/aloe gel extract film

Statement of the Problems

Due to the increasing prevalence of DFU patients and the potential bioactivities of the SF and aloe gel extract, Prof. Dr. Jarupa Viyoch, Asst. Prof. Dr. Anuphan Sittichokechaiwut and Miss Paichit Inpanya have the idea to develop innovative wound dressing based on the association of biological materials. In 2007, the researchers have succeeded the protein purification from the silk cocoons and *Aloe vera* to develop the wound dressing and applied then on the streptozotocin-induced diabetic rats [14]. The previous studies have shown that the developed wound dressing stimulated the extracellular matrix (ECM) production by fibroblasts at the wound site. The collagen deposition increased in the dermal area followed by a rearrangement of epithelial tissue and finally a completely wound healing. The animal study led to a further clinical study in DFU patients in 2016 to determine the safety and efficacy of the wound dressing. The results illustrated that enrolled 5 DFU patients have no allergy and undesired effects occurred during the study. The wounds have completely healed relating to the size of the wound and the duration time of the treatment, and any adverse effects have been observed [16].

Scope of the Study

Due to the outstanding ability of SF to promote adhesion and proliferation of various cells including keratinocytes and fibroblasts, the molecular mechanisms involved in wound healing with SF are gradually being characterized. Also, *Aloe vera* affects fibroblast growth factor and stimulates the activity and proliferation of these cells and in turn, improves collagen production and secretion. As the descriptions above, we accordingly determine experiments into 1) scaling up, we will modify the

production procedure to scale up in the larger amount for applying and transferring to the industrial field 2) sterilization procedure, we need to investigate the physical, chemical characteristics, and sterility test of the developed film using gamma-irradiated sterilization 3) biological activity, we sought to emphasize the biological activities of normal and diabetic dermal fibroblasts and diabetic wound fibroblasts to support the efficacy of the developed film described in the previous study.

Keywords

Diabetes mellitus; Diabetic foot ulcers; Chronic wound healing; Fibroin; *Aloe vera*; Wound dressing; Fibroblasts

Research Hypothesis of the study

The blended fibroin/aloe gel extract film is attributed to serve as a medical device playing preferential roles such as regulating biomolecular mechanism(s) involved in fibroblast wound healing activity.

CHAPTER II

REVIEWS OF RELATED LIERATURE AND RESEARCH

Diabetic Mellitus (DM)

Definition of Diabetic Mellitus

Diabetic Mellitus (DM) can be defined as a group of metabolic diseases identified by hyperglycemia resulting from defects in absolute or relative insulin deficiency, or both. The chronic hyperglycemia of diabetes is related to long-term damage, dysfunction, and failure of different organs including the eyes, kidneys, nerves, heart, and blood vessels especially the feet [34]. DM can be identified by characteristic symptoms including thirst, polyuria, loss of vision, and weight loss. The long-term effects of DM include the progressive development of the specific complications of retinopathy with potential blindness, neuropathy which leading to renal failure, the combination of neuropathy and vasculopathy with the risk of foot ulcers, charcot joint, failure of autonomic dysfunction, and finally amputation. Several pathogenic processes are associated with the development of DM such as dysfunction or destruct of the β-cells of the pancreas resulting in insulin deficiency and resistance to insulin action. The abnormalities of carbohydrate, protein, and fat metabolism are due to the deficient action of insulin on the target tissues which is caused by an insensitivity or lack of insulin [35]. People who suffered from DM have gotten a high risk for serious life-threatening health problems resulting in higher medical care costs, reduced quality of life, and increased mortality.

The roles of insulin

Insulin plays two important roles that relate to overall metabolic homeostasis. It maintains sufficient energy stores allowing for development, growth, and reproduction. Another role acts as a feedback regulator of plasma glucose [36]. In addition to its role in controlling blood sugar levels, insulin is also involved in the storage of fat. The amount of glucose in the bloodstream is tightly regulated by the hormone insulin. Insulin is usually secreting in small amounts by the pancreas (≤ 3.3 mmol/L) [37]. When the amount of glucose in the bloodstream raises to a certain level, the pancreas will release more insulin to uptake more glucose into the cells causing the glucose levels in the bloodstream to drop [38].

Postprandially, the secretion of insulin occurs in two phases: an initial rapid release of preformed insulin, followed by increased insulin synthesis and release in response to blood glucose. Long-term release of insulin occurs if glucose concentrations remain high (Figure1) [37, 39]. Once a significant number of islets of Langerhans cells are destructed, it results in little or lack of insulin secretion, or inability to adequately respond to insulin, leading to the development of the symptoms of diabetes.

In type 1 diabetes, the pancreas produces insufficient insulin to regulate blood glucose levels. Without the presence of insulin, many of the cells cannot uptake glucose from the blood and therefore the body uses other sources of energy. Ketones are produced by the liver as an alternative source of energy. However, high levels of ketones lead to a dangerous condition called ketoacidosis. Type 1 diabetes patients need to inject insulin to compensate for their body's lack of insulin [40].

In type 2 diabetes, cells cannot effectively respond to insulin. This is termed insulin resistance resulting in the cell is incapable of uptake glucose from the blood. In the earlier stages, the cell responds by producing more insulin than the normal condition. Due to the long-term developing, the demands on the pancreas to overproduction of insulin leads to a loss of insulin-producing cells (known as pancreatic β-cells). Depending on their level of insulin resistance, people with Type 2 diabetes may also need to take insulin injections to manage their blood sugar levels [41].

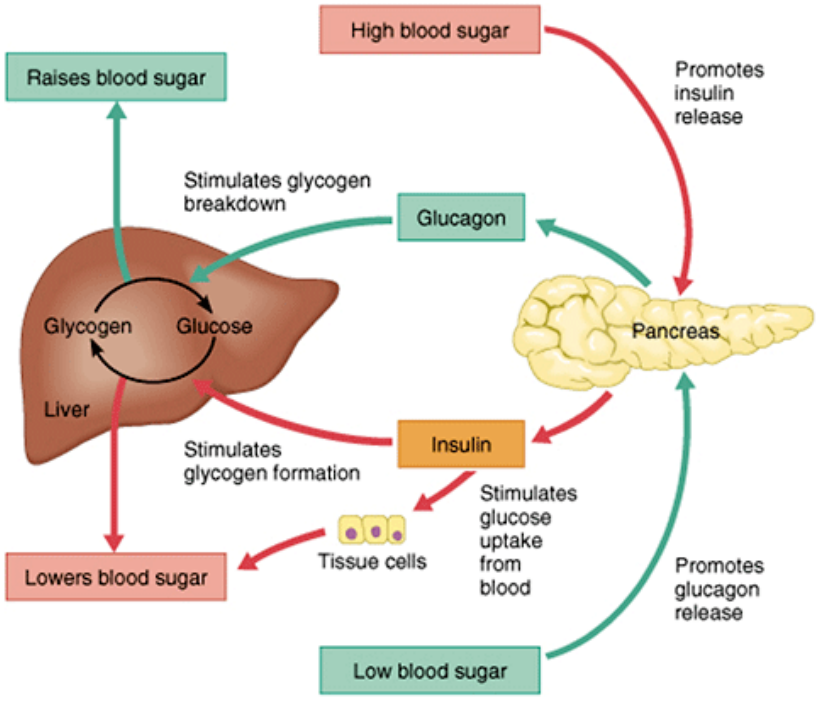

Figure 1 Complementary roles of insulin

Source: https://www.atrainceu.com/content/4-regulation-blood-glucose

Classification of Diabetic Mellitus

The World Health Organization (WHO) reported on the widely accepted and globally adopted classification of diabetes. There are two main types of DM: insulin-dependent diabetes mellitus (IDDM), or Type 1, and non-insulin-dependent diabetes mellitus (NIDDM), or Type 2, as shown in Figure 2 [42]. In another category, a degree of hyperglycemia is sufficient to cause pathological and functional changes in several target tissues, but clinical symptoms may present for a long-time before the detection of DM. During this asymptomatic period, it is possible to demonstrate an abnormality in carbohydrate metabolism by measuring glucose plasma in the fasting state or after a challenge with an oral glucose load or by A1C. The degree of hyperglycemia can be changed over time according to the extent of the emphasizing disease process [43]. Both types of DM are chronic diseases affecting the regulation of blood sugar or glucose. Although Type 1 and Type 2 DM have things in common, there are many differences. Type 1 affects 8% of people who account for DM, while Type 2 diabetes affects about 90%.

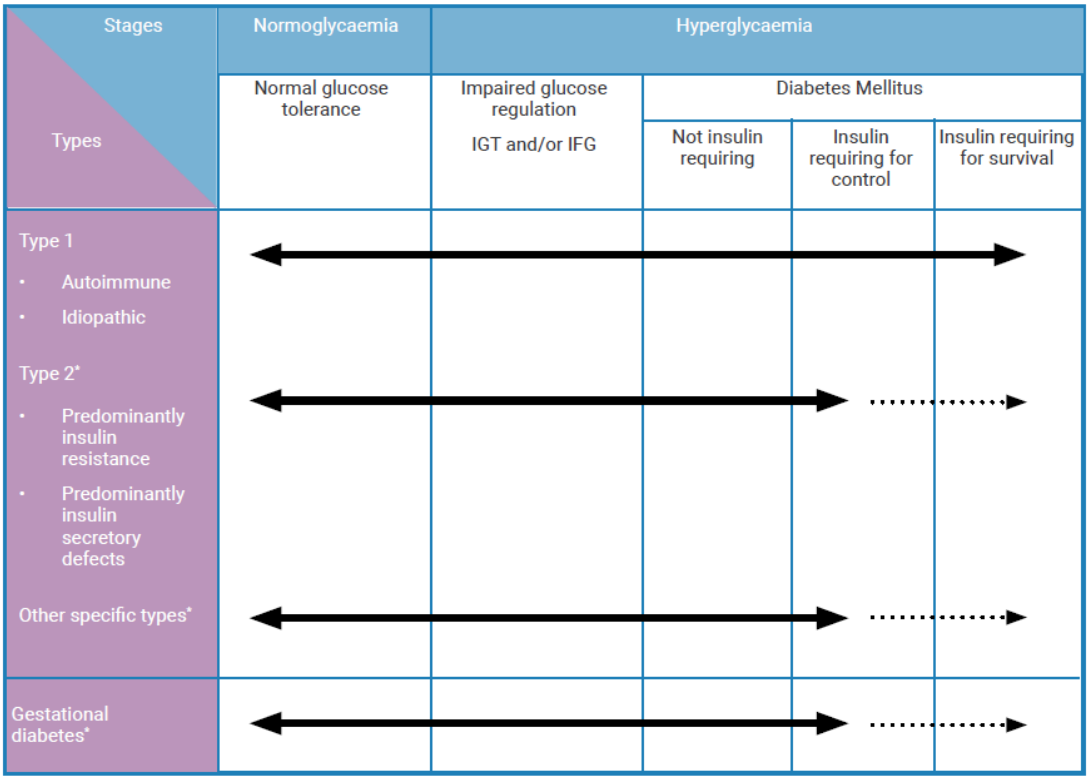

Figure 2 Disorders of glycemia: etiologic types and stages

Source: [35]

Type 1 Diabetes

Type 1 diabetes is also called IDDM. It used to be called juvenile-onset diabetes because it is usually diagnosed in children, teens, and young adults, but it can further develop at any age. IDDM is an auto-immune condition. In this type, the pancreas, a large gland secreting the insulin, stops the action to secret insulin due to the destruction of β-cells, producing the insulin by the body's immune system as antibodies (Figure 3). The rate of β-cell destruction is rapid in some individuals and slow in others [44]. Without insulin, the cells cannot uptake glucose (sugar) as energy. People with type 1 DM depend on insulin every day of their lives, replacing insulin. They have to test their blood glucose levels several times throughout the day. People who get Type 1 DM are diagnosed if they meet one of the following criteria:

Glycated hemoglobin A1C (HbA1c) test

This blood test indicates the average blood sugar level for the past two to three months. It measures the percentage of blood sugar attached to the oxygen-carrying protein in red blood cells (hemoglobin). The higher blood sugar levels, the more hemoglobin means that have sugar attached. An A1C level of 6.5 percent or higher on two tests indicates diabetes. If the A1C test is not available, or when people have certain conditions that can make the A1C test inaccurate - such as pregnancy or an uncommon form of hemoglobin (hemoglobin variant):

Random blood sugar test

A blood sample is taken randomly and may be confirmed by repeat testing. Blood sugar values are expressed in milligrams per deciliter (mg/dL) or millimoles per liter (mmol/L). Regardless of when the last meal is, a random blood sugar level of 200 mg/dL (11.1 mmol/L) or higher implies diabetes, especially when coupled with any of the signs and symptoms of diabetes, such as frequent urination and extreme thirst.

Fasting blood sugar test

A blood sample is taken after an overnight fast. A fasting blood sugar level of less than 100 mg/dL (5.6 mmol/L) is normal. A fasting blood sugar level from 100 to 125 mg/dL (5.6 to 6.9 mmol/L) is considered pre-diabetes. If it is more than 126 mg/dL (7 mmol/L) or higher on two separate tests, it means that it has gotten diabetes.

Without insulin, the body burns its fats as a substitute which releases chemical substances into the bloodstream. Without ongoing insulin injections, dangerous chemical substances accumulate and might be life-threatening, known as ketoacidosis. Many of the health problems that become further with Type 1 cause damage to tiny blood vessels in your eyes (called diabetic retinopathy), nerves (diabetic neuropathy), and kidneys (diabetic nephropathy). People with type 1 also have a higher risk of heart disease and stroke [45, 46].

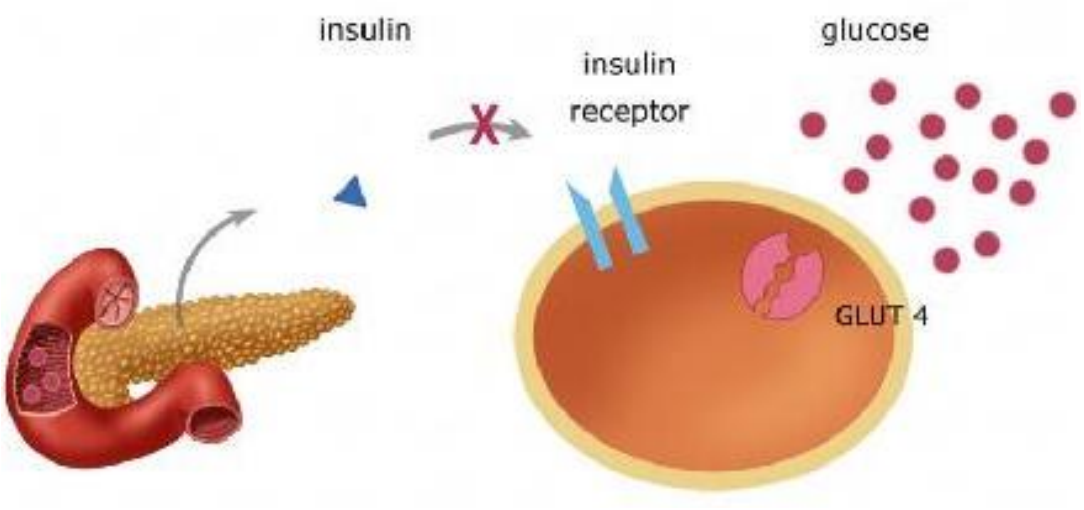

Figure 3 Type 1 diabetes mellitus: Insufficient insulin
Source:https://www.sciencesource.com/Doc/TR1_WATERMARKED/4/9/8/0/SS2573637.jpg?d6364
2786195

Type 2 Diabetes

Type 2 diabetes mellitus used to be called NIDDM or adult-onset diabetes. About 90-95% of people with diabetes have type 2 [47]. Most people with Type 2 DM are overweight or obese, which either causes or aggravates insulin resistance [48]. In this type, the cells do not react to insulin appropriately as they should, called insulin resistance (Figure 4). Firstly, the pancreas secrets typically more insulin uptake glucose into target cells where the insulin is increasingly ineffective at managing the blood glucose levels. As a result of this insulin resistance, the pancreas produces more and greater amounts of insulin to try and achieve some degree of management of the blood glucose levels as insulin overproduction. Eventually, the cells cannot uptake the glucose suitably, resulting in glucose building up in the bloodstream [49]. In this situation, they have lost 50 – 70% of their insulin-producing cells, meaning that Type 2 DM is a combination of ineffective and insufficient insulin. NIDDM can be referred to as the ongoing destruction of insulin-producing cells in the pancreas.

While people may have a strong genetic disposition toward Type 2 DM, the risk is significantly increased when people have some modifiable lifestyle factors, including high blood pressure, overweight or obesity, insufficient physical activity, poor diet, and the classic 'apple shape' body where extra weight is carried around the waist. Initially, Type 2 DM can often be managed with healthy eating and regular physical activity. While there is currently no cure for Type 2 diabetes, the condition can be managed through lifestyle modifications and medication. Type 2 diabetes is progressive and needs to be managed effectively to prevent complications. Type 2 diabetes is usually diagnosed using the following:

Glycated hemoglobin (HbA1C) test

This blood test indicates the average blood sugar level for the past two to three months. Normal levels are below 5.7 percent, and a result between 5.7 and 6.4 percent is considered prediabetes. An A1C level of 6.5 percent or higher on two separate tests means you have diabetes. If the A1C test isn't available, or when people have certain conditions - such as a distinctive form of hemoglobin (known as a hemoglobin variant) - that interfere with the A1C test, the physician may use the following tests to diagnose diabetes:

Random blood sugar test

Blood sugar values are expressed in milligrams per deciliter (mg/dL) or millimoles per liter (mmol/L). Regardless of when the last meal is, a blood sample showing a blood sugar level of 200 mg/dL (11.1 mmol/L) or higher suggests diabetes, especially if people also have signs and symptoms of diabetes, such as frequent urination and extreme thirst.

Fasting blood sugar test

A blood sample is taken after an overnight fast. A reading of less than 100 mg/dL (5.6 mmol/L) is normal. A level from 100 to 125 mg/dL (5.6 to 6.9 mmol/L) is considered prediabetes. If the fasting blood sugar is 126 mg/dL (7 mmol/L) or higher on two separate tests, which means that having diabetes.

Oral glucose tolerance test

This test is less commonly used than the others, except during pregnancy. People need to fast overnight and drink a sugary liquid at the doctor's office. Blood sugar levels are tested

periodically for the next two hours. A blood sugar level less than 140 mg/dL (7.8 mmol/L) is normal. A reading between 140 and 199 mg/dL (7.8 mmol/L and 11.0 mmol/L) indicates prediabetes. A reading of 200 mg/dL (11.1 mmol/L) or higher after two hours suggests diabetes.

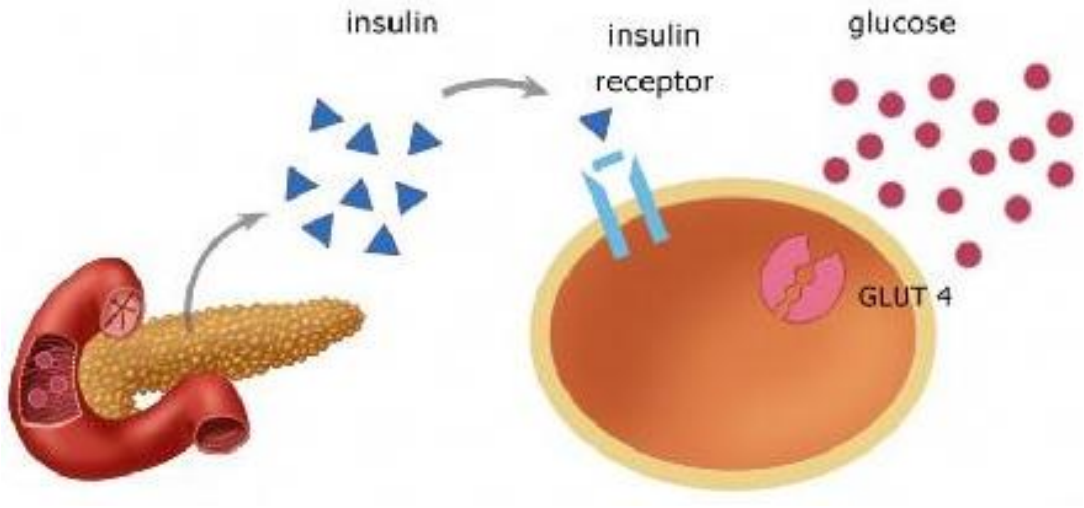

Figure 4 Type 2 diabetes mellitus: Insulin resistance
Source:https://www.sciencesource.com/Doc/TR1_WATERMARKED/4/9/8/0/SS2573637.jpg?d6364 2786195

Management of Diabetic Mellitus

Unlike many health conditions, diabetes is managed mostly by own patients, with support from your health care team (including your primary care doctor, foot doctor, dentist, eye doctor, registered dietitian nutritionist, diabetes educator, and pharmacist), family, teachers, and other important people in their life. Managing diabetes can be challenging. In type 1 DM, the patients need to take insulin shots (or wear an insulin pump) every day to manage the blood sugar levels and get the energy the body needs. Insulin cannot be taken as a pill because the acid in their stomach would destroy it before it could get into the bloodstream. DM patients need to check their blood sugar regularly and keep their blood sugar levels as close to the target as possible, which helps to prevent or delay diabetes-related complications. Stress is a part of life that makes managing diabetes harder, including controlling the blood sugar levels and dealing with daily diabetes care. Regular physical activity, getting enough sleep, and relaxation exercises can help. Healthy lifestyle habits are essential, including healthy food choices, being physically active, and controlling your blood pressure and cholesterol (Figure 5). Whether you just got diagnosed with Type 1 diabetes or have had it for some time, meeting with a diabetes educator is a great way to get support and guidance, including healthy eating and activity plan,

test the blood sugar and keep a record of the results, recognize the signs of high or low blood sugar, give insulin by syringe, pen, or pump, monitor your feet, skin, and eyes to catch problems early, manage stress and deal with daily diabetes care [50, 51].

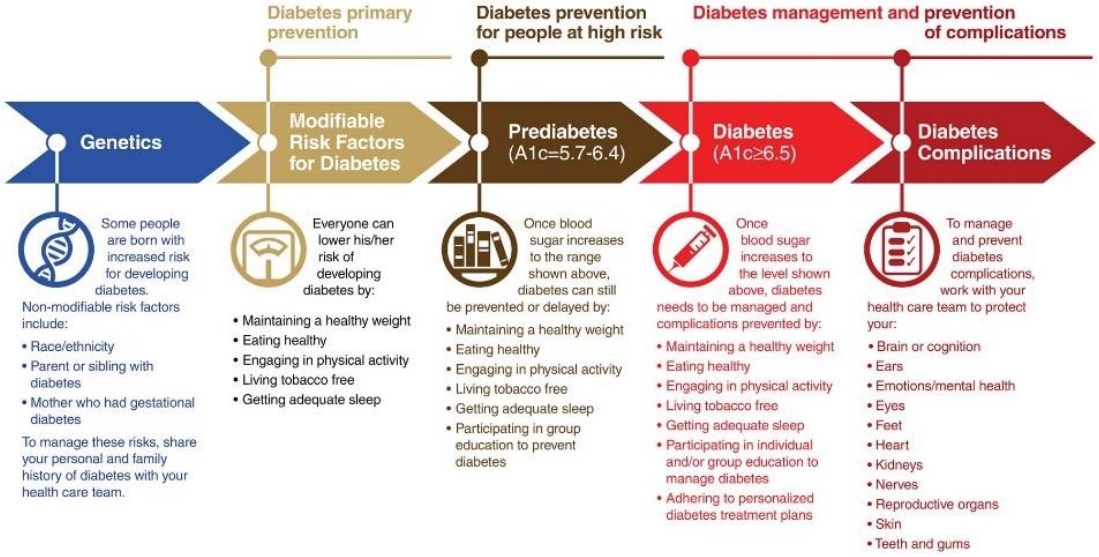

Figure 5 Guidance on how individuals can prevent and manage the disease
Source:https://www.diabetesnc.com/wpcontent/themes/dnc/assets/images/DiabetesGuide_Graphic-1800.jpg

The prevalence of Diabetic Foot Ulcers

The effects of diabetes extend further from individual to families and societies. It has broad socio-economic consequences and threatens national productivity and economies, especially in low- and middle-income countries where other diseases often accompany diabetes. The global prevalence of diabetes and impaired glucose tolerance in adults has been increasing over recent decades. International Diabetes Federation estimated that approximately 436 million of adults (20-64 years) have diabetes in 2019. In 2045, this will rise to 700 million people living with the disease, as shown in Figure 6 [1]. And 15-25% of DM patients can develop diabetic foot ulceration (DFU) [3].

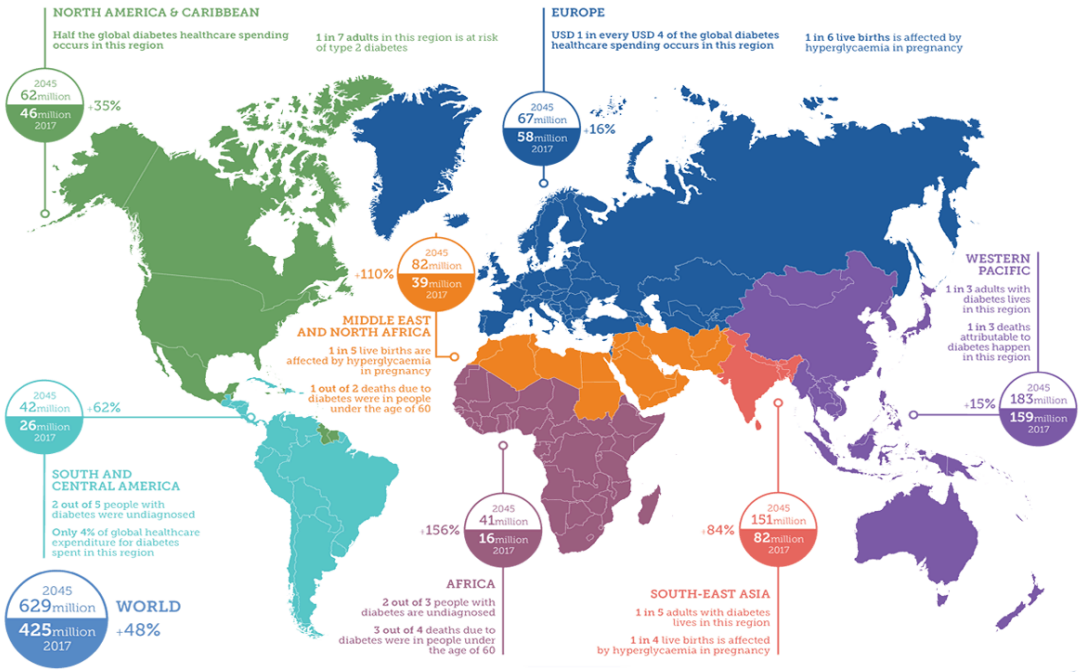

Figure 6 Number of people with diabetes worldwide and per IDF Region

Source: [52]

Diabetic foot is one of the most considerable and disastrous complications of DM. It is defined as a foot affected by ulceration related to neuropathy, vasculopathy, and immunopathy of the lower limb in a DM patient [4, 5]. Typically, the amputations of non-traumatic lower extremities happen frequently at a rate in those with diabetes as compared to other concurrent medical illnesses. The prevalence of DFUs in the DM population is 4–10%; the condition is higher in aged people. Approximately 5% of all DM patients show a record of foot ulceration, and this complication is 15% of the lifetime risk of DM patients [53, 54]. Amputations of lower extremities have constant effects on the quality of a person's life, which are related to the increasing health care costs and the elevation of the mortality risk. With the increase of individuals in the diabetes population, the number of individuals with higher lower extremity amputation [55]. Foot ulcers are the main hazard factor for the amputation case in DM patients and are regularly characterized by neuropathy, vasculopathy, or a combination of both. Nevertheless, neuropathy might be the cause of amputations in people with diabetes as well. One of the most failure outcomes and concerns for DM patients with DFUs is amputation.

Pathophysiology of diabetic foot ulcers

The patients with DM have impaired wound healing and tend to be foot ulcers, causing many severe factors, including neuropathy, ischemia, and infection. These hazards result in dangerously

chronic wound healing due to the detriment of nerves and vascular, resulting in loss of sensation on the feet [5]. Foot infection and osteomyelitis are the primary factors for the hospitalization of chronic DFUs [56]. Thus, the wound healing process may be distinct compared to non-diabetic individuals. The incident of DFU patients has the confederacy of three major factors: the degeneration of peripheral nerves leading to the deformity of the fingers and feet shape, obstruction of peripheral arteriosclerosis, and microbial infection as follows (Figure 7).

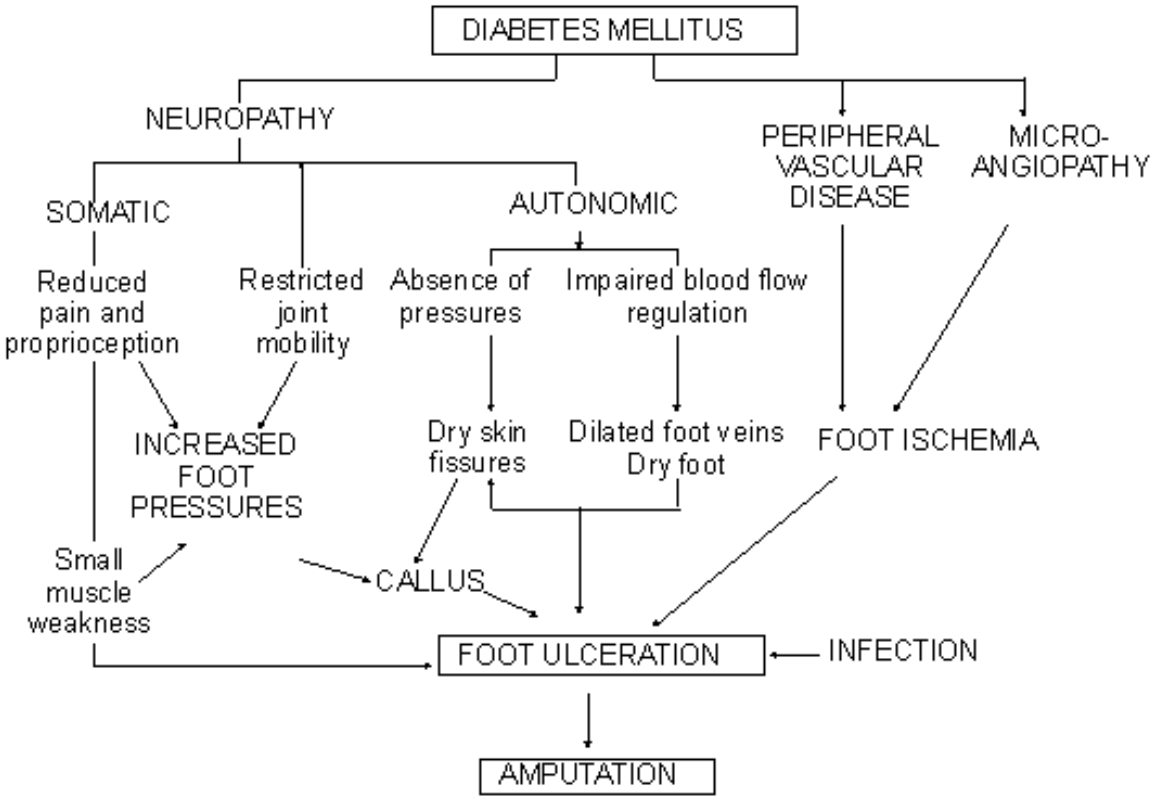

Figure 7 Development of ulcers in diabetic foot

Source: [57]

Neuropathy/peripheral neuropathy

Neuropathic ulcers are generally classified by foot deformity, high foot pressures, reduced padding of soft tissue, unassisted or unremarked trauma, and gradual tissue damage [58]. Tissue breakdown happens, resulting in ulceration and becomes chronic as the unsympathetic foot fails to conduct nociceptive stimulus, which is significant to stimulate preventive behavior. Peripheral neuropathy in DM patients is regularly located on pressure points, including the heel, head of the metatarsal bone, tip, and back of toes. This incident can initially provoke sensory, motor, and autonomic nervous systems, respectively (Figure 8).

Sensory neuropathy

Neuropathy of peripheral lower extremities is characterized by sensory, motor, and autonomic peripheral neuropathy, respectively [59]. The primary indication for sensory neuropathy is attenuation or lack of vibration sense (pallhypaesthesia), superficial sensitivity (pressure, touch), and subjective paraesthesia. Especially stress is known as "burning feet syndrome". It commonly occurs at night and is associated with a high pain sensation [60]. The decreased pain sensation is a result of chronic sensory neuropathy [61]. Therefore, the hazard of trauma is greater significant. Because of the loss of pain symptomatology, severe ulcerations are underrated by both physicians and DM patients [62]. Subsequently, injuries are barely noticed for a long time. In major cases, sensory neuropathy is associated with the reduced perception of temperature. The loss of sensation is typical of a peripheral, sock-like, symmetrical nature. This condition usually begins symmetrically. Dysfunction of muscle affects the ordinary neuropathy. Deterioration of the anterior muscular group of the lower extremity manifests the strain throughout the rollover procedure, causing high pressure on the forefoot.

Three complications occur from the loss of sensitivity:

- Steady pressure for a long time may convey to local ischemic necrosis (e.g., in the absence of pain when wearing tight footwear)
- High pressure in the short term leads to instantaneous damages. Objects with a small surface can cause direct mechanical damage.
- Repetitive modest pressure affects inflammatory autolysis of tissue. Continuous pressure on inflamed or structurally involved tissue provokes the development of ulcerations. Moreover, gangrene can occur from burns and inappropriate use of disinfection products.

Motor neuropathy

The deterioration of small foot muscles is affected by the malposition of toes (claw toe) in motoric neuropathy, including the observation of a loss of muscle self-reflexes and motor paresis. Uppermost, motor neuropathy can be defined as loss of Achilles tendon reflex, which is an early signal [59, 63]. Sensory and motor peripheral neuropathy results in an inequitable foot load associated with an unsafe walk. Over time, hyperkeratosis generates neuropathy and raises plantar loading pressure.

Autonomous neuropathy

Peripheral autonomic neuropathy occurs via vasomotor paresis, resulting in the subcutaneous vascular network in arteriovenous shunts. Furthermore, autonomic neuropathy affects the secretion of sweat, becoming dysfunctional. The increased blood perfusion of deeper skin layers results in overheating skin. Also, the absence of humidification and cooling by evaporation results from dysfunctional sweating. As a result, foot skin dries out of the described factor, leading to a reduced protective skin function and increased risk of injury. Additionally, as a result of autonomic neuropathy, medial arterial sclerosis, Charcot's foot (diabetic osteoarthropathy), neuropathic oedemas as well as alterations of skin thickness arise [59, 64]. About 40% of DM patients occur stiffness of the wrist and foot joint caused by neuropathy, non-enzymatic glycosylation, and cross-link formation of ECM impair viscoelastic foot functioning.

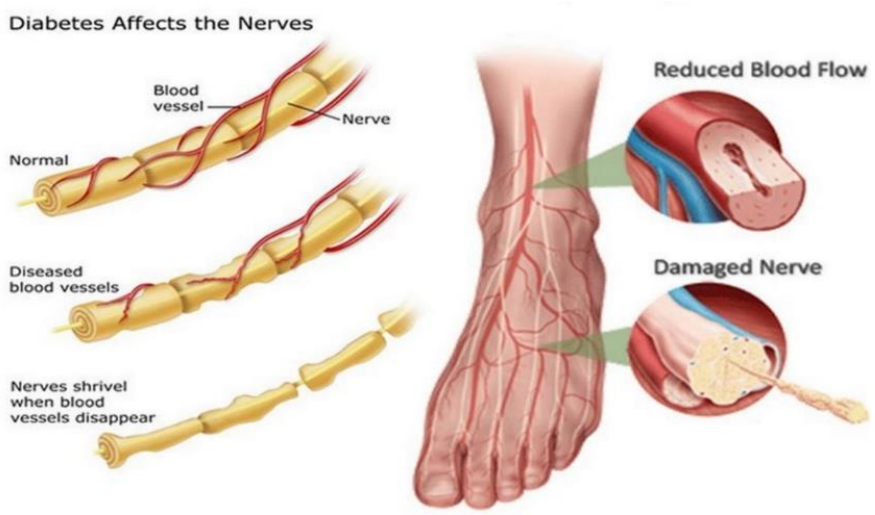

Figure 8 Neuropathy of peripheral lower extremities
Source:http://www.thailandmedical.news/uploads/editor/files/Diabetic-Neuripathy.jpg

Peripheral vascular disease

Peripheral artery disordered (PAD) is the one major cause of atherosclerosis at the lower extremity arteries. It is also involved with atherothrombosis, another vascular bed, including the cardiovascular and cerebrovascular systems (Figure 9). Additionally, PAD displays considerably over a long period of disability in DM patients, as well as expedites of the pathway, affects to greater sensible to ischemic incidence and absences the functional condition as compared to regular patients [65, 66]. Therefore, PAD patients can be treated expensively due to the need for individual diagnostic tests, therapeutic procedures, and hospitalizations.

The development of atherosclerosis is directly caused by malfunctioning metabolic events associated with DM conditions. Besides these conditions, pro-atherogenic changes include increases in vascular inflammation, and alterations in multiple cell types were involved as well [67]. Another risk factor that is determined for the development of atherosclerosis is inflammation. The development of PAD is significantly related to increased C-reactive protein (CRP) levels. Moreover, in impaired glucose tolerance patients, CRP levels are usually declining [68].

C-reactive protein is important as the procoagulant ability associated with its effects to stimulate the tissue factor expression. Additionally, increased levels of CRP imply a risk factor for PAD, a marker of atherosclerosis (Cermak et al., 1993). The endothelial cell is also interrupted with nitric oxide (NO) synthase, which causes vascular tone malfunction and elevated plasminogen activator inhibitor-1 production, which hinders the fibrinolytic plasmin formation of plasminogen [69].

Diabetes patients with the peripheral arterial disease are impacted severely by their quality of life and are related to considerable functional ulceration [66]. The progressive malfunction and long period of disability may result from reduced walking speed and distance participatory with irregular claudication. The development of critical limb ischemia (CLI) with more severe disease causes ischemic foot ulceration and risk of extremity loss. Notably, patients with the risk of fatal and non-fatal cardiovascular and cerebrovascular events may significantly increase PAD, including myocardial infarction (MI) and stroke [70, 71].

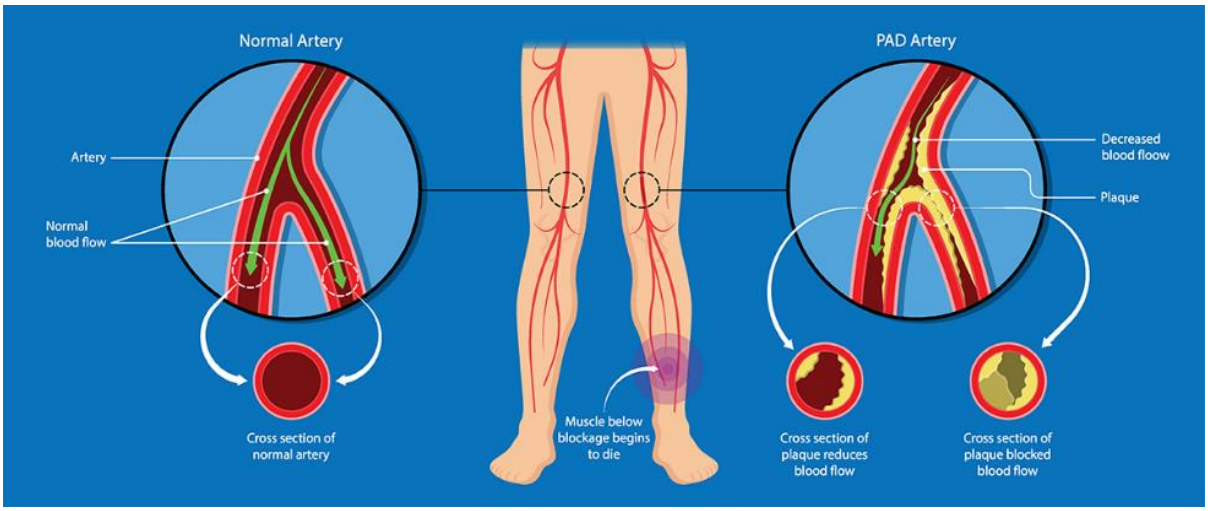

Figure 9 Peripheral arterial disease
Source:https://cdn.shortpixel.ai/client/to_webp,q_lossless,ret_img,w_1200/https://apprhs.org/wp-content/uploads/2019/05/Illustration_Peripheral_Arterial_Disease.png

Infection

Typically, immunopathy has been identified in the patient with diabetes, which is sensible to infection, and a typical inflammatory response can occur. The secondary defenses of an impaired host to hyperglycemia include the defects in functional leukocytes and the change of macrophage morphology. In diabetes patients, the leukocyte phagocytosis remarkably declines, and improvement of bactericidal levels is directly associated with hyperglycemic correction [72]. Reduction of growth factors and cytokines chemotaxis, accompanied by excessive metalloproteinases, interrupts normal wound healing by establishing an inflammatory phase over a long period. Gluconeogenesis from protein breakdown impacts negative nitrogen balance, resulting in secondary insulin deprivation. The impaired metabolism affects the synthesis of proteins, collagen and fibroblast functions, and systemic insufficiency are spread leading to the compromise of nutrition [73]. The diabetic patients' potential for infection tolerance is defective, and infection severely impacts the control of the diabetic condition. This repetitive circumstance causes an uncontrolled hyperglycemic state, also resulting in the host's response to infection.

The activity of macrophages was hindered in the inflammation phase as the cellular pathway [74, 75]. These events, including inflammatory cells, abnormality of cellular growth, and migration of the epidermis at the wound edge, are associated with localization or occlusion of the blood vessels within the edge of the wound caused by the chronic inflammatory process [76]. In a diabetic patient, the impairment of leucocyte function and the abnormalities of metabolic diabetes result in insufficient neutrophils and macrophages migration to the wound together with the reduction of leucocytes chemotaxis (Figure 10) [77]. Such increased risk of wound infection may result from the change in molecular level individuals.

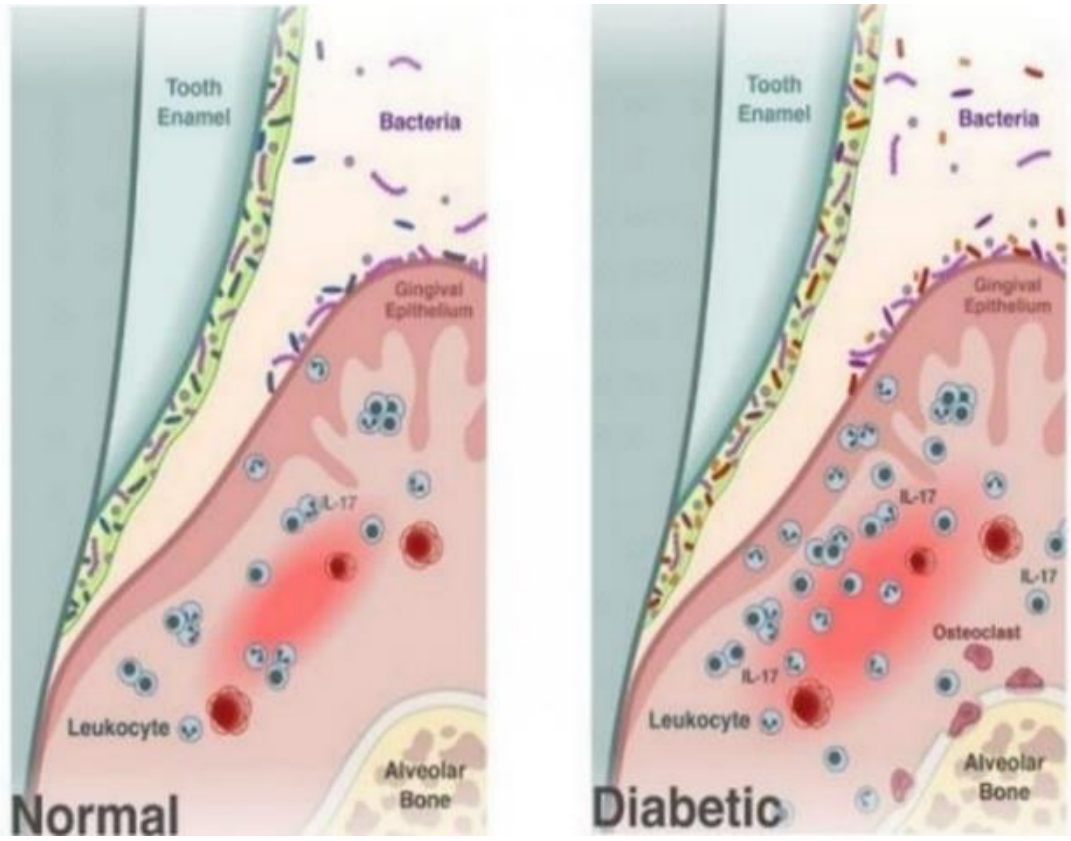

Figure 10 Impairment of leucocyte function and the abnormalities of metabolic diabetes
Source:https://www.infectioncontroltoday.com/sites/default/files/422391c4089a499aa8bebf316a13eb02.jpg

Classification of diabetic foot infections

Various categorization systems have been suggested and are utilized to determine DFU and DFI. Usually, systems engage a matrix of grades based upon the wound depth and size. Important parameters have been involved with only a few classification systems, including the presence of neuropathy and severity of the infection.

The broadest grading system for DFU is Wagner's classification, comprising six pathologic wound grades used to evaluate the depth of ulcer (grades 0-5) (Table 1). Nevertheless, this category is restrictive by the disability to notice vasculopathy and infection, an independent risk complemented in all classification grades. For instance, this system only predicates the most severe diagnosis of peripheral vascular disease in grades 4 and 5, not to clarify about more precise pathological of vasculopathy. Likewise, only grade 3 approaches the occurrence of infection and osteomyelitis, restricted to only wound depth.

Table 1 Wagner classification system

Grade	Pathology
0	Pre-ulcerative area without open lesion
1	Superficial ulcer (partial/full thickness)
2	Ulcer deep to tendon, capsule, bone
3	Stage 2 with abscess, osteomyelitis, or joint sepsis
4	Localized gangrene
5	Global foot gangrene

Source: Adapted from Wagner [78]

Normal and pathological responses to wound healing

In our body, there is one of two mechanisms, including regeneration or repair, that all tissues are proficient in the healing process. Regeneration is the restoration of the tissue to its original cellular and extracellular structure. It causes the new growth of the tissue, occurring through the proliferation of the cells of the tissue which establishes a scar and is more restricted than repair processing. The occurrence of complete regeneration is limited by several cells, such as epithelial, liver, and nerve cells. The physiology of wound healing can be clarified as the body inherits and reconstructs the function of damaged tissues [79]. Repair is the formation of scar tissue. Scar tissue is not identical to any tissue in the body which is the mechanism of the re-established equivalence between scar formation and scar remodeling, which is the response of the human body experience following injury. When the appearance of the wound healing process attempting to be maximum ability, the rearrangement of a promotional microenvironment is considerable to the utmost importance at the wound surface. Additionally, the primary aim of wound management is to support the complicated molecular pathway occurring in wound healing by maintaining a controlled set of local conditions.

Usually, the acute wound healing process is a systemically and proficient feature characterized by four distinct overlapping phases, including hemostasis, inflammation, proliferation, and remodeling, respectively (Figure 11). Moreover, pathologic responses can be considerably determined by characteristic biologic markers ensue in fibrosis and chronic wounds (Diegelmann & Evans, 2004; Reinke & Sorg, 2012). Table 2 demonstrates the biological growth factors and cytokines associated with acute wound healing.

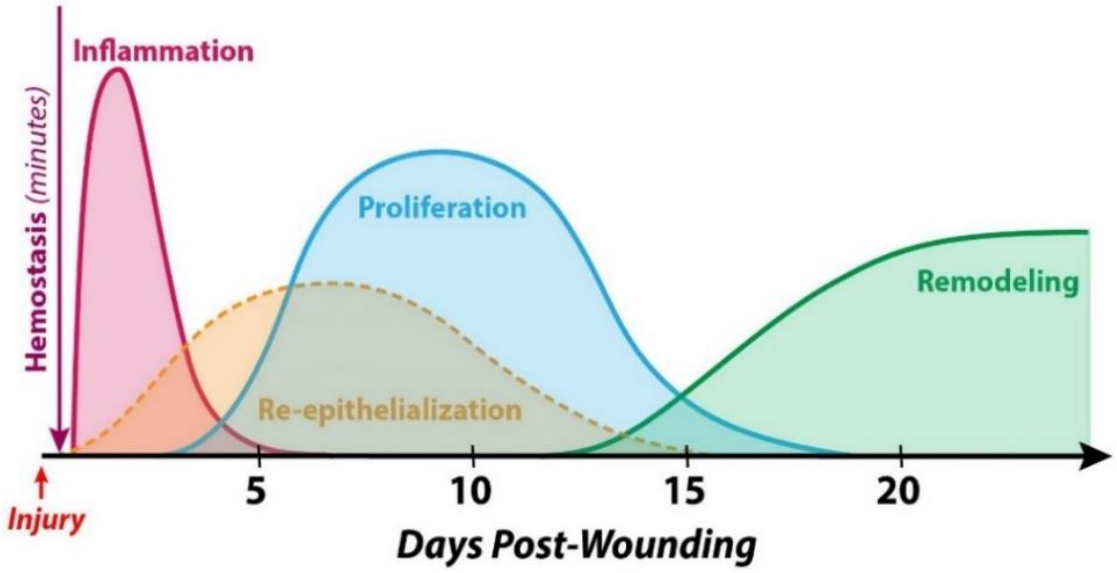

Figure 11 Sequential illustration of the stages involved in tissue repair

Source: [80]

Table 2 Growth factors in wound healing

Growth factor	Source	Wound healing-related functions
PDGF	Platelets, macrophages, endothelial cells, injured cells	Chemotaxis, fibroblast proliferation, collagenase production
TGF-β	Macrophages, platelets, neutrophils, lymphocytes, fibroblasts, epithelial and endothelial cells, injured cells	Chemotaxis, fibroblast proliferation, collagen metabolism
EGF	Macrophages, platelets, plasma, epithelial cells	Epithelial cells proliferation, granulation tissue formation
TGF-α	Activated macrophages, platelets, injured cells, epithelial cells	Epithelial cells proliferation, granulation tissue formation
KGF	Fibroblasts	Endothelial cells proliferation
IL-1	Macrophages	Fibroblast proliferation
FGF	Macrophages, fibroblasts, pituitary, endothelial cells	Fibroblast proliferation, matrix deposition, wound contraction angiogenesis
TNF-α	Macrophages, T lymphocytes	Fibroblast proliferation
IGF-1	Plasma, liver, fibroblasts	Synthesis of sulfated proteoglycans and collagen, fibroblast proliferation
IFNs	Lymphocyte, fibroblasts	Inhibition of fibroblast proliferation and collagen synthesis

Source: [81]

Hemostasis phase

Hemostasis is described as a phase of coagulation manifested promptly after wound damage (Figure 12). The primary purposes of these pathways are to prevent exsanguination accompanied by the protection of vascularization, to maintain it intact, to remain the function of the vital organs despite the injury, and to provide a matrix for invasive cells that are necessary for the afterward healing phases [82]. A dynamic equilibrium of endothelial cells, thrombocytes, coagulation, and fibrinolysis manifests in the hemostasis phase. It establishes the amount of fibrin deposited at the wound edge, thus stimulating the progression of the regenerative pathways.

In this phase, it is considered to establish the inflammatory process, known as the lag phase, which involves the recruitment of many cells and related growth factors as well as cytokines to manipulate the wound healing process [83]. The initiated clotting pathways are ensured by clotting factors from the aggregation of activated thrombocytes by which reveal collagen (intrinsic system) coupled with the skin damaged (extrinsic system). At that moment, the injured vessels follow vasoconstriction, triggered by the platelets, to reduce blood loss and fill the tissue gap with a blood clot comprised of cytokines and growth factors [84]. Accordingly, these components, including fibrin molecules, fibronectin, vitronectin, and thrombospondins which are contained in the blood clot, associate to establish the structural scaffold as a temporary matrix for the migration of leukocytes, keratinocytes, fibroblasts, and endothelial cells and as a reservoir of cytokines to the wound sites. The clot formation coupled with vasoconstriction, results in a failure of local perfusion with a coherent absence of oxygen, increasing glycolysis, and changing of blood pH, sequent followed by thrombocytes migration to the provisional wound matrix which ensues vasodilation [83]. Furthermore, the release of chemotactic factors is stimulated by the infiltration of leukocytes activated from platelets. Platelets and leukocytes play a vital role to release the related growth factors and cytokines for activation of the inflammatory pathways (IL-1α, IL 1β, IL-6, and TNF-α), provoke the synthesis of collagen (FGF-2, IGF-1, TGF-β), stimulate the differentiation of fibroblasts to myofibroblasts (TGF-β), initiate the angiogenesis (FGF-2, VEGF-A, HIF-1, TGF-β) and contribute the re-epithelialization process (EGF, FGF-2, IGF-1, TGF- β). A local redness (hyperemia) and an edema can be considerable as the vasodilation of the wound.

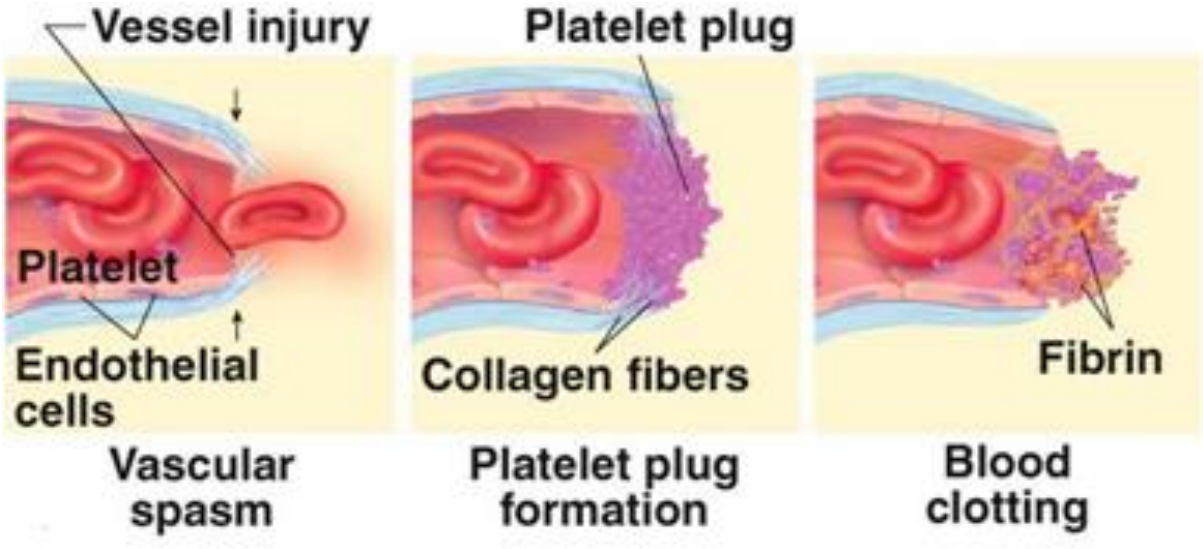

Figure 12 Hemostasis, phase of coagulation manifested promptly after wound damages
Source: http://physiologyplus.com/describe-the-three-steps-of-hemostasis/

Inflammation phase

The cellular inflammatory phase aims to provoke immune cells against invasive micro-organisms. There are two distinct phases, an early inflammatory phase and a late inflammatory phase [85]. During the hemostasis phase, the activation of the inflammatory phase is approximately divided into an early phase with the recruitment of neutrophils and a late phase with the appearance and transformation of monocytes (Figure 13). Recruitment of neutrophils is initiated to the damaged site. It occurs for 2-5 days unless the infection of the wound because of the response of the activated complement pathway, degranulated platelets, and bacterial degradation. After the injury, the neutrophils play an essential role within the first days due to the phagocytosis ability and secretion of protease, which destroy localized microbial and contribute to necrotic tissue degradation. Moreover, they are also chemoattractants for various cells associated with the inflammatory phase [86].

Therefore, these mediators, including TNF-α, IL-1α, and IL-6, are activated by neutrophils, augment the inflammatory response and trigger VEGF and IL-8 for a sufficient repairing response. Besides, debridement starts with the secretion of active antimicrobial substances, including cationic peptides, eicosanoids, and proteinases [86]. Macrophages occur in the wound and pursue the phagocytosis procession in the late inflammatory phase, 48–72 h after injury [85, 87]. These cells are known initially as blood monocytes sustaining phenotypic changes on advent into the wound to

become tissue macrophages. Chemoattractive agents, including clotting factors, complement components, cytokines such as Platelet-derived Growth Factor (PDGF), Transforming Growth Factor (TGF-β), leukotriene B4, and platelet factor IV, as well as elastin and collagen breakdown products attract to the wound site. Macrophages have a longer lifespan than neutrophils and continue to activate at a lower pH. These cells play a crucial role, including representation as key regulatory cells and offering a substantial reservoir of efficient tissue growth factors, especially TGF-β, as well as other mediators (TGF-α, heparin-binding epidermal growth factor, FGF, collagenase), stimulating keratinocytes, fibroblasts and endothelial cells for the late stages of the inflammatory response [79, 85, 88]. The severity of healing disruption is caused by the lack of monocytes and macrophages from the wound due to these events, including the low capacity of wound debridement, delay in fibroblast proliferation and maturation, as well as delay of angiogenesis which ensues the insufficient fibrosis, and a long-term weakly repaired wound [88]. Macrophages migrate into the damaged site and contribute to continuing the process by operating phagocytosis of pathogens and cell debris and by releasing growth factors, chemokines, and cytokines approximately 3 days after injury. Also, these molecules remain during the entire healing process, as some can stimulate the later phase of wound healing (proliferative phase) [89]. The inflammatory response to damaged wounds is fundamental for the provision of growth factor and cytokine signals which are accountable for cell and tissue repair pathway [86].

Lymphocytes are the last cells that infiltrate the wound site in the late inflammatory phase and are activated 72 h after injury by indicating interleukin-1 (IL-1), components, and immunoglobulin G (IgG) breakdown products [85, 90]. IL-1 is essential in regulating collagenase, which is further necessary for collagen remodeling, production of ECM components, and their degradation [85].

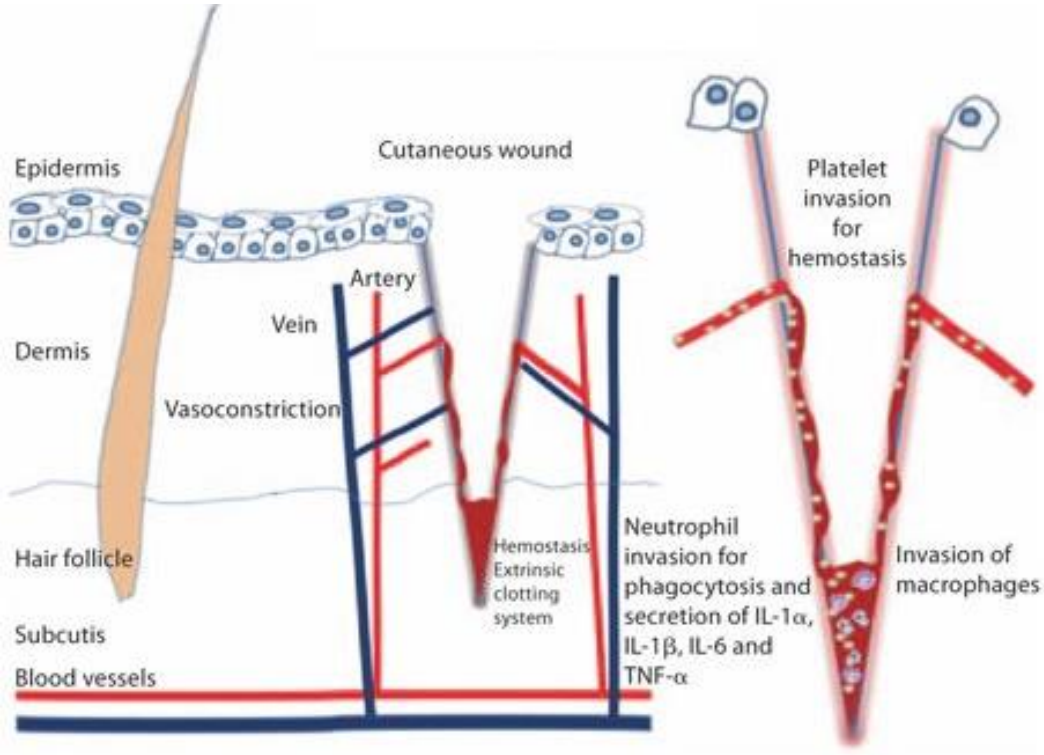

Figure 13 Inflammatory phase after a cutaneous cut; hemostasis and invasion of inflammatory cells Source: [89]

Proliferation phase

The proliferation phase begins on the third day after injury and continues approximately 2 weeks afterward. This phase can be classified by the fibroblast migration and newly synthesized ECM deposition, indicating a displacement for the fibrin and fibronectin as a provisional network. At the cellular level, there is a substantial establishing of granulation tissue in this phase of wound healing. Various processes explicate below in the proliferative phase [79, 91].

Fibroblast migration

The tissue is surrounded by fibroblasts and myofibroblasts triggered off the proliferation for the 3 days after wounding. The release of inflammatory cells and platelets attracts growth factors such as TGF-β and PDGF, leading fibroblasts and myofibroblasts to infiltrate the wound. Fibroblasts are the first arrival cells to the wound on the third day following the injury, requiring phenotypic modulation to accumulation. The advent of fibroblasts contributes to cell proliferation and generates the matrix proteins including hyaluronan, fibronectin, proteoglycans, and type 1 and 3 procollagen deposited in the local wound edge [83, 88]. The accumulation of plentiful ECM supports cell migration and is necessary for the regenerative process further by the end of the first week

[92]. At this moment, fibroblasts transform their phenotype to myofibroblasts which contain condensed actin bundles under the plasma membrane and proficiently develop pseudopodia, connecting to fibronectin and collagen in the ECM. Contraction of the wound is considered as an important state in the repair pathway contributing to close the wound edges. It happens as these cell expansions contract. The apoptosis process begins to eliminate redundant fibroblasts following accomplished this task [93].

Collagen synthesis

Collagens play a vital role as a component in all phases of wound healing. Fibroblasts synthesize collagen proteins, which provide integrity and strength to all tissues [93]. Collagens conduct as a provenance for the formation of an intracellular matrix in the wound. Usually, wound granulation tissue presents about 40% of type 3 collagen. On the other hand, the unwounded dermis consists of 80% type 1 and 25% type 3 collagen [83].

Angiogenesis and granulation tissue formation

The formation and modeling of new blood vessels are crucial and occur simultaneously throughout all phases of generative processing. In the hemostatic phase, the release of attracting neutrophils and macrophages, numerous angiogenic factors contribute to promoting angiogenesis [94]. Plenty of angiogenic factors including FGF, VEGF, PDGF, angiogenin, TGF-α, and TGF-β, are responded to inmate endothelial cells. The inhibitory factors act to balance, including angiostatin and steroids [95, 96]. On proliferating endothelial cells, both stimulatory and inhibitory agents keep balance directly and indirectly, following stimulating mitosis, activating locomotion, and promoting the release of endothelial growth factors by host cells [97]. Surrounding tissues release the molecules to promote proliferation and endothelial cell growth under hypoxia. A four-step process is happened by the reaction: (i) endothelial cells produce proteases for degradation of the basal lamina in the parent vessel to crawl through the ECM; (ii) chemotaxis; (iii) proliferation; and (iv) remodeling and differentiation. FGF and VEGF play essential regulatory roles in all processes [95-97]. Primarily, vascular cell supply absences in the center of the wound. Consequently, the wound margins limit the viable tissue perfused by undamaged vessels and by diffusion through the uninjured interstitium [79, 83].

Granulation Tissue Formation

The final state of the proliferation phase is the development of the acute granulation tissue (Figure 14). The remodeling phase is simultaneously initiated. The fibrin-fibronectin-based provisional wound matrix is taken the place of a transitional tissue, and a scar might be generated by maturation [83, 98]. Also, this stage can be featured by condensed fibroblasts, granulocytes, macrophages, capillaries, and loosely ordered collagen bundles. Because of the plenty of cellular components as granulation tissue, angiogenesis remains activated. This tissue comprises abundant vessels, which result in the appearance of redness and might be easily occurring trauma. Nevertheless, the dominating fibroblast still completes various actions, including collagen and ECM substance production (fibronectin, glycosaminoglycans (GAGs), proteoglycans, and hyaluronic acid). The formation of the ECM represents the provision of cell adhesion as a scaffold and seriously modulates and manifests the growth, movement, and differentiation of the cells [99]. Consequently, the fibroblast is the precursor of the temporary ECM, where the sequent migration of the cell followed by organization takes place. Finally, myofibroblast differentiation causes the reduction of adult fibroblasts, and then they are terminated by following apoptosis [100].

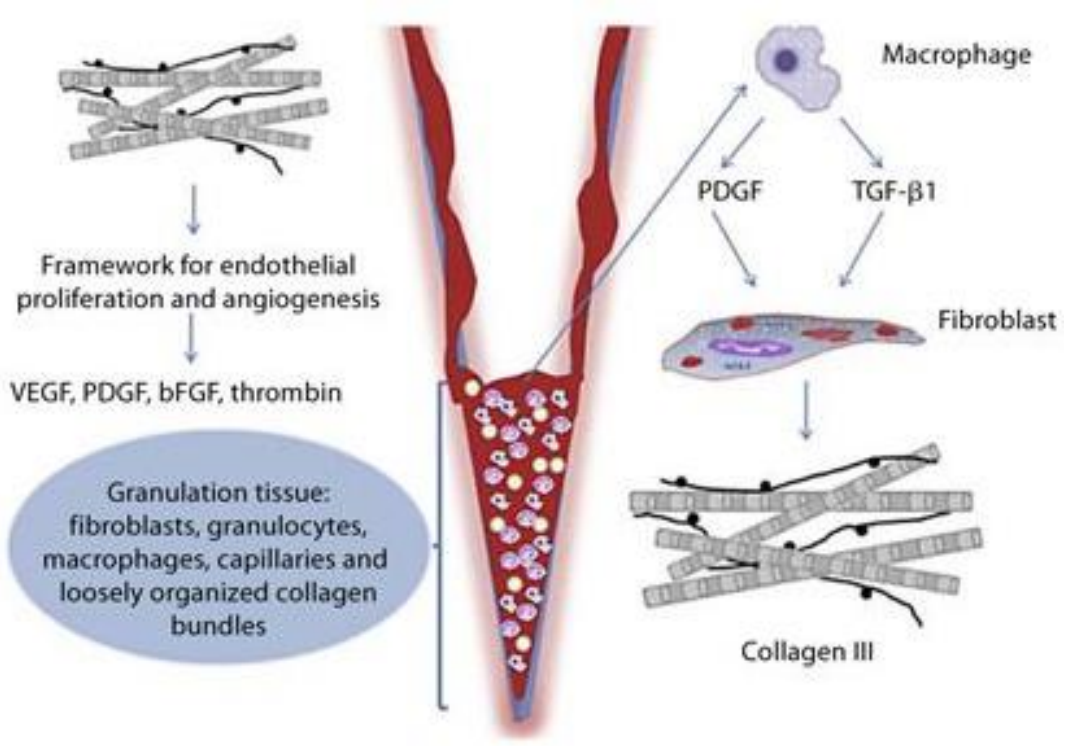

Figure 14 Proliferative phase; organization of the thrombus, secretion of growth factors, synthesis of collagen III, and the beginning of angiogenesis

Source: [89]

Remodeling

Remodeling is the final phase of the wound healing process and happens from day 21 up to at least 1 year following wounding. The apoptosis procedure affected to termination of the granulation tissue formation. Accordingly, a mature wound can be featured as avascular as well as acellular [101]. The change of ECM components encounters during the maturation of the wound. The stronger occurs in collagen type 3, produced in the proliferation phase (Figure 15). Collagen type I differs from the other basket-weave collagens since it is oriented in small parallel bundles. Following wound contractions of myofibroblasts ensue by their multiple attachments to collagen and contribute to reduce the complexion of the developing scar [102]. Moreover, the angiogenesis is diminished, affected by the decline of wound blood flow, and the metabolic activity in acute wound retards and finally stops.

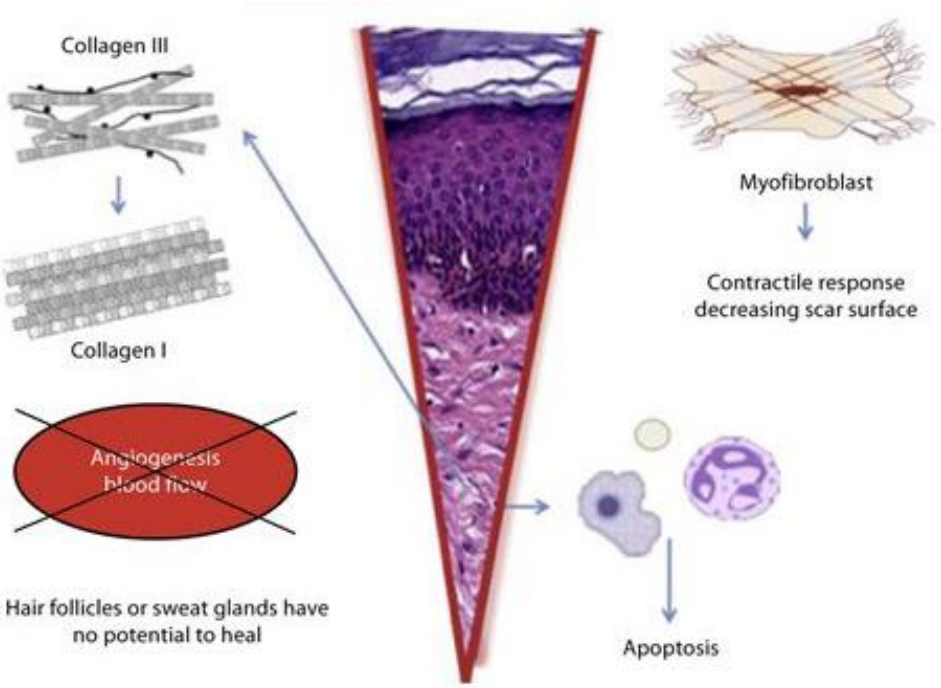

Figure 15 Remodeling phase; regenerative processes fade and are followed by a reorganization of the connective tissue and contractile response

Source: [89]

Delayed or chronic wound healing in diabetic foot ulcers

During the decades, the comprehension of the characteristics and role of diabetes at the molecular level has been widely studied in various fields. These studies indicated that the major issues caused by impaired wound healing in diabetics come from the malfunction of cellular expression and abnormality in released cytokines, growth factors and molecular factors involved in interrelating the normal wound

healing activity. The healing activity is interrupted by various factors. The inflammation and proliferation phase consumes longer, which cannot initiate the next phase. The management of the impaired diabetic wound has been studied to overcome these issues by various molecular factors/targets which directly or indirectly modulate their activity. The direct interaction targets are numerous growth factors (PDGF, TGF-α, EGF, VEGF, FGF, and KGF), keratinocytes or fibroblasts, and stem cells. The indirect target can be the up-/down-regulated expression of growth factors, pro-/anti- inflammatory macrophages, Matrix metalloproteases (MMPs), nitrous oxide level, collagen synthesis/degradation, and factors promoting angiogenesis depending on the specific target [103].

Any wound can be possible to occur the chronic or delayed wounds. In general, the chronic wound shared the similar characteristics are high level of protease, elevating inflammatory markers, low growth factor activity, and reducing cellular proliferation. The wound health society classified the chronic into 4 major categories: including pressure ulcers, venous ulcers, arterial insufficiency ulcers, and diabetic foot ulcers (Figure 16).

Figure 16 Classification of chronic wound; (A) venous ulcers (B) arterial insufficiency ulcers (C) diabetic foot ulcers (D) pressure ulcers

Source: [104]

The molecular level of delayed wound healing in diabetic foot ulcers

Diabetes mellitus is the critical factor that impairs each phase of the wound healing process, including hemostasis, inflammation, proliferation, and remodeling phase, which has a long-term adverse effect on the quality of life, morbidity, and mortality (Figure 16). Diabetic wounds can be considered as persistent acute wounds and chronic wounds revealing malfunctioning healing due to retardation, defective, or uncoordinated during healing activities. These wounds also indicate a prolonged inflammatory phase associated with an abnormality in the formation of mature granulation tissue and abatement in wound tensile strength [105]. This case is considerably different from other causes of altered tissue repair because of several factors causing an impairment. The number of patients with diabetes still exists, resulting in the magnification of the altered healing impact. The failures of the healing process which is ongoing normal condition coupled with approaching the inflammatory pathologic stage leading to the chronic wound healing. These factors affected to delay, incomplete, and irregularly proceed in a coordinated manner, following ensue as adverse anatomical and functional effects in the wound healing process [106]. Chronic wound healing is a condition that happens with patients who exert physiological failures in the healing process, including chemotherapy, steroid use, infection, and with immobile and debilitated patients. As a result, unusual infection leads to gangrene and/or amputation. The highest amputation rate results from patients with diabetes compared to any chronic wound. To clarify the consequence of this point, approximately 20% of hospitalizations for diabetes patients are constituted admissions for foot infections and up to 50% of all non-traumatic lower-extremity amputations. Harmful foot ulcerations occur in the lifetime expected of 25% of diabetes mellitus patients [107].

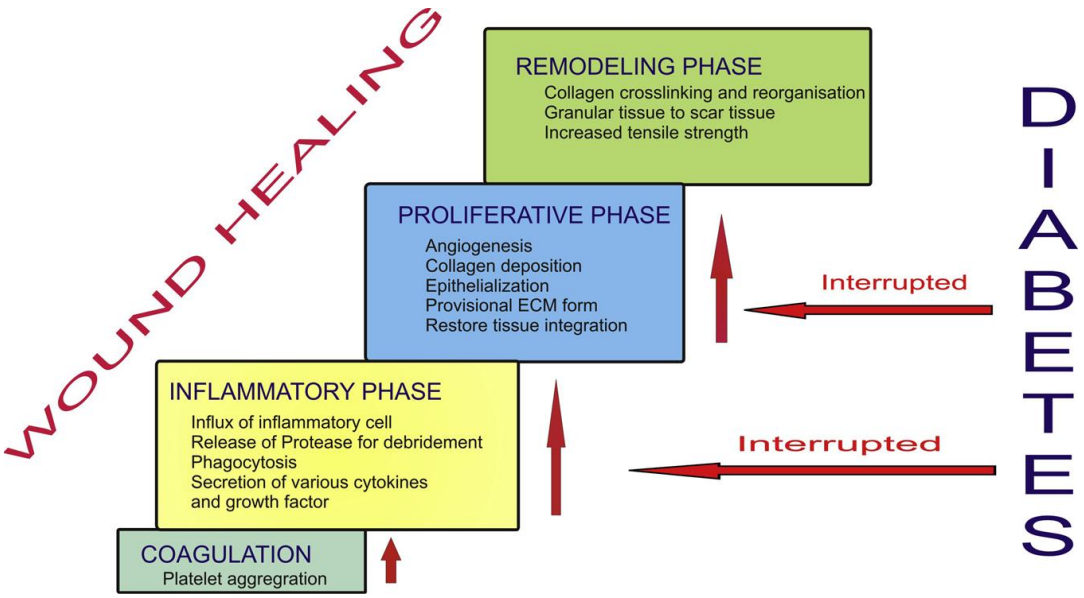

Figure 17 Interruption of the normal wound healing process in diabetes

Source: [103]

A chronic wound is an impaired healing wound. The dysfunction in diabetic wound healing was attributed to various alterations of the cellular and biochemical factors and activities. Several cell types related to wound healing include neutrophils, monocyte, macrophages, keratinocytes, fibroblasts, T cells, B cells, mast cells, and endothelial cells. These cells are proficiently associated with producing and regulating various cytokines and growth factors. Monocyte, which afterward becomes macrophages, plays an important role in producing the pro-inflammatory cytokines (IL-1β, TNF-α, IL-6 and VEGF, IGF-1, and TGF- β) in normal and diabetic conditions. Neutrophils and T- and B-cells are the major characters that also produce the TNF-α, IL-10, and other cells, keratinocytes, fibroblasts, mast cells, and endothelial cells. These cells also serve as the producer of VEGF, IGF-1 and TGF-β [108]. In hyperglycemia and oxidative stress condition, the macrophages are the essential contributor to the wound healing process. This malfunction affects their polarization and modulation, resulting in delayed wound healing [109]. There are diverse factors within the local wound environment in all phases of wound healing. There are significant abnormalities, including 1) delayed migration of neutrophils and macrophages into the wound together with declined phagocytosis activity, 2) elevated proteolytic activity coupled with decreased amounts of collagens and GAGs as well as decreased granulation tissue, 3) dysfunctions activity and proliferation of fibroblast; 4) retarded neovascularization; 5) stimulated apoptosis, and 6) reduced mechanical strength of wound [110]. Delayed wound contraction is abnormal wound healing in

diverse forms. Depending on epithelialization and angiogenesis, granulation tissue is necessary for wound healing. Recently, the treatment of growth factors has been unavailable with impaired healing patients because an angiogenic growth factor may stimulate chronic wound closure, indicating hypoxia and accommodated vascularization.

In diabetic patients, other factors interrupt the healing process, including particular metabolic default, absence of physiological responses like hypoxia owing to hemoglobin glycation and red blood cell membrane alteration, and narrowing blood vessels resulting in decreased oxygen supplied to wounds. Glycation of hemoglobin contributes to an insufficient supply of nutrients and oxygen to tissue leading to delayed wound healing. Following these features, there are also physiologic factors, including elevated matrix metalloproteinase-9 enzyme [111], aberrant accumulation of collagen and imbalance in the ratio of collagen types, insufficiency of thrombin-activatable fibrinolysis inhibitor, reduced number of epidermal nerves and barrier function [105]. Then imbalance of ECM components and matrix metalloproteinases are responsible for the delay of the wound healing process in diabetic conditions (Figure 18) [112].

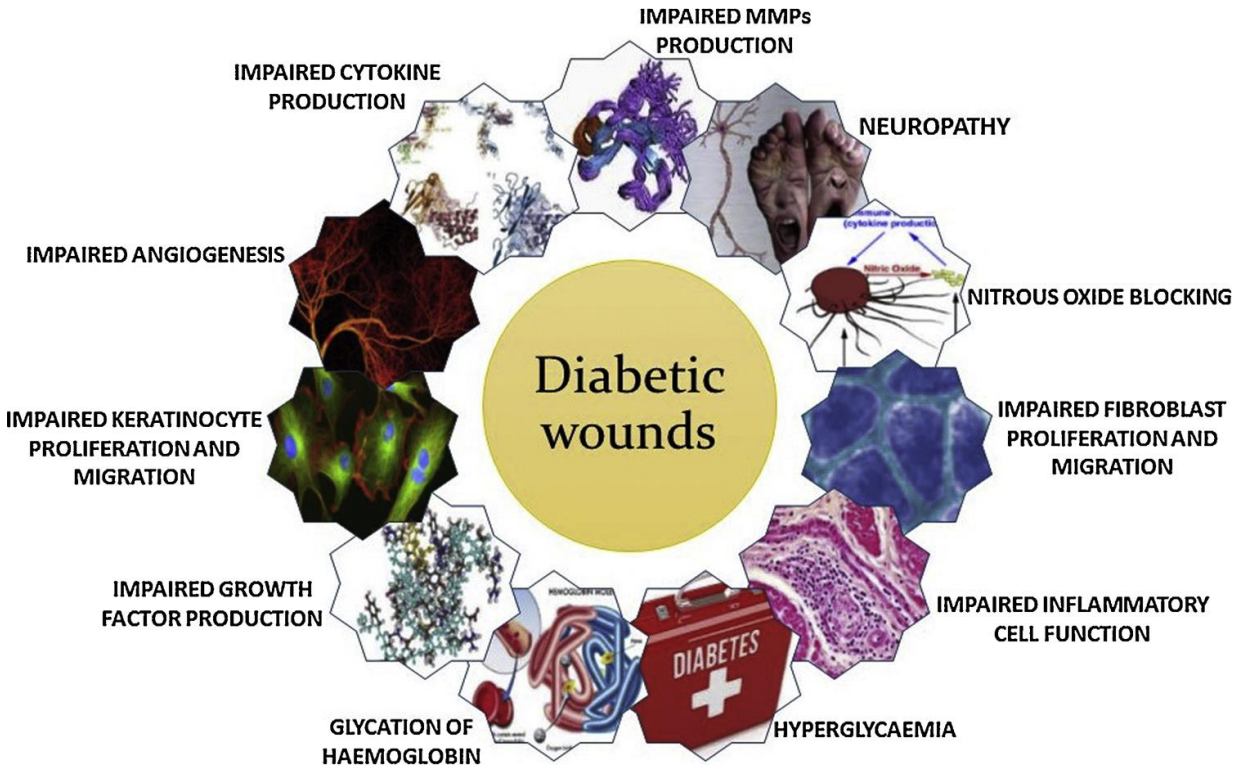

Figure 18 Associated metabolic factors responsible for diabetic wounds

Source: [109]

At the cellular pathway, the accumulation of acute inflammatory cells, the lack of cellular growth and migration of the epidermis cells are accompanied by constriction or blockage of the blood vessels within the wound edge. The malfunction of leucocytes and the metabolic abnormalities of diabetes patients cause insufficient neutrophils and macrophages migration to the wound, coupled with decreased leukocyte chemotaxis [72, 77]. The critical result affects changes in the cellular level, which attracts in-person to an increased risk of wound infection. Growth factors play an important role during normal wound healing, including mediating, coordinating, and controlling cellular interactions [90]. The stimulation of cell proliferation and activity leads to the migration of inflammatory cells into the provision of the wound and promotes protein synthesis or diminishes some conditions as healing progresses (Figure 19). In diabetes patients, the normal healing process can be absented by the changes in the levels of growth factors and timing of their expression.

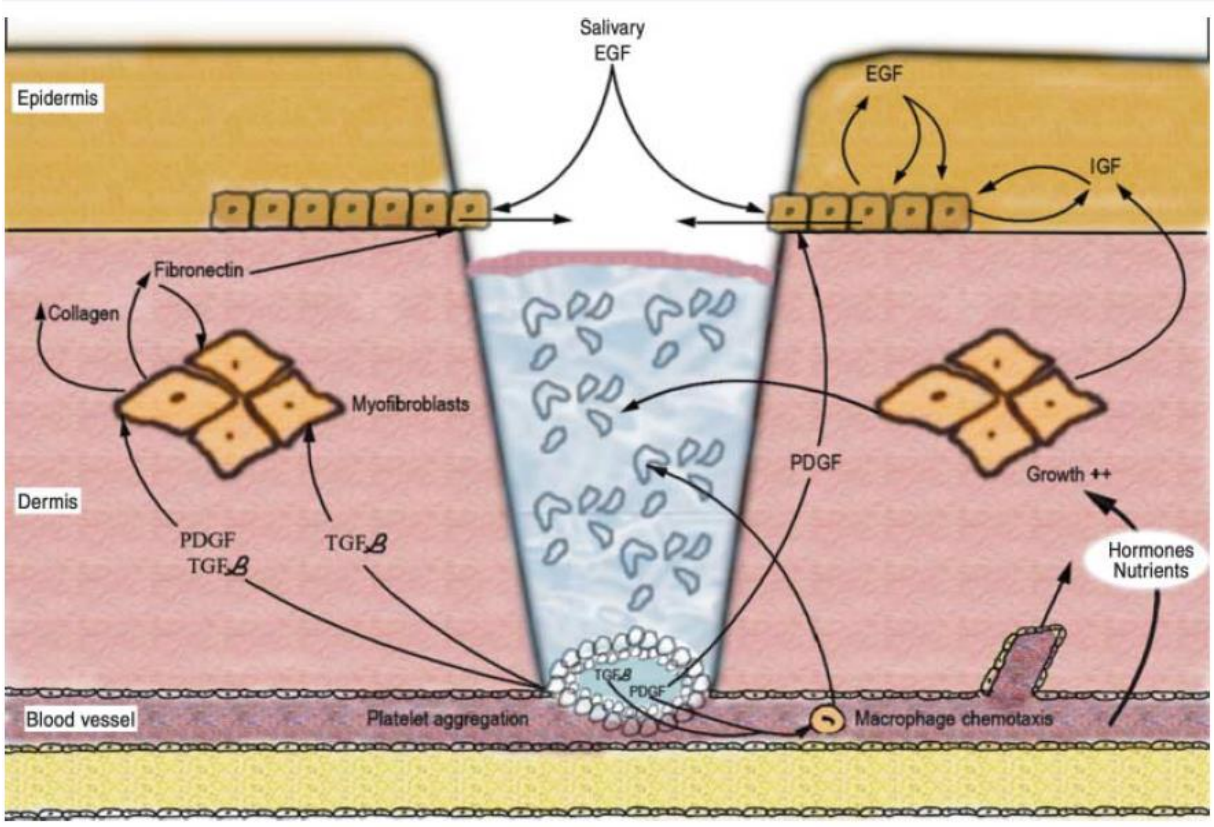

Figure 19 Overview of growth factor involvement in normal epidermal wound healing
Source: [89]

Chemokines, free radicals, and oxidative stress in diabetic wound healing

The literature reviews explicated supporting mechanisms associated with accelerated diabetic wounds like polyol pathway, hexosamine pathway, diacylglycerol pathway, nitric oxide blocking, PKC (protein kinase C) pathways, and formation of advanced glycation end products (AGEs). The overproduction of reactive oxygen species and oxidative stress by mitochondria severely affected these mentioned mechanisms. In hyperglycemia, the high oxidative stress also contributes to adverse effects and abnormal wound healing activity.

The accumulation of leukocytes (monocytes /macrophages/ neutrophils/ immature dendritic cells) is directly regulated by various pro-inflammatory cytokines as anti-bacterial properties in wound healing. All these collectively related to interfering healing rate in diabetic wounds [113, 114]

The sensory and motor malfunctions are caused by diabetic peripheral neuropathy resulting in impaired wound healing. Sensory neuropathy associated to the pain and loss of essential regulation by the growth of a diabetic wound. The absence of glycation of neural cells and the dysfunction of protein kinase C activation caused by the hyperglycemic condition and oxidative stress impair neuropathy and ischemia [115]. Irregular protection of the sensory neuropathy in diabetic patients becomes unremarked processing of the wound worse.

Immune system related to diabetic wound healing

The appropriate correlation of the inherent immune system can be considered a significant regulatory role in the wound healing process. Toll-like receptors (TLRs) are essential modulators that initiate the intrinsic immune system and allied inflammation responses [116]. In diabetic conditions, TLRs down-regulate the activities of the immune system and inflammation responses in damaged tissue, resulting in decreased chemotactic activity, which procrastinates the numerous inflammatory cell recruitment. Most diabetic patients are particularly responsive to the microorganism infection ensuing the prolonged wound healing activity and suppression of the immune system [117]. The occurrence of the microorganisms on the wound is inevitably in the etiology of diabetic wounds. They also form the biofilms, which is expedient for the microorganism to protect themselves from the antibiotic and immune ability leading to interfere the healing activity caused by the limb lower amputation [118].

Inflammation cells (neutrophils, monocyte, T cells, B cells, and mast cells play a chief role in immunity) serve as the potential regulator in the immune system. The malfunction of these cells' attributes to the irregular ability of immune cells. The overproduction of pro-inflammatory cytokines, including IL-6 and TNF-α, affects the malfunction in the inflammatory mechanisms, hyperinflammation, and insulin resistance [119].

The elevated AGEs level stimulates the immune system, which induces the activation of several cytokines, including IL-6 and TNF-α. AGEs also hinder the secretion of collagen, provoke apoptosis, overproduction of immune responses, and adversely activate cell behavior resulting in malfunctioning healing activities [120]. Mast cells act as the important producer of angiogenesis growth factors such as FGF, VEGF, and TGF-β1 and accompany macrophages, endothelial cells, and fibroblasts to play an essential role in matrix remodeling and obstruct the imbalance of pro-angiogenic factors and anti-angiogenic factors in wound tissues [121]. In diabetes, the impeded mast cells affect the prolonged proliferation phase and vascular regression in the remodeling phase. The RNA expression of MIF (Macrophage Migration Inhibitors Factor) genes diminishes in the diabetic condition, which serves as a major molecule in pro-inflammatory innate immune reactions which might be responsible for impaired production of endothelial progenitor cells and the healing process [122].

Growth factor and pathway involvement in impaired diabetic wound healing

The normal wound healing process is systematized and regulated by various growth factors, MMPs, cytokines, inflammatory cells, fibroblasts, keratinocytes, and endothelial cells. Growth factors can be considered as innate potent proteins associated with all phases in the wound healing process. In the early stage of inflammation, these factors promote tissue formation during the granulation phase. Expression changes, reduced production and secretion, obstruction, and the excessive type and amount of growth factors affect the wound adversely. The equivalence of matrix formation and matrix degradation is notable for characteristics of suitable ECM synthesis in the wound healing process. In hyperglycemic conditions, these growth factors, including VEGF, IGF-I, IGF-II, TGF-β, KGF, PDGF, EGF, FGF, TNF-α, and IL-6, are remarkably decreased, leading to dysregulation of ECM formation. Growth factors also serve as originating and supporting regulators in all wound healing phases (Figure 20).

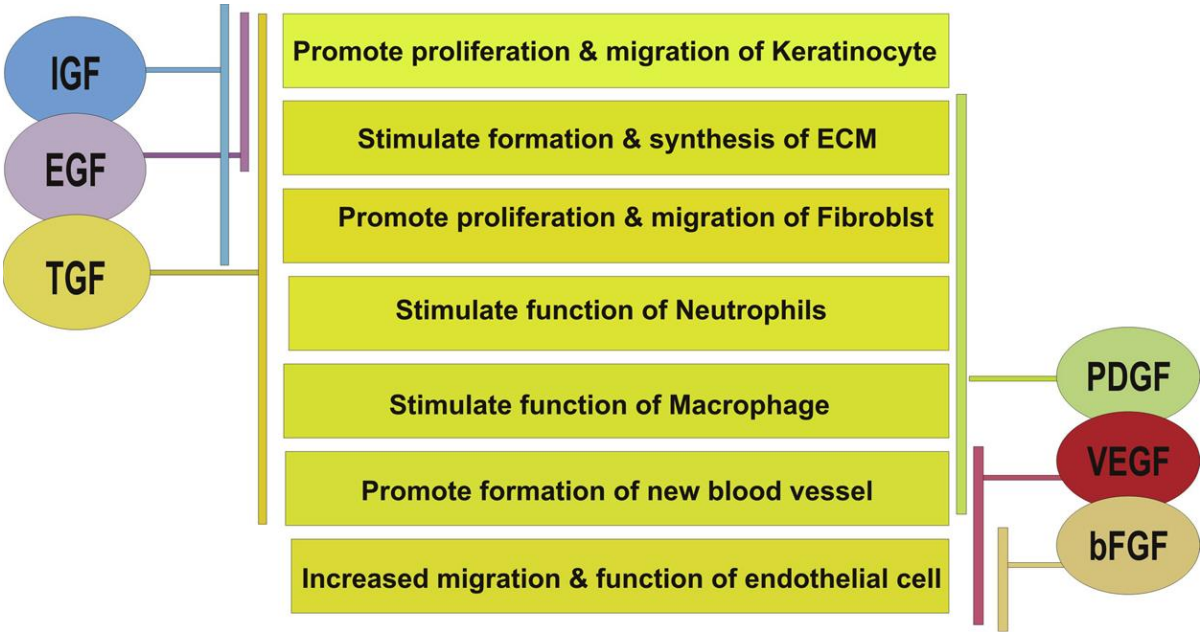

Figure 20 Growth factors controlling different cells and processes involved in wound healing
Source: [103]

Insulin-like growth factor (IGF)

Typically, the insulin-like growth factor consists of two distinct isoforms: IGF-1 and IGF-2 in mammals. IGF-1 is crucial in angiogenesis and is found in the endothelium [123]. IGF-1 can attract the chemotactic activity in endothelial cell lines, stimulates the proliferation of keratinocytes and fibroblasts and re-epithelialization, and increases the mechanical strength of the wound [124]. Genetically diabetic mice demonstrated delayed expression of IGF-1 and IGF-2 mRNA and decreased protein content within the wound. In diabetic patients, the levels of IGF-1 were decreased in fibroblasts within the basal layer of the epidermis, decelerating the re-epithelialization rate. For diabetic patients, IGF-1 and IGF-2 are raised in fibroblasts within the wound. The elevated IGF-2 may bind to the IGF-2/mannose-6-phosphate receptor, affecting to deterioration of the wound healing process by impeding the activation of TGF-β1 [125].

Transforming growth factor-β (TGF-β)

The variant patterns during normal acute wound healing depend on their occurrence time, period, and expression areas, accompanied by TGF receptors [126]. In the acute healing process, TGF-β1 has numerous fields of its function. It plays significant roles as an influential chemoattractant for monocytes, leukocytes, macrophages, lymphocytes, neutrophils, keratinocytes, and fibroblasts, facilitates cellular movement, attracts cells to release growth factors, provokes angiogenesis, and

promotes ECM deposition, simultaneously interrupting proteolytic degradation of ECM [127]. In diabetic rats, TGF-β levels were diminished within the wound fluid. In humans with venous ulcers, chronic pressure wounds and diabetic foot ulcers, the absence of the secretion of TGF-β1 is observed as compared to acute wound healing [126, 128]. In chronic pressure wounds, the amount of mRNA of TGF-βR1 is diminished. On the other hand, they are detected in repairing keratinocytes during acute wound healing [128]. The elevation may require the absence of up-regulated TGF-β 1 in the chronic wound of receptor levels. Nevertheless, a privation of elevated TGF-β receptor is found in chronic diabetic ulcers, coupled with the decline of the TGF-β1 receptor. In diabetic ulcers, the lack of TGF-β1 leads to demolishing the normal healing process, which affects the deficiency of receptors because of its central action.

Platelet-derived growth factor (PDGF)

PDGF has a considerable action in all wound healing phases similar to TGF-β [129], illustrating a diversity of functions including chemoattractant, promoting cells to release the growth factors, and attracting the several matrix molecules end products. The patients with diabetes found the absence of PDGF protein from chronic wound fluid [130]. The expression A-chain gene, which consists of PDGF in fibroblasts, is influenced by the activated TGF-β when the reduction of TGF-β1 levels results in the decrease of PDGF in diabetic wounds. Furthermore, PDGF can stimulate enhanced wound healing and promote wound-breaking strength.

Keratinocyte growth factor (KGF)

In genetically diabetic mice, the delay in expressing keratinocyte growth factor mRNA affects the exceedingly decrease in wound tissue. Also, IL-6 controls the expression of KGF mRNA and protein in fibroblasts [131]. The reduced IL-6 contents lead to decreased potential causal link for KGF in the wound fluid of streptozotocin-induced diabetic mice.

Vascular endothelial growth factor (VEGF)

In genetically diabetic mice, the secretion of mRNA and protein synthesis of VEGF is impaired, which is observed in wound tissue during granulation tissue formation. TGF-β1 and KGF provoke the release of VEGF mRNA in keratinocytes [132], which are declined in chronic wounds resulting in lowered *in vivo* VEGF. Also, VEGF accelerates wound healing in diabetic mice [133].

Angiogenesis

The pre-existing capillaries lead to the formation of new blood vessels, which can infiltrate the wound edge, important components in the wound healing process [134]. The abnormality of angiogenesis in various organs, coupled with impaired function, happens in chronic wound healing in diabetic patients [135]. Access to inflammatory cells is limited by restricting new blood vessels penetrating the wound. Alternately, the reduction of the total amount of factors is released by these cells. In the angiogenesis pathways, NO is considered as an attractor and is decreased in impaired diabetic wound. The lower amounts of other angiogenic stimulators, including Nerve growth factor (NGF), TGF-β1, VEGF, and basic Fibroblast Growth Factor (bFGF), accompanied by diminished or over-production levels of NO contribute to defining the abnormal angiogenesis in the wounds.

Extracellular matrix (ECM)

In diabetic animals and patients'skin, the capacity of collagen and GAGs is declined, resulting in a decrease in wound-breaking strength [136]. As a result, it affects the diminished synthesis of fibroblasts. The reduction of collagen content leads to decreased synthesis of NO. Both TGF-β1 and IGF-1 promote collagen synthesis in fibroblasts and the formation of GAGs. Lowered ECM production is affected by the increased MMPs and reduced NO and IGF1, and TGF-β1 as the altered biochemical mediumduring impaired wound healing. These alternative factors make the wound more sensible to erupt caused of low strength and also contribute to deficiency in the provision of a bed for the cellular tissues to generate and action accurately in the wound [137].

MAPK signaling pathway

Cytokines define as the stimulator to downstream the activated signals through the different mechanisms. Both of p38 MAPK and PI3K/Akt can be considerable as the essential protein kinase that play an essential role in cellular pathways. These pathways are associated with several molecular activities and especially the migration and proliferation of fibroblasts in the wound healing processes [138, 139]. In the wound of streptozotocin-induced diabetic rat, the expression of IL-l was decreased significantly resulting in the malfunctions of p38 MAPK or PI3K/Akt following malfunction of cell migration (Figure 21). Also, the suppression of IL-6 by SB203580 inhibitor-treating cell affected to delay the fibroblast migration in the scratching assay. These implied that upregulation of IL-6 involved to promote the migration of fibroblasts

related to wound healing, via the MAPK and PI3K/Akt pathway [140]. The MAPK pathway also regarded to diverse cells related to diabetic conditions including pancreatic β-Cell [141], retinal vascular endothelial cell (RVEC) [142], and ventricular cardiomyocytes (AC16 cells) [143].

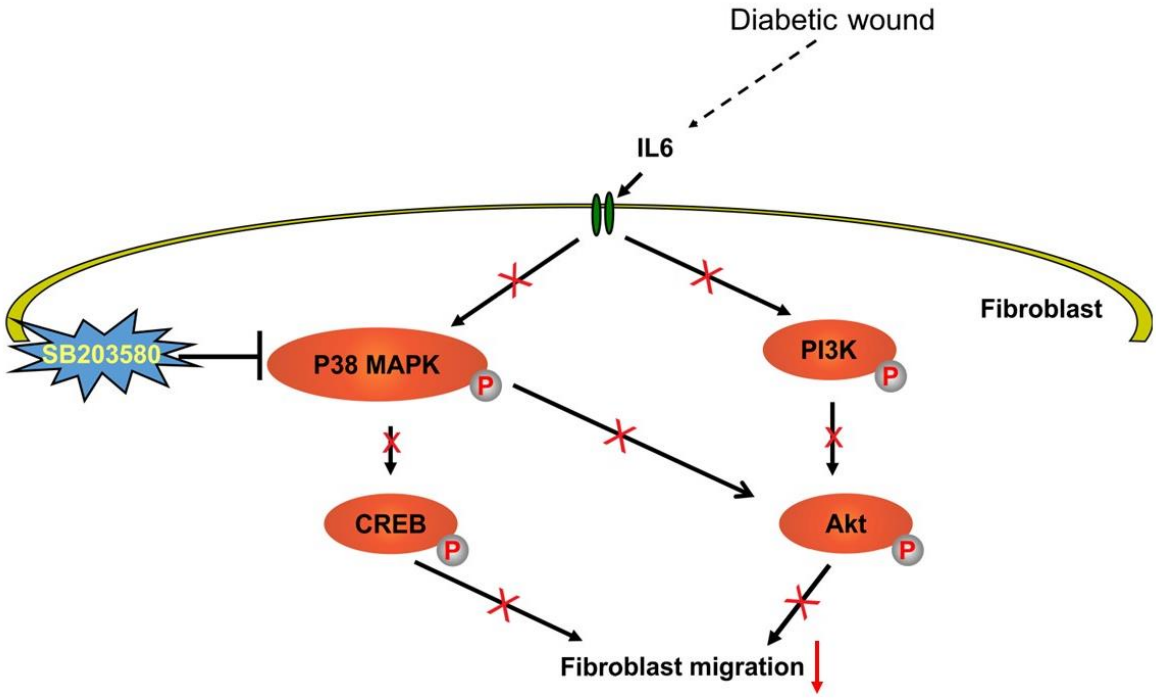

Figure 21 The malfunction mechanism of p38 MAPK and PI3K/Akt pathway in the diabetic condition related in delayed wound healing

Source: [140]

Wound dressings

Wound dressings are sterilized pad or compress conventionally utilized to accelerate healing and prevent undesirable contamination, foreign bodies, or damaging tissue forces [144]. The dressing is purposed as the direct contact with the wound, different from bandaging, typically applied to hold a wound closure. They also served as potent equipment to deliver the active compound to the damaged areas. The efficient wound dressing is supposed to manifest in a moist environment to decrease scar formation and facilitate cellular epithelization and migration into the wound. The requirements of chronic wound dressings are even more challenging [145]. The traditional dressings, including gauze and cotton wool, show the absence of active ingredients in the wound healing process, which, distinguished from advanced dressings, are designed to provide biological activity on their own and contribute to the release of bioactive constituents (drugs) incorporated within the dressing. Approximately 20 million affected patients suffer from chronic wounds, and the global

wound care market revenue rose to more than 20 billion dollars in 2016. Chronic wounds can be many adverse circumstances for the patients. Chronic wound healing has failed to progress through a timely sequence of repair or one that proceeds through the wound healing process without restoring anatomic and functional results [146].

Moreover, chronic wound affects chronic pain, loss of function and mobility, increased social stress and isolation, depression and anxiety, and prolonged hospitalization. One way to reduce inflammation time is using a wound dressing with biological activities designed to seal a wound environment from pathogens and promote the wound healing process. Wound dressing is the alternatively effective tool responsible for this problem. It plays a pivotal role in managing diabetic foot ulcers, which comprises cleaning the wound and using modern wound care techniques that promote a moist wound healing environment [147]. The management of chronic wounds has to take care of prolonged treatments and frequent dressing changes, which transfer the active compound to the damaged site in a regulated manner that stimulates the patients' compliance and therapeutic activities. Bioadhesive, polymeric (synthetic, semi-synthetic, or naturally derived) dressings, are proficiently convenient for treating tropical microorganism infection to alleviate the direct exposure concentration of the antibiotic to the wound but provide a beneficial therapeutic dose [148].

Consequently, suitable wound dressings are desired to be served as a superior healing process. The treatment of chronic wound healing is more complex in the biological pathway and healing process. The active wound healing efficacy of consisted materials can be based on different constituents, including the release of active compounds, the material of dressing, or incorporated ingredients [149].

Properties of the ideal wound dressing

Based on the types of wound, the critical requirements of wound dressings should be based on their ability in 1) controlling moist environment, 2) enhancing epidermal migration, 3) promoting angiogenesis, 4) synthesizing connective tissue, 5) allowing gas exchange between injured tissue and surrounding environment 6) maintaining proper tissue temperature to improve the blood flow to the wound bed 7) preventing against microorganism infection 8) easy to change or remove after healing 9) providing debridement action to enhance leucocytes migration and support enzyme accumulation

10) providing mechanical protection 11) possessing biocompatible, biodegradable, elastic, and nontoxic 12) relieving the wound pain, and should be costly acceptable (Figure 22) [12, 150].

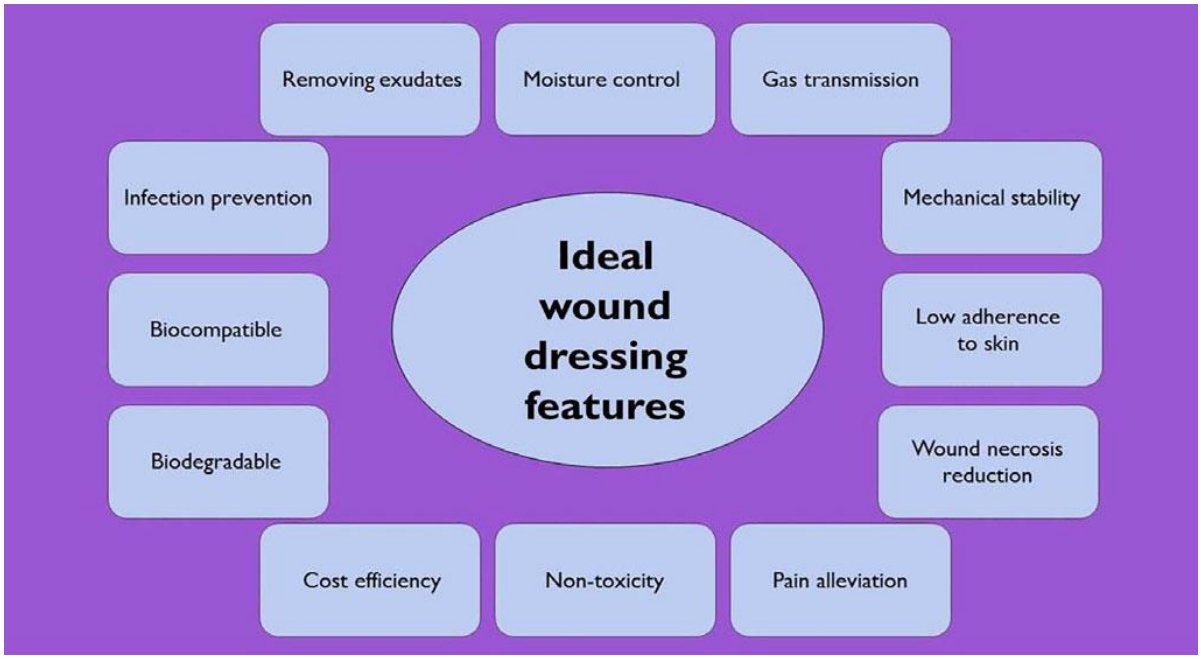

Figure 22 The ideal wound dressing features

Source: [150]

Types of biomaterials applied for diabetic wound healing

The wound dressing is chosen depending on the type, depth, location, extent of the wound, amount of release, infection, and adhesion. The components of biomaterials can be categorized into three types: (i) tissue-derived biomaterials, (ii) hydrogel-based biomaterials, and (iii) biomaterials with controlled-release of signaling molecules (Figure 23) [13].

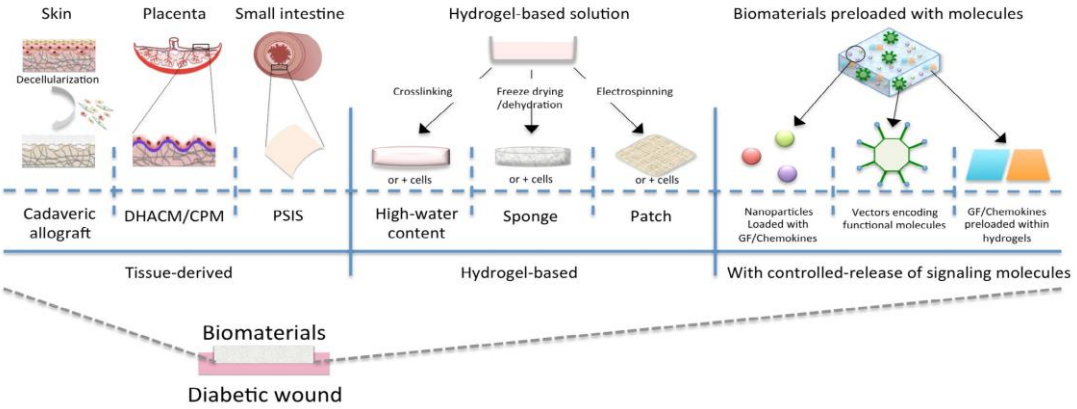

Figure 23 Type of biomaterials applied for diabetic wound healing

Source: [13]

Traditional wound dressing

Traditional wound dressing products such as bandages (natural or synthetic), gauze, lint, plasters, and cotton wool are applied as primary and secondary dressings to cover the wound from microorganism infections [145]. A gauze dressing is made from woven and non-woven fibers of cotton, rayon, and polyester to eliminate bacterial contamination. Sterilized gauze pads are applied for fluid or exudate absorption secreted from the wound. These types of wound dressing need to frequently change to reduce the risk of maceration of healthy tissues. However, they provided excessive moisture and fluid due to the excessive wound exudate leading to the wound adherent and affecting its pain when taken off. Natural bandages are produced from cotton wool and cellulose, or synthetic bandages made of polyamide materials provide different abilities. For example, cotton bandages are applied for light protection, and high compression bandages and short-stretch compression bandages are utilized for venous ulcers. Typically, the traditional dressings are illustrated for clean and dry wounds with slight exudate or used as secondary wound dressings. According to the limitation of conventional dressings to provide a moist environment for the wound, they have been taken place by modern dressings with more advanced formulations.

Modern wound dressing

Foam wound dressing

Foam dressings are semi-permeable polyurethane or silicone-based material. They provided hydrophilic or hydrophobic properties as bacterial protection and the ability to absorb the mild to high wound drainage volume [151]. These dressings are the thermal insulation for the wound, provide the wound moisture environment, non-adherent, and easy to remove. Foam dressing can be applied together with hydrogel or alginate wound dressings as the secondary wound dressing or used with antibiotic agents against infections. They can be made by the adhesive pad, which is practically applied to the wound.

Hydrofiber wound dressing

The hydrofibers are distinct from hydrocolloids with superior absorbent properties, which are up to 25 times weight its weight in exudate from the wound. These wound dressing structures

manifest vertical absorption, which alleviates the risk of skin maceration and has to be utilized with a secondary dressing, hydrocolloid.

Alginate wound dressing

Alginate wound dressings are manufactured in non-woven sheets and ropes, and the derivatives of brown seaweed as fibrous products [152]. When the alginate is contacted with the wound resulting in forming the gel effects on the surrounding fluid, they possess the absorption ability of up to 20 times their weight in the wound drainage. They are also applied for non-infected and infected wounds due to the high absorption ability of alginates. However, these types of wound dressing need supporting secondary wound dressing such as foams or hydrocolloids to assist and hold it from the vaporization of moisture.

Hydrocolloid wound dressing

Hydrocolloid wound dressings comprise absorbent compounds such as carboxymethylcellulose, pectin, or gelatin. These wound dressings provide the same absorption ability as hydrogels or hydrocolloids, which possess minimal to moderate drainage and are appropriately used for partial- or full-thickness in acute and chronic wounds. The occlusive effects of these wound dressings resulting in water, oxygen, or bacteria cannot penetrate the wound affecting the activation of angiogenesis and granulation. They also adjust the pH surrounding the wound as the acidic conditions lead to deter bacterial infections. The hydrocolloids play a vital role in the granulation and epithelialization of the wound and facilitate the autolytic debridement of necrotic or damaged sloughy tissues. However, the occlusive behavior of the hydrocolloids may not be suitable for the infected wound and diabetic foot ulcer. The hydrocolloid wound dressings are appropriate for the patient's body and can tightly adhere to high friction areas [153].

Semipermeable film dressing

The semipermeable wound dressings are transparent flexible polyurethane sheets coated with an acrylic adhesive that varies in size and thickness and has an adhesive that holds the wound dressing on the skin. They conform easily to the patient's body. As transparent property of the film resulting in the wound can be easily monitored. These wound dressings commonly need to dry site for contact with the wound and avoid the moist condition due to the adhesive dysfunction. Hence,

the assessment should be performed prior to the application. For the semi-occlusive can entrap the moisture affected to autolytic debridement of necrotic tissues and generate the moist healing condition for granulating processes.

Hydrogel wound dressing

Hydrogel wound dressings have been widely studied in various fields for their literature reviews. These wound dressings are the 3D network of polymeric hydrophilic behavior which can be made by several hydrophilic polymers [154]. They possess the excellent absorption property to hold the high volume of the exudate secreted from the wound, resulting from the appearance of the hydrophilic chains to swell tremendously without affecting their gelatinous behavior. As this ability, the hydrogel wound dressing can be considered as the wound dressing for moist absorbent. Normally, they can be applied on dry, sloughy, or necrotic wounds, but they require a secondary dressing to seize and cover the wound area. These wound dressings can be used for many uncommon shapes of wounds because of their jelly-like characteristic. Hydrogels provide non-particulate, non-toxic, and non-adherent properties. Also, they contribute to allowing the surrounding moisture to dehydrate tissue to avoid the desiccated condition and help absorb the wound drainages. Both natural polymeric and synthetic polymeric materials have been used to manufacture these wound dressings. Some of the most common commercially available hydrogel dressings include Intrasite™, Nu-gel™, Kikgel, Aqua-gel, and Aquaform™.

Bioactive wound dressing

The bioactive wound dressings are made from biomaterials that represent the healing process. These dressings provide biocompatibility, biodegradability, and non-toxic properties and are regularly synthesized from natural tissues or artificial sources, including collagen, hyaluronic acid, chitosan, alginate, and elastin. The polymeric materials can be used alone or incorporated depending on the nature and type of wound. Also, they can be applied with growth factors and antimicrobial agents, leading to the wound healing process [155].

Medicated wound dressing

Medicated wound dressing combined with drugs plays a vital role in improving the healing process directly or indirectly by removing necrotic tissues. As the functions of these wound

dressings are attained by cleaning or debriding agents for necrotic tissue, antimicrobials prevent infection and promote tissue regeneration [156]. Typically, these compounds are selected to incorporate with medicated wound dressings, including antimicrobial agents, growth factors, and enzymes. The antimicrobials are mainly purposed to prevent or struggle against microorganism infections, especially diabetic foot ulcers. The normal wound healing process is regulated by cellular activities by growth factors that naturally appear in our body. Whereas, in the chronic wound condition, the related growth factors and cytokines are hindered from migrating to the wound sites, resulting in the prolongation of the wound healing process.

Composite wound dressing

Composite wound dressings are multipurpose and comfortable for partial and full-thickness wounds. The composite or combination wound dressings provide multiple layers; each layer is physiologically individual and mainly displays three layers. They may also compose an adhesive border of non-woven fabric tape or transparent film. They possess beneficial properties as either a primary or a secondary wound dressing on a wide variety of wounds and may be used with topical medications. The outer layer can protect the wound from infection. The middle layer is usually composed of absorbent material which holds moisture and helps autolytic debridement. The bottom layer consisted of non-adherent material which prevents from sticking to provisional granulating tissues. Composite wound dressings have less flexibility and are more expensive [157].

Silk fibroin

Background

Based on history, the fibers secreted by the traditional *Bombyx mori*, indicative of Bombycidae, have been modified by humans for a long time. It has been applied in various fields, especially textile applications, because of its remarkable tensile strength and attractive abilities of material [158]. The mulberry leaf-fed, traditional *B. mori* silkworm cocoon, secreted in the pupae phase in the cycle of life, provides commercial-grade silk fibers [159]. The silk material exerts several properties, including water absorbency, dyeing affinity, thermos tolerances, insolation properties, and luster, because of its unique characteristic, thin, long, light, and soft [160]. Practically, there are various uses for the application of silk, including medical materials for human health, cosmetics, and food additives.

Structure of silk fiber

There are two majorities of fibroin protein components comprised of the silk from the cocoon of *B. mori*, light and heavy chains, 25 and 325 kDa, respectively, as shown in Figure 24. The coated sericin, a family of glue-like hydrophilic proteins, envelops these core fibers together to form the composite fibers of the cocoon case to protect the growing worm [161]. The protein is named P25, a 25 kDa non-covalent glycoprotein linked protein [162]. Beta-sheets or crystals via hydrogen bonding originated from the former blocks. SF has two distinct primary forms: silk I and silk II. Silk I provides structure as the random-coil and amorphous regions, whereas the structure of silk II is considerable to an anti-parallel β-sheet structure (Table 3). The fibroin molecule is enormous, consisting of an amorphous region of one-third, and another of about two-thirds is a crystalline portion. This portion comprises repetitive amino acids (-Gly-Ala-Gly-Ala-Gly-Ser-) through its chain to form an anti-parallel β-sheet resulting in the strength and stability of the silk fibers [162, 163]. The rearrangement of silk structure is opposite to spider silks due to the absence of these glue-like proteins. Sericulture, produced by the Silkworm or cocoon silk, provides a great percentage of yield because of the maintenance of larvae in high condensed.

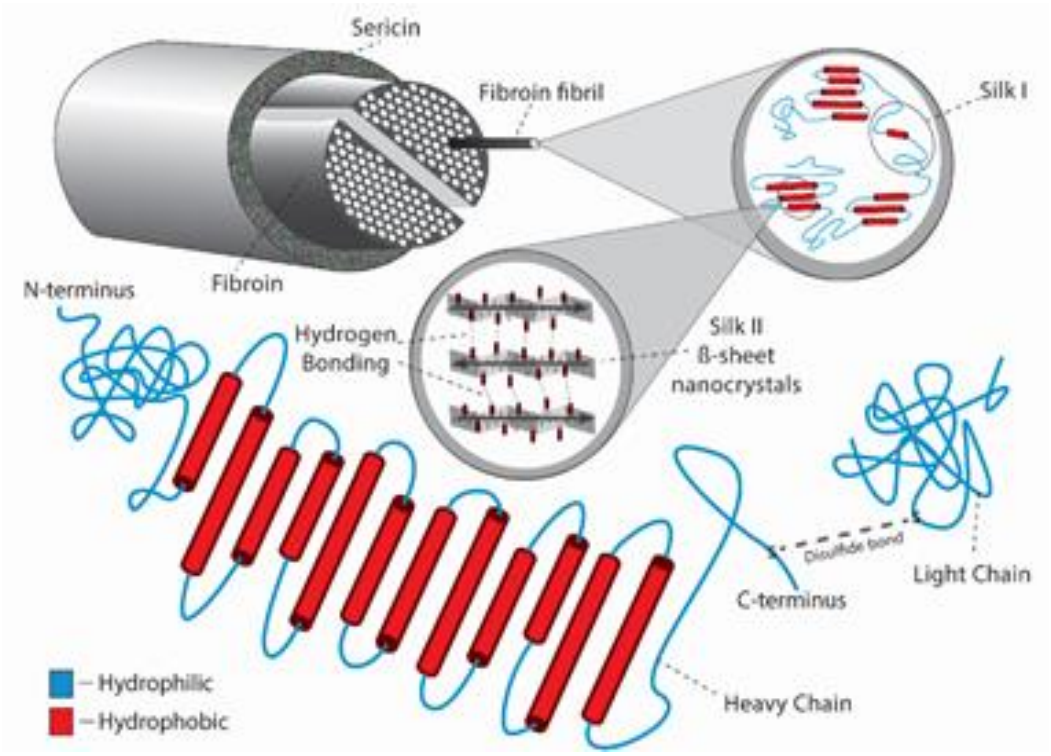

Figure 24 Structure of silk fiber

Source: [164]

Table 3 Structure of silk fibers

	Bombyx mori silk worm			
Silk fiber	Silk fibroin (72-81%)			Silk sericin (19-58%)
	H-chain	L-chain	P 25 glycoprotein	a glue-like protein
Molecular Weight	325 kDa	25 kDa	25 kDa	~300 kDa
Polarity	Hydrophobic			Hydrophilic
Structure	silk I (random-coil or unordered structure) silk II (crystalline structure) silk III (unstable structure)			non-crystalline structure
Function	the structural protein of fibers filament core protein			binds two fibroins together, coating protein

Source: [161]

The biodegradation behavior of silk biomaterials

A proteolytic enzyme, biological degradation, such as chymotrypsin, actinase, and carboxylase can adversely affect the SF protein at various times [165, 166]. There are two regular methods of biodegradation behavior; various enzymes solute the silk biomaterials to attach to the binding domains on the surface of materials. The enzymes then digest the silk biomaterials. SF wastes related to amino acids penetrate the target site, which implies that this is the superior property of silk biomaterials for biomedical applications. M. Li et al. reported that the amorphous regions of fibroins could be digested by chymotrypsin, the proteolytic enzyme, to receive practically crystallizable fibroin protein [166].

In vivo, the degradation behavior of biomaterials is considerable to significant for medical terms. The characteristic of enzymes has potentially stimulated the biodegradable process for SFs. For instance, the low molecular weight and non-compact structures contribute to greater action of degradation for the SFs because of easy for enzymes to bind on the surface of silks as well as present hydrolysis behaviors [167]. This indication defines the molecular weight and structure of polymers concerning enhancing the degradation behavior in silk biomaterials.

Biocompatibility of silk biomaterials

Silk fibers have been applied for commercially available sutures for long periods and effective biomaterials usage. However, some literature concerns the adverse biological reactions coupled with biocompatibility for medical applications. A glue-like hydrophilic protein, sericin, can seize the cored

fibroin protein and be clarified as the immunogenic reaction source. The cause of the inflammatory response is also clarified by the sericin protein as the undegummed silk, even so happening only in the case of a relationship with fibroin which occurs in terms of particular activation of macrophages [168]. Nevertheless, the occurrences of the coating glycoprotein sericin fiber lead to the possibility of inflammation, which is detached by the strong detergents, namely degumming [169]. Following the removal of sericin, the degummed silk protein is well endured on its own. From the result, the degummed SF can be applied and modified as a desirable material property for various silk-based biomedical devices.

Applications of silk fibroin as biomaterials

Plenty of silk research has been studied because of its beneficial and extraordinary properties, including mechanical strength, durability, softness, biocompatibility, and biodegradability. SF is the major component of the silk required to identify the properties, including adhesion, proliferation, and differentiation in the tissue healing process. The sutures, particularly biomedical applications, are typically made from primary silk-like fibers. As for various biomedical applications, silk fibers have been considered efficient materials for centuries.

For the SF application on skin or wound healing, Chiarini et al. 2003 reported that when fibroin coatings and scaffolds are applied, there is no expression of pro-inflammatory interleukins as well as spreading or proliferation of dermal fibroblasts [170, 171]. Min et al. studied the proliferation of oral keratinocytes. The result found that they could migrate on the woven fibroin meshes, which tend to be applied for wound healing usages [172]. Sugihara et al. reported an increase in wound healing when fibroin and fibroin-alginate sponges are applied *in vivo* compared to clinical materials. As a result, SF has the remarkable ability to enhance the re-epithelialized healing process [173].

Molecular wound healing properties of silk fibroin

SF illustrates remarkable biocompatibility with several cells and tissues because of its potent properties in stimulating the adhesion and proliferation of fibroblasts and keratinocytes. The fibroin from silk exhibits excellent ability as a biomaterial used as a wound dressing in various fields [18]. At the cellular level, SF is an ongoing clarification in the wound healing pathway. Roh et al. reported that when

they seed the keratinocytes and fibroblasts on the SF wound dressings, the proliferation and matrix deposition of these cells were increased [174].

In wound healing processing, SF exerts the synergistic effects of collagen deposition coupled with re-epithelialization enhancement which is compromised by the stimulation of the re-epithelialization process by influencing the proliferation of the epithelial cells. In the silk treatment, fibroin found that the SF has the outstanding ability to accelerate in the wound healing process compared to control [174].

The recovery of SF at the greater epithelialization or epidermal rate regards the stimulating migration and growth of keratinocytes on the provision dermis layer together with the complete basement membrane regeneration that assures the structural and mechanical stability of the dermo-epidermal junction. These conditions, including self-renewal, proliferation, and migration of keratinocytes residing, are distinctively related to the epithelialization process at the basal cell layer. SF demonstrates the attraction of the stimulating regeneration of collagen, a familiar pattern as normal skin. Collagen is of the major component of the dermis layer, which remarkably considers tissue repairing via providing the tissue mechanical strength coupled with an ECM wound bed for adhesion and migration of the cells [175]. On the cellular pathway, Roh et al. also reported that the pro-inflammatory cytokines could be manifested with the SF nano matrix in the wound healing process. Moreover, they also reported that SF displayed the potential wound healing ability to inhibit the expression of excessive pro-inflammatory cytokines within impaired wounds when applied to the damaged wound. Accordingly, controlling the balance level of pro-inflammatory cytokines (IL-1α and IL-6) and antagonistic anti-inflammatory cytokines (IL-10) when the wounding occurs, affects the prolongation of the wound damage by interfering with the normal wound healing process but controls the modulation of the balance of pro- and anti-inflammatory expression during the wound healing process [174]. TGF-β1 plays a prominent role in inflammation, stimulating angiogenesis, fibroblast proliferation, collagen synthesis, and remodeling of new ECM, which is involved in wound healing [176]. It's also essential in the formation of hypertrophic scar. The induced expression of TGF-β1 by silk fibroin contributes to stimulate wound healing following scarless wound healing [177].

Fibroblasts are essential components in the normal wound healing process from the late inflammatory phase to complete epithelialization. Qin Song et al. reported that apply SF dressings

regulated the expression of proteins, including vimentin, cyclin D1, VEGF, and fibronectin. These dressing also accompanied by cell proliferation and remodeling phases modulated by NF-κB signaling pathways in NIH3T3 cells and damaged skin rat [178], which associated with fibroblast migration and wound healing process. These coincidences were reported as the same trend that the stimulation of compromise via toll-like receptors (TLRs), interleukin-1 receptor (IL-1R), tumor necrosis factor receptor (TNFR), and antigen receptors [179, 180].

NF-κB signaling regulates various cellular activities during the wound healing process, including cell growth and adhesion, balancing the production of reactive oxygen species (ROS), stimulating the corneal epithelial healing, and stimulating the migration and inducing c-Jun expression ensuing cutaneous wounds closure at the collective cell migration leading edge. As a result, SF has notable effects to fulfill in this condition by increasing the expression of c-Jun and c-Jun protein phosphorylation in wound healing.

Furthermore, at the molecular level, SF accelerates signals, including AKT/mTOR and MAPK signaling, which provide prominent actions for the phosphorylation of ERK 1/2 and JNK 1/2 kinases and promotes cellular migration through the expression of PAI-1, regards to the promotion migration, facilitating the re-epithelialization of the provisional wound bed and stimulates complete cellular adhesion [181]. Consequently, SF also activates the expression of PAI-1, resulting in the complete acceleration of cell adhesion during the migration of cells and facilitating wound re-epithelialization. Activated JNK is essential considering the fibroblast's migration in the wound healing process. c-Jun plays an essential role in the proliferation, and motility of epithelium is promptly modified in wound healing [182]. EGF acts as an acceleratory effect on repairing the corneal epithelial wound by stimulating cellular migration [183]. Furthermore, EGF provides significant potential for cell migration involving the phosphorylation of JNK by MEKK1, extraordinarily activated JNK1, and enhances the ERK activity [184]. Activated JNK plays a crucial role in the primary mediate stages of cell migration [185]. Moreover, SF induces MEK1 upstream of both JNK1 and ERK1/2 phosphorylation in MDA-MB- 231 cells.

The stable expression of bFGF and PDGF by fibroblasts is sustained by regenerated SF film, exerting the outstanding property of enhancing angiopoiesis and stimulating wound healing. bFGF and PDGF enhance granulation tissue formation, synthesis of collagen, and angiogenesis which are

associated with the late inflammation and proliferation phase of the wound healing process [186]. VEGF plays a role as a mitogen which is particular to vascular endothelium. VEGF and its receptors on vascular endothelial cells are regarded as important modulators providing the most outstanding function and specificity in the angiogenesis process. VEGF ensures the stimulation of endothelial cell growth *in vitro* and induces angiogenesis *in vivo*. This growth factor is also involved with the initial processes of originated blood vessel formation, coupled with Ang-1, which plays a role in the stimulation of vascular remodeling and contributes to generating a developed vascular network [187]. bFGF modulates various essential functions, including the regeneration of fibroblasts in the tissue damage, the neovascularization, the proliferation of vascular smooth muscle cells and endothelial cells, and activates inflammatory pathways inrepairing tissue. bFGF also acts as chemotaxis of endothelial cells and can accelerate angiogenesis, presenting that it is a breakaway medium of angiogenesis [188]. PDGF is the accelerator providing powerful chemotactic effects on inflammatory cells in the proliferation of fibroblasts and vascular endothelial cells, resulting in aggregation of collagen, capillary angiogenesis, and production of granulation tissue.

Aloe vera

Botanical description, distribution, and cultivation

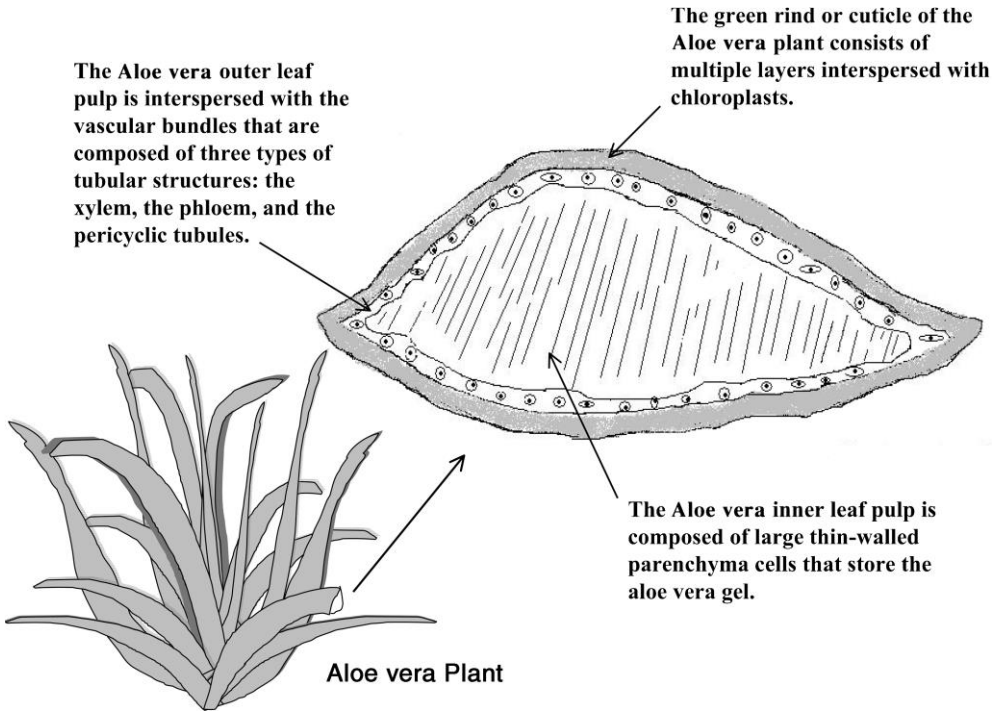

Figure 25 Schematic representation of the *Aloe vera* plant and a cross-section through *Aloe vera* leaf
Source: [189]

Typically, *Aloe vera* is known as *A. vera* Linne or *A. barbadensis* Miller. It has various identification of up to 400 species and regards the Aloeacea or Liliaceae family [190]. *Aloe vera* is characterized by a perennial, resistant-drought plant (resists up to 7 years without water) with thick, tapered, green shaft-shaped, juicy, basal, sharp-pointed, and rugged and edged leaves that rise expeditiously in tropical conditions. The leaf pulp of *Aloe vera* containing the mucilaginous gel can be applied to several fields such as cosmetic and alternative medicines for rejuvenation wound healing, and other dermatologic conditions. Although *Aloe vera* has been broadly utilized for many traditional therapeutics, but little scientific evidence has been studied which considered the molecular level involved with the wound healing process. In the *Aloe vera* leaves, the cuticle surrounding the mesophyll envelops the thick epidermis (Figure 25). This part probably transforms into chlorenchyma cells and thinner-walled cells that generate the parenchyma [191]. The leaves of *Aloe vera* contain abundant components, including 1) epidermis or the outer rind comprised of various layers distributed with chloroplasts, 2) the outer layer of leaf pulp contains vascular bundles, 3) the inner leaf pulp, mesophyll includes parenchyma cells accumulating the leaf gel which consists of many constituents such as anthraquinones, anthrones, chromones, alkaloids, pyrans and pyrones, and coumarins (Figure 26). There are two distinct primary exudate substances, including latex, which is the production of the pericyclic cells within the epidermis and provides the color of a reddish-yellow juice. Another one is a mucilaginous gel which is the production of thin-walled tubular cells in the inner central zone (parenchyma) of the leaves and classifies as transparent, slippery mucilage or gel [192]. The *Aloe vera* leaves consist of the variant three components 1) bitter yellow juice containing anthraquinones (derivatives of 1, 8-dihydroxyanthraquinone and their glycosides, as well as Aloin, is a complement of the anthraquinone complex) 2) internal mucilaginous gel or the fillet 3) the rind, composed of rinds, thorns, tips and bases [193].

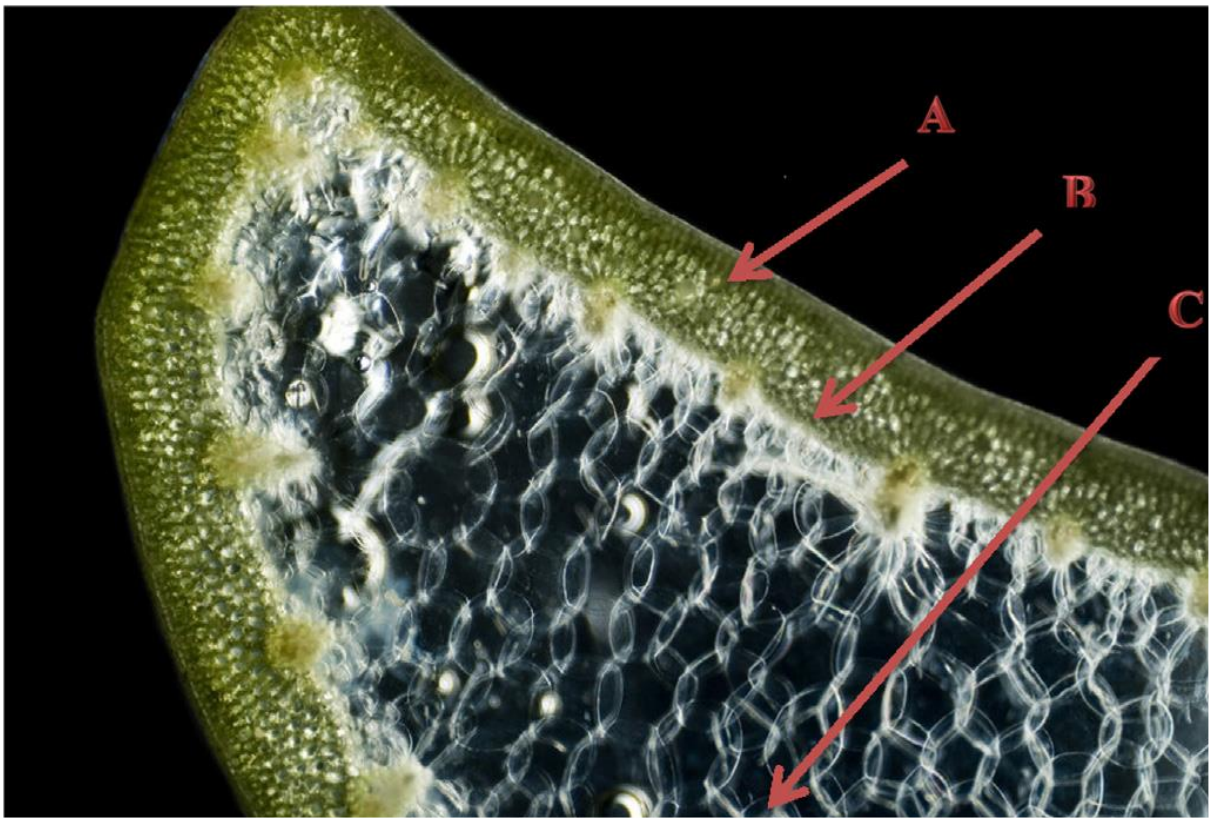

Figure 26 Cross-sectional view of Aloe vera leaf; A: epidermis; B: the outer leaf pulp; C: mesophyll or the inner leaf pulp

Source: [194]

Bioactive compounds composition

In *Aloe vera*, several alterations affect nutrient components, including diversity of species and various climatic conditions. Nevertheless, lifespan is the one factor that is considered to stimulate the components in *Aloe vera*. Several distinct scientific research has been studied about the compounds consisting of A*loe vera*, but there is no evidence of separated chemical compounds that clarify the synergistic actions [195]. Table 4 demonstrates the *Aloe vera* components and their various phytochemical identifications. The different parts of *Aloe vera* can be thoroughly classified as rind, filet, and gel [192]. Moreover, heat and dehydration have enhancing effects on the polysaccharide (acemannan) and polymers in the *Aloe vera*'s cell wall. Acemannan, known as acetylated glucomannans, is a polysaccharide enriched in mannose units instituted within the protoplast of the parenchymatous cells, providing a stimulator in wound healing and regulating immune effects. Another polysaccharide, glucomannan, consisted of *Aloe vera,* exerting an excellent moisturizer for cosmeceuticals. Glucomannan is another polysaccharide that can be found in *Aloe vera*. This is a good

moisturizer used in cosmetics [191]. The effects of the polysaccharides comprised of *Aloe vera* are associated with the degree of acetylation, molecular weight, type of sugar, and glycosidic branching. Growing conditions of *Aloe vera* contribute to the structure of polysaccharides.

Carbohydrates regard as the major components which consist of *Aloe vera.* Various procedures result from the diversity of *Aloe vera* products affecting irreversible alterations to carbohydrates. As a result, these conditions lead to their structural origin, stimulating the significant alterations of their physiological and pharmacological properties [196].

Aloe vera consists of complex chemical components approximately 75 extraordinary active compounds, including vitamins, enzymes, minerals, sugars, lignin, saponins, salicylic acids, and amino acids (Figure 27) [197]. The detail can be described below:

Vitamin

Aloe vera consists of various vitamins, such as Vitamins A, C, and E, which act as an antioxidant and comprise thiamine, niacin, riboflavin, vitamin B12, choline, and folic acid. As a result, these antioxidants neutralize ROS or free radicals.

Enzymes

Many enzymes, including amylases, lipases, alkaline phosphatases, cellulases, catalases, and peroxidases, act as biochemical catalysts manifesting in digestion by disrupting the fats and sugars. Also, bradykinins can be inactivated by carboxypeptidases and bradykinases, which provide anti-inflammatory activity [192].

Minerals

Aloe vera constitutes various minerals such as sodium, potassium, calcium, magnesium, selenium, manganese, copper, zinc, chromium, and iron. They are considered essential in activating enzymes, related to several metabolism activities. Some also act as antioxidant substances [198].

Sugars

Numerous sugars are comprised in the mucilaginous gel under the rind of the leaves. They have monosaccharides (glucose and fructose) and polysaccharides act as immune modulators, including glucomannose and polymannose. [199].

Anthraquinones

Anthraquinones and their derivatives are contained significantly in the bitter reddish-yellow juices beneath the outer green rind. They include Barbaloin, aloe-emodin-9-anthrone, lsobarbaloin, Anthrone-C-glycosides, and chromones. These compounds are classified in the phenolic group known regularly as laxatives. They display a remarkable cathartic action, contribute to gut absorption, act as powerful antibacterial substances, and indicate excellent analgesic effects [192].

Sterols

Cholesterol, Campesterol, β- Sitosterol, and Lupeol, are potent sterol substances that provide anti-inflammatory effects and antiseptic and analgesic properties [198].

Hormones

Auxins and gibberellins are the hormones that contribute to anti-inflammatory effects involving the wound healing process.

Salicylic acid

It acts as an aspirin-like compound involving anti-inflammatory possess and antimicrobial effects.

Amino acids

There are many amino acids, approximately 20 of 22 non-essential amino acids and 7 of 8 essential ones comprised in the *Aloe vera* due to involving in the wound healing process [192].

Lignin

Lignin plays an important role as an inert compound that can be applied to topical medication providing stimulating penetrative action to the other compound contained in the formulation [198].

Saponins

They act as detergent substances with cleansing and antiseptic effects [198].

Table 4 *Aloe vera* components and its various phytochemical identifications

Constituents	Identifications
Amino acids	Provides 20 of the 22 required amino acids and 7 of the 8 essential ones
Anthraquinones	aloe-emodin, aloetic acid, aloin, anthranol, barbaloin, isobarbaloin, emodin, ester of cinnamic acid
Enzymes	Alkaline phosphatase, amylase, anthranol, barbaloin, carboxypeptidase, chrysophanic acid, cyclooxidase, cyclooxygenase, smodin, ethereal oil, ester of cinnamonic acid, isobarbaloin, resistannol, lipase, oxidase, phosphoenolpyruvate carboxylase, superoxide dismutase
Hormones	Auxins and gibberellins
Minerals	Calcium, chromium, copper, iron, manganese, potassium, sodium, and zinc
Salicylic acids	Aspirin like compounds
Saponins	Glycosides
Steroids	Cholesterol, campesterol, lupeol, β-sitosterol
Sugars	Aldopentose, acetylated glucomannan, acetylated mannan (acemannan), cellulose, glucose, glucomannan, galactogalacturan, glucogalactomannan, galactoglucoarabinomannan, fructose, mannose, polymannose
Vitamins	A, B, C, E, choline, B12, folic acid

Source: [200, 201]

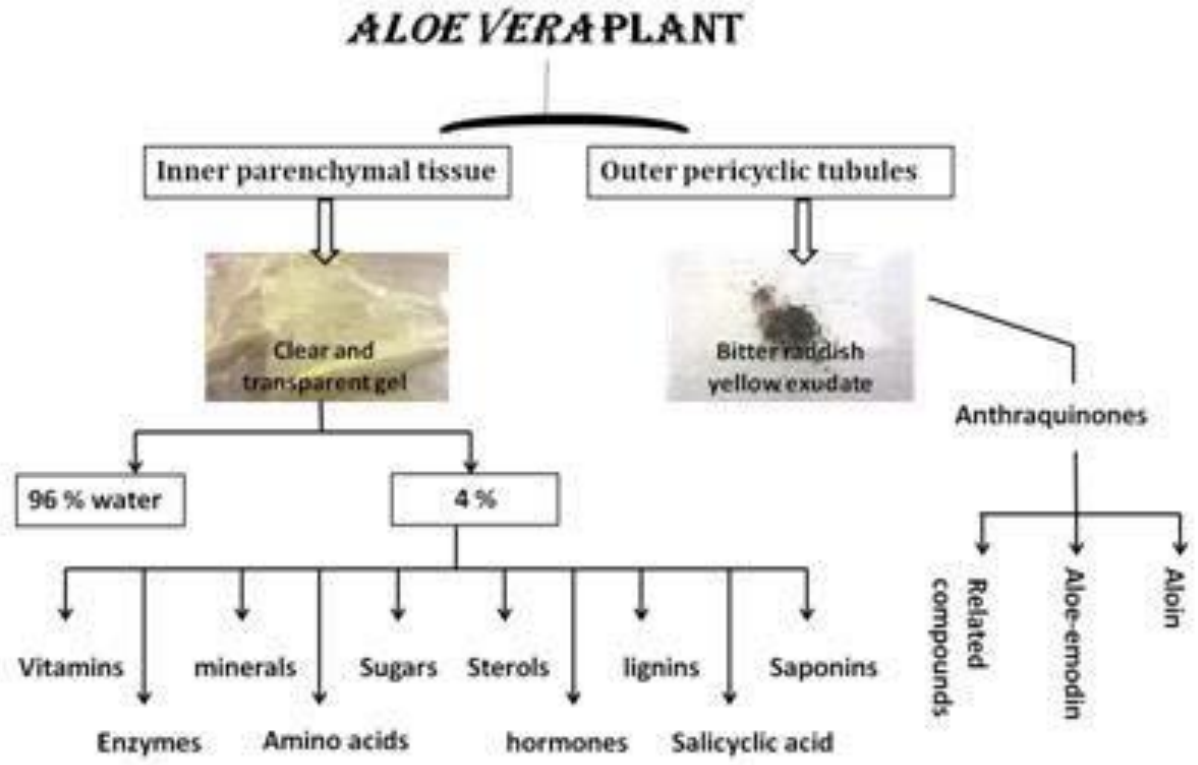

Figure 27 Components of *Aloe vera* leaves
Source: [202]

Therapeutic and Pharmacological effects on wound healing

Historically, *Aloe vera* has been utilized explicitly in various biomedical fields as well as treatments of many diseases including especially burns and wounds, as well as seborrheic dermatitis, thermal burns and sunburn, cystic acne, peptic ulcers, amputation stump ulcers, lacerations, colds, tuberculosis, gonorrhea, asthma, dysentery, and headaches. Also, it has been reported to be used as a laxative and insect repellent [203]. For the beneficial therapeutic effects, *Aloe vera* extraordinarily provides health treatment including stimulation of immune system and wound healing process, prevention against damaged skin of X-rays, lung cancer, intestinal issues, elevating high-density lipoprotein and declining low-density lipoprotein, reducing the glycemic level in people with diabetes, remedying genital herpes and psoriases.

Furthermore, *Aloe vera* contributes to pharmacological activities, including anti-inflammatory, antiarthritis, antibacterial and antifungal, and hypoglycemic effects, as demonstrated in Table5. It can prevent the production of dandruff on the head because of its antibacterial and antifungal properties and protect against fungal infections such as alopecia disease [204]. For the moisture property, *Aloe vera* greatly exerts use in topical cosmeceutical application and enhances the penetration effect into the

deeper layer of the skin to uptake the substances. Cole and Heard reported that *Aloe vera* improves the rising intake effect on drugs of caffeine, colchicines, mefenamic acid, oxybutynin, and kinin, which is caused by the increase in water content in the stratum corneum layer [205].

Table 5 Pharmaceutical activities of *Aloe vera* components

Components	Pharmacological activities
Amino acids	Basic building blocks of proteins in the body and muscle tissues
Anthraquinones	Analgesic, antibacterial property
Enzymes	Antifungal and antiviral activity but toxic at high concentrations
Hormones	Wound healing and anti-inflammatory property
Minerals	Essential for good health
Salicyclic acid	Analgesic
Saponins	Cleansing and antiseptic
Vitamins	Antioxidant (A, C, E), neutralizes free radicals

Source: [200]

Wound healing and cell proliferative effects of *Aloe vera*

Aloe vera attributes to the traditional herbal medicinal plant, which exerts outstanding healing properties and uses in various fields for skin treatment. Glycoproteins and lectins are the main components of *Aloe vera,* providing cell proliferative activities [195]. The approach to separate the compounds from *Aloe vera* into isolated glycoproteins and lectins has been approved to discover the cell proliferative activity in the wound healing process. In the past, 29 kDa glycoprotein had the potential to stimulate the proliferative activity of kidney cells in hamsters and human dermal fibroblasts by *in vitro* assays. Moreover, some scientific evidence that was studied *in vitro* and *in vivo* assay involved improving keratinocyte proliferative effects by stimulating by 5.5 kDa glycoprotein. They were verified by the enhancing the human monolayer keratinocytes closure which made by scratching. Also, the glycoprotein stimulates epidermal tissue formation and is conjugated with many saccharides, especially mannose, approximately 70% of them. *Aloe vera* displays the accelerating ability of therapeutic effects associated with wound healing via penetration into cellular tissue skin. Report [206] studied about the improvement of acemannan, main sugar residue as polysaccharides, which accelerates wound repair and hard tissue regeneration by promoting VEGF, collagen type I synthesis and collagen composition (more type III), cell proliferation as well as enhancing collagen composition

(more type III) and stimulating cross-linking of collagen for wound contraction and promoting wound-breaking strength. Furthermore, *Aloe vera* can improve hyaluronic acid and derma-tan sulfate synthesis in the granulation tissue during the wound healing process. VEGF stimulates the formation of new blood vessels and is essential as the inducer of endothelial cell proliferation and migration. The acetyl groups in acemannan and their derivatives have been investigated to be a necessary stimulator of cell proliferation, expression of VEGF, and collagen type I. Acemannan can also enhance the proliferation and migration of the fibroblasts in wound granulation tissue and collagen expression. For the mechanism pathway of acemannan, it can stimulate cell proliferation by influencing the cyclin-dependent cell cycle progress through translational regulation of cyclin D1, which is the main alteration attributed to attracting the transition of G1 to S phase. *Aloe vera* further presents the stimulating effects to elevate the expression of VEGF and TGF-β1 gene in the wound of induced-diabetes rats. TGF-β1, which plays a vital role as an accelerating induced growth factor, has the outstanding potential to enhance the reconstruction of fibroblasts in the ECM in the wound healing process. Following the regenerative process of wound healing, the rearrangement of epithelial tissue in dermal layers occurs, leading to the response of inflammatory cells and the beginning of increased collagen production. Platelet degranulation secretes the TGF-β produced by platelet sources in the wound area and is attributed to the wound healing process [207]. Also, TGF-β enhances the mitosis activity in the human fibroblasts leading to the progression of angiogenesis in many tissues via stimulating the VEGF, the angiogenesis growth factor in epithelial and fibroblast cells as promotes proliferation of fibroblasts, differentiation of myofibroblasts, and formation of ECM. It further modulates and elevates the release of bFGF at the wound edge [208]. Also, β-sitosterol is the compound consisting of mucilaginous gel in *Aloe vera*. It plays a crucial role in enhancing angiogenesis and accelerated healing of traumatic tissues by stimulating the VEGF expression and its receptors at the wounding. Mannose, the monosaccharides comprised in the *Aloe vera*, also provokes the activities of the macrophages in the injured cell by promoting the cytokines and the healing process followed by the activated with its receptor where surrounding located in the membrane of the macrophage cell.

Anti-inflammatory effects of *Aloe vera*

In our body, a defensive system reacts when the body gets injured or damaged, including burns or other skin insults, known as inflammation. This occurrence can be classified as swelling (tumor), pain (dolor), redness (rubor), and heat (calor), as well as a loss of function, respectively. Hence, treating any formulations might suppose to occur various adverse effects due to the complicated process of diseases. The production of the leucocytes coupled with accumulated fluid in the injured wound results in swelling, accelerating the permeability of the capillary. Following the release of short peptides and prostaglandins causes the complex reaction known as pain. The vasodilatation results from the redness and heat, contributing to the reduction of blood pressure and elevation of blood circulation, while this slightly declines. Infection of microorganisms is the adverse factor that causes inflammation, which also includes arthritis, which is the inflammatory condition occurring within the wounds. The inflammatory condition has been studied by various researches, providing a complicated progression associated with several biochemical mechanisms and a diversity of compounds and mediators. Especially, there are three distinct evidences, including

1. Vasoactive substrates

These agents affected the blood vessels dilation and exposure of linkages capillary cells, released by the different contractile substances in endothelial cells. These variations consist of vasoactive amines, bradykinin, and prostaglandins.

2. Chemoattractants

These substances contribute to accelerated cell motility, particularly of white blood cells (leucocytes) into target sites. These comprise several proteins and peptides.

3. Degradative enzymes

Most of them are hydrolytic enzymes that destroy tissue compositions. Proteases individually associate with inflammatory mechanisms, leading to the release of chemotactic factors. As a result, *Aloe vera* is a well-known extraordinary herbal treatment responsible for these adverse conditions, including an inhibitory stimulatory system that accelerates both inflammatory and immune responses [209].

Aloe vera displays the prevention of inflammation by reducing the adhesion of leukocytes. It also plays a role in inflammation by promoting phagocytic and proliferative activity via deterring the

cyclooxygenase (COX) regulations and decreasing the production of prostaglandin E2 (PGE2) [210]. In the primary acute inflammatory phase, transcription activities of albumin and TNF-α genes are associated with this response. Following the administration of aloe-emodin, TNF-α was slightly investigated in the treated liver cell. The histological investigation of aloe-emodin-treated rats found that inflammatory infiltration declined in the lymphocytes and Kuffer cells.

The comparison of the aloin and aloe-emodin with other polyphenols in the anti-inflammatory activity demonstrated that aloe-emodin interrupted the expression of inducible nitric oxide synthase (iNOS) mRNA and production of nitric oxide (NO) in a dose-dependent manner. Furthermore, Aloin presented its remarkable ability to hinder NO and PGE2 production. As a result, it can be implied that both aloin and aloe-emodin have the potential to suppress the responses of inflammatory cytokines by obstructing the expression of iNOS and COX-2 mRNA [211].

Anti-bacterial activities

In the progression of wound healing, antimicrobial or antibacterial activity probably improves this condition through the anti-inflammatory effects. *Aloe vera* exerts the antibacterial property by inhibiting the various bacteria, including gram-positive and gram-negative bacteria and *Streptococcus pyogenes*, *Streptococcus,* and *faecalis Pseudomonas aeruginosa* [212].

Aloe vera is a considerable antibacterial property consisting of many active compounds. Anthraquinones are the one antibacterial agent that provides structure-like tetracycline. This compound plays a similar role as tetracycline which against the synthesis of the bacterial proteins by interrupting the site of ribosomal A, where the entering of the aminoacylated tRNA. As a result, the bacteria are inhibited in the medium containing *Aloe vera* extract. For the bacterial property, polysaccharides consisting of *Aloe vera* exert directly by accelerating the phagocytic leucocytes to inhibit bacteria [213]. Pyrocatechol is a hydroxylated phenol compound in *Aloe vera*, possessing the toxic effect of antibacterial activity. From the scientific proof of glucomannan and acemannan, they provide outstanding activity, including improving wound healing, inducing macrophages, enhancing the immune system, and antibacterial properties. The antimicrobial activity could probably improve the wound healing process by inhibiting bacteria-related inflammation. Mariita et al. reported that *Aloe vera* exerted excellent antibacterial properties against Mycobacterium in the strain of M. fortuitum, M. smeg- matis, M. kansasii, and M. tuberculosis as *P. aeruginosa*, *E. coli*, *S. aureus,* and *S. Typhi* [214].

CHAPTER III

RESEARCH METHODOLOGY

Research Procedures of the study

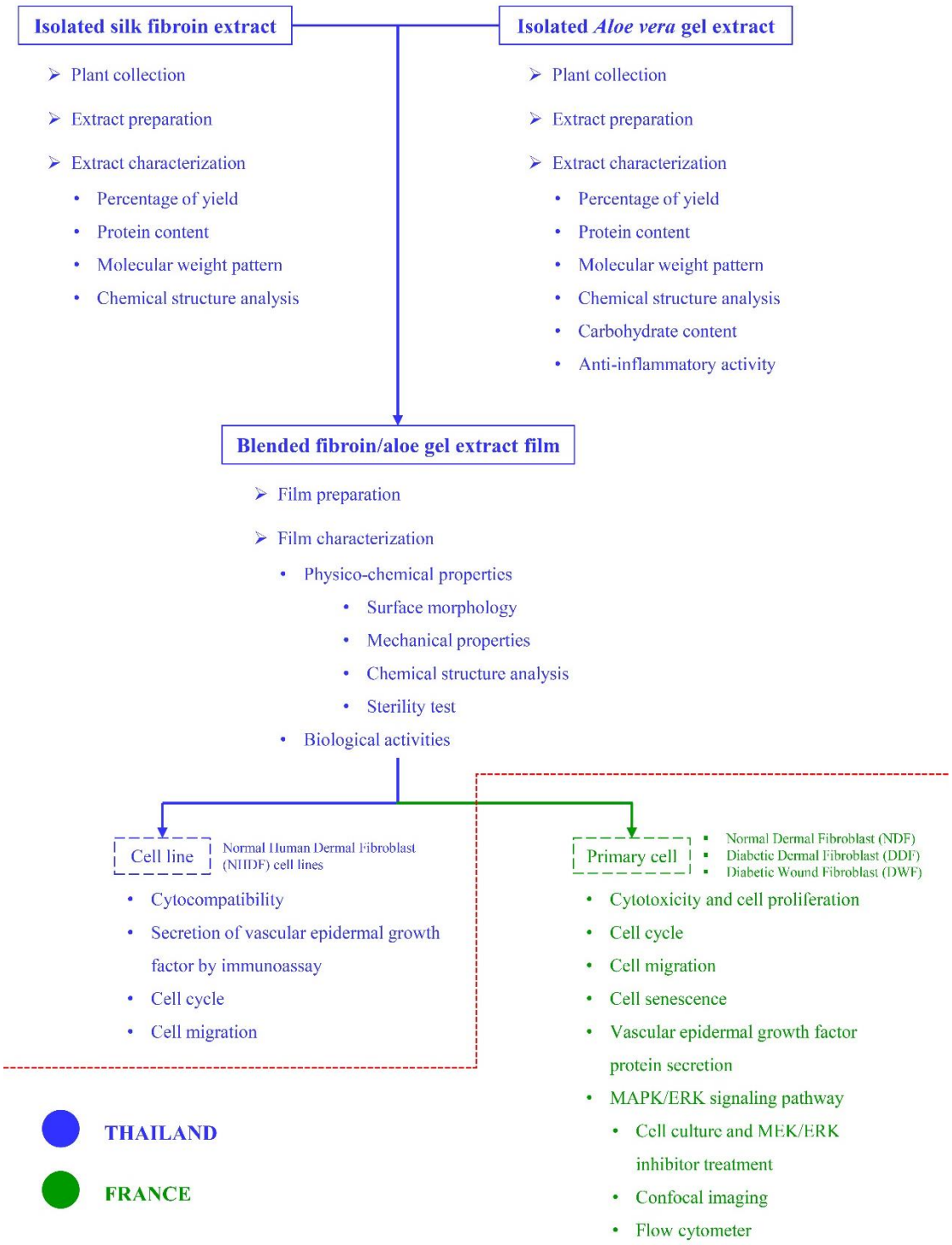

Figure 28 Scope of the study

Chemical and materials

1. Calcium chloride ($CaCl_2$, RCI Labscan, Bangkok, Thailand)
2. Sodium hydroxide (NaOH, RCI Labscan, Bangkok, Thailand
3. Ammonium sulfate ($(NH_4)_2SO_4$, RCI Labscan, Bangkok, Thailand)
4. Lactic acid solution (88%) (Sigma-Aldrich Chemie GmbH, Steinheim, Germany)
5. Sulfuric acid (Sigma-Aldrich Chemie GmbH, Steinheim, Germany)
6. Lipopolysaccharide (LPS, Sigma-Aldrich Chemie GmbH, Steinheim, Germany)
7. Dialysis membrane standard RC tubing (MWCO: 6–8 kDa) (Spectrum Laboratories, Inc., California, USA)
8. Detergent compatible (DC) protein assay kit from BIO-RAD Laboratories, Philadelphia, USA)
9. Phenol (AppliChem GmbH, Darmstadt, Germany)
10. Modified Eagle's Medium (DMEM, Sigma-Aldrich Co., Missouri, USA and PAN Biotech, Dominique Dutscher, Bernolsheim, France)
11. Fetal bovine serum (FBS, Sigma-Aldrich Co., Missouri, USA and PAN Biotech, Dominique Dutscher, Bernolsheim, France)
12. 0.25% trypsin/0.01M EDTA (Sigma-Aldrich Co., Missouri, USA)
13. Penicillin/streptomycin solution (10,000 U/m) (Gibco, Invitrogen, Massachusetts, USA and PAN Biotech, Dominique Dutscher, Bernolsheim, France
14. Amphotericin B (250 µg/ml) (Gibco, Invitrogen, Massachusetts, USA)
15. Cell proliferation kit II (2,3-bis (2-methoxy-4-nitro-5-sulphophenyl)-5-[(phenylamino)carbonyl]-2H-tetrazoliumhydroxide, XTT, Roche Diagnostics GmbH, Mannheim, Germany)
16. Mueller Hinton agar (HiMedia, Mumbai, India)
17. Muse™ Cell Cycle Assay Kit SDS (MERCK, Darmstadt, Germany)
18. Phosphate Buffer Saline (DPBS) (PAN Biotech, Dominique Dutscher, Bernolsheim, France)
19. Thiazolyl Blue Tetrazolium Bromide (MTT reagent, Sigma-Aldrich Co., Missouri, USA)
20. Dimethyl Sulfoxide (DMSO, Sigma-Aldrich Co., Missouri, USA)
21. 4′,6-Diamidine-2′-phenylindole dihydrochloride (DAPI, Sigma-Aldrich Co., Missouri, USA)
22. Bovine Serum Albumin (BSA, Sigma-Aldrich Co., Missouri, USA)

23. Propidium Iodide (PI, Sigma-Aldrich Co., Missouri, USA)
24. Copper (II) sulfate solution (Sigma-Aldrich Co., Missouri, USA)
25. Bicinchoninic Acid solution (Sigma-Aldrich Co., Missouri, USA)
26. Protease Inhibitor Cocktail (Sigma-Aldrich Co., Missouri, USA)
27. Triton™ X-100 (Sigma-Aldrich Co., Missouri, USA.)
28. 4% Formaldehyde solution (Sigma-Aldrich Co., Missouri, USA)
29. ERK inhibitor PD98059 (Sigma-Aldrich Co., Missouri, USA)
30. Phalloidin-Tetramethylrhodamine B isothiocyanate (Sigma-Aldrich Co., Missouri, USA.)
31. Senescence cells histochemical staining kit (Sigma-Aldrich Co., Missouri, USA)
32. Human VEGF ELISA kit (Diaclone, Besançon, France)
33. Cell Proliferation BrdU ELISA assay (MERCK, Darmstadt, Germany)
34. Ethanol 96% (EtOH, Carlo Erba, Val-de-Reuil, France)
35. Rabbit anti-human Phospho-p44/42 MAPK (ERK1/2) (Cell signaling TECHNOLOGY®, Massachusetts, USA)
36. Rabbit anti-human p44/42 MAPK (ERK1/2) (Cell signaling TECHNOLOGY®, Massachusetts, USA)
37. Goat anti-rabbit IgG-Alexa Fluor® 488 conjugate (Cell signaling TECHNOLOGY®, Massachusetts, USA)
38. Rabbit IgG Isotype antibodies (mAb, Cell signaling TECHNOLOGY®, Massachusetts, USA)
39. Fluoromount G® (Southern Biotech, Alabama, USA)

Instruments

1. Fourier transform infrared spectroscopy (FTIR spectrometer, Spectrum GX series, USA)
2. Magnetic stirrer (Heidolph, MR3001, ITS group, Bangkok, Thailand)
3. Hot air oven (UFP800DW, MEMMERT, Schwabach, Germany)
4. Blender (HR2020, PHILIPS, Amsterdam, Netherlands)
5. Freeze dryer (FTS systems Dura dry type FD 95C12, LabX, Ontario, Canada)
6. Laminar flow (ClassII-A/B3 Biological Safety Cabinet, BEC THAI, Bangkok, Thailand)
7. Incubator (VO400cool, MEMMERT, Schwabach, Germany)

8. Texture analyzer (TA.XT Plus, Stable Micro Systems, Ltd, Godalming, UK)
9. Rotary-Pumped Carbon Coater (Q150RS, Quorum, Laughton, UK)
10. Scanning electron microscopy (EDAX®, LEO1455VP, New Jersey, USA)
11. pH meter (PL-700, Gondo, Nangang, Taiwan)
12. Conductivity Benchtop Meter (Lab 955, Xylem Analytics Germany Sales GmbH & Co. KG, WTW, Weilheim, Germany)
13. Microplate reader (Eon™, BioTek instrument, Vermont, USA)
14. Confocal microscope (A1 HD25/A1R HD25, Nikon®, Tokyo, Japan)
15. Flow cytometry (Guava®easyCyte™, Merck Millipore, Massachusetts, USA)
16. Spectrophotometer (MULTISKAN FC, ThermoScientific, USA)
17. LSR Fortessa Flow Cytometer (Becton Dickinson, New Jersey, USA)
18. IncuCyte®S3 system (Sartorius, Goettingen, Germany)
19. Laser scanning confocal microscope (LSM 800, Zeiss, Oberkochen, Germany)

Plant collection

Silkworms yellow cocoons

Yellow Silkworms cocoons (*Bombyx mori* Linn., Nang-Laai strain) were kindly contributed by Queen Sirikit Sericulture Center, Chiang Mai province, Thailand.

Aloe vera leaves

Aloe vera plants were collected from the *Aloe vera* cultivated farm in Phrom Phiram District, Phitsanulok province, Thailand. They were then planted in the natural herbal garden in the Faculty of Pharmaceutical Sciences, Naresuan University, Thailand.

Preparation of the extracts

Preparation of silk fibroin extract

Silk fibroin extract was extracted according to a previous study with some modifications [14, 16, 215]. Briefly, silkworm cocoons were cut into small pieces and heated in deionized (DI) water at the temperature of 85-90°C for 2h. The sericin was removed then by boiling in the solution of 25mM NaOH at 70°C for 30 mins. The obtained degummed fibers were washed with DI water (3 times) and dried in the oven at 45-50°C overnight. The dried degummed silks will be dissolved in 3M $CaCl_2$ solution (1g of

samples to 60 mL of $CaCl_2$) at 85-90°C for 4-6 h. The resulting solution was filtered and dialyzed against 15 megaΩ water until salts were completely removed at 23±2°C for 2 days by changing the water every 4-6 h. The desalted silk protein was then brought to centrifuge at 8,000 rpm at 4°C for 15 mins. Finally, the supernatants were collected and lyophilized for 72 h and kept in the desiccator at 25±2°C until used. The dry silk fibroin extract was calculated as the percentage of the total extract yield.

Preparation of *Aloe vera* gel extract

Aloe vera extract was isolated, followed by a previous experiment with some modifications [14, 16, 215]. The fresh leaves of *Aloe vera* were cleaned and rinsed with DI water to remove the excess yellow bitter juice (exudate). The colorless aloe gel was collected and grounded to homogeneity by blender followed by centrifuged at 12,000 rpm at 4°C for 15 mins. The crude extract solution was precipitated with 55% $(NH_4)_2SO_4$ and stored at 4°C overnight. After that, the precipitated crude extract solution was centrifuged at 12,000 rpm at 4°C for 15 mins to collect the precipitated and dissolve it with DI water. The resultant solution was then dialyzed against 15 megaΩ water until salts were completely removed at 23±2°C for 2 days by changing the water every 6 h and brought to lyophilize for 72 h following by keeping in the desiccator at 25±2°C until used. The dry aloe gel extract was calculated as the percentage of the total extract yield.

Characterizations of the extracts

Protein determination

DC protein assay kit was used to analyze the protein content in the extracts. The standard protein or Bovine serum albumin (BSA) was diluted in various concentration (0.125, 0.25, 0.50, 1.00, 2.00, 3.00, 4.00 and 5.00 mg/mL). The extract was prepared at a concentration of 1 mg/mL. Five µl of standard protein or sample was pipetted into a 96-well plate. Twenty-five µl of reagent A (BioRad) and 200 µL of reagent B (BioRad) were pipetted into each well. The standard proteins and samples were incubated in the dark at room temperature (RT) for 15 mins. At that time, they were brought to measure the absorbance at 750 nm by a microplate reader.

$$\% \text{ Protein content} = \frac{\text{Concentration in the standard curve}}{\text{Concentration in the sample}} \times 100$$

Molecular weight pattern

The molecular weight pattern of the protein extracts was performed using the Sodium dodecyl sulfate-polyacrylamide gel electrophoresis (SDS-PAGE) method. The lyophilized extract was qualitatively analyzed in 5% stacking gel and 15% separating gel. To check the molecular weight of the extract 10 mg/mL of lyophilized extract was dropped in each well. Finally, the gel was stained in Coomassie Brilliant Blue R-250 solution for 2 h and de-stained with a destaining solution (1% acetic acid, 10% methanol in water).

Fourier Transformed Infrared (FTIR) spectroscopy

The chemical characteristic of fibroin was analyzed by the Fourier Transform Infrared (FTIR) spectroscopy technique. The extract was ground with KBr in an equal proportion to form pellets that were subjected to FTIR analysis. The spectra were scanned over the wavenumber in the range of 4,000 cm^{-1} to 400 cm^{-1}.

Carbohydrates determination of the isolated aloe gel extract

Phenol-sulfuric acid was a method that detects virtually all classes of carbohydrates. Five milligrams of lyophilized aloe gel extract were dissolved in 1 mL of DI water. D-Glucose monohydrate was used as the standard protein. D-Glucose monohydrate was dissolved in DI water in various concentrations (0.25, 0.125, 0.06, 0.03 and 0.015 mg/mL). Twenty-nine µl of standard glucose or *Aloe vera* extract solution was then added to a 96-well plate. After that, 29 µL of 5% phenol was added to each well, followed by 143 µL of concentrated sulfuric acid. The mixed solution was protected light, incubated at 80°C for 30mins in a water bath, and measured for absorbance at 490 nm by a microplate spectrophotometer.

$$\% \text{ Carbohydrate content} = \frac{\text{Concentration in the standard curve}}{\text{Concentration in the sample}} \times 100$$

In vitro assay by cell culture of the isolated aloe gel extract

Cytotoxicity

The cell culture by using RAW 264.7 cells. The raw cell ($1x10^4$ cell/well) was seeded in a 96-well plate and incubated at 37°C in a 5% CO_2 incubator for 24 h. The old medium was discarded and washed with sterilized PBS (pH 7.4). The cells were then treated with a serum-free medium of aloe gel extract in various concentrations (12.5, 25, 50, 100, and 200 µg/mL). They were incubated at 37°C in a CO_2 incubator for 24 h. At that time, the cell viability was quantified by sodium 3'-[-1-

(phenylaminocarbonyl)-3,4-tetrazolium]-bis(4-methoxy-6-nitro) benzene sulfonic acid hydrate] (XTT) assay. The supernatant was collected and brought to measure the absorbance at 490 nm using a spectrophotometer. The experiment was performed in triplicate (n = 3) per condition. Additionally, the concentration of aloe gel extract, showing non-cytotoxicity activity as compared to the control group (untreated RAW264.7 cells), was further selected to determine the anti-inflammation activity.

Anti-inflammation assay

To perform this experiment, Lipopolysaccharide (LPS) was used to activate the expression of the pro-inflammatory cytokine TNF-alpha. Firstly, the RAW 264.7 cells ($1x10^4$ cell/well) were cultured in a 96-well plate and incubated at 37˚C in a 5% CO_2 incubator for 24 h. At that time, the incubated medium was discarded and treated with serum-free medium containing *Aloe vera* extract in the various concentrations (6.25-100 µg/ml) for 1 h. and subsequently activated with the final concentration of 1 µg/mL LPS into each well for 24 h. After activating the cell, the supernatant was collected and brought to perform the anti-inflammation assay, quantified by TNF-alpha mouse ELISA Kit. The TNF-alpha released was expressed as a percentage of reduction compared with LPS-untreated cells (negative control) and LPS-treated cells (positive control). The experiment was performed in triplicate (n = 4) per condition.

Preparation of sterilized blended fibroin/aloe gel extract film

The method for film formation was modified from a previous study [14, 16, 215]. Briefly, 540 mg of lyophilized fibroin was dissolved in 10 mL of lactic acid solution (pH 4.0±2), and 15 mg of *Aloe vera* extract was dissolved in 5 mL of lactic acid solution. Both solutions were agitated with a magnetic stirrer and mixed continuously at RT for 2 h. The mixed solution was added to the mold (6x6 cm^2) and allowed to dry at 47±2°C for 4 h. In this study, the gamma irradiation technique (facilitated by THAI ADHESIVE TAPES INDUSTRY CO., LTD., Bangkok, Thailand) was used to sterilize the developed film.

Characteristics of sterilized blended fibroin/aloe gel extract film

Physico-chemical characteristics of blended fibroin/aloe gel extract film

Surface morphology

Morphology of the surface of sterilized and non-sterilized blended fibroin/aloe gel extract film was coated with Au^+ particles by cathodic spreading in a Rotary-Pumped Sputter Coater/Carbon

Coater and examined under a Scanning Electron Microscope, SEM with the operating at an accelerating voltage of 15 kV.

Mechanical properties

Texture analyzer was performed for measuring maximum force and elongation at break of sterilized and non-sterilized blended fibroin/aloe gel extract film. They were cut into a rectangular shape (10x50 mm^2), and the thickness was approximately 0.05 mm. The samples were clamped and adhered tape on the top and end using a 50 kg, 49 N load cell. The crosshead rate set in the test was 1.00 mm/sec, and the distance between grips used was 30 mm. At least three samples of the sterilized and non-sterilized film in dried and wet states (soak in 95% EtOH for 1 h) were tested for each set, being average values reported.

Fourier transformed infrared spectroscopy

The chemical characteristic of fibroin will be analyzed by the FTIR spectroscopy technique. The sterilized and non-sterilized blended fibroin/aloe gel extract film were ground with KBr in proportion to form pellets subjected to FTIR analysis. The spectra were scanned over the wavenumber in the range of 4,000 cm^{-1} to 400 cm^{-1}.

Sterility test by using agar gel plate technique

The agar plate culture technique was used to test microbial contamination of the sterilized film. The sterilized dressing was received from THAI ADHESIVE TAPES INDUSTRY CO., LTD. using sterilization techniques by gamma irradiation. The sterilized film was compared with non-sterilized film by placing the film on a nutrient agar medium for a contamination test. The nutrient agar culture was incubated at 37°C for 24 h. The results were recorded. In the case that showed colonies of microbes or bacteria growth, it was contamination.

Biological activities of the blended fibroin/aloe gel extract film

Fibroblast cell culture

In this study, fibroblast cells were classified into 2 major types: Cell line and Primary cell

Cell line

Normal Human Dermal Fibroblast (NHDF) cell lines (Lot no. C-12302) were purchased from Promocell, Eppelheim, Germany.

Cells were cultured in complete DMEM supplemented with 10% FBS and 1% PS (10,000 U/mL Penicillin, and 10 mg/mL Streptomycin) at 37°C in a humidified 5% CO_2 atmosphere. Cells were trypsinized when they reached a confluency of 80% and used up to passage 8.

Cytocompatibility

NHDF cells ($1x10^5$ cell/well) were seeded in 24-well plates for 24 h. The incubated medium was then replaced with a serum-free medium. The sterilized film was cut into a circle shape with a diameter of 6 mm (4.56 mg) and placed in trans-well cell seeding. Subsequently, they were put into each well with the adherent fibroblasts for 24 h. After treating cells, the trans-wells were removed, followed by immersed medium was discarded and replaced with 250 µL of serum-free medium and XTT reagent for 4 h. The supernatant was measured the absorbance at 490 nm using a microplate reader. The experiment was performed in triplicate (n = 3) per condition. Additionally, the percentage of viability of the control group (untreated fibroblasts) was adjusted to 100% and compared with the treated group (developed film).

Secretion of VEGF by immunoassay

The production of VEGF by fibroblast cells stimulates the formation of blood vessels (angiogenesis). The qualitative evaluation was performed using the Anti-VEGFA antibody (ab39250, Abcam, Massachusetts, USA). Briefly, film extracts were prepared by incubating 1x1 cm^2 sterilized films in 1 mL of DMEM serum-free and incubated for 24 h. NHDF) cell ($1x10^5$ cell/well) was seeded in cell culture slide with DMEM containing 10% FBS and incubated for 24 h. The incubated medium was then replaced with a serum-free medium and film extract. After treating cells, the cells were fixed with 4% paraformaldehyde in PBS pH 7.4 for 10 mins at RT, followed by permeabilizing with 0.1% Triton X-100 and washed cells in PBS three times for 5 mins. For Blocking and immunostaining, the cells were incubated with 1% BSA, 22.52 mg/mL glycine in PBST (PBS+0.1% Tween 20) for 30 mins to block unspecific binding of the antibodies and then incubated with anti-VEGF antibody (diluted in 1% BSA in PBST) in a humidified chamber for 1 h at RT or overnight at 4°C. At that time, the solution was decanted and washed the cells three times in PBS, 5 mins each wash. Then, the cells were incubated with the secondary antibody in 1% BSA for 1 h at RT in the dark. The secondary antibody solution was decanted and washed three times with PBS for 5 mins each in the dark. For counter staining, the cells were

incubated with 100 µL of Hoechst stain or DAPI (DNA stain) for 1 min and rinsed with PBS. Finally, the mounting method, the coverslips were mounted with a drop of mounting medium, sealed with nail polish to prevent drying and movement under a microscope, and stored in the dark at 4°C.

Cell migration

The cell migration was performed by the scratch assay, typically utilized to quantify the migration of cells on two-dimensional (2-D) surfaces over time which is performed and modified following this study [216]. NHDF cells ($1x10^5$ cell/well) were seeded in a 24-well plate and incubated for 24-48 h allowing the cells were grown to confluency in a monolayer. The scratch was then made with a pipette tip to create an incision-like gap. After that, the cells were washed twice with sterilized PBS (pH 7.4) followed by replaced with 800 µL of DMEM serum-free. The sterilized dressing was cut into a circle shape of a diameter of 6 mm and placed into trans-well cell seeding. The wounded area was photographed immediately after wounding and at defined time points (0, 12, 24, and 36 h) after that, cell migration was monitored as completed closure of the scratching gap by visualization under an inverted microscope. The experiment was performed in triplicate (n = 3) per condition.

Cell cycle

The analysis of the cell cycle is the quantitation of DNA content which was determined by flow cytometry by the alteration method according to [217]. NHDF cells ($1x10^5$ cell/well) were seeded in a 24-well plate and incubated for 24 h. The incubated medium was then replaced by DMEM serum-free, and the trans-well cell containing sterilized dressing (diameter of 6 mm) was put into each well with the adherent fibroblasts for 24 h. After incubation time, the immersed medium was discarded and replaced with 0.25%Trypsin/0.01M EDTA to trypsinize the cell. The cells were then counted in the amount of $2x10^5$ cells/ml and centrifuged to discard the supernatant, followed by washing the cell with PBS (pH7.4). The cells were fixed with 70% EtOH for 3 h. The fixed solution was replaced by PBS (pH7.4) to wash the cell, and then the cells were stained with 150 µL of Muse™ Cell Cycle Assay Kit reagent at RT for 30 mins (light protection). After incubation, the strained cells were measured by the cell cycle assay using Guava® easyCyte Flow Cytometer (Merck Ltd, Darmstadt, Germany). The experiment was performed in triplicate (n = 3) per condition. Additionally, the percent of total cells for each phase of the cell cycle

(G0/G1, S, and G2/M), as well as chromatogram profiles and flow cytometry dot plots of the control group (untreated fibroblasts), were compared with the treated group (developed film).

Primary cells

Primary fibroblast cells were classified into 3 groups: Normal Dermal Fibroblast (NDF), Diabetic Dermal Fibroblast (DDF), and Diabetic Wound Fibroblast (DWF). NDF and DWF were obtained from one patient undergoing skin-abdominal plastic surgery and one patient with diabetic foot ulcers. The experiment was approved by the medical ethics committee of Besançon University Hospital, France, and patients were informed about the purpose of the research study and provided written consent. Fibroblasts' isolation and culture methods were consistent with previous reports [218]. DDF was purchased from PELOBIOTECH GmbH, Germany.

Cells were cultured in complete DMEM supplemented with 10% FBS and 1% PS (10,000 U/mL Penicillin, and 10 mg/mL Streptomycin) at 37°C in a humidified 5% CO_2 atmosphere. Cells were trypsinized when they reached a confluency of 80% and used up to passage 8.

Cytotoxicity and cell proliferation

The fibroblast cells ($1x10^4$ cell/well) using NDF, DDF, and DWF were seeded in a 96-well plate and incubated for 24 h. At that time, the incubated medium was discarded and washed with sterilized PBS (pH 7.4) followed by replaced with DMEM serum-free (w/o FBS), DMEM containing 2% FBS (2% FBS), and film extracts made by incubating 1x1 cm^2 sterilized developed films in 1 mL of DMEM serum-free and incubated for 24 h. The cell viability was quantified by MTT assay. The 3-(4,5-dimethylthiazol-2-yl)-2,5-diphenyltetrazolium bromide (MTT) assay was used to determine the cytotoxicity assay of developed film to primary fibroblast cells. The supernatant was collected and brought to measure the absorbance at 517 nm using a spectrophotometer. The experiment was performed in triplicate (n = 8) per condition. Additionally, the percentage of viability of the control group (DMEM w/o FBS) will be adjusted to 100% and compared with the treated group (DMEM with 2% FBS and film extract).

The quantification cell of proliferation assay was performed by colorimetric BrdU assay. Briefly, NDF, DDF, and DWF ($1x10^4$ cell/well) were seeded in 96-well plate and incubated for 24 h. At that time, the incubated medium was discarded and washed with sterilized PBS (pH 7.4)

followed by replaced with DMEM w/o FBS, DMEM 2% FBS, and film extracts and incubated for 24 h. The cell proliferation was quantified by BrdU assay kit. Briefly, treated cells were replaced by 100 µL of BrdU labeling solution and incubated at 37°C for 24 h. The incubated BrdU labeling solution was then replaced by 200 µL of Fixdent and incubated at RT for 30 mins, followed by 100 µL of Anti-BrdU-POD working solution at RT for 2 h. At that time, the supernatants were discarded and washed with 1x PBS (3 times). One hundred µL of substrate solution was then added and incubated at RT for 15-30 mins, followed by added 25 µL of 1M sulfuric acid. The supernatant was collected and brought to measure the absorbance at 450 nm using spectrophotometer. The experiment was performed in triplicate (n = 8) per condition. Additionally, the percentage of cell proliferation of the control group (DMEM w/o FBS) will be adjusted to 100% and compared with the treated group (DMEM with 2% FBS and film extract).

Cell cycle

The analysis of the cell cycle is the quantitation of DNA content which was determined by flow cytometry by the alteration method according to [215]. Fibroblast cells (NDF, DDF, and DWF) ($1x10^5$ cell/well) were seeded in a 6-well plate and incubated for 24 h. The incubated medium was discarded and washed with sterilized PBS (pH 7.4) followed by replaced with DMEM w/o FBS, DMEM 2% FBS, and film extracts and incubated for 24 h. After incubation time, the supernatant was discarded and washed with sterilized PBS (pH 7.4), followed by adding 0.25%Trypsin/0.01M EDTA to trypsinize the cell. The cells were then counted in the amount of $2x10^5$ cells/ml and centrifuged at 1,100 rpm for 5 mins to discard the supernatant. The cells were fixed with 70% EtOH at 4°C overnight. The fixed solution was added directly with cold PBS (pH7.4) to wash the cell and centrifuged at 1,100 rpm at 4°C for 5 mins to discard the supernatant (2 times). The cells were stained with 300 µL of mixture IP staining reagent (light protection). The strained cells were measured by the cell cycle assay using LSR Fortessa Flow Cytometer (Becton Dickinson, France). The experiment was performed in triplicate (n = 3) per condition. Additionally, the percent of total cells for each phase of the cell cycle (G0/G1, S, and G2/M), as well as chromatogram profiles and flow cytometry dot plots of the control group (DMEM w/o FBS), was compared with the treated group (DMEM with 2% FBS and film extract).

Cell migration

The cell migration was performed by the scratch assay, typically utilized to quantify the migration of cells on two-dimensional (2-D) surfaces over time which is performed and modified following this study. NDF, DDF, and DWF ($3x10^5$ cell/well) were seeded in a 96-well plate and incubated for 24 h allowing the cells were grown to confluency in a monolayer. The scratch was then made by Incucyte® cell migration kit (Cat. no. 4563, Sartorius, Goettingen, Germany) to create an incision-like gap. After that, the cells were washed twice with sterilized PBS (pH 7.4), then replaced with DMEM w/o FBS, 2% FBS, and film extract for 48 h. The scratched areas were photographed immediately after scratching at defined time points (every 2 h) for 48 h. After incubation, cell migration was observed as completed closure of the scratching gap by visualization by IncuCyte®S3 (Cat. No. 4763, Sartorius, Goettingen, Germany) and the percentage of relative wound density. The experiment was performed in triplicate (n = 5) per condition.

Cell senescence

Fibroblast cells (NDF, DDF, and DWF) ($1x10^4$ cell/well) were seeded in 96-well plate and incubated for 24 h. The incubated medium was discarded and washed with sterilized PBS (pH 7.4) followed by replaced with DMEM w/o FBS, DMEM 2% FBS, and film extracts and incubated at 37°C in 5% CO_2 incubator for 24 h. The cell senescence was quantified by Senescence cells histochemical staining kit. Briefly, the cells were washed twice with PBS and fixed with 1x Fixation buffer for 5 mins. The fixed cells were washed with s PBS (3 times) and stained with a Staining mixture at 37°C for 24 h (without CO_2 atmosphere). After incubation, the stained cells were washed with PBS (3 times) and stained with DAPI (DNA stain) for 10 mins, and rinsed with PBS for 5 mins (3 times). The cells were observed under an inverted fluorescence microscope (Olympus IX50, Tokyo, Japan). The SA-β-Gal cell (blue-stained cell) was counted as the cell senescence. The percentage of cell senescence was presented as (SA-β-Gal positive cell/total cell)x100. The experiment was performed in triplicate (n = 8) per condition.

Vascular epidermal growth factor protein secretion

NDF, DDF, and DWF (2×10^5 cells/well) were seeded in 12-well plate and incubated for 24 h. The incubated medium was replaced by DMEM w/o FBS, 2% FBS, and film extract

for 24 h. Supernatants were collected with 10% v/v anti-protease solution. The concentration of VEGF from the supernatant was assessed using a VEGF ELISA kit following the manufacturer's protocol. Briefly, 50 µL of assay solution was added, followed by 200 µL of standards or cell culture supernatant, and incubated at RT for 2 h. Then 200 µL of Human VEGF-conjugated antibody was added and incubated at RT for 2 h. After washing, 200 µL of substrate solution was added and incubated at RT for 30mins. The reaction was stopped with 50 µL of stop solution. Then, absorbance was measured at 450 nm using a spectrophotometer. The amount of VEGF was expressed in pg/mg protein. Protein content was determined by Bradford assay with BSA as the protein standard. Briefly, BSA standard solution (concentration 0-2 mg/mL) and samples were distributed separately, followed by adding 200 µL of Pierce solution (20 µL of Copper(II) sulfate:1,000 µL of Bicinchoninic acid solution). The samples were incubated at 37°C for 30 mins and measured the absorbance at 571 nm using a spectrophotometer. The experiment was performed in triplicate (n = 4) per condition.

MAPK/ERK signaling pathway

Cell culture and MEK/ERK inhibitor treatment

NDF was cultured in a 12-well plate in a complete DMEM for 24 h. The incubated DMEM was then replaced by DMEM w/o FBS with or without PD98059 solution (concentration of 10 µM) for 1 h, followed by 24 h incubation in DMEM w/o FBS, 2% FBS, and film extract. At that time, the cell proliferation assay was quantified by the BrdU assay kit described above.

Confocal imaging

NDF ($1x10^5$ cell/well) was cultured on the coverslips in a 12-well plate in a complete DMEM for 24 h. The incubated DMEM was then replaced by DMEM w/o FBS with or without PD98059 solution (concentration of 10 µM) for 1 h. The cells were washed and incubated with DMEM w/o FBS, 2% FBS or film extract for 1 and 24 h. After treating cells, the cells were fixed by 4% PFA in PBS pH 7.4 for 10 mins at RT followed by permeabilizing with 0.1% Triton X-100 for 10 mins and washed cells in PBS three times for 5 mins. For Blocking and immunostaining, the cells were incubated with 5% goat serum + 0.3% Triton X-100 in PBS for 1 h at 4°C to block the unspecific binding of the antibodies and then incubated with phospho-p44/42 MAPK (ERK1/2) (Thr202/Tyr204) XP® rabbit mAb (1:200 in diluent (PBS with 1% BSA + 0.3% Triton X-100)) in a humidified chamber at 4°C for overnight. At that time, the solution

was decanted and washed the cells three times in PBS, 5 mins each wash. Then, the cells were incubated with goat anti-rabbit IgG Alexa Fluor®488-conjugated secondary antibody (1:100 in diluent) for 1 h at 4°C. The secondary antibody solution was then decanted and washed three times with PBS for 5 mins each in the dark. For counter staining, the cells were incubated with 100 µL of Hoechst stain or DAPI (DNA stain) for 5 mins to visualize nuclei and rinsed with PBS. Finally, the mounting method, the cover slips were mounted with a drop of Fluoromount reagent to prevent drying and movement under a microscope and stored in the dark at 4°C. The immunofluorescence images were captured with LSM 800 laser scanning confocal microscope (Zeiss, Germany).

Flow cytometer

NDF ($6x10^5$ cell/well) was cultured in a 12-well plate in a complete DMEM for 24 h. The supernatant was then discarded and replaced with DMEM w/o FBS, 2% FBS, and film extract for 24 h. After treating, cells were detached and fixed with 4% PFA at RT for 10 mins. After washing, the cells were permeabilized with 0.1% Triton X-100 for 15 mins and washed cells in PBS three times for 5 mins. The permeabilized cells were suspended in blocking buffer containing 5% goat serum + 0.3% Triton X-100 in PBS for 1 h at 4°C followed by incubating overnight at 4°C with p44/42 MAPK (ERK1/2) Rabbit mAb (1:400 in diluent), phospho-p44/42 MAPK (ERK1/2) (Thr202/Tyr204) XP®rabbit mAb (1:800 in diluent) and rabbit mAb Isotype control (1:200 in diluent). At that time, the solution was decanted and washed the cells three times in PBS, 5mins each wash. The cells were then incubated with goat anti-rabbit IgG Alexa Fluor®488-conjugated secondary antibody (1:100 in diluent) for 1 h at 4°C. Finally, cells were washed the cells three times in PBS, 5 mins each wash, suspended in 2 mM EDTA/PBS and analyzed on a flow cytometer (LSR Fortessa, Becton Dickinson, USA). FACS analysis was performed using FACSDiva software (Becton Dickinson). Twenty thousand events were recorded for each sample. The results are mean values of Fluorescence Intensity ± SD of triplicate (n = 4) per condition.

The statistics analysis

The mean, standard deviation (SD), and frequency of collected data were determined by paired *t*-test. The significance criteria for the correlation measurement were set at *** $p<0.001$, ** $p<0.01$, * $p<0.05$. The experiment was performed in triplicate.

CHAPTER IV

RESULTS AND DISCUSSIONS

Characteristics of the fibroin extract

The lyophilized fibroin extract prepared from silkworm cocoons (Nang-Laai strain) presented yellowish cotton-like characteristics (Figure 29A). One gram of silk cocoons yielded 0.58 g (58% w/w) of the extract corresponding to our previous report . A DC protein assay showed a protein content of 97.43±0.44% w/w of the extract.

Infrared spectra obtained using FTIR spectroscopy showed the frequency peaks at 1634 (amide I), 1513 (amide II), and 1232 (amide III) cm^{-1} (Figure 29B). Amide I is useful for the analysis of the secondary structure of the proteins and is mainly related to the C=O stretching, and it occurs in the range of 1696-1611 cm^{-1}. Amide II, which falls in 1550-1501 cm^{-1} range, is related to the N-H bending and C-H stretching vibration. Amide III occurs in the range of 1320-1200 cm^{-1}, resulting in a phase combination of C-N stretching and C=O bending vibration. The presence of amides I, II, and III and the random coil groups in the FTIR spectrum confirmed that the extract structure consists of water-soluble random coil conformation [219].

The SDS-PAGE method was used to check the molecular weight pattern of silk fibroin as show in Figure 29C. The appearance of the smeared band may result from degradation of the heavy (H) chain (325-350 kDa) of silk fibroin protein through the dissolving process. For the band at 17-25 kDa, it is related to the light (L) chain of fibroin [161]. The SDS-PAGE result indicated a specific L-chain band at approximately 25 kDa and a smear brand of H-chain range of 30 to 245 kDa.

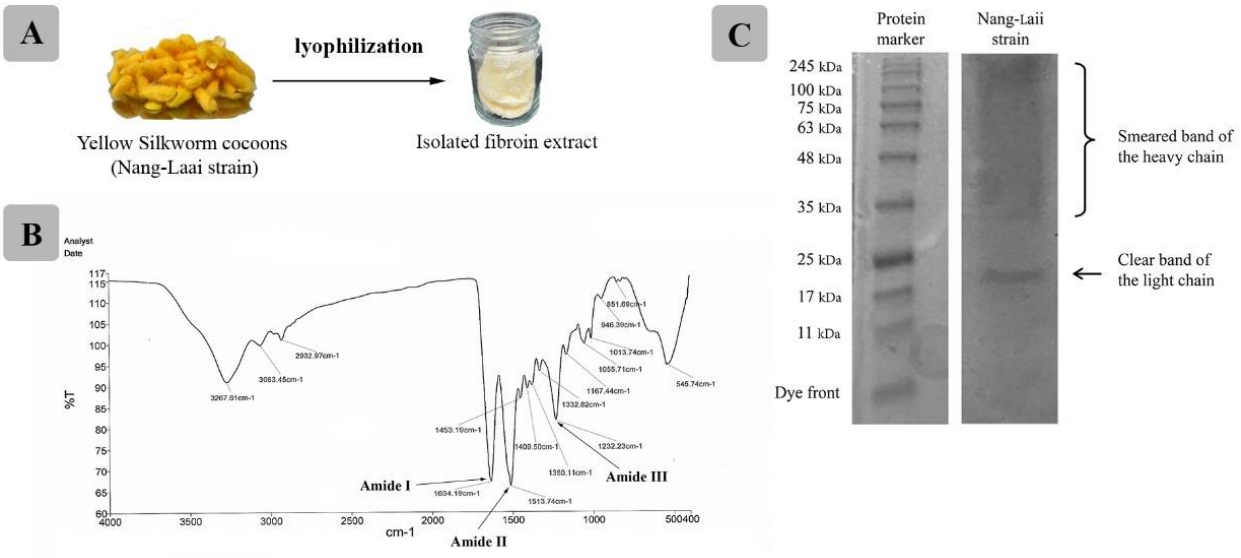

Figure 29 Physical characteristic (A) Infrared spectrum (B) and molecular weight pattern of the isolated fibroin extract prepared from yellow silkworm cocoons (Nang-Laai strain) (C)

Characteristics of the aloe extract

The lyophilized extract of the *Aloe vera* gel showed white cotton-like characteristics (Figure 30A), and 100 g of the gel produced 6 g (0.06% w/w) of the extract were similar to our previous findings [14]. The protein content in the extract was 6.86±1.15% w/w of the extract. For the content of carbohydrates that is also important for the healing capacity of the extract, the amount of carbohydrate found was 58.76±4.89% w/w of the lyophilized aloe gel extract.

Figure 30B demonstrated the IR spectra of the lyophilized aloe gel extract with 55% $(NH_4)_2SO_3$ precipitated, indicating peak at 1731 (O-acetyl ester), 1238 (O-acetyl ester), 1059 (glucan units), 955 (pyranoside ring), and 807 (mannose) cm^{-1}. The FTIR spectrum showed the presence of functional groups, including glucan units, pyranoside, and mannose, relating to the anti-inflammatory and healing activities of the aloe gel extract [199, 220].

The molecular weight pattern of the extract contained in the anti-inflammatory characteristic of aloe protein with molecular weights in range of 20 to 100 kDa showed a clear band at approximately 14 and 35 kDa (Figure 30C), also indicating the activities of anti-inflammatory [221], hemagglutinating and mitogenic activities [222] of the extract.

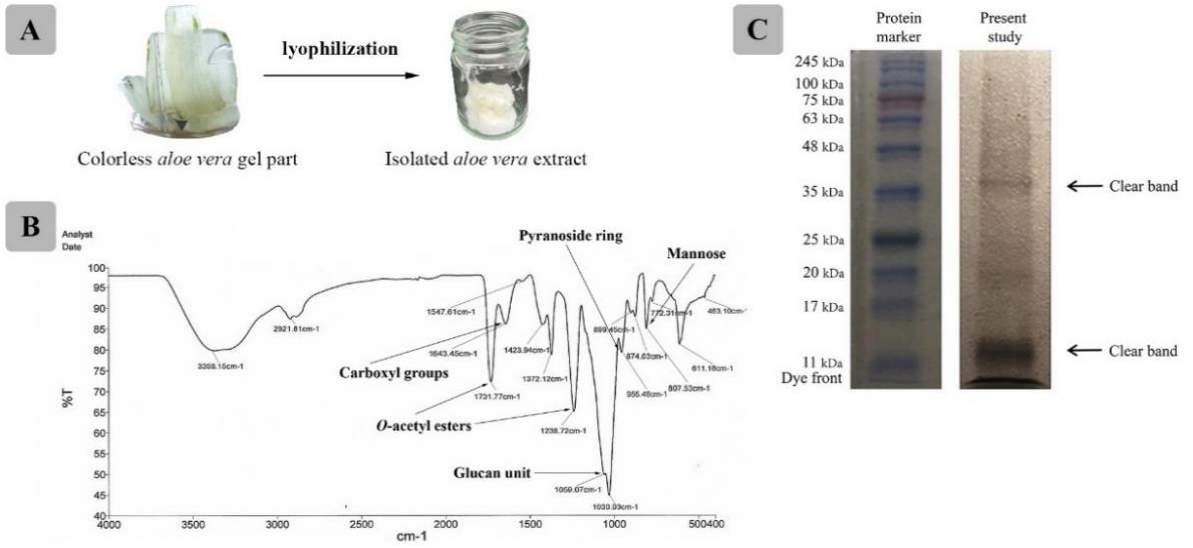

Figure 30 Physical characteristic (A) Infrared spectrum (B) and molecular weight pattern of the aloe gel extract prepared from the gel part of *Aloe vera* leaves (C)

For the cytotoxicity, the results found that RAW 264.7 cells pre-treated with aloe gel extract at the concentration of 6.25, 12.5, 25, 50, and 100 µg/mL for 24 h have the percentage of viability of 99.76±1.44, 97.83±3.18, 99.44±1.03, 98.93±1.59, 99.93±1.35, respectively. These viability percentages were not significantly different compared with the control group (untreated RAW 264.7 cells), which has a percentage of viability of 100±2.58. These results can be implied that aloe gel extract did not show any effect on the viability of the treated cells (Figure 31). Additionally, the morphology of the cells treated with the extract did not change compared to the control group. Therefore, this concentration range was selected for further studies in the pro-inflammatory cytokines release.

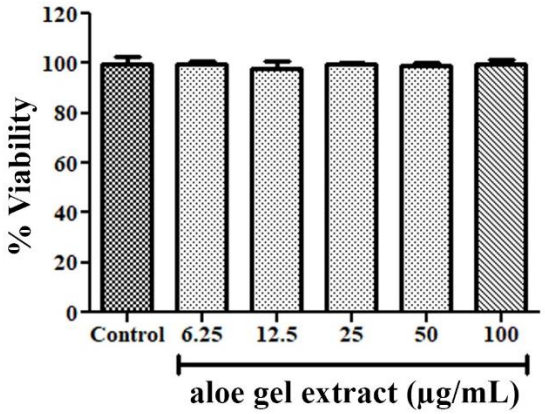

Figure 31 Effect of aloe gel extract (concentration of 6.25 - 100 µg/mL) on the viability of RAW 264.7 cells. Each bar represents mean ± SD in triplicate (n = 4) compared to the control group (untreated cell).

The anti-inflammation activity of aloe gel extract was quantified by TNF-alpha Mouse ELISA Kit. The TNF-alpha released was expressed as a percentage of reduction compared with LPS-treated cells (positive control). The results demonstrated the *Aloe vera* extract in the various concentrations (6.25, 12.5, 25, 50, 100 µg/ml) provided the percentage of reduction as 84.49±2.76, 84.44±3.89, 82.03±2.31, 80.31±0.99 and 76.79±2.24% as compared to LPS-treated cell (100±3.59%) which has potential to inhibit significantly (p<0.001) as shown in Figure 32. The production of TNF-α is released as dose-dependent behavior. It can be implied that the aloe gel extract plays an important role in the inflammatory process, which is directly associated with facilitating rapid wound healing.

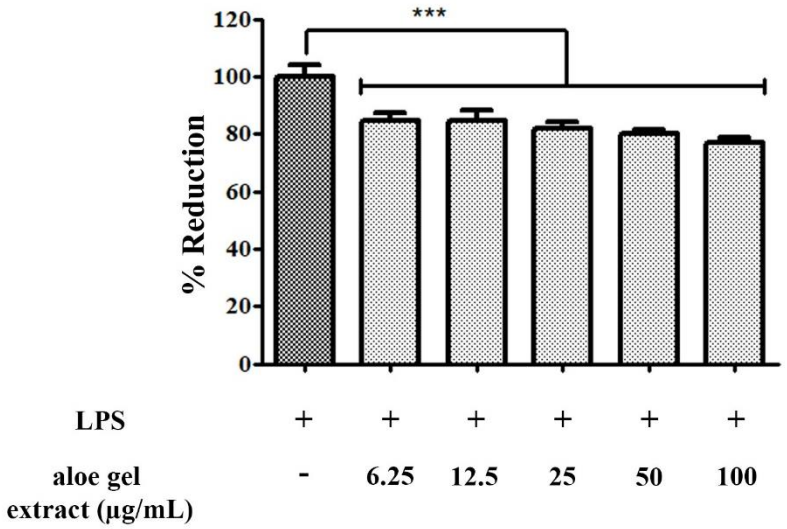

Figure 32 The percentage of reduction of TNF-alpha released of aloe gel extract as anti-inflammatory activity. Each bar represents mean ± SD in triplicate (n = 4), ***p<0.001 compared to LPS-treated cell (control group).

Characteristics of the blend fibroin/aloe gel extract film

Physico-chemical characteristics of blended fibroin/aloe gel extract film

The characteristics of fibroin extract blended with aloe gel extracts film were prepared by casting the solution into a smooth suitable mold were yellowish smooth homogeneous tough, and quite brittle film has approximately thickness 0.05 mm, shown in Figure 33A. Then, the developed film was sterilized using gamma irradiation facilitated by THAI ADHESIVE TAPES INDUSTRY CO., LTD. In this study, the developed film was sterilized by gamma irradiation which is one of the most common sterilization methods for health care products, including wound dressing [32] and temperature-sensitive materials [223]. However, some

studies indicated the adverse effects on molecular mechanisms involving gamma rays-induced cell damage [224], microorganisms resistance [225], and structural changes in medical devices made of polymer [226]. For these reasons, the physical characteristics, chemicals, and sterility of the gamma-irradiated film were determined in the present study. The SEM images showed a non-porous morphology on the surface of the non-sterilized (Figure 33B1) as well as sterilized film (Figure 33B2). For the mechanical properties, the non-sterilized film provided the breaking force and percentage of elongation at break at 6.038±0.746 N and 1.147±0.119%, respectively, which are not significantly different (p>0.5) to the sterilized film (6.26±0.44 N for the breaking force and 1.20±0.07% for percent elongation at break). Thus, the sterilized blended fibroin/aloe gel extract film provided an appropriate toughness and flexibility which were achieved in this study. Figure 33C1 and 33C2 demonstrated the infrared spectra obtained from the FTIR spectroscopy technique indicated that the chemical characteristics of the sterilized film was not different from non-sterilized film. For the comparison between the absorption bands of non-sterilized and sterilized film at 1633 and 1634 cm^{-1} were amide I, 1514 and 1513 cm^{-1} were amide II, and 1231 and 1228 cm^{-1} were amide III, respectively which belongs to fibroin. From the results can be implied that amide I is useful for the analysis of the secondary structure of the proteins and is mainly related to the C=O stretching, and it occurs in the range of 1696-1611 cm^{-1}. Amide II, which falls in 1550-1501 cm^{-1} range, is related to the N-H bending and C-H stretching vibration. Amide III occurs in the range of 1320-1200 cm^{-1}, resulting from in phase combination of C-N stretching and C=O bending vibration. Additionally, the infrared spectra also illustrated that the peaks of aloe gel extract in both non-sterilized and sterilized film at 1055 and 1057 cm^{-1} were clearly as certain as the presence of glucan unit. A further peak at 1013 and 1013 cm^{-1} was due to the pyranoside ring. The characteristic of mannose absorption peak 826 and 828 was detected in non-sterilized and sterilized film. The sterility teat was performed by agar plate culture technique to test microbial contamination of the sterilized film compared to non-sterilized film for 24 h. The result showed that the sterilized film did not find any colonies of microbes or bacteria growth, as shown in Figure 33D. The results showed that gamma irradiation efficiently killed the microorganisms on the film; the physicochemical properties of the film were not affected, i.e. its physical appearance, surface morphology, mechanical properties, and chemical characteristics remained unchanged

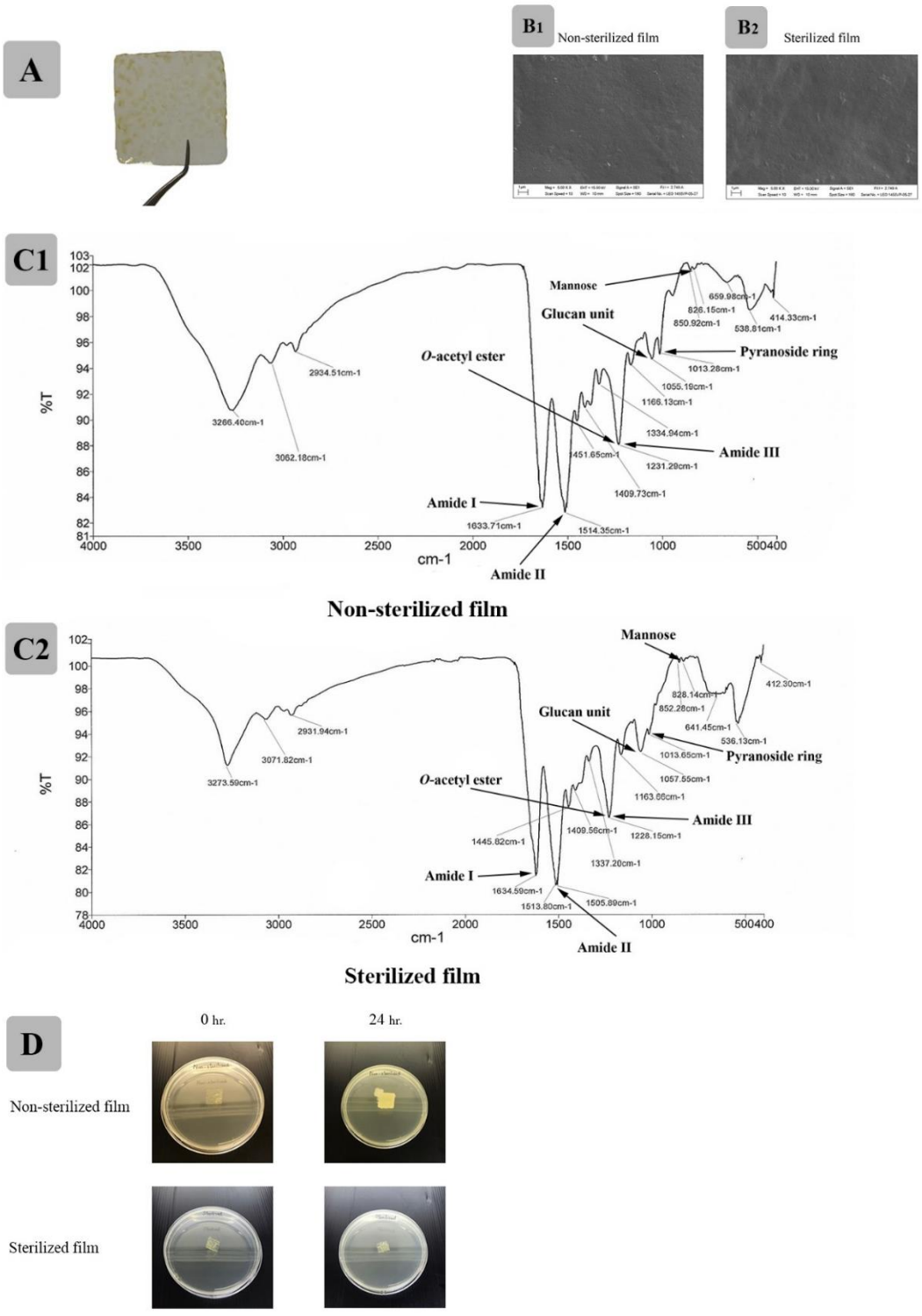

Figure 33 Developed blended fibroin/aloe gel extract film (A); SEM images of surface photomicrographs of the non-sterilized film (B1) and the sterilized film (B2); Infrared spectra of the non-sterilized film (C1) and the sterilized film (C2); and Sterility test of the non-sterilized and the sterilized films after incubation for 24 h (D)

Biological activities of the blend fibroin/aloe gel extract film

Cell line

Cytocompatibility

Results from our previous study showed that the fibroin/aloe gel film exerted potential healing effects, *in vitro* and *in vivo*, and promoted wound closure by 7 days compared with the untreated cells in streptozotocin-induced diabetic rats [14]. In a preliminary clinical study, the developed film accelerated the healing rate in 5 DFU patients within 4 weeks [16]. However, in the current study, we sought to emphasize the biological activities associated with healing properties to support the efficacy of the film sterilized by gamma irradiation. For the cytocompatibility, the results found that the film-treated NHDF cells for 24 h have the percentage of viability of 145.95±1.86. These percentages of viability which significantly higher than control group (untreated NHDF) as 100±5.34 (p<0.001). These results can be implied that the prepared film did not show any effects on the viability and cell morphology of the treated cells (Figure 34A).

Secretion of VEGF by immunoassay

Following the immunofluorescence assay, the film extract can potentially promote the VEGF expression compared to the control group. Moreover, the number and the size/shape of the treated NHDF cells were elevated (Figure 34B). An XTT assay demonstrated that the percentage of cell viability relating to the number of cells had a higher OD value, implying a higher proliferation rate. VEGF can be considered a key angiogenesis regulator secreted by fibroblasts. It is also one of the essential mediators associated with the wound healing process because it improves the survival, proliferation, and migration of endothelial cells [227, 228]. The results on the expression of VEGF indicated that the sterilized film did not induce any adverse effect but stimulated an increase in cell number, or the expression of VEGF, indicating the improvement of cell attachment and proliferation as well as the growth factor expression by the primary skin fibroblasts seeded on the film [14]. Many studies have supported the potential of the silk fibroin and aloe gel extracts on the acceleration of cell proliferation and migration in the wound healing process [14, 229, 230]. To determine the essential role of the developed film in the migration and proliferation of fibroblast cells in the wound healing process, we further performed flow cytometry and scratching assay.

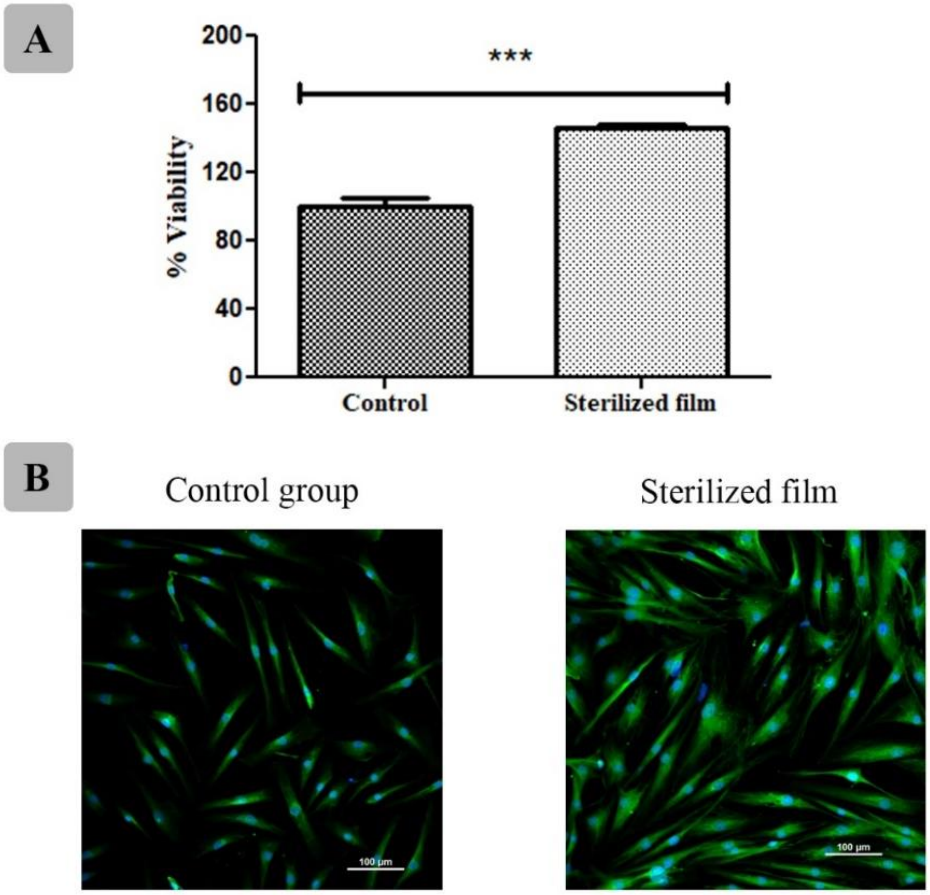

Figure 34 Viability of NHDF cells treated with the blended fibroin/aloe gel extract film for 24 h (A). Data are expressed as percent of control group (untreated cells), and each column represents mean ± S.D in triplicate (n = 3); ***p<0.001. Immunofluorescence for VEGF expression of control group (untreated NHDF cells) and the film-treated group at magnification of 20x (B).

Cell cycle

The cell cycle of the developed films was illustrated as flow cytometry dot plots and histogram profiles, as shown in Figure 35A. Figure 35B showed the cell cycle data as the percent of total cells for each phase of the cell cycle (G0/G1, S, and G2/M). A decrease in the percentage of total cells was found in G0/G1 phase of the film-treated group compared to the control group. The percentage of total cells in S and G2/M phase increased in the film-treated cells group to 7.19±0.23 and 16.09±0.58%, respectively, which are significantly higher than the untreated cells (2.53±0.92 and 4.67±1.61%, respectively) (p<0.001). Focusing on cell proliferation relating to the cell cycle, which is the complex and orderly cellular process through specific phases during the replication of DNA into two daughter cells, our data revealed that the film-treated cells initiated to shift from G0/G1 phase to S phase and G2/M phase, respectively. The results showed biological effect of the

developed film by promoting cells to enter in S and G2/M phases, essential stages for mitosis and cell growth, respectively [231]. They also concurred with Wei X et al., showing that an acemannan consisting of *Aloe vera* can stimulate cell proliferation by influencing the cyclin-dependent cell cycle progress through translational regulation of cyclin D1 [232]. This is the main alteration attributed to the transition of G1 to S phase.

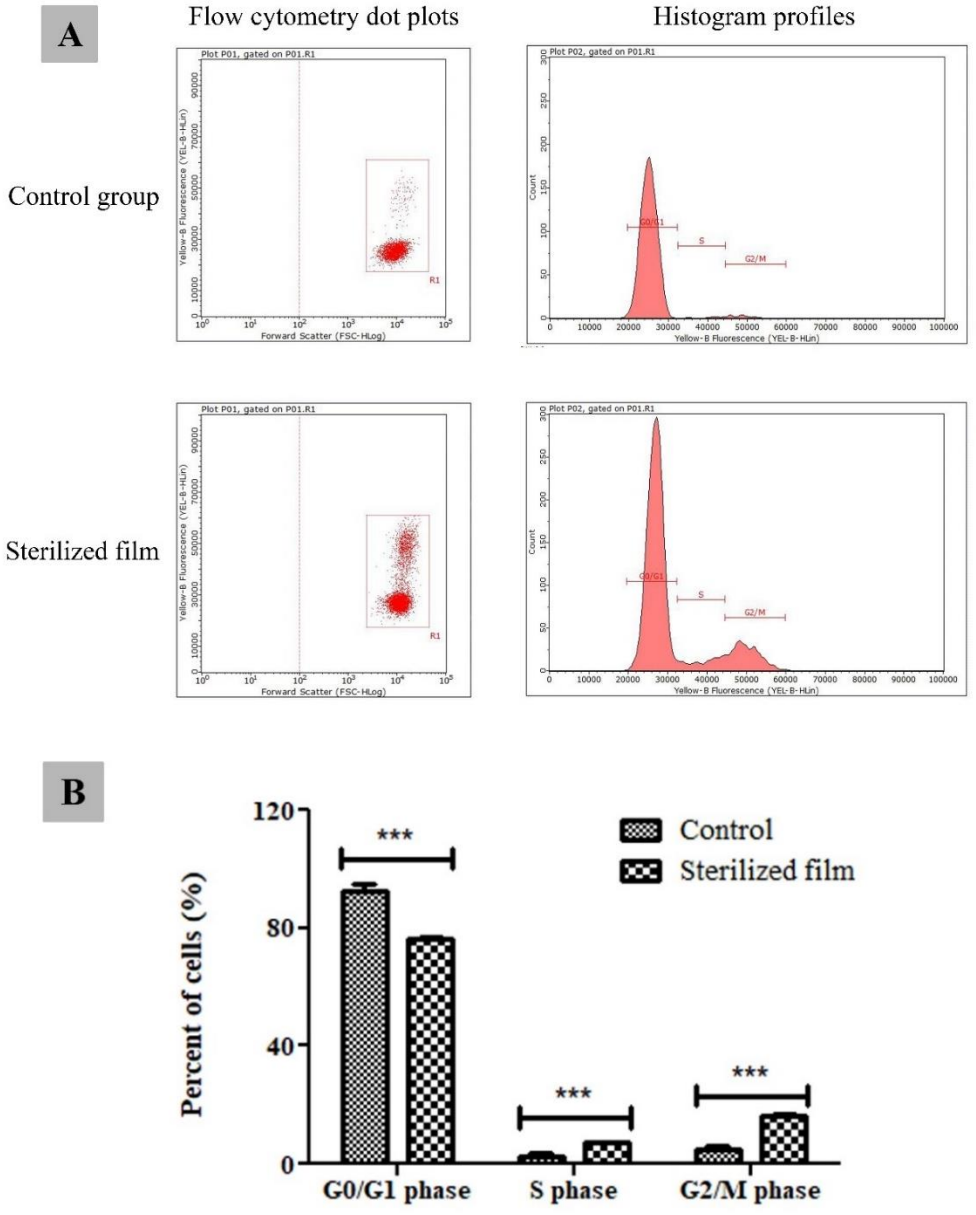

Figure 35 Cell cycle phases of NHDF cells treated with the blended fibroin/aloe gel extract film for 24 h as compared to the control group (untreated cells). This figure shows the examples of cell cycle distribution in dot plots, histogram profiles (A) and percent of total cell (B), and each column represents mean ± S.D. in triplicate (n = 3); ***p<0.001

Cell migration

Determination of cell migration, measured as the closure of the scratch gap at various times, indicated that the film-treated cells provided a completely healed scratch at 36 h after scratch creation. In contrast, the scratch of the untreated cells was not healed simultaneously, as shown in Figure 36. Furthermore, it was found that the developed film exerted a beneficial effect by promoting the migration of fibroblasts and thereby stimulating wound closure [233]. Cell proliferation and cell migration are also correlated in the cell cycle, particularly in the mitosis phase (M phase). M phase is associated with the cell division process, which divides duplicated DNA and cytoplasm to create two identical cells [234]. Cell migration can also be correlated to cytoskeletal reorganization and focal adhesion receptors [235]. Interestingly, cell proliferation result described above showed that the percentage of total cells in the film-treated group was the highest accumulated in G2/M phase, which implied that the film-treated cells contributed to the promotion of cell differentiation and migration processes. They referred to several prior studies which determined that natural compounds promoted G2/M phase and fibroblast migration [236, 237].

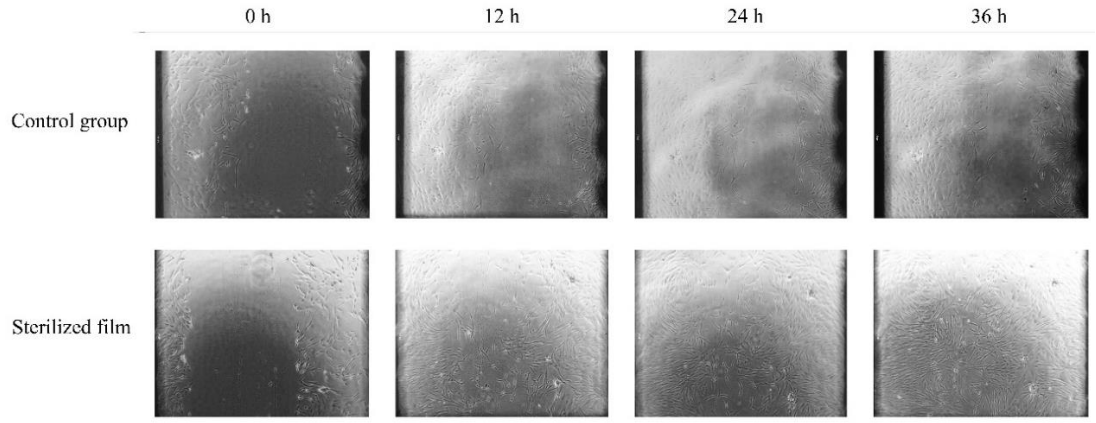

Figure 36 Cell migration of NHDF cells treated with the blended fibroin/aloe gel extract film at 0, 12, 24, and 36 h as compared to control group (untreated cells) at magnification of 10x

Primary cells

Cytotoxicity and cell proliferation

The wound healing process is usually delayed or impaired for patients with diabetic conditions. A primary chronic complication is diabetic foot ulcers. A diabetic environment could be associated with dermal fibroblast dysfunction, reduced angiogenesis, the release of pro-inflammatory cytokines, and senescence features. Alternative therapeutic treatments using natural products highly

demand their high potential for bioactive activity in skin repair. We developed a dressing comprising silk fibroin and *Aloe vera* gel extract for a novel approach to treating chronic wound pathologies. Previously, the primary markers during the wound healing process were investigated. This study aimed to elucidate the possible MAPK/ERK signaling pathway related to the biological effects of the dressing on fibroblast cells. This investigation was conducted on NDF, DDF, and DWF for the cellular responses and NDF for the MAPK/ERK signaling pathway.

The cytotoxicity of fibroblasts was evaluated by MTT colorimetric assay [238], which provides a readout of cell viability and growth by measuring metabolic activity if any viable or proliferative cells with NADPH-dependent enzymes that reduce MTT. The results found that NDF, DDF, and DWF treated with the film extract for 24 h have the percentage of viability of 242.77±8.95, 193.24±6.91, and 215.52±5.22, respectively, which is significantly higher than DMEM w/o FBS (100±8.34 and 151.26±5.12, 100±4.21) and DMEM with 2% FBS (127.15±7.83, and 100±3.79 and 141.64±4.69), as shown in (Figure 37A). These results implied that the film extract behaved non-cytotoxicity effect on fibroblast cells and might also have the potential to stimulate cell viability and proliferation. Also, the results were similar to our previous study [215]. The quantification of cell proliferation of fibroblast cells was performed by colorimetric BrdU assay [239]. This quantification of cell proliferation is based on the measurement of the incorporation of BrdU (bromodeoxyuridine is a synthetic nucleoside, a structural analog of thymidine) during DNA synthesis. The results found that NDF, DDF, and DWF treated with film extract for 24 h have the percentage of cell proliferation of 608.83±6.39, 515.42±10.26, and 576.90±6.87, respectively, which are significantly higher than DMEM w/o FBS (100±7.35, 231.49±9.73, and 100±9.54) and DMEM with 2% FBS (225.63±9.51, 100±9.37, and 198.30±9.02) (Figure 37B). The quantification of cell proliferation of fibroblast cells was performed by colorimetric BrdU assay. This quantification of cell proliferation is based on the measurement of the incorporation of BrdU (bromodeoxyuridine is a synthetic nucleoside, a structural analog of thymidine) during DNA synthesis. The results were related to cell viability, which implied a higher rate of cell viability as a higher rate of cell proliferation. In the hyperglycemic environment, the absence of cell proliferation is caused by several issues, such as the increase of L-lactate secretion [240], pro-inflammatory mediators, and AGEs, leading to enhance the apoptosis via activation of ROS, pro-apoptotic transcription factor FOXOI and caspase [241]. As an outcome, the film extract exerts exaggerated

properties on cell growth and cell proliferation in fibroblast cells. To its remarkable properties, silk fibroin regulates the expression of proteins, including vimentin, cyclin D1, VEGF, and fibronectin accompany the proliferation and remodeling phases modulated by NF-κB signaling pathways in NIH3T3 cells [242]. Regarding two peptides, VITTDSDGNE and NINDFDED were identified and located in the N-terminal region, serving as the active principle of fibroblast growth-promoting activity [243]. Simultaneously, 29 kDa glycoprotein displayed the potential to stimulate the proliferative activity of kidney cells in hamsters and human dermal fibroblasts by *in vitro* assays [244]. Moreover, acemannan is one of the main compounds of *Aloe vera*, providing synergistic effects to promote cell proliferation and skin wound healing through AKT/mTOR signaling pathway [245].

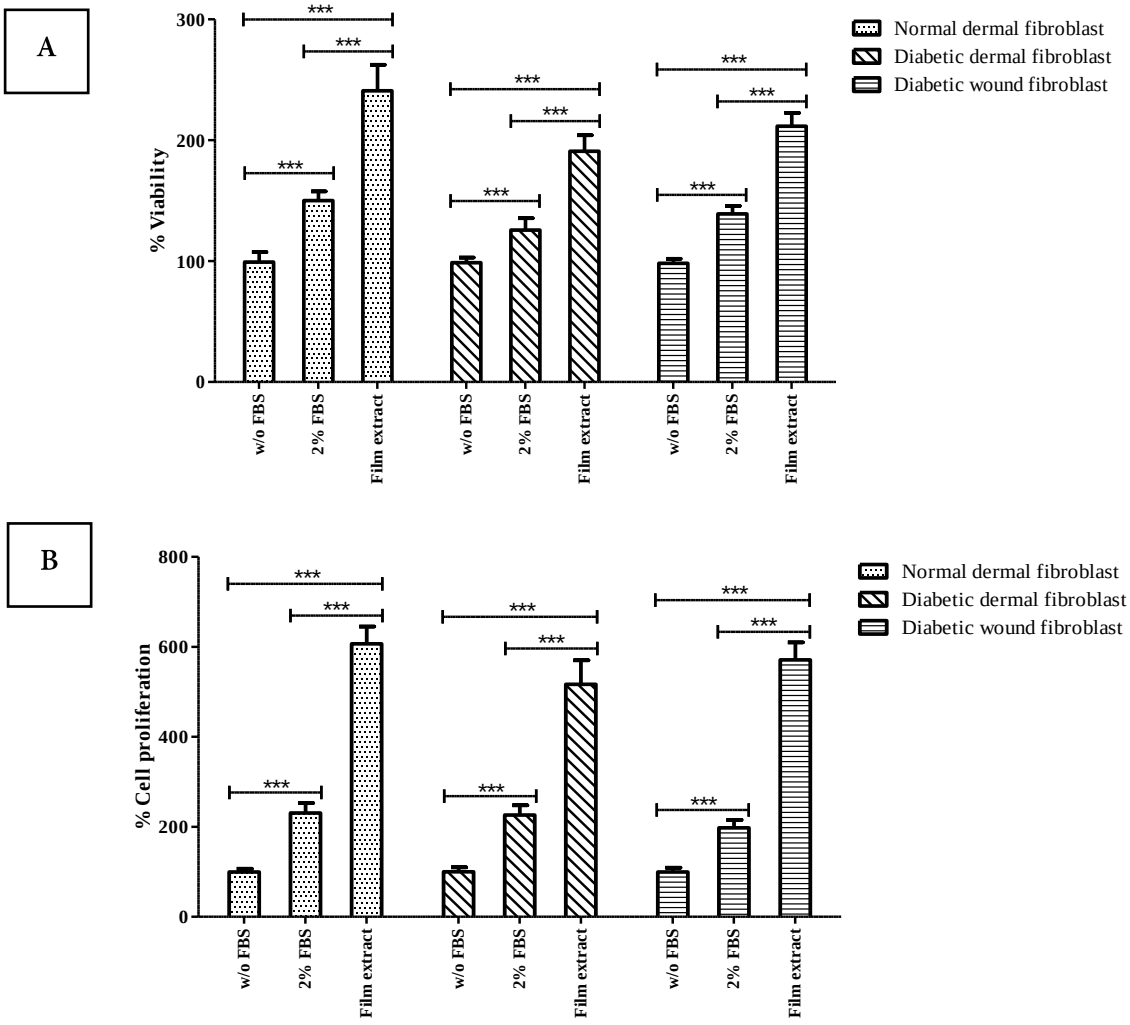

Figure 37 Viability (A) and Proliferation (B) of fibroblasts (NDF, DDF, DWF) cultured for 24 h with DMEM w/o FBS, DMEM 2% FBS, and DMEM film extract. Data are expressed as percentage of the control DMEM w/o FBS considered as 100% viability and each column represents mean ± S.D. in triplicate (n = 8); *** $p<0.001$.

Cell cycle

The effect of the film extract on the fibroblast cell cycle as the percent of cells in cell cycle phases (G0/G1, S, and G2/M) was shown in Figure 38. The percentage of NDF in G0/G1 phase was significantly lower with film extract (48.76±1.15) than with DMEM w/o FBS (73.80±1.65) and DMEM with 2% FBS (57.38±2.54). Whereas, in S phase the percentage of NDF was significantly higher with film extract (51.03±1.45%) compared to DMEM w/o FBS (21.12±3.40%) and DMEM with 2% FBS (40.22±5.12%). The same trend was observed for DDF and DWF, S phase was significantly higher with film extract (45.81±3.98%, 47.92±0.93%, respectively) compared to DMEM w/o FBS (28.72±2.43%, 11.28±9.82%) and DMEM with 2% FBS (29.12±3.60%, 40.78±0.50%). Stain DNA with PI and flow cytometry experiments were performed for cell cycle analysis. Typically, $p21^{Cip1}$ and $p27^{Kip1}$ are the cyclin-dependent kinase (CDK)-inhibitors (CKIs) that are essential in interfering with the kinase activities related to the cell cycle. These CKIs are significantly elevated at high glucose levels and inhibit the cyclin/CDK complexes. In cell cycle progression, cells are arrested in G1 phase, and the proliferation rate is restricted, followed by impaired wound healing processes [246]. As the depicted cell cycle data implies, the film-treated cells shifted from G0/G1 phase to S phase by binding to cyclin D/CDK4,6 complexes that regulate G1-S phase transit. The film extract promoted cells to enter in S phase via the pathway of Acemannan, which is a crucial stage for mitosis and cell growth by influencing cyclin-dependent cell cycle progress through translational regulation of cyclin D1[215]. Also, Yuan L. et al. reported that after treating with aloe polysaccharide, the number of cells was increased in S and G2/M phases preparing for mitosis, and cyclin D1 protein was up-regulated in a concentration-dependent manner[247]. Thus, we hypothesized that the film extract stimulates cyclin D1 expression in cultured fibroblasts and functions as a transcriptional co-regulator to initiate the shift from cell arrest (G0/G1 phase) to cell synthesis (S phase).

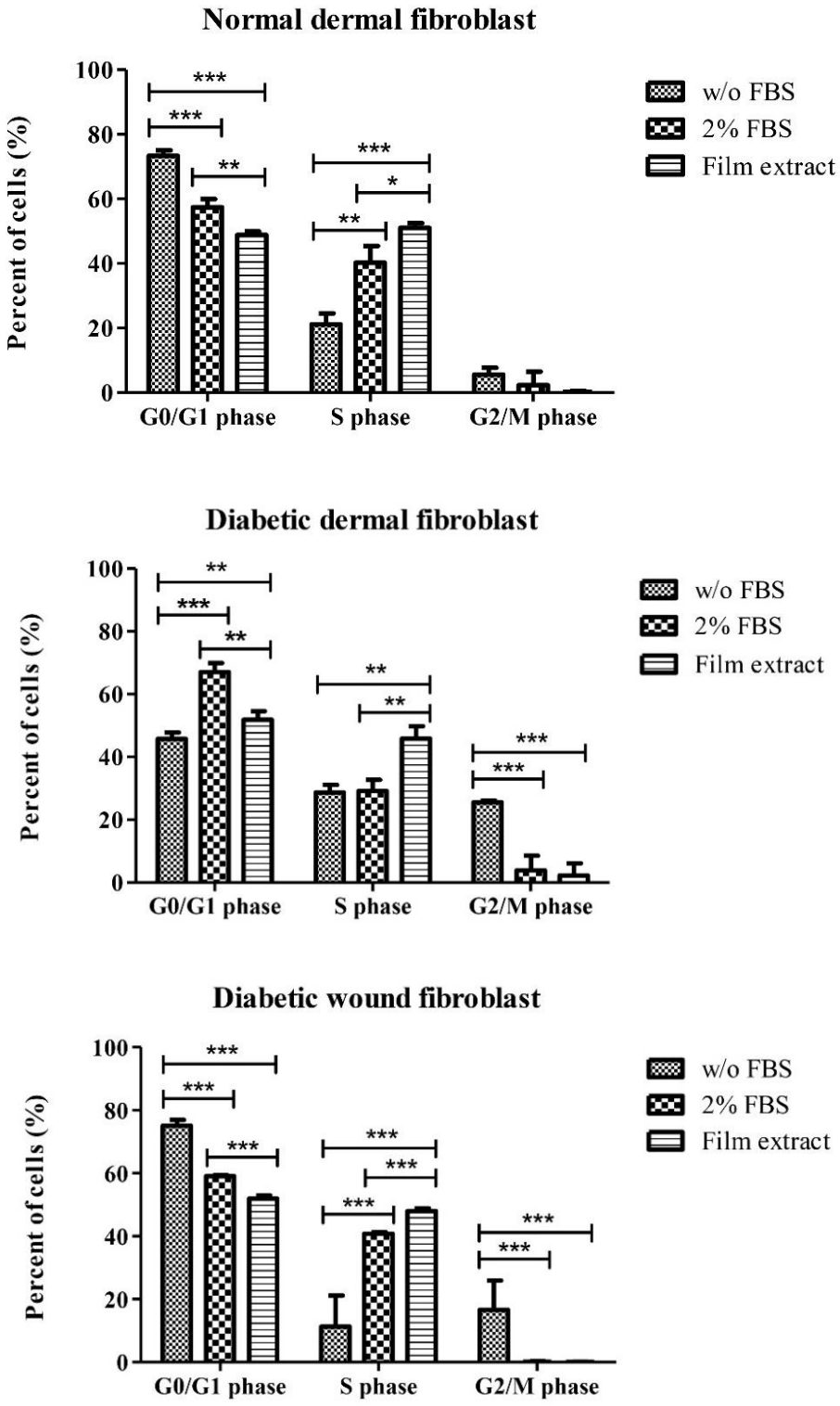

Figure 38 Cell cycle phases of fibroblasts (NDF, DDF, DWF) cultured for 24 h with DMEM w/o FBS, DMEM 2% FBS, and DMEM film extract. Figure shows the percentage of cells in G0/G1 phase, S phase, and G2/M phase. Each column represents mean ± S.D. in triplicate (n = 3); *** $p<0.001$, ** $p<0.01$, * $p<0.05$.

Cell migration

The cell migration was performed by the scratch assay modified by [215]. The fibroblast cells were seeded in a 96-well plate for 24 h to reach 100% confluence before scratching. The scratch was created by the Incucyte® cell migration kit on the cell surface. The results found that fibroblast cells treated with film extract for 24 h elucidated a completely healed scratch after 48 h, while other groups (DMEM w/o FBS and 2% FBS) were not healed at the same time as shown in Figure 39A. Figure 39B explicated the percentage of relative wound density of fibroblast cells (NDF, DDF, and DWF). The film-treated cells were 99.73±5.01%, 98.01±0.26%, and 93.47±2.86%, which reached the relative wound density of almost 100%, whereas the group of w/o FBS-treated cells was 32.65±3.52%, 37.01±1.75%, and 38.63±2.36% and 2% FBS-treated cells was 68.15±4.91% (NDF), 84.36±1.85%, and 48.27±2.71% after 48 h. Regarding the hyperglycemic condition, the excessive production of ROS is accumulated, resulting in protein structure dysfunction and aberration of cell migration directly by over-activation of the small Rho GTPase Racl and affected cell polarity and morphology [248]. To its remarkable properties, silk fibroin stimulated the pathway of canonical NF-κB signaling, which is associated with fibroblast migration and wound healing process in both NIH3T3 cells and damaged skin rats [242]. Coincidences contributed to these studies, which reported that the stimulation of compromise via toll-like receptors (TLRs), interleukin-1 receptor (IL-1R), tumor necrosis factor receptor (TNFR), and antigen receptors [249]. Moreover, 5.5 kDa glycoprotein isolated from the *Aloe vera* gel, improved keratinocyte proliferative and migration effects, which resulting in enhancing the human monolayer keratinocytes closure which made by scratching [250].

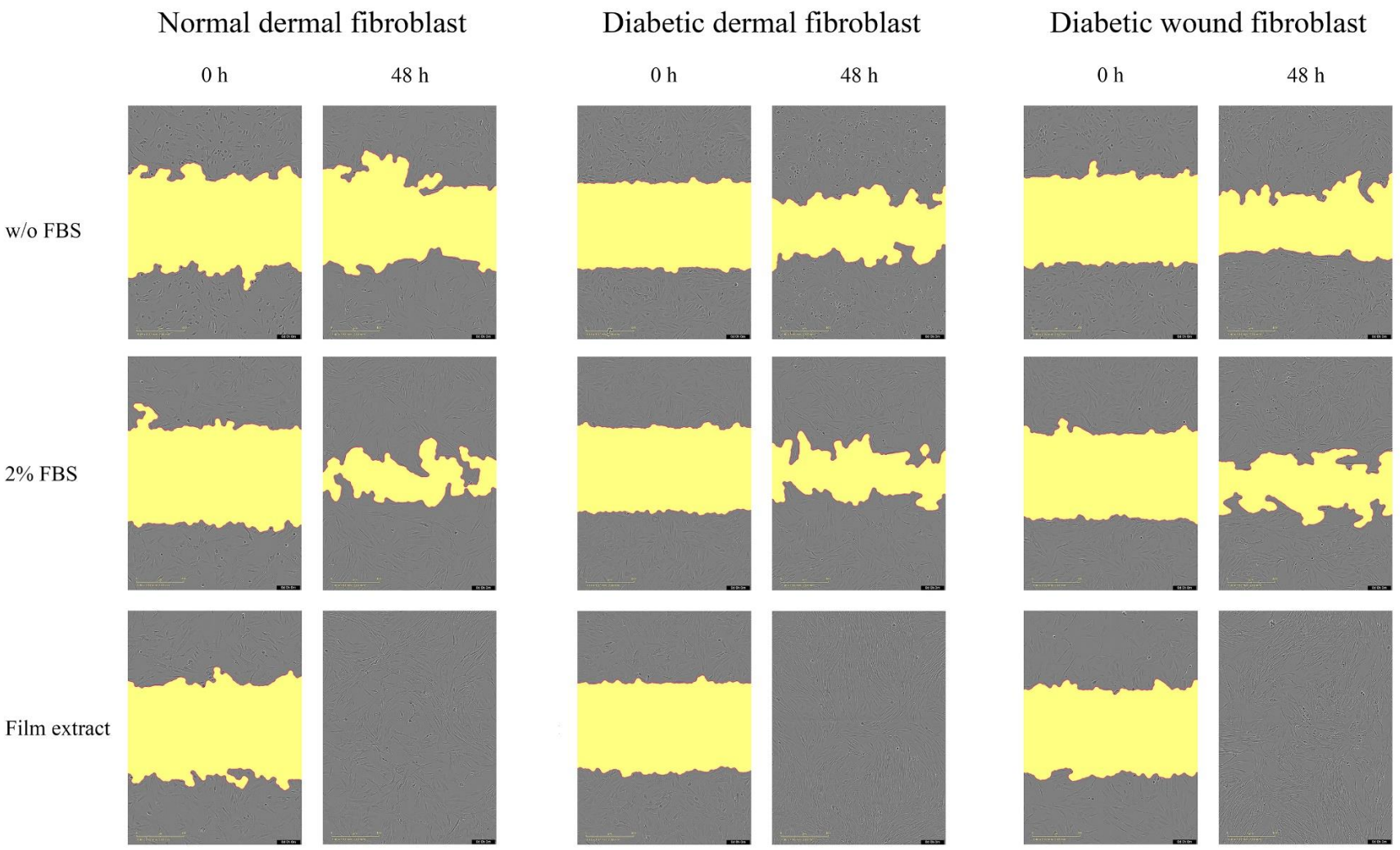
Normal dermal fibroblast
Diabetic dermal fibroblast
Diabetic wound fibroblast
0 h
48 h
0 h
48 h
0 h
48 h
w/o FBS
2% FBS
Film extract

B

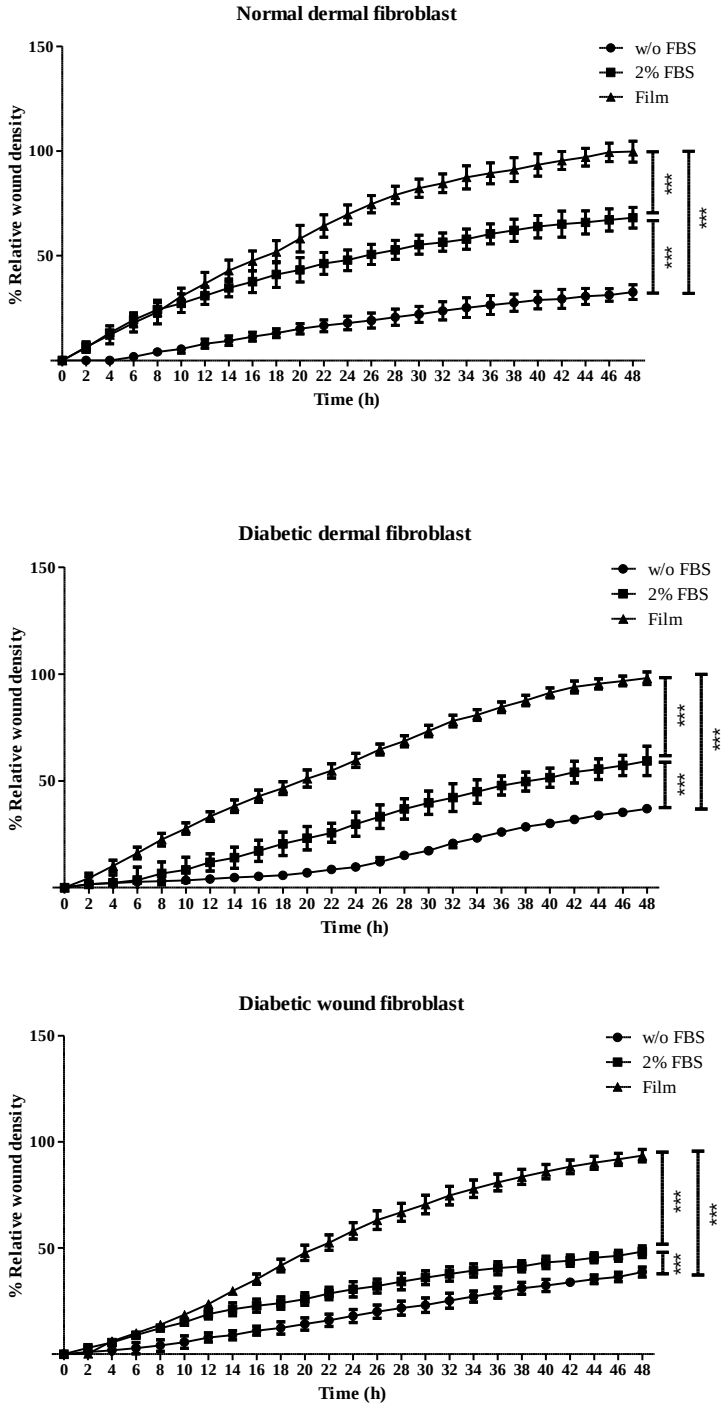

Figure 39 Migration of fibroblasts (NDF, DDF, DWF) cultured for 48 h with DMEM w/o FBS, DMEM 2% FBS, and DMEM film extract. Visualization of the scratching gap at 10x magnification (A); Percentage of relative wound density (B). Each timepoint represents mean ± S.D. in triplicate (n = 5); *** p<0.001 at 48 h.

Cell senescence

The cell senescence was quantified by Senescence cells histochemical staining kit. Senescence is related to a substantial DNA damage response resulting in irreparable DNA damage and permanent cell-cycle arrest. Its character was determined by cell cycle arrest, which is regulated by activating p53/$p21^{CIP1}$ and $p16^{INK4a}$/Rb tumor suppression pathway [251, 252]. For diabetic conditions, the cell senescence impacts several downstream cellular abnormalities, especially for the cutaneous fibroblast, which demonstrated the aggrandized activation of p53/p21-dependent pathways and increased senescence-associated β-galactosidase (SA-b-Gal) activity resulting in cellular senescence and wound healing dysfunction [253, 254]. In this study, the film extract contributed to significantly inhibiting the percentage of cell senescence in NDF, DDF, and DWF as 0.39±0.43%, 11.30±2.39%, and 0.63±0.51%, respectively, compared to DMEM w/o FBS (2.04±1.09%, 35.18±3.22%, and 12.43±2.57%) and DMEM with 2% FBS (1.77±1.16%, 21.15±1.67%, and 2.27±1.03%), as shown in Figure 40. These data corresponded to Xiang-Yu Ma et al. reported that fibroin improved the osseointegration of porous titanium Implants under diabetic conditions via activation of the PI3K/Akt signaling pathway [255]. Also, Yun Hu et al. found that polysaccharides and flavonoids contained in *Aloe vera* possessed the potential for radical scavenging activity [256], which causes activating delayed inflammatory and oxidative environment affected to the abnormality of cell proliferation causing cell senescence perverse innate wound healing process [257]. Subsequently, acemannan enhanced cyclin D1 expression in cultured fibroblast cells, which is an essential regulator of cell cycle progression and can function as a transcriptional co-regulator [258] ensuing to initiate the shift from cell arrest (G0/G1 phase) to cell synthesis (S phase) which correlated to the results of cell cycle mentioned above. We suggested that the film extract has a protective effect on cellular senescence by regulating ROS-induced stress pathways.

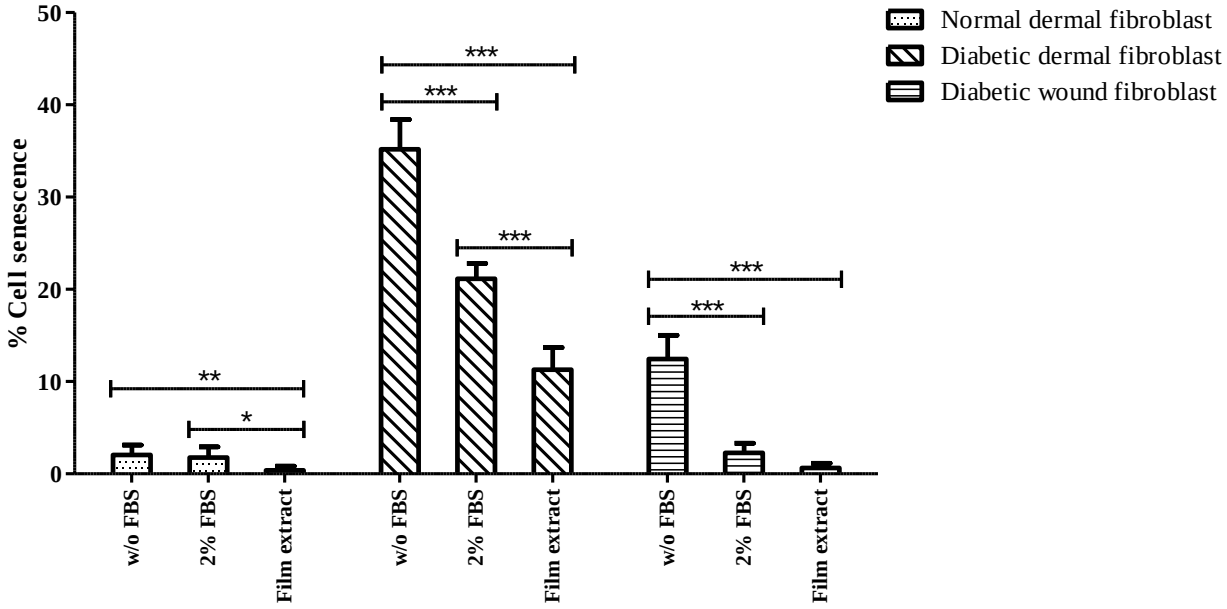

Figure 40 Senescence of fibroblasts (NDF, DDF, DWF) cultured for 24 h with DMEM w/o FBS, DMEM 2% FBS, and DMEM film extract. Data are expressed as the ratio percentage of SA-β-gal *positive cells* to the *total cell count*, each column represents mean ± S.D. in triplicate (n = 8); * $p<0.05$, ** $p<0.01$, *** $p<0.001$.

VEGF secretion

The production of VEGF by fibroblast cells stimulates the formation of blood vessels (angiogenesis) and the expansion of an existing vascular bed by sprouting new blood vessels as it acts as a highly specific mitogen for endothelial cells [259]. The quantitative VEGF evaluation was performed using the Human VEGF165 ELISA kit. Figure 41 illustrated that fibroblast cells (NDF, DDF, and DWF), which were treated with film extract for 24 h, provided the VEGF expression of 1072±35.85, 979.28±70.97, and 828.24±87.33 pg/mg protein, respectively which is higher than DMEM w/o FBS group (448.06±70.96, 349.62±39.20, and 140.59±62.68 pg/mg protein) and DMEM with 2% FBS (650.51±41.41, 569.87±43.77, and 430.69±50.26 pg/mg protein) significantly (p value<0.001). Impaired-glucose tolerance condition leads to the malfunction of VEGF expression resulting in cell proliferation and cell migration disturbances and also affected to prolonged-wound healing rate [260]. Following the results can be implied that the fibroblast cells treated with film extract can stimulate the expression of VEGF, a key angiogenesis regulator secreted by fibroblast. It is also one of the essential mediators associated with wound healing because it improves endothelial cells' survival, proliferation, and migration. The acetyl groups in acemannan and their derivatives have been investigated to be an

essential stimulator of cell proliferation, VEGF expression, and collagen type I together with the β-Sitosterol compound of *Aloe vera* promotes VEGF expression in brain ischemic reperfusion animals [261, 262]. Additionally, we also studied many growth factors by immunoassays, including TGF-β1 and bFGF (data not shown).

In summary, for the effects on cellular activities, including cell viability, cell proliferation, cell migration, and cell senescence can be proven that film extract clarifies the preferential properties of the wound healing process in all types of fibroblast cells (NDF, DDF, and DWF). Therefore, normal dermal fibroblast was selected further to determine the underlying mechanism, particularly the principal intracellular signaling pathway targeted by the film extract.

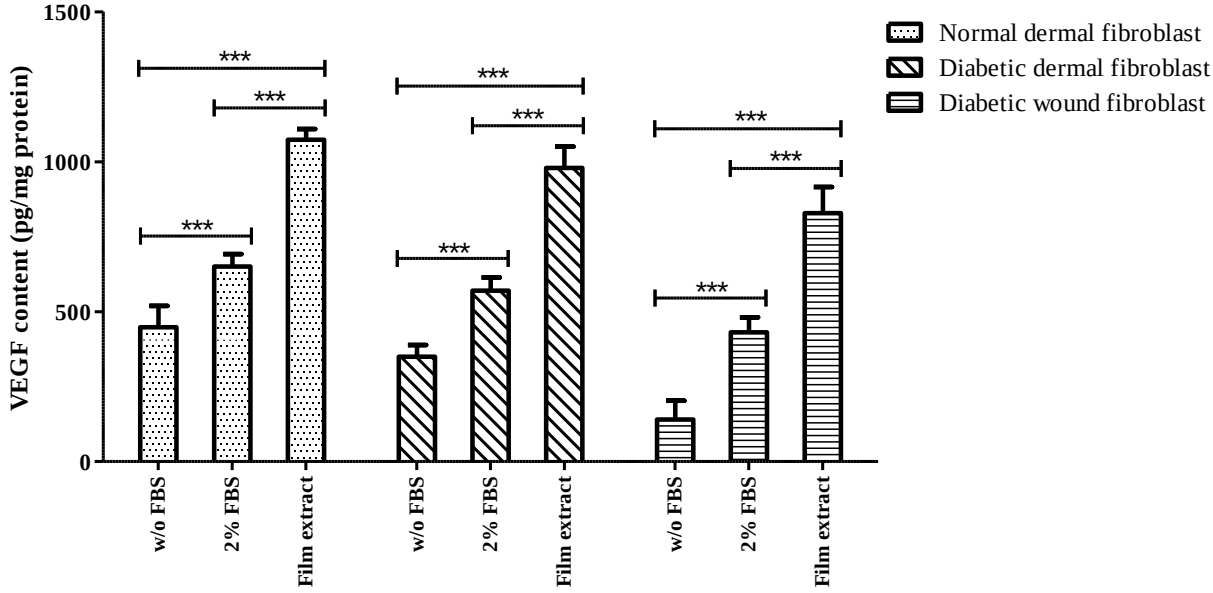

Figure 41 VEGF secretion by fibroblasts (NDF, DDF, DWF) cultured for 24 h with DMEM w/o FBS, DMEM 2% FBS, and DMEM film extract. Data are expressed as VEGF content (pg/mg protein), and each column represents mean ± S.D. in triplicate (n = 4); *** p<0.001.

MAPK/ERK pathway

Mitogen-activated protein kinase (MAPK) pathways are the primary key driving the signaling events that facilitate the wound healing processes, including cell proliferation, cell migration, cell differentiation, and angiogenesis [263, 264]. Activation of MAPK complexes regulates the transcription factor by phosphorylating downstream proteins and finally initiates the cell proliferation and differentiation signals to the nucleus. The activation of the ERK/MAPK cascade can be stimulated via various factors, including 1) variety of growth factors and cytokines; 2) Ca^{2+} influx; 2) activation of receptor tyrosine kinase

Ras, Protein kinase-mediated, G-protein-coupled receptor ligands; and 3) membrane depolarization [265]. Furthermore, to determine the effects of transcription factor inhibitors on cell proliferation and expression of a transcription factor. In this study, we utilized PD98059 is flavonoid compound can be considered a potent inhibitor of MEK1/2 and MAPK cascade by binding to MEK1/2 in an inactive form and preventing the activation of upstream activator (c-Raf) [266]. Figure42A illustrated the cell proliferation of NDF was determined by colorimetric BrdU assay. The results found that NDF treated with MEK1/2 for 1hr was significantly decreased in DMEM w/o FBS, 2% FBS, and Film extract as 49.17±13.57, 121.74±6.09, and 133.65±12.39%, respectively (p value<0.001). In contrast, the MEK1/2 non-treated NDF displayed the percentage of cell proliferation as 100.00±7.69, 307.63±16.29, and 404.74±8.85%, respectively. These results were correlated to fluorescence microscopy imaging that explicated that after treating with MEK1/2 for 1hr, the expression of green fluorescence was attenuated as compared to the MEK1/2 non-treated NDF (Figure42B). Blocking the ERK/MAPK signaling pathway inhibited the proliferation of a diffuse large B cell lymphoma cell line as well as inhibiting the expression of the ERK/MAPK signaling pathway to inhibit tumor cell proliferation may involve inhibition of cell cycle [267, 268]. At present, p44/42 MAP kinase is the only known substrate for MEK1/2. A synthetic inhibitor of MEK1/2, PD98059 binds to the dephosphorylated form of MEK1/2, preventing its phosphorylation, activation, and thus the subsequent activation of p44/42 MAP kinase. In this study, we investigated the expression of transcription factors related to the cell proliferation pathway, including p44/42 MAPK (ERK1/2) and phosphor-p44/42 MAPK (ERK1/2). Figure42C showed the flow cytometry data affirmed the immunofluorescence imaging and illustrated that the film extracts significantly promoted the FITC-A mean as 2082.50±41.41, while DMEM w/o FBS group and DMEM with 2% FBS were 1206.00±56.23 and 1611.50±126.74 (p value < 0.001). Immunofluorescence microscopy image further indicated an increase of green fluorescence compared to others which defined that the film extract stimulated the up-regulation of phosphor-p44/42 MAPK (ERK1/2), downstream further to protein regulation and wound healing process as shown in Figure42B. Maemura K et al. reported that ERK/MAPK signaling pathway promotes cell proliferation and inhibits the apoptotic cell by influencing the activity of downstream cell cycle regulatory proteins, apoptosis-related proteins, and other effector molecules, such as G1/S specific cyclin D1 [269]. Park K-J et al. found that fibroin provided the sensitizing effects to increase the JNK phosphorylation and c-Jun accumulation and alter the regulation of

the MAP kinase pathway [22]. Aloesin is one of the active secondary metabolites in *Aloe vera*, indicating the activation of the Smad and MAPK signaling cascade, which contributes to cell migration, angiogenesis, and tissue development [270].

A

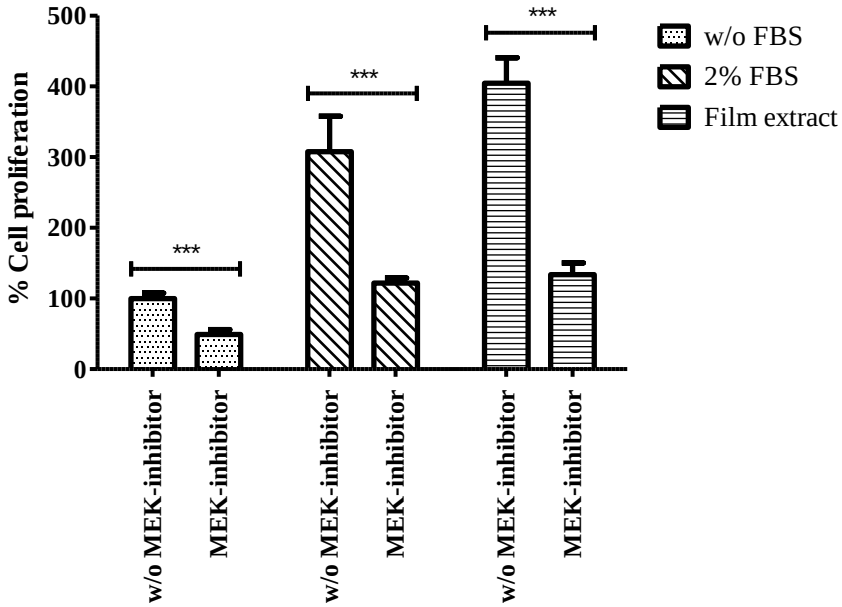

B

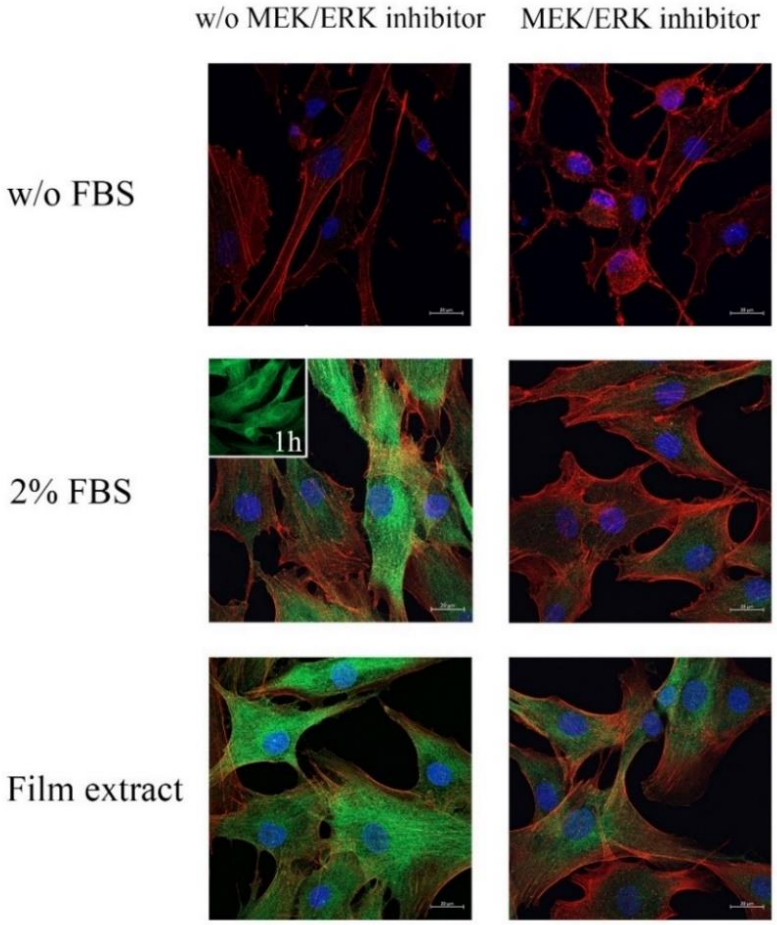

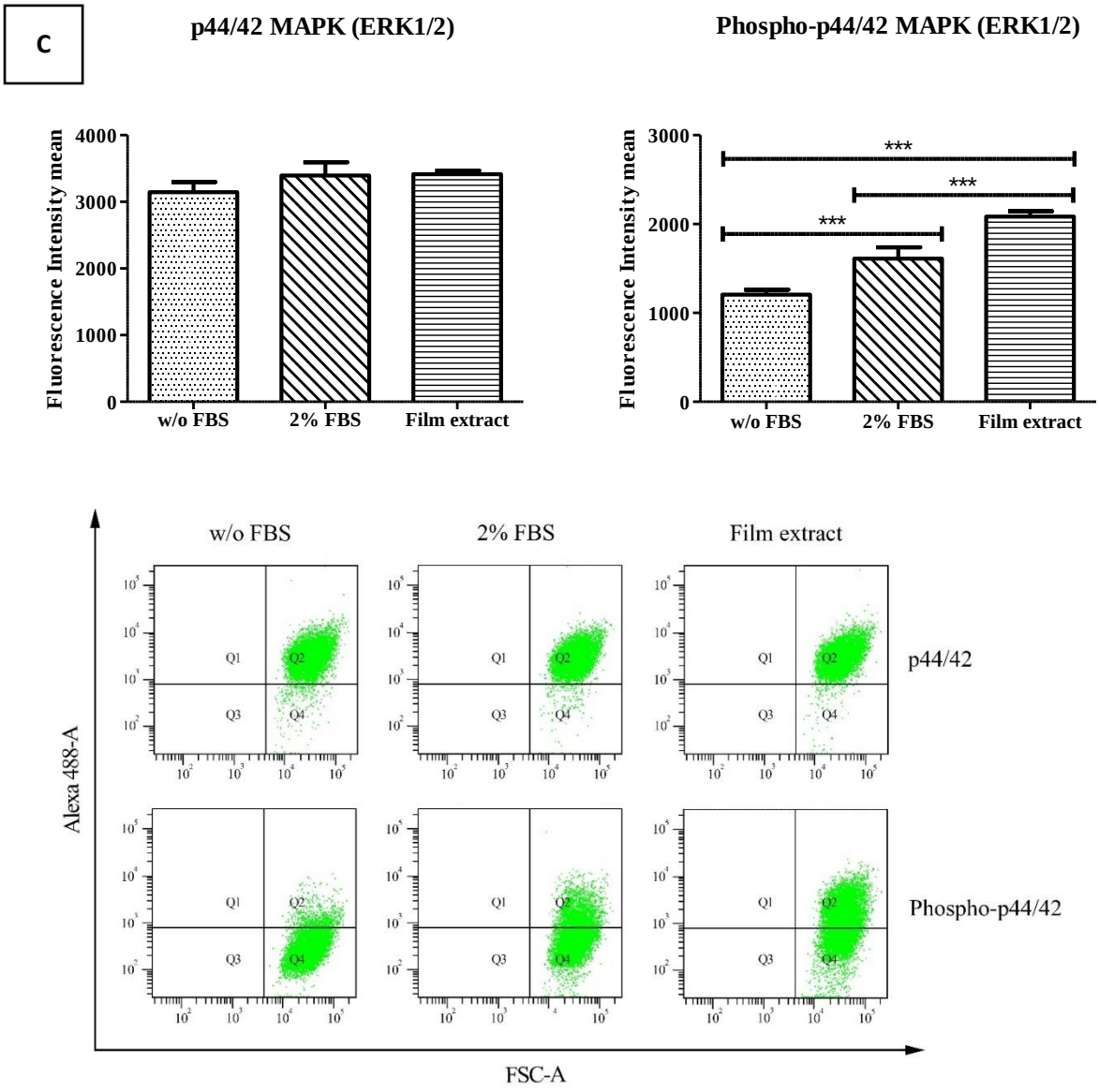

Figure 42 ERK1/2 activity in NDF fibroblasts cultured for 24 h with DMEM w/o FBS, DMEM 2% FBS, and DMEM film extract. (A); Proliferation of NDF treated 1 h with or without MEK/ERK inhibitor PD98059 and cultured for 24 h with DMEM w/o FBS, DMEM 2% FBS, and DMEM film extract. Data are expressed as percentage of the control DMEM w/o FBS untreated with PD98059 and considered as 100% viability, and each column represents mean ± S.D. in triplicate (n = 4); *** $p<0.001$ (B); Immunofluorescence images of phospho-p44/42 protein (green), F-actin (red) and nucleus (blue) by confocal microscopy (40x objective magnification). Box area at 1 h after DMEM 2% FBS culture, Bars: 20 μm. (C); Flow cytometry analysis with plots and histograms identifying p44/42 and Phospho-p44/42 protein levels. Each column of histograms represents mean ± S.D. in triplicate (n = 4); *** $p<0.001$)

CHAPTER V

CONCLUSION

The physicochemical characteristics of silk fibroin and aloe gel extract, and of prepared film, were similar as in previous studies. Gamma irradiation was utilized to sterilize the film and was found to have no effect on physicochemical properties of the prepared film. The experiments of this PhD work supported the beneficial activities of the blended fibroin/aloe gel extract film on the biomolecular mechanism(s) including cell proliferation, cell migration, cell senescence, the expression of growth factor and transcription factor associated with diabetic wound healing. The mechanism of action of the prepared film was mainly linked to the activation of the MAPK/ERK pathway known to regulate various cellular activities, including proliferation. Therefore, the blended fibroin/aloe gel extract film can be considered as an effective therapeutic approach in treating diabetic non-healing ulcers and/or other chronic skin wound.

LIST OF PUBLICATION & COMMUNICATION

Publications

- **Phimnuan, P.,** Dirand, Z., Tissot, M., Worasakwutiphong, S., Sittichokechaiwut, Grandmottet F., Viyoch J., Viennet C. **Beneficial effects of blended fibroin/aloe gel extract film on the biomolecular mechanism(s) via MAPK/ERK pathway relating to the diabetic wound healing.** (in preparation)
- **Phimnuan, P.,** Worasakwutiphong, S., Sittichokechaiwut, A., Grandmottet, F., Nakyai, W., Luangpraditkun, K., . . . Viyoch, J. **Physicochemical and biological activities of the gamma-irradiated blended fibroin/aloe gel film.** (Original Article. Submitted to Journal of ScienceAsia)

Poster

- **Effect of the blended fibroin/aloe gel extract dressing on skin wound healing process** (Fourmis de la Recherche, Besançon, France, 2022)

Oral presentation

- **Investigation of the blended fibroin/aloe gel extract film on the biomolecular mechanism(s) relating to wound healing activity** (Forum de Jeunes Chercheurs, Dijon, France, 2022)

Publication

RESEARCH ARTICLE

ScienceAsia 48 (2022): **278–286**

doi: 10.2306/scienceasia1513-1874.2022.048

Physicochemical and biological activities of the gamma-irradiated blended fibroin/aloe gel film

Preeyawass Phimnuan[a], Saran Worasakwutiphong[b], Anuphan Sittichokechaiwut[c], Francois Grandmottet[d], Wongnapa Nakyai[e], Kunlathida Luangpraditkun[a], Céline Viennet[f], Jarupa Viyoch[a,*]

[a] Department of Pharmaceutical Technology, Faculty of Pharmaceutical Sciences and Center of Excellence for Innovation in Chemistry, Naresuan University, Phitsanulok 65000 Thailand

[b] Division Plastic and Reconstructive Surgery, Department of Surgery, Faculty of Medicine, Naresuan University, Phitsanulok 65000 Thailand

[c] Department of Preventive Dentistry, Faculty of Dentistry, Naresuan University, Phitsanulok 65000 Thailand

[d] Department of Biochemistry, Faculty of Medical Science, Naresuan University, Phitsanulok 65000 Thailand

[e] Department of Chemistry, Faculty of Science, Ramkhamhaeng University, Bangkok 10240 Thailand

[f] UMR 1098 RIGHT INSERM EFS BFC, University of Bourgogne Franche-Comté, Besançon, 25000 France

*Corresponding author, e-mail: jarupav@nu.ac.th

Received 12 Jul 2021, Accepted 17 Dec 2021
Available online 28 Feb 2022

ABSTRACT: The physicochemical and biological properties of the blended fibroin/aloe gel film as a wound dressing were investigated to support the wound healing efficacy of the film described in our previous study. In the current study, protein content, molecular weight pattern, and chemical characteristics of the silk fibroin and the aloe gel extracts were analyzed. The two extracts were then dissolved in lactic acid solution and casted to obtain the blended fibroin/aloe gel film. We found that gamma irradiation did not affect any physicochemical properties of the film, i.e., the irradiated and the non-sterilized films had similar physical appearance, surface morphology, mechanical properties, and chemical characteristics. On normal human fibroblast cultures, the film induced non-cytotoxicity and stimulated the expression of vascular epidermal growth factor. The film-treated cells were shown to proliferate by shifting from G_0/G_1 phase ($76.26 \pm 0.72\%$) to S phase ($7.19 \pm 0.23\%$) and G_2/M phase ($16.09 \pm 0.58\%$) which are higher than the untreated cells. The film-treated cells provided a completely healed scratch at 36 h after scratch creation, while the created scratch of the untreated cells was not healed, indicating that the biological activity of the film enhanced the proliferation and the migration of fibroblast cells. We speculated that the prepared film might be able to use as wound dressing for the diabetic foot ulcer.

KEYWORDS: silk fibroin, aloe gel, gamma-irradiation, wound dressing

INTRODUCTION

Diabetic foot ulcer (DFU), defined as a foot affected by ulceration, is one of the most serious complications of diabetes mellitus (DM) [1]. Several artificial DM polymeric materials have been developed for application as wound dressings. Besides, the utilization of natural biomaterials based on silk fibroin and aloe gel extracts, shown to have wound healing properties *in vitro*, *in vivo*, and clinical trial, has also been reported [2, 3].

Silk fibroin, from the cocoons of *Bombyx mori* silk worm, has been highlighted for various applications in the biomedical field due to its superior mechanical properties, controllable biodegradability, hemostatic properties, non-cytotoxicity, and non-inflammatory characteristics [4, 5]. Silk fibroin also exhibits exceptional compatibility with a variety of cells and tissues [2]. Because of its properties on enhancing the migration and proliferation of various cells, silk fibroin has been considered as a potential biomaterial to be used as wound dressings with many formulations.

Aloe vera has been traditionally used in diverse cultures for its therapeutic properties including rejuvenation, dermatologic conditions, and especially wound healing properties [6, 7]. Many chemical compounds are found in the *Aloe vera* leaf, including acetylated mannans, polymannans, anthraquinone C-glycosides, anthrones, anthraquinones, and lectins [8]. Although it has been widely used as a folk treatment, few scientific studies have been reported on the incorporation of *Aloe vera* with silk fibroin and the effects of the product' biological properties in wound healing [9].

Our previous studies showed that a film prepared from a blend of silk fibroin and aloe gel extracts significantly accelerated the wound healing rate in streptozotocin-induced diabetic rats [2]. In addition, the film rapidly attenuated the healing time and the wound size in 5 DFU patients with complete healing within 4 weeks. In the current study, a blended fibroin/aloe gel film was prepared and sterilized by gamma irradiation. Then, the physicochemical and biological properties of the film were analyzed, and the effects on the wound healing efficacy of the film were determined.

For the biological effects, we focused on the expression of growth factor, proliferation, and migra-

tion of skin fibroblast activities associated with wound granulation and subsequent wound closure. We also expected to demonstrate that the physicochemical properties of the sterilized film would not be altered by gamma irradiation process, and that the biological activities of gamma-irradiated film would enhance wound healing.

MATERIALS AND METHODS

Materials

Yellow silkworm cocoons (*Bombyx Mori*, Nang-Laai strain) were contributed by the Queen Sirikit Sericulture Center, Chiang Mai Province, Thailand. *Aloe vera* was cultured and collected from Phitsanulok Province, Thailand. Chemicals/materials were purchased from different companies: calcium chloride, sodium hydroxide, and ammonium sulfate from RCI Labscan, Bangkok, Thailand; lactic acid solution (88%), sulfuric acid, and lipopolysaccharide (LPS) from Sigma-Aldrich Chemie GmbH, Steinheim, Germany; dialysis membrane standard RC tubing (MWCO: 6–8 kDa) from Spectrum Laboratories, Inc., California, USA; detergent compatible (DC) protein assay kit from BIO-RAD Laboratories, Philadelphia, USA; phenol from AppliChem GmbH, Darmstadt, Germany; Modified Eagle's Medium (DMEM), fetal bovine serum (FBS), and 0.25% trypsin/0.01M EDTA from Sigma-Aldrich Co., Missouri, USA; penicillin/streptomycin solution (10 000 U/ml) and amphotericin B (250 µg/ml) from Gibco, Invitrogen, Massachusetts, USA; cell proliferation kit II (2,3-bis (2-methoxy-4-nitro-5-sulphophenyl)-5-[(phenylamino)carbonyl]-2H-tetrazoliumhydroxide, XTT) from Roche Diagnostics GmbH, Mannheim, Germany; Mueller Hinton Agar from HiMedia, Mumbai, India; and Muse™ Cell Cycle Assay Kit SDS from MERCK, Darmstadt, Germany.

Preparation and characteristic determination of the fibroin extract

The extraction of silk fibroin was performed according to the method described our previous study with some modifications [2]. Briefly, small pieces of silkworm cocoons were treated with hot deionized (DI) water at 85–90 °C for 2 h followed by 25 mM NaOH at 70 °C for 30 min to remove silk gum protein. The degummed fibers were washed with DI water and dried at 45 °C overnight. The dried samples were dissolved in 3 M $CaCl_2$ solution (1 g of samples to 60 ml of $CaCl_2$) at 85–90 °C for 4–6 h. The resulting solution was filtered and dialyzed against 15 MΩ water using dialysis membrane standard RC tubing (MWCO 6–8 kDa) at 23 ± 2 °C for 2 days, with changes of water every 4–6 h, until salts were completely removed. The desalted solution was then centrifuged at 8000 rpm at 4 °C for 15 min. Finally, the supernatants were collected and lyophilized, and the lyophilized fibroin extract was kept in the desiccator at 25 ± 2 °C until further use. The protein content and the molecular weight pattern of the fibroin extract were determined using DC protein assay kit and sodium dodecyl sulfate polyacrylamide gel electrophoresis (SDS-PAGE) method, respectively [2]. The chemical characteristics of the extract were analyzed using Fourier transform infrared spectroscopy (FTIR spectrometer, Spectrum GX series, USA) [2].

Preparation and characteristic determination of the *Aloe vera* gel extract

The extract of *Aloe vera* gel was prepared according to the method described our previous study with some modifications [2]. Briefly, the colorless gel part was collected, homogenized, and centrifuged at 12 000 rpm at 4 °C for 15 min. The supernatant was collected and precipitated by adding $(NH_4)_2SO_4$ to get 55% (w/v) of $(NH_4)_2SO_4$. The resulting precipitates were isolated, dissolved in DI water. The obtained solution was dialyzed against 15 MΩ water using dialysis membrane standard RC tubing (MWCO 6–8 kDa) at 23 ± 2 °C for 1 day with changes of water every 4–6 h. The desalted solution was lyophilized, and the lyophilized aloe gel extract was kept in the desiccator at 25 ± 2 °C until further use. The protein content and the molecular weight pattern of the extract were determined by DC protein assay kit and SDS-PAGE, respectively. Functional groups of the extract were determined using FTIR spectrometry [2].

Preparation and characteristic determination of the blended fibroin/aloe gel film

The blended fibroin/aloe gel film was prepared by casting method described in our previous study with some modifications [2]. 540 mg of the fibroin extract and 15 mg of the aloe gel extract were separately dissolved for 1 h in aqueous solution (with maintained pH 4.0 ± 0.2 using lactic acid) to a final volume of 15 ml. The mixture solution was then filtered and subsequently cast in a square-shaped silicone mold (6 cm × 6 cm) under a dust-free condition and a maintained temperature of 47 ± 2 °C. The ratio of the fibroin extract and the aloe gel extract in the film (36 cm^2) was 97.3% to 2.7% by weight. The physicochemical characteristics of the films were done as follows; (1) scanning electron microscopy (SEM, DAX®, LEO1455VP, New Jersey, USA) for surface morphology observation; (2) mechanical texture analysis (TA.XT Plus, Stable Micro Systems, Ltd, Godalming, UK) including determination of tensile strength and elongation at break; and (3) Fourier transform infrared spectroscopy (FTIR) for chemical characteristics determination. The film was sterilized by gamma irradiation technique (facilitated by Thai Adhesive Tapes Industry Co., Ltd, Bangkok, Thailand), and the sterility of the irradiated film was confirmed by observing the appearance of bacteria

growth using the agar plate culture technique [10].

Determination of biological activities of the blended fibroin/aloe gel film

Cytocompatibility and expression of growth factor by skin fibroblast cells

Normal human dermal fibroblast (NHDF) cells (Lot no. C-12302, Promocell, Eppelheim, Germany) (1×10^5 cells/well, passage number 6) were seeded in a 24-well plate, cultured in DMEM containing 10% FBS, and incubated at 37 °CC in a humidified 5% CO_2 atmosphere for 24 h. The incubated medium was then replaced with serum-free medium. The sterilized films were cut into pieces in a circular shape (6 mm in diameter and 4.56 mg in weight) and placed into trans-well inserts which were, then, put into individual wells of the 24-well plate containing fibroblast cells and incubated for 24 h. After the incubation, the trans-well inserts were removed from the 24-well plate, and the incubated serum-free medium was then discarded and replaced with 250 µl of new serum-free medium plus XTT reagent. The seeded cells were further incubated for 4 h, and the supernatant was then collected for absorbance measurement at 490 nm using microplate reader (Eon™, BioTek instrument, Vermont, USA). The optical density of the control (untreated cells) was adjusted to 100%, and the cell viability was thus shown in percentage. The experiment was performed in triplicates.

Expression of vascular epidermal growth factor (VEGF) was qualitatively determined using the Anti-VEGFA antibody (ab39250, Abcam, Massachusetts, USA). In brief, film extracts were prepared by incubating 1×1 cm^2 sterilized films in 1 ml of DMEM serum-free and incubated at 37 °C in 5% CO_2 incubator for 24 h. NHDF cells (2×10^5 cells/well, passage number 11) were seeded in a cell culture slide with DMEM containing 10% FBS and incubated at 37 °C in a humidified 5% CO_2 atmosphere for 24 h. The cultured medium was then replaced with the film extracts and incubated for 24 h. Subsequently, cells were fixed with 4% paraformaldehyde in PBS for 10 min at room temperature, permeabilized by 0.1% Triton-X 100 at room temperature for 10 min, and washed 3 times with PBS for 5 min. Cells were then incubated with 1% BSA, 22.52 mg/ml glycine in PBST to block unspecific binding of antibodies. At 30 min later, they were incubated with Anti-VEGFA antibody (diluted in 1% BSA in PBST) in a humidified chamber at 4 °C overnight. After washes with PBS for 3 min (5 times), cells were then incubated with Alexa Fluor®488 conjugated secondary antibody (diluted in 1% BSA in PBST) at room temperature for 1 h in the dark. The secondary antibody solution was discarded, and the cells were washed with PBS for 3 min (5 times). After the washes, the cells were incubated with 100 µl of DAPI (DNA stain) for 1 min and rinsed with PBS for 3 min (5 times). Finally, the cells were mounted with anti-fade mounting solution and observed under Laser confocal microscope (A1 HD25/A1R HD25, Nikon®, Tokyo, Japan).

Cell cycle

NHDF cells (1×10^5 cells/well, passage number 6) were seeded in a 24-well plate and incubated at 37 °C in 5% CO_2 incubator for 24 h. The medium was then replaced by DMEM serum-free. Trans-well inserts containing 6 mm diameter sterilized films were put into a 24-well plate with the adherent fibroblasts and incubated for 24 h. After the incubation, cells were trypsinized using 0.25% trypsin/0.01 M EDTA. Cell suspensions (2×10^5 cells/ml) were centrifuged, and the cell pellet was then washed with PBS (pH 7.4) and fixed with 70% EtOH for 3 h. After the wash, cells were stained with 150 µl of Muse™ Cell Cycle Assay Kit reagent at room temperature for 30 min (protected from light). Cell cycle was then analyzed by flow cytometry. The percentages of total cells for the cell cycle phases (G_0/G_1, S, and G_2/M) of the control (untreated cells) and the film-treated sample were calculated. The experiment was done in 3 replicates.

Migration of skin fibroblasts

The skin fibroblast migration was studied using the scratch assay, which is typically utilized to quantify the migration of cells on two-dimensional (2-D) surfaces over time, following a modified method described in [11, 12]. NHDF cells (1×10^5 cells/well, passage number 7) were seeded in a 24-well plate and incubated at 37 °C in 5% CO_2 incubator for 48 h, during which cells had grown to confluency in a monolayer. A scratch was then made with a pipette tip by creating an incision-like gap in the confluent monolayer of the fibroblasts in each well. The fibroblast scratches were washed twice with sterilized PBS (pH 7.4) followed by adding 800 µl of DMEM serum-free into each well. The trans-well inserts containing the sterilized films (circular shape, 6 mm in diameter) were put into the 24-well plate with fibroblast scratches, and the plate was further incubated at 37 °C in 5% CO_2 incubator for 36 h. The scratched gaps were photographed immediately after scratching at defined time points (0, 12, 24, and 36 h). At 36 h, cell migration was observed as a completed closure of the scratched gaps under an inverted microscope [13]. The experiment was done in three replicates.

Statistical analysis

All values were expressed as mean ± SD. The student's unpaired t-test was used to compare between the control and the sample. $p < 0.01$ was considered significant difference.

RESULTS

Characteristics of the fibroin extract

The lyophilized fibroin extract prepared from silkworm cocoons (Nang-Laai strain) presented yellowish cotton-like characteristics. One gram of silk cocoons yielded 0.58 g (58% w/w) of the extract. A DC protein assay showed a protein content of 97.43 ± 0.44% w/w of the extract. Infrared spectra obtained using FTIR spectroscopy showed the frequency peaks at 1634 (amide I), 1513 (amide II), and 1232 (amide III) cm^{-1} (Fig. 1A). The molecular weight pattern of the extract, as shown in Fig. 1B, indicated a specific band of L-chain at approximately 25 kDa and a smear band of H-chain in the range of 30 to 245 kDa.

Characteristics of the aloe gel extract

The lyophilized extract of the *Aloe vera* gel showed white cotton-like characteristics, and 100 g of the gel produced 6 g (0.06% w/w) of the extract. The protein content in the extract was 6.86 ± 1.15% w/w of the extract. Fig. 2A shows the IR spectra of the aloe gel extract indicating peak at 1731 (*O*-acetyl ester), 1238 (*O*-acetyl ester), 1059 (glucan units), 955 (pyranoside ring), and 807 (mannose) cm^{-1}. The molecular weight pattern of the extract showed a clear band at approximately 14 and 35 kDa (Fig. 2B).

Characteristics of the blended fibroin/aloe gel extract

The physical appearance of the prepared film was flexible, translucent, and yellowish with uniform thickness of 50 μm. The SEM images showed a non-porous morphology on the surface of the non-sterilized (Fig. 3A1) as well as sterilized film (Fig. 3A2). For the mechanical properties, the non-sterilized film provided the breaking force and percentage of elongation at break at 6.038 ± 0.746 N and 1.147 ± 0.119%, respectively, which are not significantly different ($p > 0.5$) to the sterilized film (6.26 ± 0.44 N for the breaking force and 1.20 ± 0.07% for percent elongation at break). The FTIR spectroscopy presented infrared spectra of the non-sterilized and sterilized film at 1633 and 1634 (amide I), 1514 and 1513 (amide II), 1231 and 1228 (amide III), 1055 and 1057 (glucan units), 1013 and 1013 (pyranoside ring), 826 and 828 (mannose), respectively, as shown in Fig. 3(B1,B2). Focusing on the sterility test using agar plate culture, the sterilized film showed no colonies of microbes or bacteria growth (Fig. 3C).

Biological activities of the blended fibroin/aloe gel film

For the cytocompatibility of the fibroin/aloe gel film, the viability percentage of the treated NHDF cells was 145.95 ± 1.86, which is significantly higher than the control's (100 ± 5.34) ($p < 0.01$) (Fig. 4A). In the immunofluorescence experiment, the film significantly stimulated the expression of VEGF. Compared with the control, the number and the size/shape of the treated cells were increased (Fig. 4B). In comparison to the control, the treated cells showed a decrease in the percentage of total cells in the G_0/G_1 phase; on the other hand, increases in the percentages of total cells of 7.19 ± 0.23% and 16.09 ± 0.58% were found in the S and the G_2/M phases, respectively, which were higher than those of the untreated cells (2.53 ± 0.92 and 4.67 ± 1.61%, respectively) (Fig. 5). Fig. 6 shows the result of cell migration, measured as the closure of the scratch gap at various times, indicating that at 36 h after scratch creation, the treated cells provided a completely healed scratch, while the scratch of the untreated cells was not healed.

DISCUSSION

In this study, Nang-Laai strain cocoons provided the percentage of yield and the protein content of the fibroin extract corresponding to our previous report [2]. The presence of amides I, II, and III and the random coil groups in the FTIR spectrum confirmed that the extract structure consists of water-soluble random coil conformation [14]. The appearance of the smeared band in the analysis of protein, using SDS-PAGE technique, might be a consequence of the degradation of the heavy (H) chain (325–350 kDa) of silk fibroin protein during the extraction process. The clear band at the range of 17–25 kDa is related to the light (L) chain of fibroin [15].

The percentage of yield and the protein content of the aloe gel extract were similar to our previous findings [2]. The FTIR spectrum showed the presence of functional groups, including glucan units, pyranoside, and mannose relating to anti-inflammatory and healing activities of the aloe gel extract [16, 17]. The SDS-PAGE molecular weight pattern was observed with two clear bands of mannose-binding lectin at approximately 14 and 35 kDa, also indicating the activities of anti-inflammatory [18], hemagglutinating, and mitogenic activities [19] of the extract.

In our current study, the fibroin/aloe gel film was sterilized by gamma irradiation which is one of the most common sterilization methods for health care products including wound dressing [20] and temperature-sensitive materials [21]. However, some studies indicated the adverse effects on molecular mechanisms involving gamma rays-induced cell damages [22], microorganisms resistance [23], and structural changes in medical devices made of polymer [24]. For these reasons, the physical characteristics, chemical, and sterility of the gamma-irradiated film were determined in the present study. The results showed that gamma irradiation efficiently killed the microorganisms on the film; the physicochemical properties of the film were not affected; i.e. its physical appearance, surface morphology, mechanical properties, and chem-

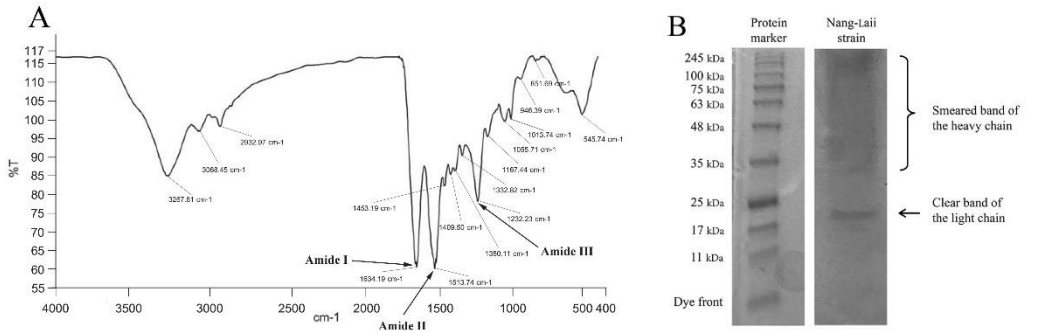

Fig. 1 (A) Infrared spectrum and (B) molecular weight pattern of the fibroin extract prepared from yellow silkworm cocoons (Nang-Laai strain).

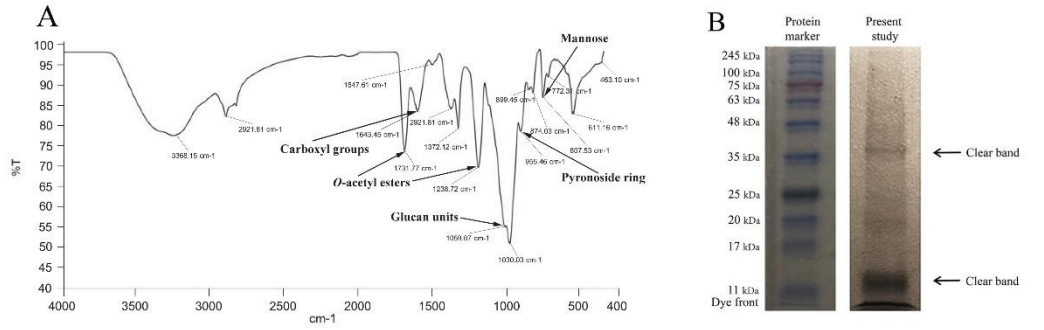

Fig. 2 (A) Infrared spectrum and (B) molecular weight pattern of the aloe gel extract prepared from the gel part of *Aloe vera* leaves.

ical characteristics remained unchanged.

Results from our previous study showed that the fibroin/aloe gel film exerted potential healing effects, *in vitro* and *in vivo*, and promoted wound closure by 7 days compared with the untreated cells in streptozotocin-induced diabetic rats [2]. In a preliminary clinical study, the developed film accelerated the healing rate in 5 DFU patients within 4 weeks. However, in the current study, we sought to emphasize the biological activities associated with healing property to support the efficacy of the film sterilized by gamma irradiation. The cytotoxicity results showed that the sterilized film did not affect the cell viability and morphology. An XTT assay demonstrated that the percentage of cell viability relating to the number of cells had a higher OD value, implying a higher proliferation rate. VEGF can be considered as a key angiogenesis regulator secreted by fibroblasts. It is also one of the most essential mediators associated with the wound healing process because it improves the survival, the proliferation, and the migration of endothelial cells [25, 26]. The results on the expression of VEGF indicated that the sterilized film did not induce any adverse effect, but stimulated an increase in cell number, or the expression of VEGF, indicating the improvement of cell attachment and proliferation as well as the growth factor expression by the primary skin fibroblasts seeded on the film [2]. There have been many studies supporting the potential of the silk fibroin and aloe gel extracts on the acceleration of cell proliferation and cell migration in the wound healing process [2, 27, 28]. To determine the essential role of the fibroin/aloe gel film in the migration and the proliferation of fibroblast cells on the wound healing process, we further performed the flow cytometry and the scratch assay.

Focusing on cell proliferation relating to the cell cycle, which is the complex and orderly cellular process through specific phases during the replication of DNA into two daughter cells, our data revealed that the film-treated cells shifted from G_0/G_1 phase to S phase and then G_2/M phase. Hence, the film promoted the cells to enter into the S and G_2/M phases, which are essential stages for cell mitosis and cell growth, respectively [29]. Besides, Wei et al [30] showed that an acemannan consisting of *Aloe vera* can stimulate cell proliferation by influencing the cyclin-dependent cell cycle through translational regulation of cyclin D1,

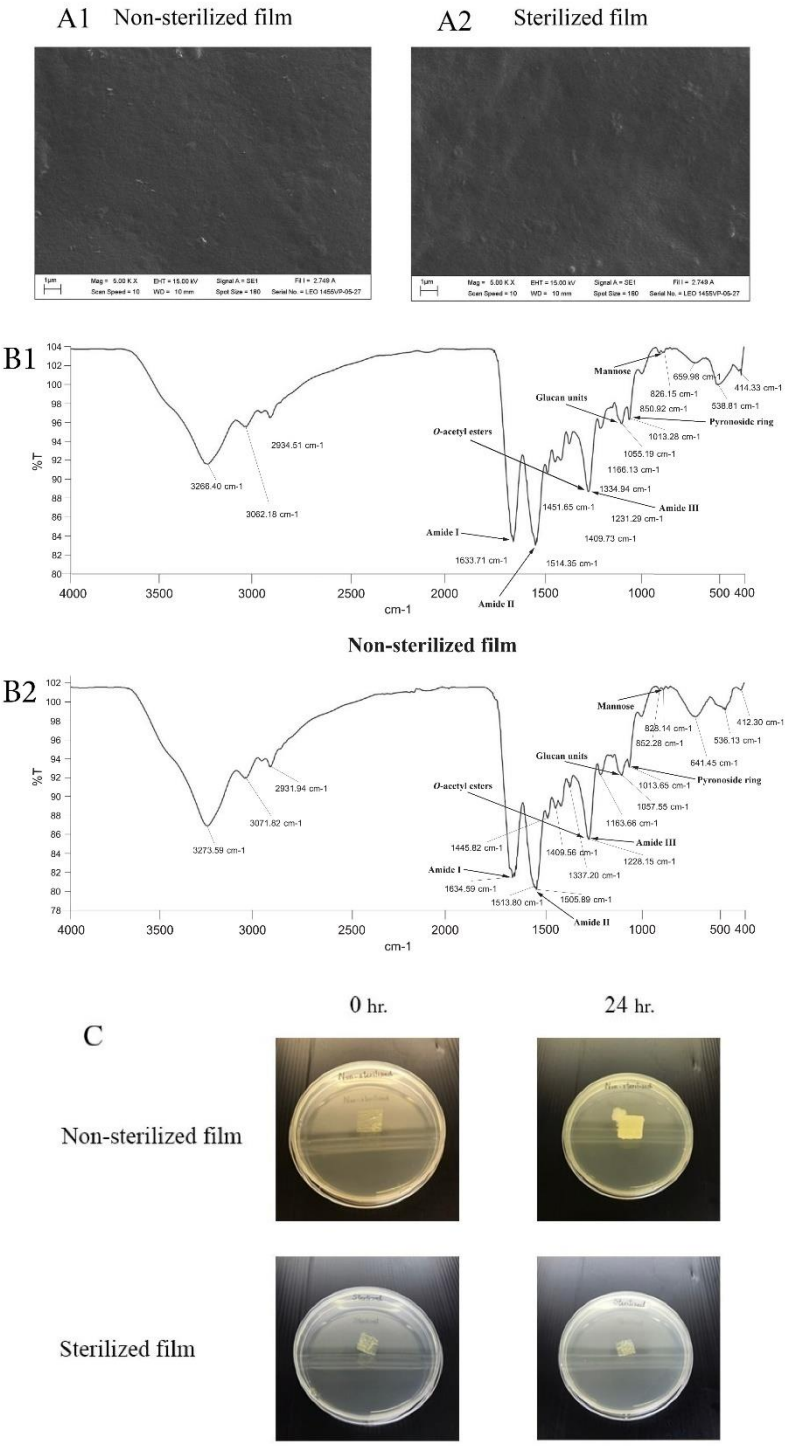

Fig. 3 (A1) SEM images of surface photomicrographs of the non-sterilized film and (A2) the sterilized film; (B1) infrared spectra of the non-sterilized film and (B2) the sterilized film; and (C) sterility test of the non-sterilized and the sterilized films after incubation for 24 h.

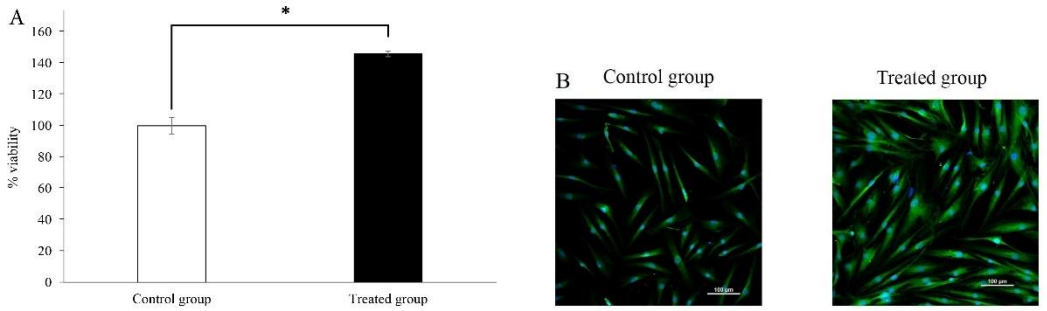

Fig. 4 (A) Viability of NHDF cells treated with the blended fibroin/aloe gel film for 24 h. Data are expressed as percentage of the control (untreated cells), and each column represents mean ± S.D. of triplicate study; * $p < 0.01$. (B) Immunofluorescence for VEGF expression of the control (untreated NHDF cells) and the treated cells at 20 × magnification.

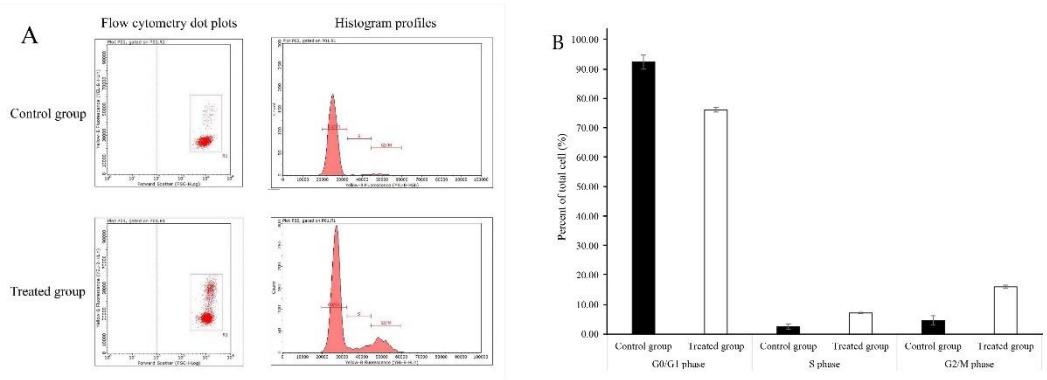

Fig. 5 Cell cycle phases of NHDF cells treated with the blended fibroin/aloe gel film for 24 h compared with the control (untreated cells). The figure shows the examples of cell cycle distribution in: (A) dot plots and histogram profiles; (B) percentage of the total cell. Each column represents mean ± S.D. of triplicate study.

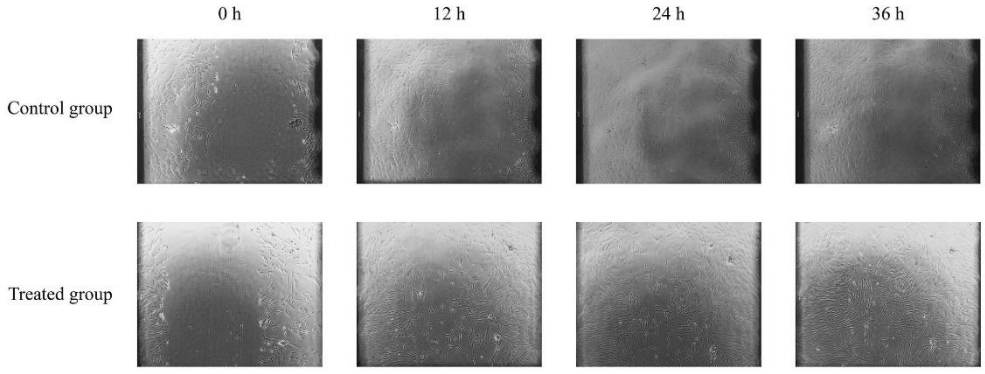

Fig. 6 Cell migration of NHDF cells treated with the blended fibroin/aloe gel film at 0, 12, 24, and 36 h compared with the control (untreated cells) at 10x magnification.

which is the main alteration attributed to the transition of G_1 phase to S phase.

Furthermore, it was found that the fibroin/aloe gel film exerted a beneficial effect by promoting the migration of fibroblasts and, thereby, stimulating wound closure [31]. Additionally, cell proliferation and cell migration are correlated in the cell cycle, particularly in mitosis phase (M phase), associated with the cell division process when duplicated DNA and cytoplasm were divided to create two identical cells [32]. Cell migration can be also correlated to cytoskeletal reorganization and focal adhesion receptors [33]. Interestingly, cell proliferation result described above showed that the highest percentage of total cells in the fibroin/aloe gel film treated cells was found accumulated in the G_2/M phase, implying the promotion of cell differentiation and cell migration processes by the treated cells. The result was consistent with several prior studies reporting that natural compounds promoted G_2/M phase and fibroblast migration [34, 35].

The limitation of this study due to the use of normal fibroblast cells should be noted. In our previous study, the activities of the fibroin/aloe gel film were evaluated in the streptozotocin-induced diabetic rat and the diabetic fibroblast cells related to the DFU patients [2]. In general, the growth factor functions of the diabetic fibroblast cells are impaired leading to the delayed cell proliferation and cell migration when compared with the normal fibroblast cells [36, 37]. However, the presence of functional groups in the fibroin/aloe gel film, including amides (I, II, III), glucan units, pyranoside ring, and mannose, may enhance the proliferation and the migration of cells, leading to wound healing improvement in the diabetic foot ulcers. Nevertheless, further studies on the expression of growth factors and transcription factors of the film in biomolecular level should be performed using human diabetic dermal fibroblast cells to investigate its wound healing efficacy.

CONCLUSION

The physicochemical and biological activities of gamma-irradiated fibroin/aloe gel film were determined to support the wound healing efficacy reported in our previous study. The gamma irradiation was found to have no effects on the film's physicochemical properties (physical appearance, surface morphology, mechanical properties, and chemical characteristics). For biological activities, the blended fibroin/aloe gel film enhanced the proliferation and the migration of the fibroblast cells and, thereby, might be able to help in stimulating the DFU wound healing process.

Acknowledgements: We would like to thank Naresuan University for financial support for graduate student. We also thank the Center of Excellence for Innovation in Chemistry (PERCH-CIC), Office of the Higher Education Commission and the Faculty of Pharmaceutical Sciences, Naresuan University for facility supports. We wish to thank Mr. Roy I. Morien of the Naresuan University Graduate School for his efforts in editing the English grammar and expression in this paper.

REFERENCES

1. Alexiadou K, Doupis J (2012) Management of diabetic foot ulcers. *Diabetes ther* **3**, ID 4.
2. Inpanya P, Faikrua A, Ounaroon A, Sittichokechaiwut, Viyoch J (2012) Effects of the blended fibroin/aloe gel film on wound healing in streptozotocin-induced diabetic rats. *Biomed Mater* **7**, ID 035008.
3. Zhang W, Chen L, Chen J, Wang L, Gui X, Ran J, Xu G, Zhao H, et al (2017) Silk fibroin biomaterial shows safe and effective wound healing in animal models and a randomized controlled clinical trial. *Adv Healthc Mater* **6**, ID 1700121.
4. Mori H, Tsukada M (2000) New silk protein: modification of silk protein by gene engineering for production of biomaterials. *J Biotechnol* **74**, 95–103.
5. Meinel L, Hofmann S, Karageorgiou V, Kirker-Head C, McCool J, Gronowicz G, Zichner L, Langer R, et al (2005) The inflammatory responses to silk films *in vitro* and *in vivo*. *Biomaterials* **26**, 147–155.
6. Chithra P, Sajithlal GB, Chandrakasan G (1998) Influence of *Aloe vera* on the glycosaminoglycans in the matrix of healing dermal wounds in rats. *J Ethnopharmacol* **59**, 179–186.
7. Maenthaisong R, Chaiyakunapruk N, Niruntraporn S, Kongkaew C (2007) The efficacy of *Aloe vera* used for burn wound healing: A systematic review. *Burns* **33**, 713–718.
8. Femenia A, Sánchez ES, Simal S, Rosselló C (1999) Compositional features of polysaccharides from *Aloe vera* (*Aloe barbadensis* Miller) plant tissues. *Carbohydr Polym* **39**, 109–117.
9. Sahu PK, Giri DD, Singh R, Pandey P, Gupta S, Shrivastava AK, Kumar A, Pandey KD (2013) Therapeutic and medicinal uses of *Aloe vera*: A Review. *Pharmacol Pharm* **4**, 599–610.
10. Sanders ER (2012) Aseptic laboratory techniques: plating methods. *J Vis Exp* **63**, e3064.
11. Pinto Bi, Cruz ND, Lujan OR, Propper CR, Kellar RS (2019) *In vitro* scratch assay to demonstrate effects of arsenic on skin cell migration. *J Vis Exp* **144**, e58838.
12. He S, Shi D, Han Z, Dong Z, Xie Y, Zhang F, Zeng W, Yi Q (2019) Heparinized silk fibroin hydrogels loading FGF1 promote the wound healing in rats with full-thickness skin excision. *Biomed Eng Online* **18**, ID 97.
13. Monsuur HN, Boink MA, Weijers EM, Roffel S, Breetveld M, Gefen A, Broek LJ, Gibbs S (2016) Methods to study differences in cell mobility during skin wound healing *in vitro*. *J Biomech* **49**, 1381–1387.
14. Zhong J, Ma M, Li W, Zhou J, Yan Z, He D (2014) Self-assembly of regenerated silk fibroin from random coil nanostructures to antiparallel β-sheet nanostructures. *Biopolymers* **101**, 1181–1192.
15. Altman GH, Diaz F, Jakuba C, Calabro T, Horan RL, Chen J, Lu H, Richmond J, et al (2003) Silk-based biomaterials. *Biomaterials* **24**, 401–416.
16. Esua MF, Rauwald J-W (2006) Novel bioactive maloyl glucans from *Aloe vera* gel: Isolation, structure elucidation and *in vitro* bioassays. *Carb Res* **341**, 355–364.
17. Kumar K, Bhowmik D, Bhattacharjee C, Biswajit (2010)

Aloe vera: a potential herb and its medicinal importance. *J Chem Pharm Res* **2**, 21–29.

18. Das S, Mishra B, Gill K, Ashraf MS, Singh AK, Sinha M, Sharma S, Xess I, et al (2011) Isolation and characterization of novel protein with anti-fungal and anti-inflammatory properties from *Aloe vera* leaf gel. *Int J Biol Macromol* **48**, 38–43.
19. Koike T, Beppu H, Kuzuya H, Maruta K, Shimpo K, Suzuki M, Titani K, Fujita K (1995) A 35 kDa mannose-binding lectin with hemagglutinating and mitogenic activities from "Kidachi Aloe" (*Aloe arborescens Miller var. natalensis Berger*). *J Biochem* **118**, 1205–1210.
20. Fairand BP (2001) *Radiation Sterilization for Health Care Products. X-Ray, Gamma, and Electron Beam*, 1st edn, CRC Press, Boca Raton, Florida, USA.
21. Aquino K (2012) *Sterilization by Gamma Irradiation, Gamma Radiation*, IntechOpen Limited, London, UK.
22. AlZahrani K, Al-Sewaidan HA (2017) Nanostructural changes in the cell membrane of gamma-irradiated red blood cells. *Indian J Hematol Blood Transfus* **33**, 109–115.
23. Grieb TA, Forng R-Y, Stafford RE, Lin J, Almeida J, Bogdansky S, Ronholdt C, Drohan WN, et al (2005) Effective use of optimized, high-dose (50 kGy) gamma irradiation for pathogen inactivation of human bone allografts. *Biomaterials* **26**, 2033–2042.
24. Araújo ES, Khoury HJ, Silveira SV (1998) Effects of gamma-irradiation on some properties of durolon polycarbonate. *Radiat Phys Chem* **53**, 79–84.
25. Khan S, Villalobos MA, Choron RL, Chang S, Brown SA, Carpenter JP, Tulenko TN, Zhang P (2017) Fibroblast growth factor and vascular endothelial growth factor play a critical role in endotheliogenesis from human adipose-derived stem cells. *J Vasc Surg* **65**, 1483–1492.
26. Ferrara N (2000) VEGF: an update on biological and therapeutic aspects. *Curr Opin Biotechnol* **11**, 617–624.
27. Mandal BB, Kundu SC (2009) Cell proliferation and migration in silk fibroin 3D scaffolds. *Biomaterials* **30**, 2956–2965.
28. Teplicki E, Ma Q, Castillo DE, Zarei M, Hustad AP, Chen J, Li J (2018) The effects of *Aloe vera* on wound healing in cell proliferation, migration, and viability. *Wounds* **30**, 263–268.
29. Hengst L, Nigg EA (2006) Cell cycle: Overview. In: *Encyclopedic Reference of Genomics and Proteomics in Molecular Medicine*, Springer, Berlin, Heidelberg, pp 228–233.
30. Wei X, Guo W, Zou C-H, Fu T-T, Li X-Y, Zhu M, Qi J-H, Song J, et al (2015) Acemannan accelerates cell proliferation and skin wound healing through AKT/mTOR signaling pathway. *J Dermatol Sci* **79**, 101–109.
31. Bainbridge P (2013) Wound healing and the role of fibroblasts. *J Wound Care* **22**, 407–408, 410–412.
32. Yang VW (2012) Chapter 15: The cell cycle. In: Johnson LR, et al (eds) *Physiology of the Gastrointestinal Tract*, 5th edn, Academic Press, Boston, pp 451–471.
33. Kodama A, Lechler T, Fuchs E (2004) Coordinating cytoskeletal tracks to polarize cellular movements. *J Cell Biol* **167**, 203–207.
34. Harishkumar M, Masatoshi Y, Hiroshi S, Tsuyomu I, Masugi M (2013) Revealing the mechanism of *in vitro* wound healing properties of *Citrus tamurana* extract. *Biomed Res Int* **2013**, ID 963457.
35. Zhang S-L, Li B-L, Li W, Lu M, Ni L-Y, Ma H-L, Meng Q-G (2018) The Effects of ludartin on cell proliferation, cell migration, cell cycle arrest and apoptosis are associated with upregulation of p21WAF1 in Saos-2 osteosarcoma cells *in vitro*. *Med Sci Monit* **16**, 4926–4933.
36. Lamers ML, Almeida ME, Vicente-Manzanares M, Horwitz AF, Santos MF (2011) High glucose-mediated oxidative stress impairs cell migration. *PLoS One* **6**, ID e22865.
37. Desta T, Li J, Chino T, Graves DT (2010) Altered fibroblast proliferation and apoptosis in diabetic gingival wounds. *J Dent Res* **89**, 609–614.

Poster

Effect of the blended fibroin/aloe gel extract dressing on skin wound healing process

Preeyawass Phimnuan[1, 2], Saran Worasakwutiphong[1], Anuphan Sittichokechaiwut[1], Francois Grandmottet[1], Wongnapa Nakyai[1], Kunlathida Luangpraditkun[1], Marion Tissot[2], Céline Viennet[2], Jarupa Viyoch[1]

[1]Naresuan university, Phitsanulok, Thailand

[2]Bourgogne Franche-Comté University, INSERM, EFS BFC, UMR1098 RIGHT, UFR Santé, Besançon, France

Introduction

Silk fibroin and *aloe vera* gel extract have shown beneficial activities for delayed wound healing and can be used as biomaterial wound dressing [1-3].

Objectives

1. **To develop the Gamma-irradiated blended fibroin/aloe gel extract as a biomaterial wound dressing**
2. **To determine the Gamma-irradiated blended fibroin/aloe gel extract on the potential wound healing activities including *in vitro*, *in vivo*, clinical study**

Physicochemical properties
(sized of 5.5 x 5.5 cm^2, 50±5 µm thickness)
Tensile strength 6.26±0.44 N
Percent elongation at break 1.20±0.07%

SEM images of surface photomicrographs

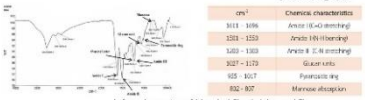

Infrared spectra of blended fibroin/aloe gel film

Results

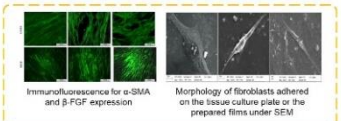

Immunofluorescence for α-SMA and β-FGF expression

Morphology of fibroblasts adhered on the tissue culture plate or the prepared films under SEM

Conclusion: Developed wound dressing promotes the attachment and α-SMA and β-FGF expression of the normal dermal fibroblast cell [1].

Wound characteristics of each patient at each visit after treatment

Conclusion: Developed wound dressing can reduce the healing time and the wound size effectively within 4 weeks and no one got the adverse effects during the experiment [2].

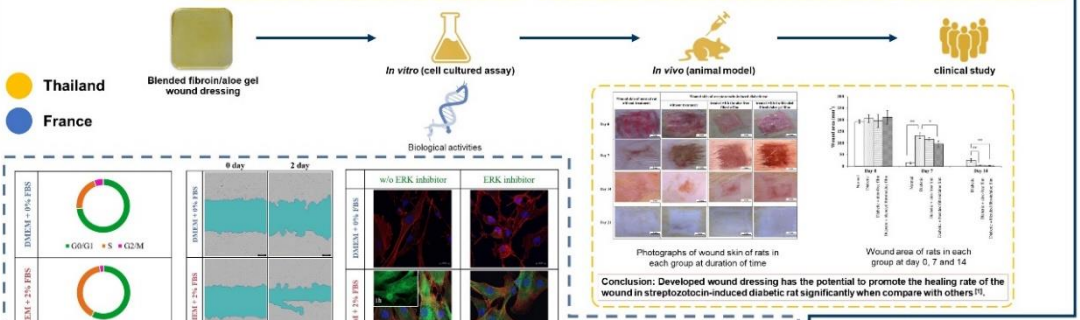

Cell cycle phases of NDF cells for 24h

Cell migration of NDF cells for 2 days

Immunofluorescence for ERK transcription factor

VEGF content (pg/mg protein) of NDF (***; p<0.001)

NDF : Normal human dermal fibroblast
VEGF : Vascular epidermal growth factor

Photographs of wound skin of rats in each group at duration of time

Wound area of rats in each group at day 0, 7 and 14

Conclusion: Developed wound dressing has the potential to promote the healing rate of the wound in streptozotocin-induced diabetic rat significantly when compare with others [3].

Conclusion: Developed wound dressing improves the parameters of wound healing process including cell cycle, cell migration, cell proliferation, and growth factor/transcription factor expression in normal dermal fibroblast cell

Perspective

To detect the biomolecular mechanism(s) of the Gamma-irradiated blended fibroin/aloe gel extract wound dressing, by western blot and qPCR techniques via MAPK pathway

References

1. Inpanya, P., et al., Effects of the blended fibroin/aloe gel film on wound healing in streptozotocin-induced diabetic rats. *Biomedical Materials*, 2012. **7**(3):035008.
2. Worasakwutiphong S, et al. Evaluation of Safety and Healing Potential of Fibroin-Aloe Gel Film in Diabetic Foot Ulcer. *Journal of Wound Care*, 2022. **30**:1020-1028.
3. Phimnuan P, et al. Physicochemical and biological activities of the gamma-irradiated blended fibroin/aloe gel film. *ScienceAsia*, 2022. **48**:278-286.

*Contact email: p.preeyawass@gmail.com

Oral presentation

Investigation of the blended fibroin/aloe gel extract film on the biomolecular mechanism(s) relating to wound healing activity

Preeyawass Phimnuan

Double doctoral degree program: Université de Bourgogne Franche-Comté & Naresuan University

Advisor: **Dr. Céline Viennet-Steiner & Prof. Dr. Jarupa Viyoch**

REFERENCES

1. Saeedi P, Petersohn I, Salpea P, Malanda B, Karuranga S, Unwin N, et al. Global and regional diabetes prevalence estimates for 2019 and projections for 2030 and 2045: Results from the International Diabetes Federation Diabetes Atlas, 9th edition. Diabetes research and clinical practice. 2019;157.
2. American Diabetes A. Diagnosis and classification of diabetes mellitus. Diabetes care. 2013;36 Suppl 1(Suppl 1):S67-S74.
3. Singh N, Armstrong DG, Lipsky BA. Preventing foot ulcers in patients with diabetes. The journal of the American medical association. 2005;293(2):217-28.
4. Alexiadou K, Doupis J. Management of diabetic foot ulcers. Diabetes therapy : research, treatment and education of diabetes and related disorders. 2012;3(1):4-.
5. Hobizal KB, Wukich DK. Diabetic foot infections: current concept review. Diabetic foot & ankle. 2012;3:10.3402/dfa.v3i0.18409.
6. Griffioen AW, Molema G. Angiogenesis: potentials for pharmacologic intervention in the treatment of cancer, cardiovascular diseases, and chronic inflammation. Pharmacological reviews. 2000;52(2):237-68.
7. Hehenberger K, Kratz G, Hansson A, Brismar K. Fibroblasts derived from human chronic diabetic wounds have a decreased proliferation rate, which is recovered by the addition of heparin. Journal of dermatological science. 1998;16(2):144-51.
8. Nass SJ, Li M, Amundadottir LT, Furth PA, Dickson RB. Role for Bcl-xL in the regulation of apoptosis by EGF and TGF beta 1 in c-myc overexpressing mammary epithelial cells. Biochemical and biophysical research communications. 1996;227(1):248-56.
9. Yamakawa S, Hayashida K. Advances in surgical applications of growth factors for wound healing. Burns & trauma. 2019;7:10.
10. Demidova-Rice TN, Hamblin MR, Herman IM. Acute and impaired wound healing: pathophysiology and current methods for drug delivery, part 1: normal and chronic wounds: biology, causes, and approaches to care. Advances in skin & wound care. 2012;25(7):304-14.
11. Edmonds M. Diabetic foot ulcers: practical treatment recommendations. Drugs. 2006;66(7):913-29.
12. Dhivya S, Padma VV, Santhini E. Wound dressings - a review. Biomedicine (Taipei). 2015;5(4):22-.
13. Liu J, Zheng H, Dai X, Sun S, Machens H, Schilling A. Biomaterials for promoting wound healing in diabetes. Journal of tissue science & engineering. 2017;08.

14. Inpanya P, Faikrua A, Ounaroon A, Sittichokechaiwut A, Viyoch J. Effects of the blended fibroin/aloe gel film on wound healing in streptozotocin-induced diabetic rats. Biomedical materials. 2012;7(3):035008.
15. Zhang W, Chen L, Chen J, Wang L, Gui X, Ran J, et al. Silk fibroin biomaterial shows safe and effective wound healing in animal models and a randomized controlled clinical trial. Advanced healthcare materials. 2017;6(10):1700121.
16. Worasakwutiphong S, Termwattanaphakdee T, Kamolhan T, Phimnuan P, Sittichokechaiwut A, Viyoch J. Evaluation of safety and healing potential of fibroin-aloe gel film in diabetic foot ulcer. Journal of wound care. 2021.
17. Mori H, Tsukada M. New silk protein: modification of silk protein by gene engineering for production of biomaterials. Reviews in molecular biotechnology. 2000;74(2):95-103.
18. Horan RL, Antle K, Collette AL, Wang Y, Huang J, Moreau JE, et al. *In vitro* degradation of silk fibroin. Biomaterials. 2005;26(17):3385-93.
19. Meinel L, Hofmann S, Karageorgiou V, Kirker-Head C, McCool J, Gronowicz G, et al. The inflammatory responses to silk films *in vitro* and *in vivo*. Biomaterials. 2005;26(2):147-55.
20. Mauney JR, Nguyen T, Gillen K, Kirker-Head C, Gimble JM, Kaplan DL. Engineering adipose-like tissue *in vitro* and *in vivo* utilizing human bone marrow and adipose-derived mesenchymal stem cells with silk fibroin 3D scaffolds. Biomaterials. 2007;28(35):5280-90.
21. Czekay RP, Wilkins-Port CE, Higgins SP, Freytag J, Overstreet JM, Klein RM, et al. PAI-1: An Integrator of cell signaling and migration. International journal of cell biology. 2011;2011:562481.
22. Park KJ, Shin EJ, Kim SH, Hyun CK. Insulin sensitization of MAP kinase signaling by fibroin in insulin-resistant Hirc-B cells. Pharmacological research. 2005;52(4):346-52.
23. Femenia A, Sánchez ES, Simal S, Rosselló C. Compositional features of polysaccharides from *Aloe vera* (*Aloe barbadensis* Miller) plant tissues. Carbohydrate polymers. 1999;39(2):109-17.
24. Chithra P, Sajithlal GB, Chandrakasan G. Influence of *Aloe vera* on the glycosaminoglycans in the matrix of healing dermal wounds in rats. Journal of ethnopharmacology. 1998;59(3):179-86.
25. Maenthaisong R, Chaiyakunapruk N, Niruntraporn S, Kongkaew C. The efficacy of *Aloe vera* used for burn wound healing: A systematic review. Burns. 2007;33(6):713-8.
26. Bautista R, Segura D, Vázquez-Cruz B. *In vitro* antibradykinin activity of Aloe barbadensis gel. Journal of ethnopharmacology. 2004;93:89-92.
27. Teplicki E, Ma Q, Castillo DE, Zarei M, Hustad AP, Chen J, et al. The Effects of *Aloe vera* on Wound Healing in Cell Proliferation, Migration, and Viability. Wounds : a compendium of clinical research and practice. 2018;30(9):263-8.
28. Atiba A, Ueno H, Uzuka Y. The effect of *Aloe vera* oral administration on cutaneous wound healing in type 2 diabetic rats. The Journal of veterinary medical science. 2011;73(5):583-9.
29. Song QH, Klepeis VE, Nugent MA, Trinkaus-Randall V. TGF-beta1 regulates TGF-beta1 and FGF-2 mRNA expression during fibroblast wound healing. Mol Pathol. 2002;55(3):164-76.

30. Akaberi M, Sobhani Z, Javadi B, Sahebkar A, Emami SA. Therapeutic effects of Aloe spp. in traditional and modern medicine: A review. Biomedicine & pharmacotherapy. 2016;84:759-72.
31. Caesar LK, Cech NB. Synergy and antagonism in natural product extracts: when 1 + 1 does not equal 2. Natural Product Reports. 2019;36(6):869-88.
32. Fairand BP. Radiation Sterilization for Health Care Products. 1st Edition ed. Boca Raton: CRC Press; 2001. 160.
33. Adrovic F. Gamma Radiation: IntechOpen; 2012. 320.
34. Diagnosis and classification of diabetes mellitus. Diabetes care. 2014;37(Supplement 1):S81-S90.
35. World Health O. Definition, diagnosis and classification of diabetes mellitus and its complications : report of a WHO consultation. Part 1, Diagnosis and classification of diabetes mellitus. Geneva: World Health Organization; 1999.
36. Porte D. Central regulation of energy homeostasis. The key role of insulin. 2006;55(Supplement 2):S155-S60.
37. Aronoff SL, Berkowitz K, Shreiner B, Want L. Glucose metabolism and regulation: beyond insulin and glucagon. Diabetes spectrum. 2004;17(3):183-90.
38. Qaid M, Abdelrahman M. Role of insulin and other related hormones in energy metabolism- A review. Cogent Food & Agriculture. 2016;2.
39. Williams R. Williams' textbook of endocrinology, Wilson JD, Foster DW, eds. Philadelphia: WB Saunders; 1992.
40. Wilcox G. Insulin and insulin resistance. The Clinical biochemist Reviews. 2005;26(2):19-39.
41. Maria Rotella C, Pala L, Mannucci E. Role of insulin in the type 2 diabetes therapy: past, present and future. International journal of endocrinology and metabolism. 2013;11(3):137-44.
42. Mellitus WHOECoD, World Health O. WHO expert committee on diabetes mellitus [meeting held in Geneva from 25 September to 1 October 1979] : second report. Geneva: World Health Organization; 1980.
43. Diagnosis and classification of diabetes mellitus. Diabetes care. 2013;36(Supplement 1):S67-S74.
44. Hagopian WA, Karlsen AE, Gottsäter A, Landin-Olsson M, Grubin CE, Sundkvist G, et al. Quantitative assay using recombinant human islet glutamic acid decarboxylase (GAD65) shows that 64K autoantibody positivity at onset predicts diabetes type. The Journal of clinical investigation. 1993;91(1):368-74.
45. Haller MJ, Atkinson MA, Schatz D. Type 1 diabetes mellitus: etiology, presentation, and management. Pediatric clinics. 2005;52(6):1553-78.
46. Chiang JL, Kirkman MS, Laffel LMB, Peters AL. Type 1 diabetes through the life span: a position statement of the american diabetes association. Diabetes care. 2014:DC_141140.
47. Roglic G. WHO Global report on diabetes: A summary. International journal of noncommunicable diseases. 2016;1(1):3.

48. Stumvoll M, Goldstein BJ, Van Haeften TW. Type 2 diabetes: principles of pathogenesis and therapy. The lancet. 2005;365(9467):1333-46.
49. Zhao Y, Xu G, Wu W, Yi X. Type 2 diabetes mellitus-disease, diagnosis and treatment. Journal of diabetes & metabolism. 2015;6(533):2.
50. Organization WH. Guidelines for the prevention, management and care of diabetes mellitus2006.
51. Baynes H. Classification, pathophysiology, diagnosis and management of diabetes mellitus. Journal of diabetes & metabolism. 2015;06.
52. Cho NH, Shaw JE, Karuranga S, Huang Y, da Rocha Fernandes JD, Ohlrogge AW, et al. IDF Diabetes Atlas: Global estimates of diabetes prevalence for 2017 and projections for 2045. Diabetes research and clinical practice. 2018;138:271-81.
53. Abbott C, Carrington A, Ashe H, Bath S, Every L, Griffiths J, et al. The North-West Diabetes Foot Care Study: incidence of, and risk factors for, new diabetic foot ulceration in a community-based patient cohort. Diabetic medicine. 2002;19(5):377-84.
54. Lauterbach S, Kostev K, Kohlmann T. Prevalence of diabetic foot syndrome and its risk factors in the UK. Journal of wound care. 2010;19(8):333-7.
55. Margolis DJ, Allen-Taylor L, Hoffstad O, Berlin JA. Diabetic neuropathic foot ulcers and amputation. Wound repair and regeneration. 2005;13(3):230-6.
56. Groupa FWHCF. Guidance for industry: Chronic cutaneous ulcer and burn wounds-developing products for treatment. Wound repair and regeneration. 2001;9(4):258-68.
57. Coce F, Car N, Pavlić-Renar I, Metelko Z, Rogić M, Jandrić M, et al. The diabetic foot. The Croatian model-national consensus (clinical recommendations for diagnosis, prevention and therapy). Lijecnicki vjesnik. 1999;121(6):175-80.
58. Ndip A, Ebah L, Mbako A. Neuropathic diabetic foot ulcers - evidence-to-practice. International journal of general medicine. 2012;5:129-34.
59. Volmer-Thole M, Lobmann R. Neuropathy and diabetic foot syndrome. International journal of molecular sciences. 2016;17(6):917.
60. Tavee J. Small fiber neuropathy: a burning problem. Cleveland clinic journal of medicine. 2009;76(5):297-305.
61. Boulton AJ, Kirsner RS, Vileikyte L. Neuropathic diabetic foot ulcers. New England journal of medicine. 2004;351(1):48-55.
62. Boulton AJ, Malik RA, Arezzo JC, Sosenko JM. Diabetic somatic neuropathies. Diabetes care. 2004;27(6):1458-86.
63. Andersen H. Motor dysfunction in diabetes. Diabetes/metabolism research and reviews. 2012;28:89-92.
64. Vinik AI, Maser RE, Mitchell BD, Freeman R. Diabetic autonomic neuropathy. Diabetes care. 2003;26(5):1553-79.

65. Marso SP, Hiatt WR. Peripheral arterial disease in patients with diabetes. Journal of the American College of Cardiology. 2006;47(5):921-9.
66. Vogt MT, Cauley JA, Kuller LH, Nevitt MC. Functional status and mobility among elderly women with lower extremity arterial disease: the Study of Osteoporotic Fractures. Journal of the American geriatrics society. 1994;42(9):923-9.
67. Beckman JA, Creager MA, Libby P. Diabetes and atherosclerosis: epidemiology, pathophysiology, and management. The journal of the American medical association. 2002;287(19):2570-81.
68. Ridker PM, Cushman M, Stampfer MJ, Tracy RP, Hennekens CH. Plasma concentration of C-reactive protein and risk of developing peripheral vascular disease. Circulation. 1998;97(5):425-8.
69. Vinik AI, Erbas T, Park TS, Nolan R, Pittenger GL. Platelet dysfunction in type 2 diabetes. Diabetes care. 2001;24(8):1476-85.
70. O'Donnell M, Reid J, Lau L, Hannon R, Lee B. Optimal management of peripheral arterial disease for the non-specialist. The ulster medical journal. 2011;80(1):33.
71. Weitz JI, Byrne J, Clagett GP, Farkouh ME, Porter JM, Sackett DL, et al. Diagnosis and treatment of chronic arterial insufficiency of the lower extremities: a critical review. Circulation. 1996;94(11):3026-49.
72. Bagdade JD, Root RK, Bulger RJ. Impaired leukocyte function in patients with poorly controlled diabetes. Diabetes. 1974;23(1):9-15.
73. Inzucchi SE. Management of hyperglycemia in the hospital setting. New England journal of medicine. 2006;355(18):1903-11.
74. Blakytny R, Jude E. The molecular biology of chronic wounds and delayed healing in diabetes. Diabetic medicine. 2006;23(6):594-608.
75. Brem H, Tomic-Canic M. Cellular and molecular basis of wound healing in diabetes. The Journal of clinical investigation. 2007;117(5):1219-22.
76. Ferguson M, Herrick S, Spencer M-J, Shaw J, Boulton A, Sloan P. The histology of diabetic foot ulcers. Diabetic medicine. 1996;13:S30-S3.
77. Wysocki J, Wierusz-Wysocka B, Wykretowicz A, Wysocki H. The influence of thymus extracts on the chemotaxis of polymorphonuclear neutrophils (PMN) from patients with insulin-dependent diabetes mellitus (IDD). Thymus. 1992;20(1):63-7.
78. Wagner Jr FW. The dysvascular foot: a system for diagnosis and treatment. Foot & ankle. 1981;2(2):64-122.
79. Hunt TK, Hopf H, Hussain Z. Physiology of wound healing. Advances in skin & wound care. 2000;13:6.
80. desJardins-Park HE, Mascharak S, Chinta MS, Wan DC, Longaker MT. The spectrum of scarring in craniofacial wound repair. Frontiers in physiology. 2019;10(322).
81. Ganapathy N, Venkataraman S, Daniel R, Aravind R, Kumarakrishnan V. Molecular biology of wound healing. Journal of pharmacy and bioallied sciences. 2012;4(6):334-7.

82. Li J, Chen J, Kirsner R. Pathophysiology of acute wound healing. Clinics in dermatology. 2007;25(1):9-18.
83. Robson MC, Steed DL, Franz MG. Wound healing: biologic features and approaches to maximize healing trajectories. Current problems in surgery. 2001;2(38):72-140.
84. Martin P. Wound healing-aiming for perfect skin regeneration. Science. 1997;276(5309):75-81.
85. Hart J. Inflammation 1: its role in the healing of acute wounds. Journal of wound care. 2002;11(6):205-9.
86. Eming SA, Krieg T, Davidson JM. Inflammation in wound repair: molecular and cellular mechanisms. Journal of investigative dermatology. 2007;127(3):514-25.
87. Young A, McNaught C-E. The physiology of wound healing. Surgery (Oxford). 2011;29(10):475-9.
88. Witte MB, Barbul A. General principles of wound healing. Surgical clinics of north America. 1997;77(3):509-28.
89. Reinke J, Sorg H. Wound repair and regeneration. European surgical research. 2012;49(1):35-43.
90. George Broughton I, Janis JE, Attinger CE. Wound healing: an overview. Plastic and reconstructive surgery. 2006;117(7S):1e-S-32e-S.
91. Diegelmann RF, Evans MC. Wound healing: an overview of acute, fibrotic and delayed healing. Frontiers in bioscience. 2004;9:283-9.
92. Ramasastry SS. Acute wounds. Clinics in plastic surgery. 2005;32(2):195-208.
93. Baum CL, Arpey CJ. Normal cutaneous wound healing: clinical correlation with cellular and molecular events. Dermatologic surgery. 2005;31(6):674-86.
94. Pierce G, Berg JV, Rudolph R, Tarpley J, Mustoe T. Platelet-derived growth factor-BB and transforming growth factor beta 1 selectively modulate glycosaminoglycans, collagen, and myofibroblasts in excisional wounds. The American journal of pathology. 1991;138(3):629.
95. Risau W. Angiogenic growth factors. Progress in growth factor research. 1990;2(1):71-9.
96. Ribatti D, Vacca A, Roncali L, Dammacco F. Angiogenesis under normal and pathological conditions. Haematologica. 1991;76(4):311-20.
97. Folkman J, Klagsbrun M. Angiogenic factors. Science. 1987;235(4787):442-7.
98. Lazarus GS, Cooper DM, Knighton DR, Margolis DJ, Percoraro RE, Rodeheaver G, et al. Definitions and guidelines for assessment of wounds and evaluation of healing. Wound repair and regeneration. 1994;2(3):165-70.
99. Eckes B, Nischt R, Krieg T. Cell-matrix interactions in dermal repair and scarring. Fibrogenesis & tissue repair. 2010;3(1):4.
100. Hinz B. Formation and function of the myofibroblast during tissue repair. Journal of investigative dermatology. 2007;127(3):526-37.
101. Greenhalgh DG. The role of apoptosis in wound healing. The international journal of biochemistry & cell biology. 1998;30(9):1019-30.

102. Gurtner GC, Evans GR. Advances in head and neck reconstruction. Plastic and reconstructive surgery. 2000;106(3):672-82.
103. Patel S, Srivastava S, Singh MR, Singh D. Mechanistic insight into diabetic wounds: Pathogenesis, molecular targets and treatment strategies to pace wound healing. Biomedicine & pharmacotherapy. 2019;112:108615.
104. Bowers S, Franco E. Chronic wounds: evaluation and management. American family physician. 2020;101(3):159-66.
105. Alavi A, Sibbald RG, Mayer D, Goodman L, Botros M, Armstrong DG, et al. Diabetic foot ulcers: part I. Pathophysiology and prevention. Journal of the American academy of dermatology. 2014;70(1):1.e-.e18.
106. Menke NB, Ward KR, Witten TM, Bonchev DG, Diegelmann RF. Impaired wound healing. Clinics in dermatology. 2007;25(1):19-25.
107. Bao P, Kodra A, Tomic-Canic M, Golinko MS, Ehrlich HP, Brem H. The role of vascular endothelial growth factor in wound healing. Journal of surgical research. 2009;153(2):347-58.
108. Babaei S, Bayat M, Nouruzian M, Bayat M. Pentoxifylline improves cutaneous wound healing in streptozotocin-induced diabetic rats. European journal of pharmacology. 2013;700(1):165-72.
109. Basu Mallik S, Jayashree BS, Shenoy RR. Epigenetic modulation of macrophage polarization-perspectives in diabetic wounds. Journal of diabetes and its complications. 2018;32(5):524-30.
110. Grazul-Bilska AT, Johnson ML, Bilski JJ, Redmer DA, Reynolds LP, Abdullah A, et al. Wound healing: the role of growth factors. 2003.
111. Li Z, Guo S, Yao F, Zhang Y, Li T. Increased ratio of serum matrix metalloproteinase-9 against TIMP-1 predicts poor wound healing in diabetic foot ulcers. Journal of diabetes and its complications. 2013;27(4):380-2.
112. Gooyit M, Peng Z, Wolter WR, Pi H, Ding D, Hesek D, et al. A chemical biological strategy to facilitate diabetic wound healing. ACS chemical biology. 2014;9(1):105-10.
113. Badr G. Camel whey protein enhances diabetic wound healing in a streptozotocin-induced diabetic mouse model: the critical role of β-Defensin-1, -2 and -3. Lipids in health and disease. 2013;12(1):46.
114. Badr G. Supplementation with undenatured whey protein during diabetes mellitus improves the healing and closure of diabetic wounds through the rescue of functional long-lived wound macrophages. Cellular physiology and biochemistry : international journal of experimental cellular physiology, biochemistry, and pharmacology. 2012;29(3-4):571-82.
115. Clayton W, Jr., Elasy TA. A Review of the pathophysiology, classification, and treatment of foot ulcers in diabetic patients. Clinical diabetes. 2009;27(2):52-8.
116. Singh K, Agrawal NK, Gupta SK, Mohan G, Chaturvedi S, Singh K. Genetic and epigenetic alterations in Toll like receptor 2 and wound healing impairment in type 2 diabetes patients. Journal of diabetes and its complications. 2015;29(2):222-9.

117. Peleg AY, Weerarathna T, McCarthy JS, Davis TME. Common infections in diabetes: pathogenesis, management and relationship to glycaemic control. Diabetes/metabolism research and reviews. 2007;23(1):3-13.
118. Smith K, Collier A, Townsend EM, O'Donnell LE, Bal AM, Butcher J, et al. One step closer to understanding the role of bacteria in diabetic foot ulcers: Characterizing the microbiome of ulcers. BMC microbiology. 2016;16(1).
119. Moura J, Rodrigues J, Gonçalves M, Amaral C, Lima M, Carvalho E. Impaired T-cell differentiation in diabetic foot ulceration. Cellular & molecular immunology. 2016:21.
120. Abiko Y, Selimovic D. The mechanism of protracted wound healing on oral mucosa in diabetes. Review. Bosnian journal of basic medical sciences. 2010;10(3):186-91.
121. Tellechea A, Leal EC, Kafanas A, Auster ME, Kuchibhotla S, Ostrovsky Y, et al. Mast cells regulate wound healing in Diabetes. Diabetes. 2016;65(7):2006-19.
122. Grieb G, Simons D, Eckert L, Hemmrich M, Steffens G, Bernhagen J, et al. Levels of macrophage migration inhibitory factor and glucocorticoids in chronic wound patients and their potential interactions with impaired wound endothelial progenitor cell migration. Wound repair and regeneration. 2012;20(5):707-14.
123. Dennis PA, Rifkin DB. Cellular activation of latent transforming growth factor beta requires binding to the cation-independent mannose 6-phosphate/insulin-like growth factor type II receptor. Proceedings of the national academy of sciences. 1991;88(2):580-4.
124. Kratz G, Lake M, Ljungström K, Forsberg G, Hægerstrand A, Gidlund M. Effect of recombinant IGF binding protein-1 on primary cultures of human keratinocytes and fibroblasts: selective enhancement of IGF-1 but not IGF-2-induced cell proliferation. Experimental cell research. 1992;202(2):381-5.
125. Brown DL, Kane CD, Chernausek SD, Greenhalgh DG. Differential expression and localization of insulin-like growth factors I and II in cutaneous wounds of diabetic and nondiabetic mice. The American journal of pathology. 1997;151(3):715.
126. Levine J, Moses H, Gold L, Nanney L. Spatial and temporal patterns of immunoreactive transforming growth factor beta 1, beta 2, and beta 3 during excisional wound repair. The American journal of pathology. 1993;143(2):368.
127. Roberts AB. Transforming growth factor-β: activity and efficacy in animal models of wound healing. Wound repair and regeneration. 1995;3(4):408-18.
128. Schmid P, Cox D, Bilbe G, McMaster G, Morrison C, Stähelin H, et al. TGF-βs and TGF-β type II receptor in human epidermis: differential expression in acute and chronic skin wounds. The journal of pathology. 1993;171(3):191-7.
129. Heldin C-H, Westermark B. Mechanism of action and *in vivo* role of platelet-derived growth factor. Physiological reviews. 1999;79(4):1283-316.

130. Castronuovo Jr J, Ghobrial I, Giusti A, Rudolph S, Smiell J. Effects of chronic wound fluid on the structure and biological activity of becaplermin (rhPDGF–BB) and becaplermin gel. The American journal of surgery. 1998;176(2):61S-7S.
131. Brauchle M, Angermeyer K, Hübner G, Werner S. Large induction of keratinocyte growth factor expression by serum growth factors and pro-inflammatory cytokines in cultured fibroblasts. Oncogene. 1994;9(11):3199-204.
132. Frank S, Hübner G, Breier G, Longaker MT, Greenhalgh DG, Werner S. Regulation of vascular endothelial growth factor expression in cultured keratinocytes. Implications for normal and impaired wound healing. Journal of biological chemistry. 1995;270(21):12607-13.
133. Wetzler C, Kämpfer H, Stallmeyer B, Pfeilschifter J, Frank S. Large and sustained induction of chemokines during impaired wound healing in the genetically diabetic mouse: prolonged persistence of neutrophils and macrophages during the late phase of repair. Journal of investigative dermatology. 2000;115(2):245-53.
134. Tonnesen MG, Feng X, Clark RA, editors. Angiogenesis in wound healing. Journal of investigative dermatology symposium proceedings; 2000: Elsevier.
135. Martin A, Komada MR, Sane DC. Abnormal angiogenesis in diabetes mellitus. Medicinal research reviews. 2003;23(2):117-45.
136. Altavilla D, Saitta A, Cucinotta D, Galeano M, Deodato B, Colonna M, et al. Inhibition of lipid peroxidation restores impaired vascular endothelial growth factor expression and stimulates wound healing and angiogenesis in the genetically diabetic mouse. Diabetes. 2001;50(3):667-74.
137. Reed MJ, Vernon RB, Abrass IB, Sage EH. TGF-β1 induces the expression of type I collagen and SPARC, and enhances contraction of collagen gels, by fibroblasts from young and aged donors. Journal of cellular physiology. 1994;158(1):169-79.
138. Li G, Li Y-Y, Sun J-E, Lin W-h, Zhou R-x. ILK–PI3K/AKT pathway participates in cutaneous wound contraction by regulating fibroblast migration and differentiation to myofibroblast. Laboratory investigation. 2016;96(7):741-51.
139. Loughlin DT, Artlett CM. Modification of collagen by 3-deoxyglucosone alters wound healing through differential regulation of p38 MAP Kinase. PLOS ONE. 2011;6(5):e18676.
140. Nishikai-Yan Shen T, Kanazawa S, Kado M, Okada K, Luo L, Hayashi A, et al. Interleukin-6 stimulates Akt and p38 MAPK phosphorylation and fibroblast migration in non-diabetic but not diabetic mice. PLOS ONE. 2017;12(5):e0178232.
141. Sidarala V, Kowluru A. The regulatory roles of mitogen-activated protein kinase (MAPK) pathways in health and diabetes: lessons learned from the pancreatic β-Cell. Recent patents on endocrine, metabolic and immune drug discovery. 2017;10(2):76-84.
142. Guo Y, Guo C, Ha W, Ding Z. Carnosine improves diabetic retinopathy via the MAPK/ERK pathway. Experimental and therapeutic medicine. 2019;17(4):2641-7.

143. Wang S, Ding L, Ji H, Xu Z, Liu Q, Zheng Y. The role of p38 MAPK in the development of diabetic cardiomyopathy. International journal of molecular. 2016;17(7).
144. Boateng J, Catanzano O. Advanced therapeutic dressings for effective wound healing--A review. Journal of pharmaceutical sciences. 2015;104(11):3653-80.
145. Boateng JS, Matthews KH, Stevens HN, Eccleston GM. Wound healing dressings and drug delivery systems: a review. Journal of pharmaceutical sciences. 2008;97(8):2892-923.
146. Fonder MA, Lazarus GS, Cowan DA, Aronson-Cook B, Kohli AR, Mamelak AJ. Treating the chronic wound: A practical approach to the care of nonhealing wounds and wound care dressings. The journal of the American academy of dermatology. 2008;58(2):185-206.
147. Koehler J, Brandl FP, Goepferich AM. Hydrogel wound dressings for bioactive treatment of acute and chronic wounds. European polymer journal. 2018;100:1-11.
148. Vowden K, Vowden P. Wound dressings: principles and practice. Surgery (Oxford). 2017;35(9):489-94.
149. Dabiri G, Damstetter E, Phillips T. Choosing a wound dressing based on common wound characteristics. Advances in wound care. 2016;5(1):32-41.
150. Rezvani Ghomi E, Khalili S, Nouri Khorasani S, Esmaeely Neisiany R, Ramakrishna S. Wound dressings: Current advances and future directions. Journal of applied polymer science. 2019;136(27):47738.
151. Morgan DA. Wounds-What should a dressing formulary include? Hospital pharmacist. 2002;9:261-6.
152. Thomas A, Harding KG, Moore K. Alginates from wound dressings activate human macrophages to secrete tumour necrosis factor-alpha. Biomaterials. 2000;21(17):1797-802.
153. Agren MS, Mertz PM, Franzén L. A comparative study of three occlusive dressings in the treatment of full-thickness wounds in pigs. The journal of the American academy of dermatology. 1997;36(1):53-8.
154. Tavakoli S, Klar AS. Advanced hydrogels as wound dressings. Biomolecules. 2020;10(8).
155. Nathoo R, Howe N, Cohen G. Skin substitutes: an overview of the key players in wound management. The Journal of clinical and aesthetic dermatology. 2014;7(10):44-8.
156. Sood A, Granick MS, Tomaselli NL. Wound dressings and comparative effectiveness data. Advances in wound care. 2014;3(8):511-29.
157. Broussard KC, Powers JG. Wound dressings: selecting the most appropriate type. American journal of clinical dermatology. 2013;14(6):449-59.
158. Shao Z, Vollrath F. Surprising strength of silkworm silk. Nature. 2002;418(6899):741.
159. Valluzzi R, Winkler S, Wilson D, Kaplan DL. Silk: molecular organization and control of assembly. Philosophical transactions of the royal society of London series B: Biological sciences. 2002;357(1418):165-7.

160. Mondal M, Trivedy K, Kumar N. The silk proteins, sericin and fibroin in silkworm, *Bombyx mori* Linn. A review. 2006;5.
161. Altman GH, Diaz F, Jakuba C, Calabro T, Horan RL, Chen J, et al. Silk-based biomaterials. Biomaterials. 2003;24(3):401-16.
162. Tanaka K, Inoue S, Mizuno S. Hydrophobic interaction of P25, containing Asn-linked oligosaccharide chains, with the HL complex of silk fibroin produced by *Bombyx mori*. Insect biochemistry and molecular biology. 1999;29(3):269-76.
163. Kim U-J, Park J, Kim HJ, Wada M, Kaplan DL. Three-dimensional aqueous-derived biomaterial scaffolds from silk fibroin. Biomaterials. 2005;26(15):2775-85.
164. DeBari MK, Abbott RD. Microscopic considerations for optimizing silk biomaterials. WIREs nanomedicine and nanobiotechnology. 2019;11(2):e1534.
165. Li J, Zhu H, Lei C, Chen J. Enzymatic hydrolysis of silk fibroin peptide for hemorrhage control. DEStech transactions on materials science and engineering. 2015(icmea).
166. Li M, Ogiso M, Minoura N. Enzymatic degradation behavior of porous silk fibroin sheets. Biomaterials. 2003;24(2):357-65.
167. Zuo B, Dai L, Wu Z. Analysis of structure and properties of biodegradable regenerated silk fibroin fibers. Journal of materials science. 2006;41(11):3357-61.
168. Panilaitis B, Altman GH, Chen J, Jin H-J, Karageorgiou V, Kaplan DL. Macrophage responses to silk. Biomaterials. 2003;24(18):3079-85.
169. Barker RH. Additives in fibers and fabrics. Environmental health perspectives. 1975;11:41-5.
170. Chiarini A, Petrini P, Bozzini S, Dal Pra I, Armato U. Silk fibroin/poly (carbonate)-urethane as a substrate for cell growth: *in vitro* interactions with human cells. Biomaterials. 2003;24(5):789-99.
171. dal Prà I, Petrini P, Charini A, Bozzini S, Farè S, Armato U. Silk fibroin-coated three-dimensional polyurethane scaffolds for tissue engineering: interactions with normal human fibroblasts. Tissue engineering. 2003;9(6):1113-21.
172. Min B-M, Lee G, Kim SH, Nam YS, Lee TS, Park WH. Electrospinning of silk fibroin nanofibers and its effect on the adhesion and spreading of normal human keratinocytes and fibroblasts *in vitro*. Biomaterials. 2004;25(7-8):1289-97.
173. Sugihara A, Sugiura K, Morita H, Ninagawa T, Tubouchi K, Tobe R, et al. Promotive effects of a silk film on epidermal recovery from full-thickness skin wounds (44552). Proceedings of the society for experimental biology and medicine. 2000;225(1):58-64.
174. Roh D-H, Kang S-Y, Kim J-Y, Kwon Y-B, Kweon HY, Lee K-G, et al. Wound healing effect of silk fibroin/alginate-blended sponge in full thickness skin defect of rat. Journal of materials science: materials in medicine. 2006;17(6):547-52.
175. Aukhil I. Biology of wound healing. Periodontology 2000. 2000;22(1):44-50.
176. Roberts AB, Sporn MB, Assoian RK, Smith JM, Roche NS, Wakefield LM, et al. Transforming growth factor type beta: rapid induction of fibrosis and angiogenesis *in vivo* and stimulation of

collagen formation *in vitro*. Proceedings of the national academy of sciences. 1986;83(12):4167-71.

177. Hashimoto T, Kojima K, Otaka A, Takeda YS, Tomita N, Tamada Y. Quantitative evaluation of fibroblast migration on a silk fibroin surface and TGFBI gene expression. Journal of biomaterials science, polymer edition. 2013;24(2):158-69.
178. Song Q, Gou Q, Xie Y, Zhang Z, Fu C. Periplaneta americana extracts promote skin wound healing via nuclear factor kappa B canonical pathway and extracellular signal-regulated kinase signaling. Evidence-based complementary and alternative medicine. 2017;2017.
179. Schmid JA, Birbach A. IκB kinase β (IKKβ/IKK2/IKBKB)-A key molecule in signaling to the transcription factor NF-κB. Cytokine & growth factor reviews. 2008;19(2):157-65.
180. Hoesel B, Schmid JA. The complexity of NF-κB signaling in inflammation and cancer. Molecular cancer. 2013;12:86-.
181. Czekay R-P, Wilkins-Port CE, Higgins SP, Freytag J, Overstreet JM, Klein RM, et al. PAI-1: an integrator of cell signaling and migration. International journal of cell biology. 2011;2011.
182. Huang C, Rajfur Z, Borchers C, Schaller MD, Jacobson K. JNK phosphorylates paxillin and regulates cell migration. Nature. 2003;424(6945):219-23.
183. Tao W, Liou GI, Wu X, Abney T, Reinach P. ETB and epidermal growth factor receptor stimulation of wound closure in bovine corneal epithelial cells. Investigative ophthalmology & visual science. 1995;36(13):2614-22.
184. Yujiri T, Ware M, Widmann C, Oyer R, Russell D, Chan E, et al. MEK kinase 1 gene disruption alters cell migration and c-Jun NH2-terminal kinase regulation but does not cause a measurable defect in NF-κB activation. Proceedings of the national academy of sciences. 2000;97(13):7272-7.
185. You H, Padmashali RM, Ranganathan A, Lei P, Girnius N, Davis RJ, et al. JNK regulates compliance-induced adherens junctions formation in epithelial cells and tissues. The journal of cell science. 2013;126(12):2718-29.
186. Liu T-l, Miao J-c, Sheng W-h, Xie Y-f, Huang Q, Shan Y-b, et al. Cytocompatibility of regenerated silk fibroin film: a medical biomaterial applicable to wound healing. Journal of Zhejiang University scienceB. 2010;11(1):10-6.
187. Augustin HG, Breier G. Angiogenesis: molecular mechanisms and functional interactions. Thrombosis and haemostasis. 2003;89(01):190-7.
188. Nissen NN, Polverini P, Koch AE, Volin MV, Gamelli RL, DiPietro LA. Vascular endothelial growth factor mediates angiogenic activity during the proliferative phase of wound healing. The American journal of pathology. 1998;152(6):1445.
189. Boudreau MD, Beland FA. An evaluation of the biological and toxicological properties of *Aloe barbadensis* (miller), *Aloe vera*. Journal of Environmental Science and Health Part C. 2006;24(1):103-54.

190. Sánchez-Machado DI, López-Cervantes J, Sendón R, Sanches-Silva A. *Aloe vera*: Ancient knowledge with new frontiers. Trends in food Science & technology. 2017;61:94-102.
191. Chandegara V, Varshney A. *Aloe vera* L. processing and products: A review. 2013.
192. Joseph B, Raj SJ. Pharmacognostic and phytochemical properties of *Aloe vera* Linn an overview. 2010.
193. Eshun K, He Q. *Aloe vera*: a valuable ingredient for the food, pharmaceutical and cosmetic industries—a review. Critical reviews in food science and nutrition. 2004;44(2):91-6.
194. Akaberi M, Sobhani Z, Javadi B, Sahebkar A, Emami SA. Therapeutic effects of Aloe spp. in traditional and modern medicine: A review. Biomedicine & pharmacotherapy. 2016;84:759-72.
195. Reynolds T, Dweck A. *Aloe vera* leaf gel: a review update. Journal of ethnopharmacology. 1999;68(1-3):3-37.
196. Femenia A, García-Pascual P, Simal S, Rosselló C. Effects of heat treatment and dehydration on bioactive polysaccharide acemannan and cell wall polymers from *Aloe barbadensis* Miller. Carbohydrate polymers. 2003;51(4):397-405.
197. Vogler B, Ernst E. *Aloe vera*: a systematic review of its clinical effectiveness. The British journal of general practice. 1999;49(447):823-8.
198. Surjushe A, Vasani R, Saple D. *Aloe vera*: a short review. Indian journal of dermatology. 2008;53(4):163.
199. Kumar K, Bhowmik D, Bhattacharjee C, Biswajit. *Aloe vera* : A potential Herb and its medicinal importance. 2010:21-9.
200. Sahu PK, Giri DD, Singh R, Pandey P, Gupta S, Shrivastava AK, et al. Therapeutic and medicinal uses of *Aloe vera*: a review. Pharmacology & pharmacy. 2013;4(08):599.
201. Choi S, Chung M-H, editors. A review on the relationship between *Aloe vera* components and their biologic effects. Seminars in integrative medicine; 2003: Elsevier.
202. Shrivastava N, Mahajan S, Jain A, Sharma P, Kharakwal AC, Varma A. Mutualistic interaction of *Piriformospora indica* (Serendipita indica) with *Aloe vera*, the wonder plant for modern living. American journal of plant sciences. 2019;10(11):2002-11.
203. Shelton RM. *Aloe vera*: its chemical and therapeutic properties. International journal of dermatology. 1991;30(10):679-83.
204. Rosca-Casian O, Parvu M, Vlase L, Tamas M. Antifungal activity of *Aloe vera* leaves. Fitoterapia. 2007;78(3):219-22.
205. Cole L, Heard C. Skin permeation enhancement potential of *Aloe Vera* and a proposed mechanism of action based upon size exclusion and pull effect. International journal of pharmaceutics. 2007;333(1-2):10-6.
206. Chantarawaratit P, Sangvanich P, Banlunara W, Soontornvipart K, Thunyakitpisal P. Acemannan sponges stimulate alveolar bone, cementum and periodontal ligament regeneration in a canine class II furcation defect model. Journal of periodontal research. 2014;49(2):164-78.

207. Shi Y, Massagué J. Mechanisms of TGF-β signaling from cell membrane to the nucleus. Cell. 2003;113(6):685-700.
208. Song Q, Klepeis V, Nugent M, Trinkaus-Randall V. TGF-β1 regulates TGF-β1 and FGF-2 mRNA expression during fibroblast wound healing. Molecular ฆathology. 2002;55(3):164.
209. Davis RH, Maro NP. *Aloe vera* and gibberellin. Anti-inflammatory activity in diabetes. Journal of the American podiatric medical association. 1989;79(1):24-6.
210. Im S-A, Oh S-T, Song S, Kim M-R, Kim D-S, Woo S-S, et al. Identification of optimal molecular size of modified Aloe polysaccharides with maximum immunomodulatory activity. International immunopharmacology. 2005;5(2):271-9.
211. Park M-Y, Kwon H-J, Sung M-K. Intestinal absorption of aloin, aloe-emodin, and aloesin; A comparative study using two *in vitro* absorption models. Nutrition research and practice. 2009;3(1):9-14.
212. Habeeb F, Shakir E, Bradbury F, Cameron P, Taravati MR, Drummond AJ, et al. Screening methods used to determine the anti-microbial properties of *Aloe vera* inner gel. Methods. 2007;42(4):315-20.
213. Pugh N, Ross SA, ElSohly MA, Pasco DS. Characterization of Aloeride, a new high-molecular-weight polysaccharide from *Aloe vera* with potent immunostimulatory activity. Journal of agricultural and food chemistry. 2001;49(2):1030-4.
214. Mariita RM, Orodho JA, Okemo PO, Kirimuhuzya C, Otieno JN, Magadula JJ. Methanolic extracts of Aloe secundiflora Engl. inhibits *in vitro* growth of tuberculosis and diarrhea-causing bacteria. Pharmacognosy research. 2011;3(2):95.
215. Phimnuan P, Worasakwutiphong S, Sittichokechaiwut A, Grandmottet F, Nakyai W, Luangpraditkun K, et al. Physicochemical and biological activities of the gamma-irradiated blended fibroin/aloe gel film. ScienceAsia. 2022;48:278.
216. Pinto BI, Cruz ND, Lujan OR, Propper CR, Kellar RS. *In Vitro* scratch assay to demonstrate effects of arsenic on skin cell migration. Journal of visualized experiments : JoVE. 2019(144):10.3791/58838.
217. Toledo-Piza AR, Nakano E, Rici REG, Maria DA. Proliferation of fibroblasts and endothelial cells is enhanced by treatment with Phyllocaulis boraceiensis mucus. Cell proliferation. 2013;46(1):97-108.
218. Nakyai W, Tissot M, Humbert P, Grandmottet F, Viyoch J, Viennet C. Effects of repeated UVA irradiation on human skin fibroblasts embedded in 3D tense collagen matrix. Photochemistry and photobiology. 2018;94(4):715-24.
219. Zhong J, Ma M, Li W, Zhou J, Yan Z, He D. Self-assembly of regenerated silk fibroin from random coil nanostructures to antiparallel β-sheet nanostructures. Biopolymers. 2014;101(12):1181-92.
220. Esua M, Rauwald J-W. Novel bioactive maloyl glucans from *Aloe vera* gel: Isolation, structure elucidation and *in vitro* bioassays. Carbohydrate research. 2006;341:355-64.

221. Das S, Mishra B, Gill K, Ashraf MS, Singh AK, Sinha M, et al. Isolation and characterization of novel protein with anti-fungal and anti-inflammatory properties from *Aloe vera* leaf gel. International journal of biological macromolecules. 2011;48(1):38-43.
222. Koike T, Beppu H, Kuzuya H, Maruta K, Shimpo K, Suzuki M, et al. A 35 kDa Mannose-binding lectin with hemagglutinating and mitogenic activities from "Kidachi Aloe" *Aloe arborescens* Miller var. natalensis Berger. The journal of biochemistry. 1995;118(6):1205-10.
223. Aquino K. Sterilization by gamma irradiation. 2012.
224. AlZahrani K, Al-Sewaidan HA. Nanostructural changes in the cell membrane of gamma-irradiated red blood cells. Indian journal of hematology and blood transfusion. 2017;33(1):109-15.
225. Grieb TA, Forng RY, Stafford RE, Lin J, Almeida J, Bogdansky S, et al. Effective use of optimized, high-dose (50 kGy) gamma irradiation for pathogen inactivation of human bone allografts. Biomaterials. 2005;26(14):2033-42.
226. Araújo ES, Khoury HJ, Silveira SV. Effects of gamma-irradiation on some properties of durolon polycarbonate. Radiation physics and chemistry. 1998;53(1):79-84.
227. Ferrara N. VEGF: an update on biological and therapeutic aspects. Current opinion in biotechnology. 2000;11(6):617-24.
228. Khan S, Villalobos MA, Choron RL, Chang S, Brown SA, Carpenter JP, et al. Fibroblast growth factor and vascular endothelial growth factor play a critical role in endotheliogenesis from human adipose-derived stem cells. Journal of vascular surgery. 2017;65(5):1483-92.
229. Mandal BB, Kundu SC. Cell proliferation and migration in silk fibroin 3D scaffolds. Biomaterials. 2009;30(15):2956-65.
230. Teplicki E, Ma Q, Castillo D, Zarei M, Hustad A, Chen J, et al. The effects of *Aloe vera* on wound healing in cell proliferation, migration, and viability. wounds : a compendium of clinical research and practice. 2018;30:263-8.
231. Hengst L, Nigg EA. Cell Cycle – Overview. Encyclopedic reference of genomics and proteomics in molecular medicine. Berlin, Heidelberg: Springer Berlin Heidelberg; 2006. p. 228-33.
232. Wei X, Guo W, Zou C-H, Fu T-T, Li X-Y, Zhu M, et al. Acemannan accelerates cell proliferation and skin wound healing through AKT/mTOR signaling pathway. Journal of dermatological science. 2015;79.
233. Bainbridge P. Wound healing and the role of fibroblasts. Journal of wound care. 2013;22(8):407-8, 10-12.
234. Yang VW. Chapter 15 - The Cell Cycle. In: Johnson LR, Ghishan FK, Kaunitz JD, Merchant JL, Said HM, Wood JD, editors. Physiology of the gastrointestinal tract (5th Edition). Boston: academic press; 2012.451-71.
235. Kodama A, Lechler T, Fuchs E. Coordinating cytoskeletal tracks to polarize cellular movements. Journal of cell biology. 2004;167(2):203-7.

236. Harishkumar M, Masatoshi Y, Hiroshi S, Tsuyomu I, Masugi M. Revealing the mechanism of *in vitro* wound healing properties of *Citrus tamurana* extract. Biomed Res Int. 2013;2013:963457.
237. Zhang S-L, Li B-L, Li W, Lu M, Ni L-Y, Ma H-L, et al. The effects of ludartin on cell proliferation, cell migration, cell cycle arrest and apoptosis are associated with upregulation of p21WAF1 in Saos-2 osteosarcoma cells *in vitro*. Medical science monitor : international medical journal of experimental and clinical research. 2018;24:4926-33.
238. Ghasemi M, Turnbull T, Sebastian S, Kempson I. The MTT assay: utility, limitations, pitfalls, and interpretation in bulk and single-cell analysis. International journal of molecular sciences. 2021;22(23).
239. Mead TJ, Lefebvre V. Proliferation assays (BrdU and EdU) on skeletal tissue sections. Methods in molecular biology (Clifton, NJ). 2014;1130:233-43.
240. Aleksandar J, Vladan P, Markovic-Jovanovic S, Stolic R, Mitic J, Smilic T. Hyperlactatemia and the outcome of type 2 diabetic patients suffering acute myocardial infarction. Journal of diabetes research. 2016;2016:6901345.
241. Mahali S, Raviprakash N, Raghavendra PB, Manna SK. Advanced glycation end products (AGEs) induce apoptosis via a novel pathway: involvement of Ca^{2+} mediated by interleukin-8 protein. The journal of biological chemistry. 2011;286(40):34903-13.
242. Park YR, Sultan MT, Park HJ, Lee JM, Ju HW, Lee OJ, et al. NF-κB signaling is key in the wound healing processes of silk fibroin. Acta biomaterialia. 2018;67:183-95.
243. Yamada H, Igarashi Y, Takasu Y, Saito H, Tsubouchi K. Identification of fibroin-derived peptides enhancing the proliferation of cultured human skin fibroblasts. Biomaterials. 2004;25(3):467-72.
244. Yagi A, Egusa T, Arase M, Tanabe M, Tsuji H. Isolation and characterization of the glycoprotein fraction with a proliferation-promoting activity on human and hamster cells *in vitro* from *Aloe vera* gel. Planta medica. 1997;63(1):18-21.
245. Xing W, Guo W, Zou C-H, Fu T-T, Li X-Y, Zhu M, et al. Acemannan accelerates cell proliferation and skin wound healing through AKT/mTOR signaling pathway. Journal of dermatological science. 2015;79(2):101-9.
246. Wolf G. Cell cycle regulation in diabetic nephropathy. Kidney international. 2000;58:S59-S66.
247. Yuan L, Duan X, Zhang R, Zhang Y, Qu M. Aloe polysaccharide protects skin cells from UVB irradiation through Keap1/Nrf2/ARE signal pathway. Journal of dermatological treatment. 2020;31(3):300-8.
248. Lamers ML, Almeida ME, Vicente-Manzanares M, Horwitz AF, Santos MF. High glucose-mediated oxidative stress impairs cell migration. PloS one. 2011;6(8):e22865.
249. Hoesel B, Schmid JA. The complexity of NF-κB signaling in inflammation and cancer. Molecular cancer. 2013;12(1):86.

250. Moriyama M, Moriyama H, Uda J, Kubo H, Nakajima Y, Goto A, et al. Beneficial effects of the genus aloe on wound healing, cell proliferation, and differentiation of epidermal keratinocytes. PLoS One. 2016;11(10):e0164799.
251. Herranz N, Gil J. Mechanisms and functions of cellular senescence. The journal of clinical investigation. 2018;128(4):1238-46.
252. Mijit M, Caracciolo V, Melillo A, Amicarelli F, Giordano A. Role of p53 in the regulation of cellular senescence. Biomolecules. 2020;10(3).
253. Berlanga-Acosta JA, Guillén-Nieto GE, Rodríguez-Rodríguez N, Mendoza-Mari Y, Bringas-Vega ML, Berlanga-Saez JO, et al. Cellular senescence as the pathogenic hub of diabetes-related wound chronicity. Frontiers in endocrinology. 2020;11:573032.
254. Bitar MS, Abdel-Halim SM, Al-Mulla F. Caveolin-1/PTRF upregulation constitutes a mechanism for mediating p53-induced cellular senescence: implications for evidence-based therapy of delayed wound healing in diabetes. American journal of physiology endocrinology and metabolism. 2013;305(8):E951-63.
255. Ma XY, Cui D, Wang Z, Liu B, Yu HL, Yuan H, et al. Silk fibroin/hydroxyapatite coating improved osseointegration of porous titanium implants under diabetic conditions via activation of the PI3K/Akt signaling pathway. ACS biomaterials science & engineering. 2022;8(7):2908-19.
256. Hu Y, Xu J, Hu Q. Evaluation of antioxidant potential of *Aloe vera* (*Aloe barbadensis* Miller) extracts. Journal of agricultural and food chemistry. 2003;51(26):7788-91
257. Weinberg E, Maymon T, Weinreb M. AGEs induce caspase-mediated apoptosis of rat BMSCs via TNFα production and oxidative stress. Journal of molecular endocrinology. 2014;52(1):67-76.
258. Alao JP. The regulation of cyclin D1 degradation: roles in cancer development and the potential for therapeutic invention. Molecular cancer. 2007;6(1):24.
259. Hoeben A, Landuyt B, Highley MS, Wildiers H, Van Oosterom AT, De Bruijn EA. Vascular endothelial growth factor and angiogenesis. Pharmacological reviews. 2004;56(4):549-80.
260. Firdaus I, Arfian N, Wahyuningsih MSH, Agustiningsih D. *Aloe vera* stimulate cell proliferation, cell migration, expression of vascular endothelial growth factor-A (VEGF-A), and c-Jun N-terminal kinase-1 (JNK-1) on fibroblast of diabetic rat models. Journal of thee medical sciences (Berkala ilmu kedokteran). 2019.
261. Jettanacheawchankit S, Sasithanasate S, Sangvanich P, Banlunara W, Thunyakitpisal P. Acemannan stimulates gingival fibroblast proliferation; expressions of keratinocyte growth factor-1, vascular endothelial growth factor, and type I collagen; and wound healing. Journal of pharmacological sciences. 2009;109(4):525-31.
262. Choi S, Kim KW, Choi JS, Han ST, Park YI, Lee SK, et al. Angiogenic activity of beta-sitosterol in the ischaemia/reperfusion-damaged brain of Mongolian gerbil. Planta medica. 2002;68(4):330-5.
263. Guo YJ, Pan WW, Liu SB, Shen ZF, Xu Y, Hu LL. ERK/MAPK signaling pathway and tumorigenesis. Experimental and therapeutic medicine. 2020;19(3):1997-2007.

264. Plotnikov A, Zehorai E, Procaccia S, Seger R. The MAPK cascades: Signaling components, nuclear roles and mechanisms of nuclear translocation. Biochimica et Biophysica Acta (BBA) - Molecular Cell Research. 2011;1813(9):1619-33.
265. Avruch J, Khokhlatchev A, Kyriakis JM, Luo Z, Tzivion G, Vavvas D, et al. Ras activation of the Raf kinase: tyrosine kinase recruitment of the MAP kinase cascade. Recent progress in hormone research. 2001;56:127-55.
266. Di Paola R, Galuppo M, Mazzon E, Paterniti I, Bramanti P, Cuzzocrea S. PD98059, a specific MAP kinase inhibitor, attenuates multiple organ dysfunction syndrome/failure (MODS) induced by zymosan in mice. Pharmacological research. 2010;61(2):175-87.
267. Huang Y, Zou Y, Lin L, Ma X, Zheng R. miR-101 regulates the cell proliferation and apoptosis in diffuse large B-cell lymphoma by targeting MEK1 via regulation of the ERK/MAPK signaling pathway. Oncology reports. 2019;41(1):377-86.
268. Shah S, Brock EJ, Ji K, Mattingly RR. Ras and Rap1: A tale of two GTPases. Seminars in cancer biology. 2019;54:29-39.
269. Maemura K, Shiraishi N, Sakagami K, Kawakami K, Inoue T, Murano M, et al. Proliferative effects of gamma-aminobutyric acid on the gastric cancer cell line are associated with extracellular signal-regulated kinase 1/2 activation. Journal of gastroenterology and hepatology. 2009;24(4):688-96.
270. Wahedi HM, Jeong M, Chae JK, Do SG, Yoon H, Kim SY. Aloesin from *Aloe vera* accelerates skin wound healing by modulating MAPK/Rho and Smad signaling pathways *in vitro* and *in vivo*. Phytomedicine. 2017;28:19-26.

APPENDIX

APPENDIX A STABILITY TEST

Infrared spectra reference

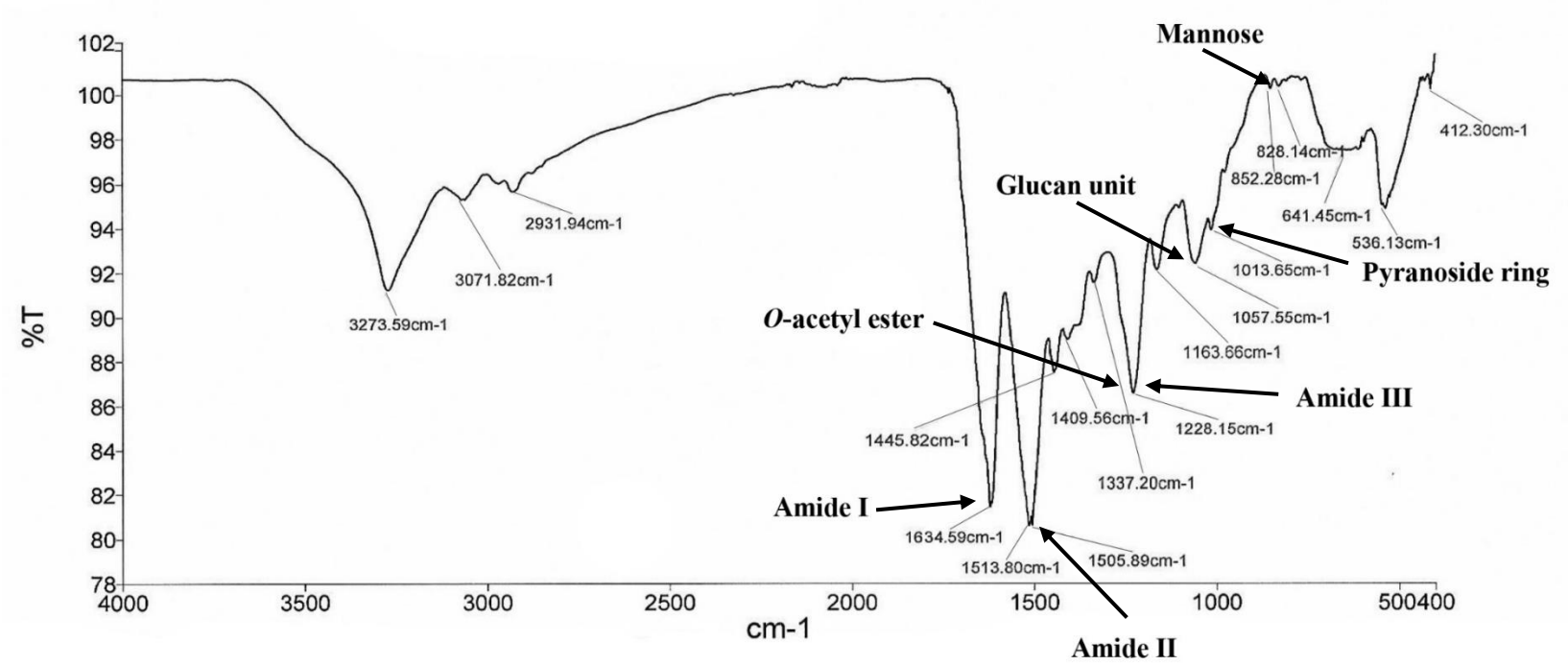

Figure 43 Chemical structure analysis by Fourier Transformed Infrared (FTIR) spectroscopy of gamma-irradiated blended fibroin/aloe gel extract film (reference)

Storage temperature: 4˚C for 7 days

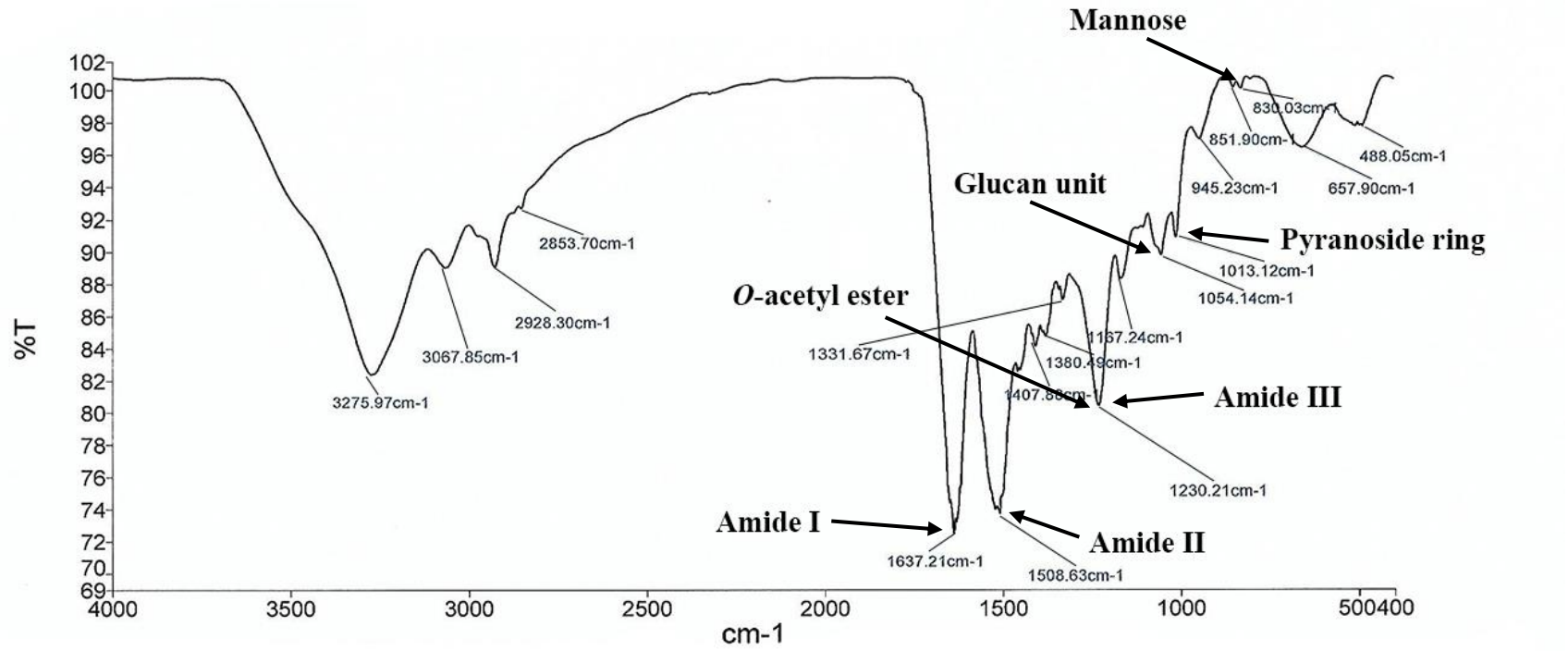

Figure 44 Chemical structure analysis by Fourier Transformed Infrared (FTIR) spectroscopy of gamma-irradiated blended fibroin/aloe gel extract film at 4˚C for 7 days

Storage temperature: 45˚C for 7 days

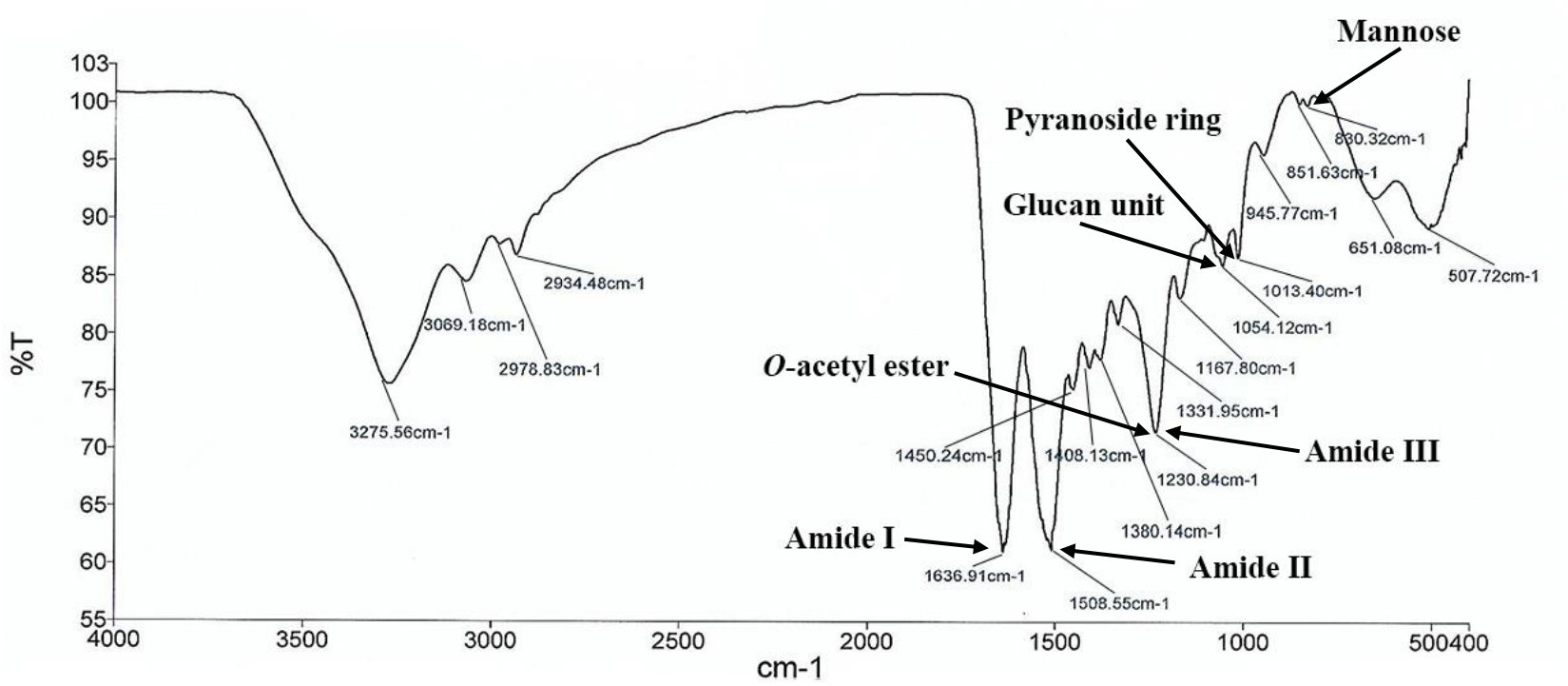

Figure 45 Chemical structure analysis by Fourier Transformed Infrared (FTIR) spectroscopy of gamma-irradiated blended fibroin/aloe gel extract film at 45˚C for 7 days

Storage temperature: 4˚C for 30 days

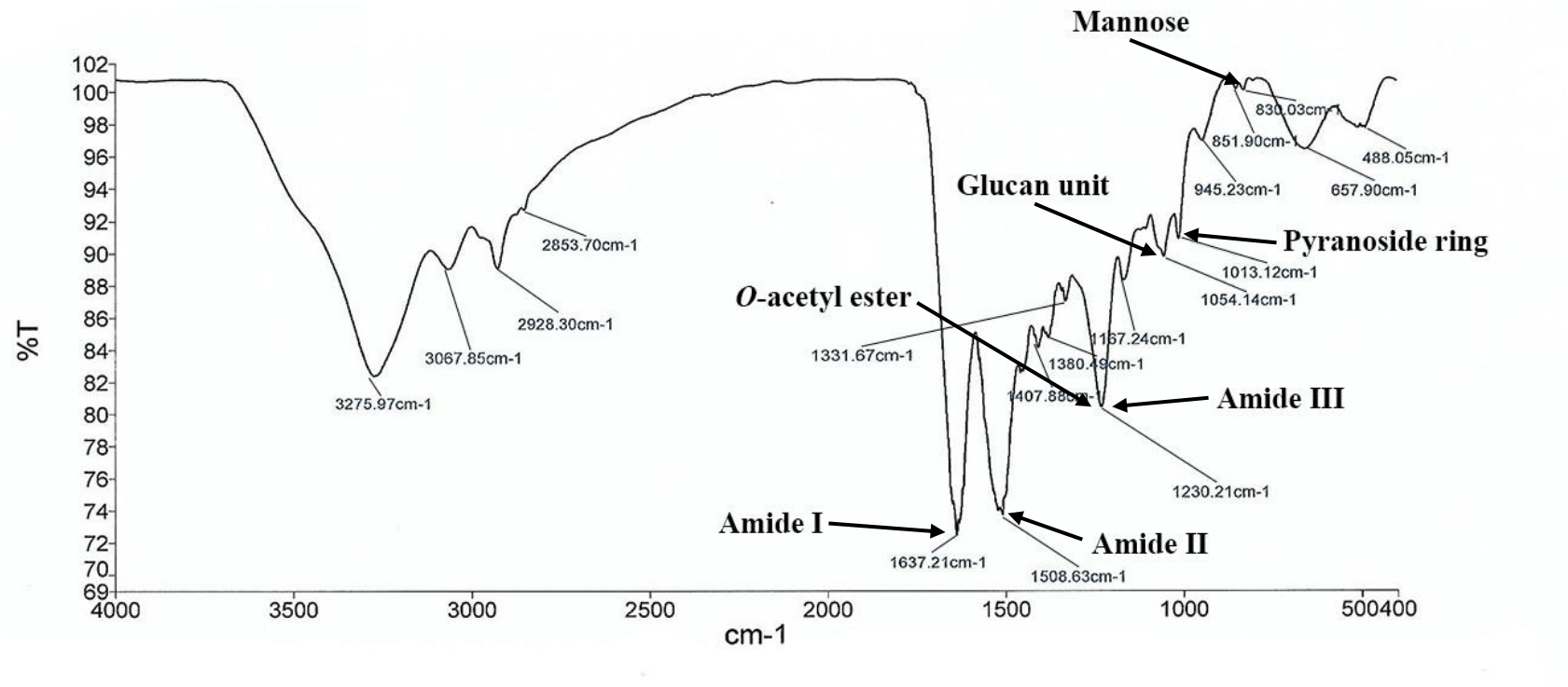

Figure 46 Chemical structure analysis by Fourier Transformed Infrared (FTIR) spectroscopy of gamma-irradiated blended fibroin/aloe gel extract film at 4˚C for 30 days

Storage temperature: 45˚C for 30 days

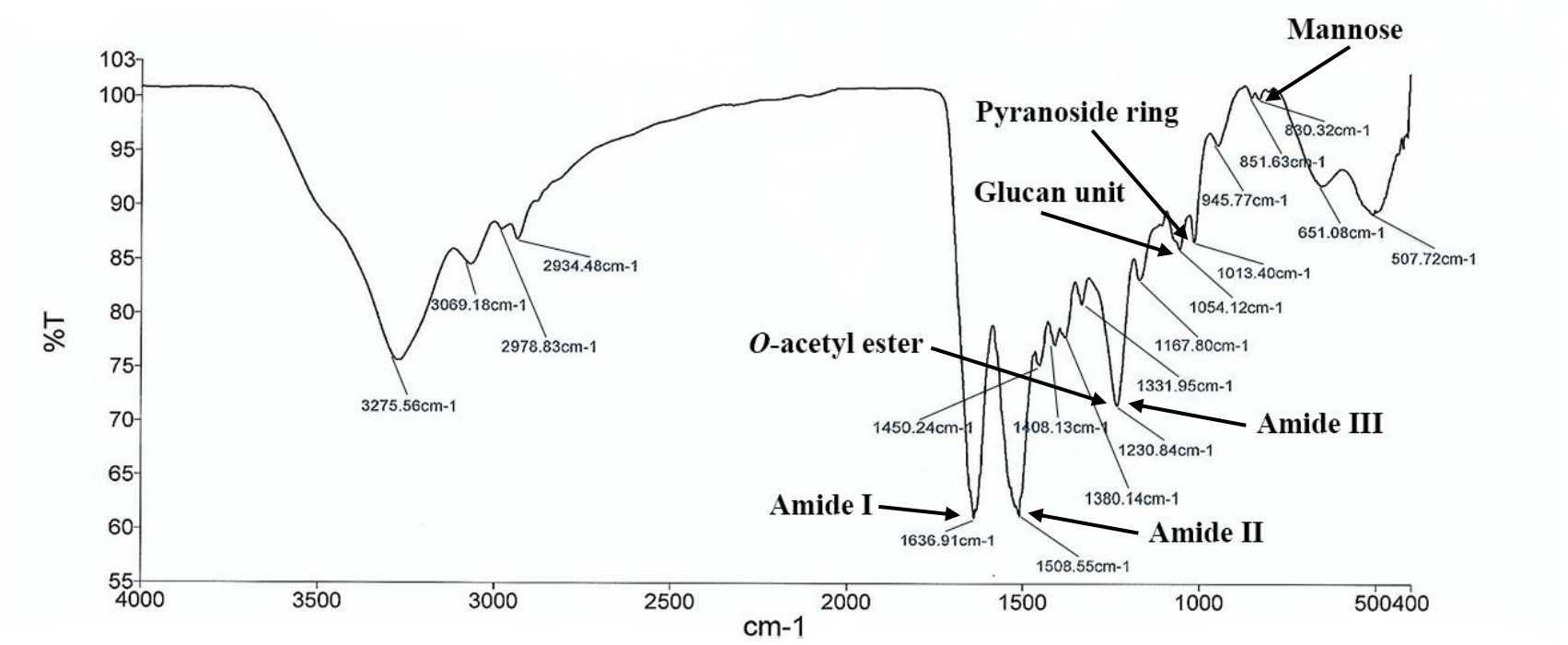

Figure 47 Chemical structure analysis by Fourier Transformed Infrared (FTIR) spectroscopy of gamma-irradiated blended fibroin/aloe gel extract film at 45˚C for 30 days

Storage temperature: 4˚C for 90 days

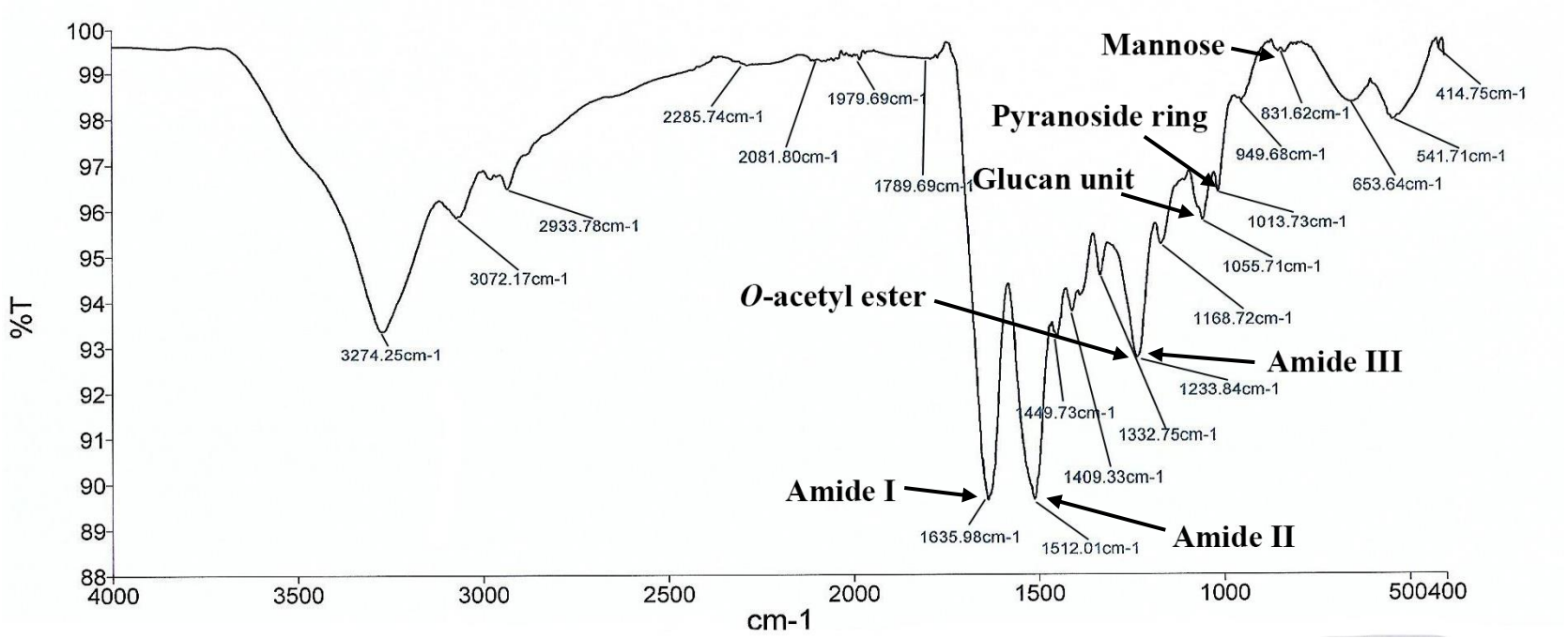

Figure 48 Chemical structure analysis by Fourier Transformed Infrared (FTIR) spectroscopy of gamma-irradiated blended fibroin/aloe gel extract film at 4˚C for 90 days

Storage temperature: 45˚C for 90 days

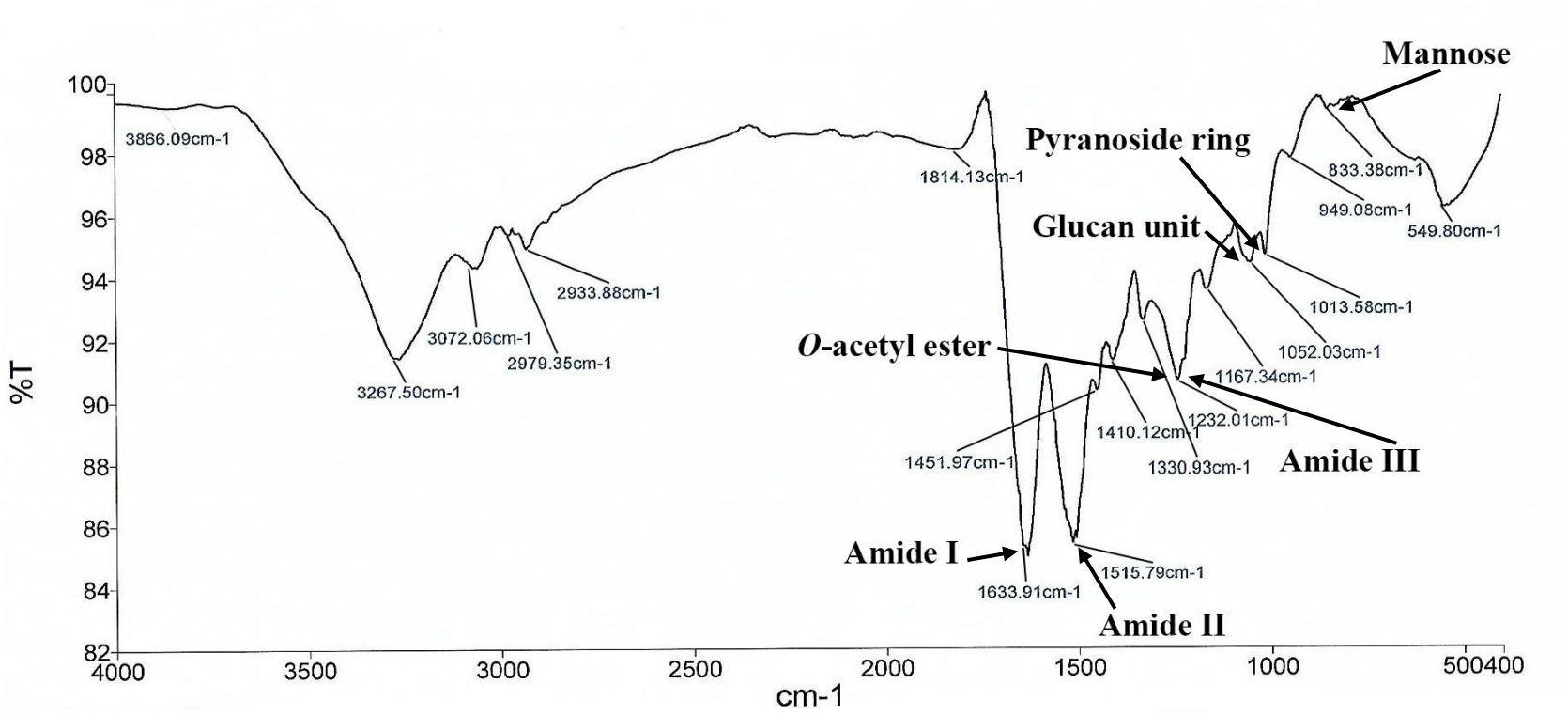

Figure 49 Chemical structure analysis by Fourier Transformed Infrared (FTIR) spectroscopy of gamma-irradiated blended fibroin/aloe gel extract film at 45˚C for 90 days

APPENDIX B BIOLOGICAL ACTIVITIES OF BLENDED FIBROIN/ALOE GEL EXTRACT FILM USING NORMAL HUMAN DERMAL FIBROBLAST (NHDF) CELL LINES

Table 6 Cytotoxicity test

	Control group (untreated cell)		Film extract	
	OD value	% Viability	OD value	% Viability
1	1.010	105.67	1.373	143.71
2	0.909	95.07	1.387	145.17
3	0.949	99.26	1.424	148.97
Average	0.9556	100	1.3947	145.95
SD	5.34		1.86	

Table 7 Cell cycle

	G0/G1 phase		S phase		G2/M phase	
	Control group	Film extract	Control group	Film extract	Control group	Film extract
1	91.14	75.36	2.72	7.32	5.84	16.68
2	95.29	76.56	1.53	6.93	2.83	16.07
3	90.98	76.84	3.33	7.33	5.33	15.53
Average	92.47	76.25	2.53	7.19	4.67	16.09
SD	2.44	0.79	0.92	0.23	1.61	0.58

APPENDIX C BIOLOGICAL ACTIVITIES OF BLENDED FIBROIN/ALOE GEL EXTRACT FILM USING PRIMARY CELL (NORMAL DERMAL FIBROBLAST, DIABETIC DERMAL FIBROBLAST, DIABETIC WOIUND FIBROBLAST)

Table 8 Cytotoxicity test

%Viability	Normal dermal fibroblast			Diabetic wound fibroblast			Diabetic dermal fibroblast		
	w/o FBS	2% FBS	Film	w/o FBS	2% FBS	Film	w/o FBS	2% FBS	Film
1	106.84	156.84	237.89	106.15	118.46	212.69	93.33	131.43	201.90
2	85.79	158.42	243.16	99.23	141.92	178.85	98.10	134.76	210.95
3	102.63	146.84	250.53	101.54	123.85	181.15	91.90	145.71	194.29
4	97.37	152.63	260.53	95.00	119.62	186.54	102.38	136.19	216.19
5	106.32	140.53	254.21	100.38	115.00	181.92	101.43	134.76	215.71
6	92.11	158.42	263.16	96.54	124.23	186.15	99.05	142.86	231.90
7	93.68	147.37	206.32	92.69	122.31	210.38	99.52	150.48	213.33
8	108.95	139.47	211.05	98.85	139.62	189.62	100.00	136.67	209.05
Average	99.21	150.07	240.86	98.80	125.63	190.91	98.21	139.11	211.67
SD	8.34	5.12	8.95	4.21	7.83	6.91	3.79	4.69	5.22

Table 9 Cell proliferation

% Cell proliferation	Normal dermal fibroblast			Diabetic wound fibroblast			Diabetic dermal fibroblast		
	w/o FBS	2% FBS	Film	w/o FBS	2% FBS	Film	w/o FBS	2% FBS	Film
1	99.22	272.94	615.49	91.96	268.48	501.52	99.66	206.10	632.20
2	109.02	245.29	588.04	98.48	244.13	598.04	92.88	188.31	596.61
3	98.24	238.04	643.92	89.13	221.09	570.22	111.02	170.00	571.19
4	97.45	223.53	555.88	87.83	212.83	498.04	95.76	199.15	525.25
5	111.57	207.25	631.57	108.70	210.43	446.74	97.46	181.02	565.08
6	96.47	225.88	583.33	107.61	200.22	469.78	91.19	216.78	579.49
7	88.82	201.57	665.88	109.57	227.83	491.09	116.78	196.44	508.98
8	96.27	230.59	568.63	109.13	225.43	560.22	92.54	223.22	588.81
Average	99.63	230.64	606.59	100.30	226.30	516.96	99.66	197.63	570.95
SD	7.35	9.73	6.39	9.54	9.51	10.26	9.37	9.02	6.87

Table 10 Cell cycle: Normal dermal fibroblast

Cell cycle	G0/G1 phase			S phase			G2/M phase		
	w/o FBS	2% FBS	Film	w/o FBS	2% FBS	Film	w/o FBS	2% FBS	Film
1	74.03	57.72	48.80	17.84	35.08	51.17	8.04	7.20	0.03
2	74.45	54.68	49.89	20.90	45.32	49.52	4.64	0.00	0.59
3	71.41	59.73	47.60	24.63	40.27	52.40	3.96	0.00	0.00
Average	73.30	57.38	48.76	21.12	40.22	51.03	5.55	2.40	0.21
SD	1.65	2.54	1.15	3.40	5.12	1.45	2.19	4.16	0.33

Table 11 Cell cycle: Diabetic dermal fibroblast

Cell cycle	G0/G1 phase			S phase			G2/M phase		
	w/o FBS	2% FBS	Film	w/o FBS	2% FBS	Film	w/o FBS	2% FBS	Film
1	74.37	58.67	51.50	17.90	41.33	48.31	7.73	0.00	0.19
2	73.70	59.23	53.14	0.00	40.35	46.86	26.30	0.42	0.00
3	77.22	59.24	51.24	15.95	40.66	48.60	15.95	0.10	0.16
Average	75.10	59.05	51.96	11.28	40.78	47.92	16.66	0.17	0.12
SD	1.87	0.33	1.03	9.82	0.50	0.93	9.31	0.22	0.10

Table 12 Cell cycle: Diabetic wound fibroblast

Cell cycle	G0/G1 phase			S phase			G2/M phase		
	w/o FBS	2% FBS	Film	w/o FBS	2% FBS	Film	w/o FBS	2% FBS	Film
1	47.19	66.69	51.11	27.37	33.26	42.22	25.44	0.04	6.67
2	46.56	70.02	54.88	27.26	27.33	45.12	26.18	2.65	0.00
3	43.37	64.22	49.73	31.53	26.77	50.09	25.10	9.01	0.18
Average	45.71	66.98	51.91	28.72	29.12	45.81	25.57	3.90	2.28
SD	2.05	2.91	2.67	2.43	3.60	3.98	0.55	4.61	3.80

Table 13 Cell migration: Normal dermal fibroblast

Elapsed	w/o FBS		2% FBS		Film	
	% Relative density	SD	% Relative density	SD	% Relative density	SD
0	0.00	0.00	0.00	0.00	0.00	0.00
2	0.00	1.43	6.22	2.17	6.45	2.45
4	0.00	1.05	13.17	1.96	12.26	4.26
6	1.79	1.88	19.47	3.32	18.02	4.39
8	4.12	1.81	24.37	3.27	23.18	5.70
10	5.51	1.97	27.33	4.44	30.68	3.92
12	8.02	2.14	30.99	4.21	36.66	5.38
14	9.46	2.29	34.67	4.20	42.86	5.12
16	11.40	2.09	37.61	5.17	47.57	4.70
18	13.02	2.17	41.03	6.19	51.91	5.30
20	15.16	2.37	43.28	5.77	58.13	6.34
22	16.62	2.81	46.33	5.25	64.24	5.34
24	17.92	3.22	47.86	4.93	69.69	4.59
26	19.11	3.67	50.65	4.77	74.59	4.12
28	20.69	3.91	52.82	4.51	79.00	4.18
30	22.02	3.89	55.28	4.48	82.23	4.38
32	23.77	4.34	56.48	4.38	84.55	4.48
34	25.23	4.72	57.92	4.79	87.43	5.56
36	26.50	4.52	60.40	4.75	89.38	5.03
38	27.63	4.12	62.15	5.29	91.10	5.69
40	28.90	4.21	63.91	5.30	93.40	5.34
42	29.46	4.54	65.10	6.16	95.43	4.26
44	30.63	3.83	65.96	5.49	97.07	4.23
46	31.32	3.02	67.10	5.28	99.36	4.41
48	32.65	3.52	68.15	4.91	99.73	5.01

Table 14 Cell migration: Diabetic dermal fibroblast

Elapsed	w/o FBS		2% FBS		Film	
	% Relative density	SD	% Relative density	SD	% Relative density	SD
0	0.00	0.00	0.00	0.00	0.00	0.00
2	1.68	0.49	1.53	3.72	4.46	2.32
4	2.20	0.49	2.31	3.66	10.19	2.76
6	2.75	0.84	3.59	6.13	16.24	2.65
8	3.08	0.82	6.68	5.38	22.55	2.91
10	3.44	1.07	8.37	5.86	27.75	2.64
12	4.13	1.42	11.86	3.99	33.39	2.25
14	4.76	1.58	14.03	4.98	38.17	2.94
16	5.30	1.77	17.25	4.93	42.78	2.88
18	5.81	1.86	20.56	5.40	46.60	3.01
20	7.00	1.56	23.20	5.49	51.06	4.04
22	8.47	1.60	25.70	4.40	54.75	3.33
24	9.70	1.92	29.73	5.65	59.59	3.28
26	12.11	2.00	33.25	5.49	64.73	2.50
28	15.10	1.46	36.88	4.71	68.57	2.57
30	17.32	1.74	39.76	5.47	73.34	2.63
32	20.76	1.97	42.16	6.46	78.03	2.66
34	23.34	1.59	44.98	5.57	80.82	2.51
36	26.07	1.46	47.80	4.40	84.45	2.51
38	28.49	1.35	49.65	4.41	87.61	2.42
40	30.13	1.31	51.42	4.49	91.16	2.27
42	31.89	1.63	54.08	5.05	93.94	2.73
44	33.89	1.49	55.50	4.81	95.43	2.36
46	35.30	1.62	57.24	4.74	96.78	2.23
48	37.01	1.75	59.37	6.85	98.01	2.90

Table 15 Cell migration: Diabetic wound fibroblast

Elapsed	w/o FBS		2% FBS		Film	
	% Relative density	SD	% Relative density	SD	% Relative density	SD
0	0.00	0.00	0.00	0.00	0.00	0.00
2	0.94	2.64	3.04	0.63	0.23	0.43
4	1.79	2.75	5.43	1.61	6.11	0.64
6	2.80	2.71	8.98	1.63	9.95	0.89
8	4.10	2.75	12.27	1.53	13.89	0.92
10	5.63	2.94	14.99	1.91	18.58	0.94
12	7.88	2.12	18.81	2.16	23.60	1.35
14	8.92	2.10	21.12	3.07	29.80	1.81
16	11.05	2.13	22.82	3.03	35.27	2.48
18	12.30	2.88	24.03	2.87	41.70	2.99
20	14.20	2.91	25.97	2.97	47.68	3.61
22	15.92	2.95	28.55	2.90	52.50	3.70
24	17.96	3.12	30.57	3.59	58.05	3.87
26	20.03	3.15	32.04	3.27	63.10	4.34
28	21.69	3.25	34.20	3.88	66.79	4.24
30	23.08	3.36	36.01	3.23	70.49	4.37
32	25.17	3.52	37.69	3.36	74.64	4.37
34	27.11	2.60	39.37	3.06	77.87	4.17
36	28.98	2.56	40.49	3.07	80.83	3.87
38	31.03	2.81	41.40	2.63	83.47	3.55
40	32.35	2.88	43.17	2.90	85.93	3.37
42	33.81	1.96	43.99	2.65	88.20	3.19
44	35.29	2.02	45.39	2.35	90.06	3.06
46	36.37	2.16	46.29	2.53	91.66	2.83
48	38.63	2.36	48.27	2.71	93.47	2.86

Table 16 Cell senescence: Normal dermal fibroblast

Cell senescence	w/o FBS			2% FBS			Film extract		
	Blue-stained cell	Total cell	Cell senescence	Blue-stained cell	Total cell	Cell senescence	Blue-stained cell	Total cell	Cell senescence
1	4	131	0.0305	1	93	0.0108	0	178	0.0000
2	2	120	0.0167	2	114	0.0175	1	100	0.0100
3	1	120	0.0083	4	130	0.0308	0	138	0.0000
4	1	119	0.0084	6	151	0.0397	1	169	0.0059
5	2	52	0.0385	2	122	0.0164	2	240	0.0083
6	2	80	0.0250	1	111	0.0090	0	167	0.0000
7	1	81	0.0123	1	108	0.0093	1	144	0.0069
8	2	86	0.0233	1	125	0.0080	0	124	0.0000
Average		0.0204			0.0177			0.0039	
% Cell senescence		2.04			1.77			0.39	
SD		1.09			1.16			0.43	

Table 17 Cell senescence: Diabetic dermal fibroblast

Cell senescence	w/o FBS			2% FBS			Film extract		
	Blue-stained cell	Total cell	Cell senescence	Blue-stained cell	Total cell	Cell senescence	Blue-stained cell	Total cell	Cell senescence
1	22	69	0.3188	31	140	0.2214	11	122	0.0902
2	18	47	0.3830	23	117	0.1966	22	163	0.1350
3	24	66	0.3636	31	137	0.2263	16	158	0.1013
4	25	64	0.3906	33	161	0.2050	22	176	0.1250
5	18	59	0.3051	31	138	0.2246	22	148	0.1486
6	20	60	0.3333	35	159	0.2201	15	120	0.1250
7	21	62	0.3387	37	169	0.2189	11	111	0.0991
8	24	63	0.3810	27	151	0.1788	7	88	0.0795
Average		0.3518			0.2115			0.1130	
% Cell senescence		35.18			21.15			11.30	
SD		3.22			1.67			2.39	

Table 18 Cell senescence: Diabetic wound fibroblast

Cell senescence	w/o FBS			2% FBS			Film extract		
	Blue-stained cell	Total cell	Cell senescence	Blue-stained cell	Total cell	Cell senescence	Blue-stained cell	Total cell	Cell senescence
1	17	120	0.1417	5	129	0.0388	1	279	0.0036
2	9	82	0.1098	1	119	0.0084	2	116	0.0172
3	10	103	0.0971	2	107	0.0187	1	226	0.0044
4	10	98	0.1020	5	136	0.0368	0	308	0.0000
5	21	120	0.1750	2	111	0.0180	2	229	0.0087
6	11	100	0.1100	2	108	0.0185	2	280	0.0071
7	11	88	0.1250	3	172	0.0174	1	264	0.0038
8	13	97	0.1340	2	80	0.0250	2	360	0.0056
Average		0.1243			0.0227			0.0063	
% Cell senescence		12.43			2.27			0.63	
SD		2.57			1.03			0.51	

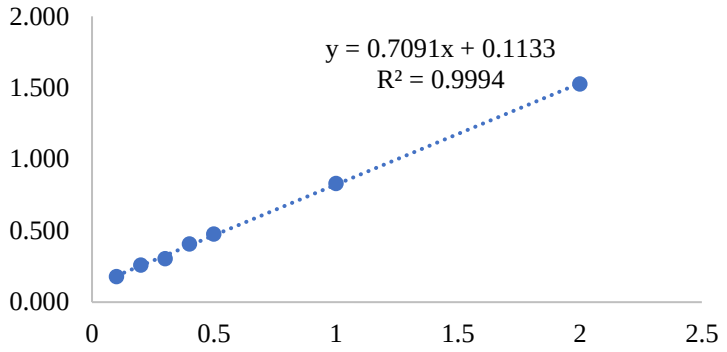

Figure 50 BSA standard curve standard solution (concentration 0-2 mg/mL) by Bradford assay

Table 19 Intracellular protein analysis

Intracellular protein analysis	Normal dermal fibroblast			Diabetic wound fibroblast			Diabetic dermal fibroblast		
	w/o FBS	2% FBS	Film	w/o FBS	2% FBS	Film	w/o FBS	2% FBS	Film
1	0.394	0.574	0.722	0.297	0.506	0.603	0.359	0.472	0.647
2	0.393	0.578	0.686	0.328	0.508	0.614	0.345	0.506	0.656
3	0.416	0.572	0.702	0.369	0.505	0.589	0.389	0.516	0.624
4	0.395	0.545	0.747	0.377	0.492	0.623	0.396	0.509	0.625
Average	0.400	0.567	0.714	0.343	0.503	0.607	0.372	0.501	0.638
mg/mL	0.40	0.64	0.84	0.33	0.55	0.69	0.37	0.55	0.74
SD	0.015	0.021	0.037	0.052	0.010	0.020	0.034	0.027	0.022

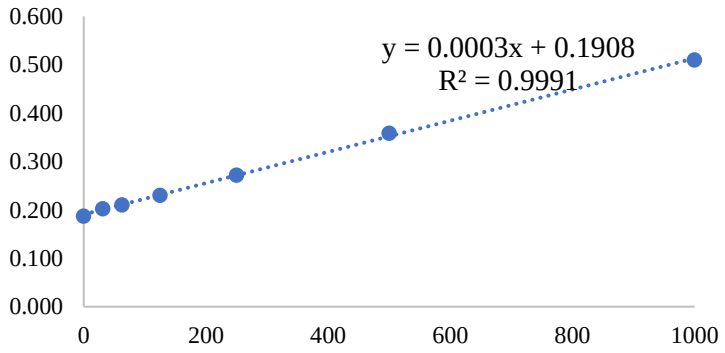

Figure 51 VEGF standard curve standard solution (concentration 0 - 1,000 μg/mL)

Table 20 VEGF secretion by VEGF ELISA colorimetric assay

VEGF secretion	Normal dermal fibroblast			Diabetic wound fibroblast			Diabetic dermal fibroblast		
	w/o FBS	2% FBS	Film	w/o FBS	2% FBS	Film	w/o FBS	2% FBS	Film
1	0.248	0.287	0.304	0.221	0.264	0.285	0.203	0.227	0.264
2	0.233	0.308	0.306	0.227	0.258	0.284	0.203	0.233	0.262
3	0.244	0.294	0.314	0.229	0.268	0.276	0.203	0.237	0.256
4	0.253	0.297	0.309	0.235	0.277	0.279	0.217	0.255	0.291
Average	0.245	0.297	0.308	0.228	0.267	0.281	0.207	0.238	0.268
mg/mL	179.00	352.33	782.17	124.00	253.17	598.83	52.33	157.33	515.50
VEGF (mg protein)	448.060	621.125	1095.088	361.780	503.564	986.140	140.587	314.195	807.994
SD	70.963	51.341	19.277	56.149	52.869	22.227	62.682	80.249	81.900

Table 21 Phospho-nF-kB p65 signaling pathway at the various time (1, 4, 18, and 24 h) by immunofluorescence assay using normal dermal fibroblast

Normal dermal fibroblast - Control (untreated group)			
1 H	4 H	18 H	24 H
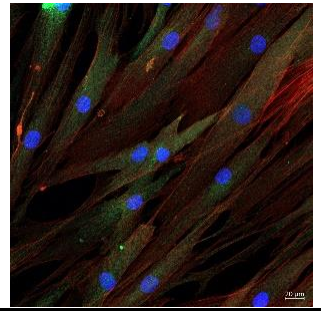	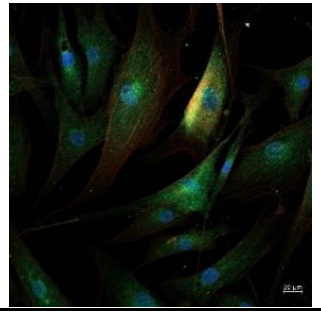	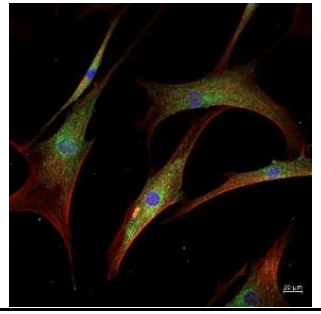	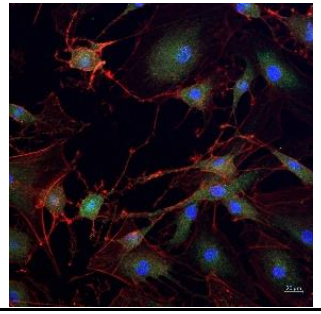
Normal dermal fibroblast - Film extract (treated group)			
1 H	4 H	18 H	24 H
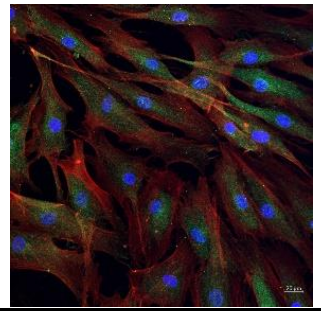	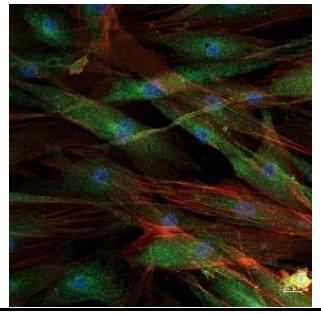	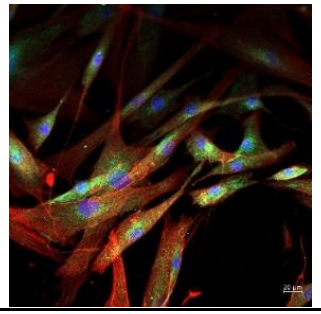	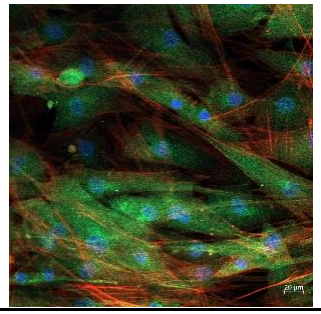

Table 22 Phospho-p44/42 MAPK signaling pathway at the various time (1, 4, 18, and 24 h) by immunofluorescence assay using normal dermal fibroblast

Normal dermal fibroblast - Control (untreated group)			
1 H	4 H	18 H	24 H
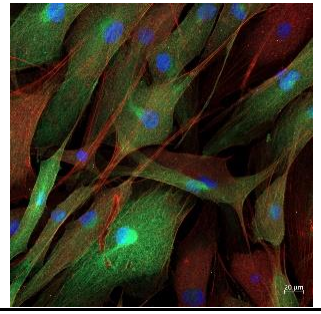	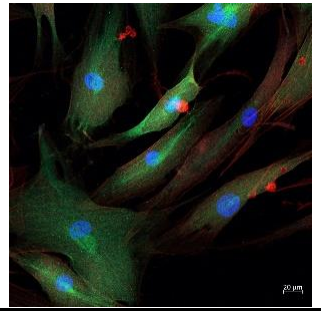	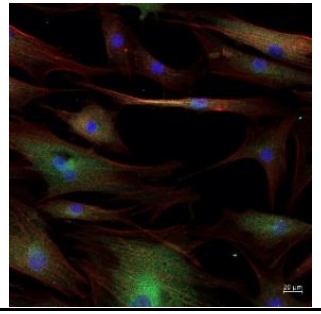	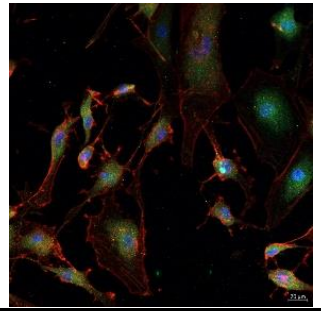
Normal dermal fibroblast - Film extract (treated group)			
1 H	4 H	18 H	24 H
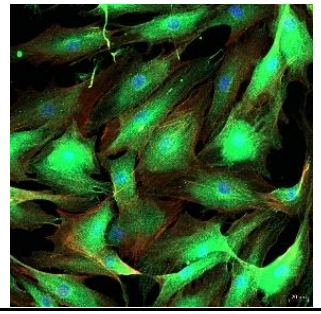	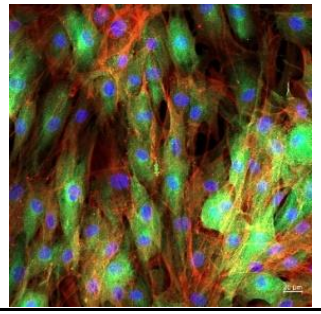	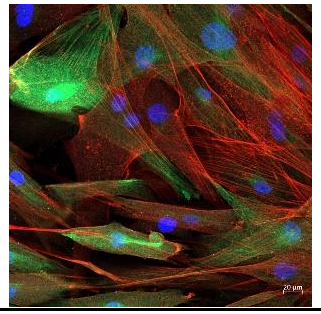	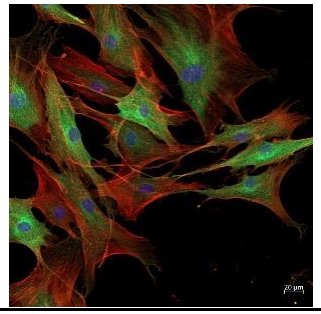

Table 23 Phospho-p38 MAPK signaling pathway at the various time (1, 18, and 24 h) by immunofluorescence assay using normal dermal fibroblast

Normal dermal fibroblast - Control (untreated group)		
1 H	18 H	24 H
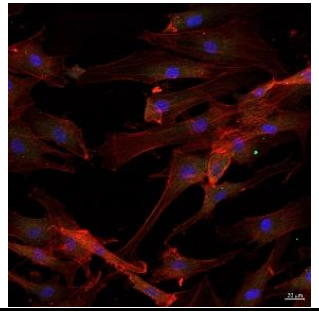	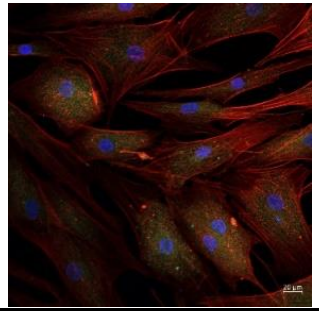	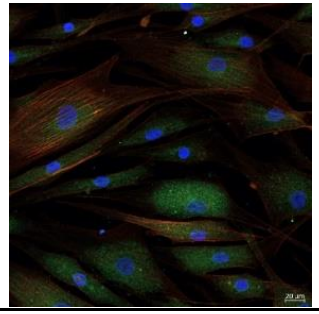
Normal dermal fibroblast - Film extract (treated group)		
1 H	18 H	24 H
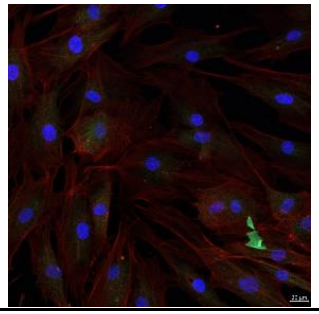	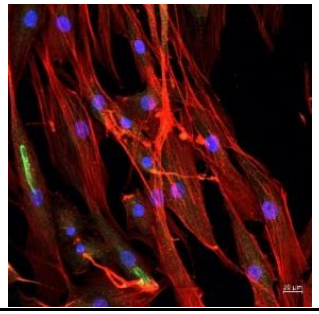	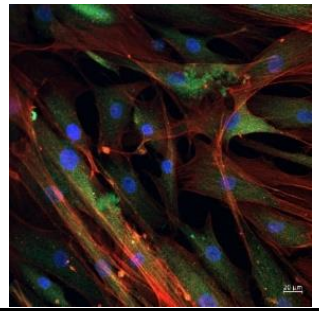

Table 24 Phospho-JNK/SAPK signaling pathway at the various time (1, 18, and 24 h) by immunofluorescence assay using normal dermal fibroblast

Normal dermal fibroblast - Control (untreated group)		
1 H	18 H	24 H
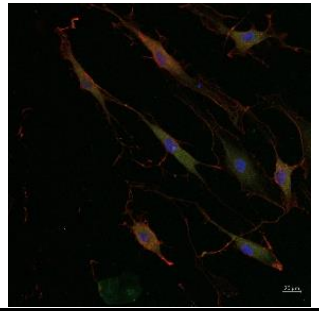	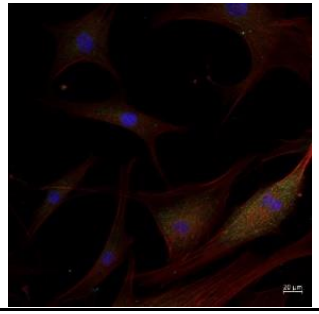	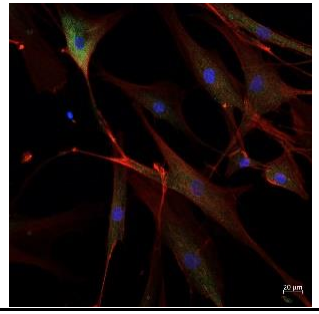
Normal dermal fibroblast - Film extract (treated group)		
1 H	18 H	24 H
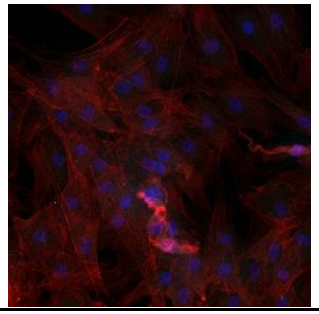	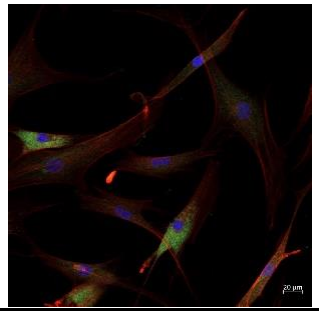	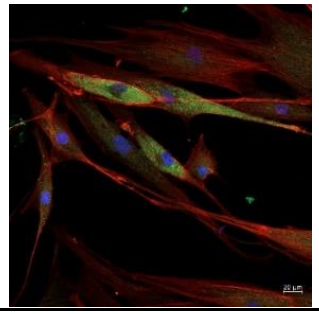

Table 25 Immunofluorescence assay (Phospho-nF-kB p65, Phospho-p44/42 MAPK, Phospho-p38 MAPK, and Phospho-JNK/SAPK signaling pathway) using diabetic dermal fibroblast at 24 h

Diabetic dermal fibroblast (24 H) - Control (untreated group)			
Phospho-nF-kB p65	Phospho-p44/42 MAPK	Phospho-p38 MAPK	Phospho-JNK/SAPK
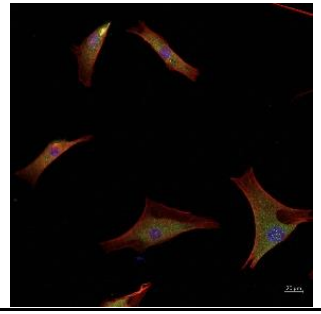	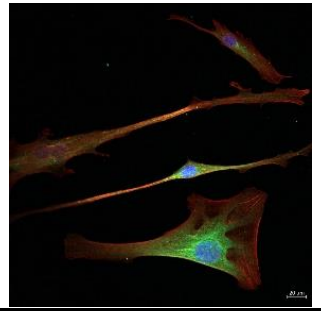	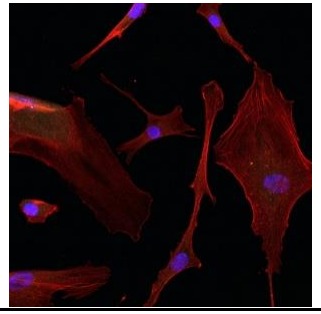	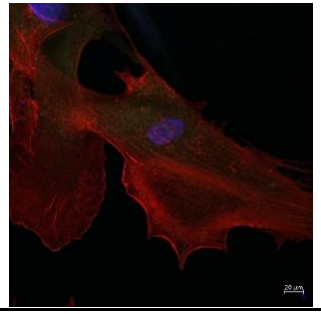
Diabetic dermal fibroblast (24 H) - Film extract (treated group)			
Phospho-nF-kB p65	Phospho-p44/42 MAPK	Phospho-p38 MAPK	Phospho-JNK/SAPK
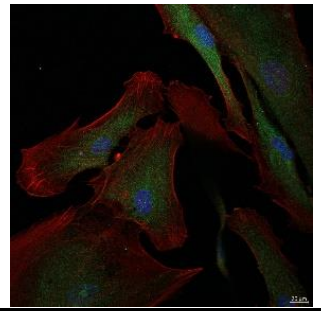	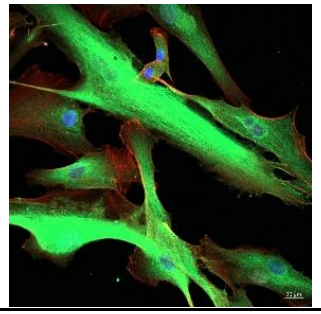	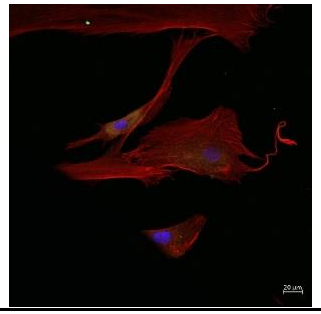	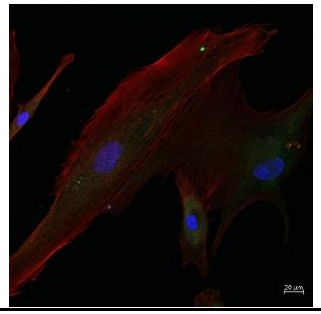

Table 26 Immunofluorescence assay (Phospho-nF-kB p65, Phospho-p44/42 MAPK, Phospho-p38 MAPK, and Phospho-JNK/SAPK signaling pathway) using diabetic wound fibroblast at 24 h

Diabetic wound fibroblast (24 H) - Control (untreated group)			
Phospho-nF-kB p65	Phospho-p44/42 MAPK	Phospho-p38 MAPK	Phospho-JNK/SAPK
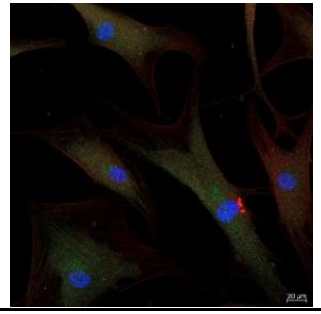	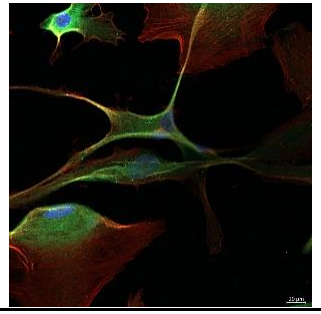	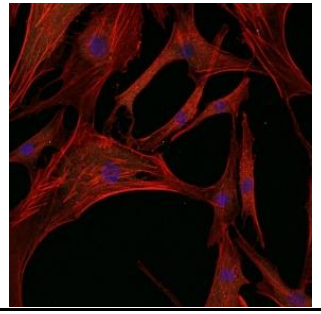	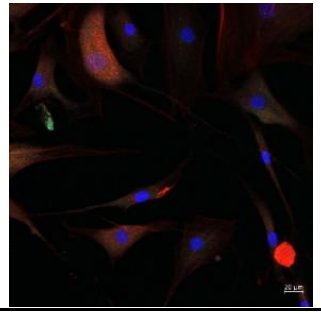
Normal wound fibroblast - Film extract (treated group)			
Phospho-nF-kB p65	Phospho-p44/42 MAPK	Phospho-p38 MAPK	Phospho-JNK/SAPK
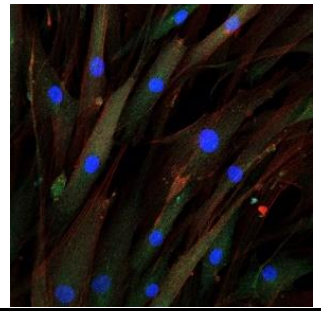	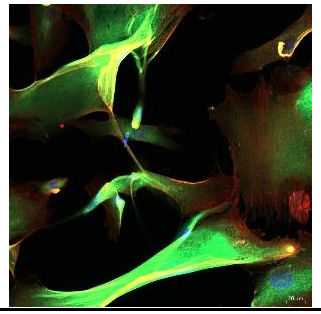	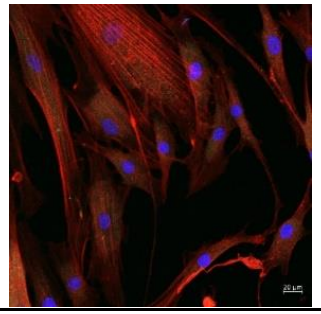	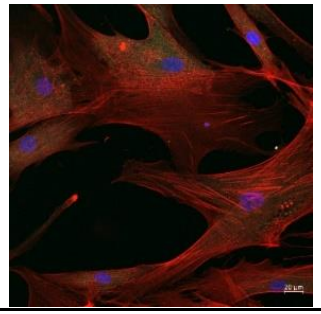

Table 27 MAPK/ERK inhibitor treatment on cell proliferation using Normal dermal fibroblast

MAPK/ERK inhibitor treatment on cell proliferation	DMEM w/o serum		DMEM 2% serum		Film extract	
	w/o ERK-inhibitor	ERK-inhibitor	w/o ERK-inhibitor	ERK-inhibitor	w/o ERK-inhibitor	ERK-inhibitor
1	0.45	0.18	1.61	0.58	1.72	0.52
2	0.43	0.23	1.48	0.61	1.69	0.65
3	0.52	0.22	1.47	0.55	1.92	0.59
4	0.49	0.22	1.25	0.51	2.05	0.58
Average	0.46	0.23	1.42	0.56	1.86	0.62
%Cell proliferation	100.00	49.17	307.63	121.74	404.74	133.65
SD	7.69	13.57	16.29	6.09	8.85	12.39

.

Table 28 MAPK/ERK signaling pathway by Flow cytometer using Normal dermal fibroblast: P-ERK

MAPK/ERK signaling pathway by Flow cytometer	DMEM w/o serum		DMEM 2% serum		Film extract	
	% Parent	FITC-A	% Parent	FITC-A	% Parent	FITC-A
1	98.5	3207	98.8	3147	98.8	3398
2	98.2	2954	99.3	3404	98.8	3354
3	99.1	3100	99.2	3399	98.4	3486
4	99.2	3314	98.7	3632	98.2	3419
Average	98.8	3143.8	99.0	3395.5	98.6	3414.3
SD	0.5	153.7	0.3	198.1	0.3	55.0

Table 29 MAPK/ERK signaling pathway by Flow cytometer using Normal dermal fibroblast: Phospho-P-ERK

MAPK/ERK signaling pathway by Flow cytometer	DMEM w/o serum		DMEM 2% serum		Film extract	
	% Parent	FITC-A	% Parent	FITC-A	% Parent	FITC-A
1	14.9	1261	48.0	1716	71.0	2155
2	12.5	1237	43.5	1710	67.8	2071
3	11.9	1193	35.2	1569	65.4	2007
4	19.4	1133	38.6	1451	69.1	2097
Average	14.7	1206.0	41.3	1611.5	68.3	2082.5
SD	3.4	56.2	5.6	126.7	2.4	61.4